Technische Universität München
Lehrstuhl für Steuerungs- und Regelungstechnik

Wholesale Energy Market in a Smart Grid: Dynamic modeling, stability, and robustness

Arman Kiani Bejestani

Vollständiger Abdruck der von der Fakultät für Elektrotechnik und Informationstechnik der Technischen Universität München zur Erlangung des akademischen Grades eines

Doktor-Ingenieurs (Dr.-Ing.)

genehmigten Dissertation.

Vorsitzender: Univ.-Prof. Dr. rer. nat. Thomas Hamacher

Prüfer der Dissertation:

1. Univ.-Prof. Dr.-Ing. Sandra Hirche
2. Prof. Anuradha Annaswamy, Ph. D.
   Massachusetts Institute of Technology, USA

Die Dissertation wurde am 20.09.2012 bei der Technischen Universität München eingereicht und durch die Fakultät für Elektrotechnik und Informationstechnik am 24.01.2013 angenommen.

Acknowledgement

I am very grateful to my thesis supervisor, Professor Anuradha Annaswamy, for her motivation, guidance, encouragement, and high research and ethical standards. She always made plenty of time to talk about the research, open to possibilities, and dedicated to working through the uncertainties and difficulties in pursuit of the solutions to problems that are both challenging and practical. I have benefitted enormously from her numerous insights in these discussions. It is a great fortune that I have the privilege to work with her, and know her not only as an advisor but also as a friend. Watching her approach in research with calmness, patience and dedication was a valuable lesson for me. I want to thank her especially for giving me the chance to work with her, for letting me grow and find my way, this experience has forever changed my perspective on research, and will have a long-lasting influence on my career.

This thesis was made possible by financial support from Institute for Advanced Study, funded by the German Excellence Initiative and by Deutsche Forschungsgemeinschaft (DFG) through the Technische Universität München International Graduate School of Science and Engineering (IGSSE). I would like to gratefully acknowledge Professor Martin Buss for giving me support and encouragement that really helped me, Professor Sandra Hirche for helping me gain perspective by her appreciation for broader issues and implications, and taking the time to discuss the work with me and share her technical and physical insights, and Professor Thomas Hamacher as a head of my defense committee.

Parts of the work reported here were carried out when I was a visiting student at the Laboratory of Information and Decision Systems (LIDS) in 2010, and Active Adaptive Control Laboratory in 2011 at MIT. I gratefully acknowledge my discussions and kind hospitality of Professor Munther Dahleh and the members of LIDS, specially Dr. Mardavij Roozbehani, and Ali Faghih. Special thanks go to Professor Ozdaglar for her wonderful classes on game theory. I really appreciate her taking the time to talk to me about my work and helpful discussions on the game theory and mechanism design. I would like to extend special thanks to Dr. Tariq Samad, Honeywell, for his invaluable comments for helping me make my explanations clearer.

Many heartfelt thanks go to my great friend, and colleague, Harald Voit, who always offered me assistance, whether for research or for my daily life in Munich, for the unforgettable conference trips and his constructive feedback during my thesis; Special thanks go to friends and colleagues, Vahid Mamduhi, Markus Rank, and Alan Walbridge for their useful comments and proof reading of this thesis. Finally special thanks go to my office-mates Andreas Schmid, Dr. Iason Vittorias, and Stefan Kersting and all my other colleagues and lab mates at LSR for giving me insights, support, and friendship throughout these years. I am also very grateful to the great administrative support I received at LSR, treated with professionalism and help in every matter I had. To my friends and colleagues at MIT, Travis Gibson, Dr. Yoav Sharon, Dr. Damoon Soudbakhsh, Manohar Srikanth, and Daniel Wiese

for the useful and critical technical and theoretical comments and for the nice atmosphere in the office we shared during my stay in Active Adaptive Control Laboratory.

Above all, no words can fully express my thankfulness to my parents. I am extremely grateful for introducing me to mathematics and science, for teaching me to persist and for always taking the time to listen, encourage, love, care, and faith in me. I am forever grateful to my dear wife, Yasaman, for her understanding during the late nights I was working, her continuos support, and encouragements. It is because of her that I have been able to successfully complete this endeavor.

Dedicated to my beloved parents and my wife, Yasaman.

Abstract

The recent paradigm shift in the architecture of the smart grid is driven by the need to integrate Renewable Energy Resources (RER), the availability of information through communication networks, and an emerging policy of demand that is intertwined with pricing. A major component of this architecture is the design of electricity markets, which pertains to the optimal scheduling of power generation and reserve requirements. The challenge is to carry out this scheduling with a high level of integration of renewable generation sources, a formidable task due to intermittency and uncertainty. Introducing huge intermittency and uncertainty in the smart grid will demand a dynamic framework for addressing the operation, scheduling and financial settlements in the uncertain environment. The temporal components in scheduling generation are necessary due to increasing penetration of renewable sources, and increasing potential of adjustable demand via Demand Response (DR). The former brings issues of strong intermittency and uncertainty, and the latter brings a feedback structure, where demand can be modulated over a range of time-scales. Both of these components are dictating a new look at market mechanisms, with a controls viewpoint enabling a novel framework for analysis and synthesis.

This dissertation provides static and dynamic models that capture the various aspects of electrical power systems, including the dynamics of market participants, the physical and technical constraints of power systems, and the uncertainty of RER. The proposed models shed new light on wholesale electricity market design, allowing an understanding to be gained of how to create markets, which enhance the stability of price profiles, and efficiency of the power systems, in the presence of uncertain demand and intermittent resources. The notion of market equilibrium in the presence of RER and DR is presented. The effects of uncertainties due to forecast errors in RER and variations due to DR on the market equilibrium are analyzed using perturbation analysis. Then, the notion of a disequilibrium process is provided as an indispensable market mechanism to attain market equilibrium in the presence of perturbations due to renewables and Demand Response. Associated with this notion is the design of dynamic mechanisms whose roles become more crucial as one moves from a day-ahead to a real time market and the underlying forecast models of renewables become more accurate. Introduction of dynamics and feedback brings in questions of stability. A systematic stability framework is studied, which analyzes the interplay between pricing strategies, adjustable demand, and generation while guaranteeing a stable price profile.

Furthermore, an analytical modeling of a Transactive control architecture is provided, which incorporates the interaction between market transactions, real-time pricing, physical constraints, and DR in the presence of uncertainty of RER. Transactive control consists of three hierarchical levels: (i) primary control, where power is regulated at a unit level, (ii) secondary control, where frequency is regulated at an area-level, and (iii) tertiary control, which includes market transactions between the generating and consumer companies in order to dispatch the resources economically. With a goal of ensuring frequency regulation using optimal allocation of resources in the presence of uncertainties in renewables and load, an analytical framework of Transactive control is presented. Global asymptotic stability of the overall system is established in the presence of uncertainties at all three time-scales, and this overall hierarchical Transactive controller is then shown to be effective through numerical simulations in the presence of generation and load uncertainties.

Zusammenfassung

Der Paradigmenwechsel in der Architektur von Smart Grids, der sich in letzter Zeit vollzogen hat, ist getrieben von der Notwendigkeit erneuerbare Energiequellen in das Stromnetz zu integrieren, der Verfügbarkeit von Informationen durch fortschrittliche Mess- und Kommunikationstechnik und der sich abzeichnenden Strategie die Nachfrage mit der Preisgestaltung zu verflechten. Ein bedeutender Aspekt dieser Architektur ist das Design von Elektrizitätsmärkten für Großkunden. Hierzu gehört die optimale Planung der Stromproduktion und die Anforderungen an die Reserve. Die Herausforderung besteht darin, diese Planung unter Berücksichtigung eines hohen Maßes an erneuerbaren Energien auszuführen; eine anspruchsvolle Aufgabe angesichts der Periodizität und Unsicherheit von letzterem. Durch die Einführung von Periodizitäten und Unsicherheiten im Smart Grid bedarf es einer dynamischem Lösung, die den Betrieb, die Planung und die finanziellen Vereinbarungen in einer dynamischen und unsicheren Umwelt anspricht. Es ist notwendig die zeitlichen Aspekte bei der Produktionsplanung zu berücksichtigen, da durch das vermehrte Auftreten von erneuerbaren Energiequellen sowohl Periodizitäten als auch Unsicherheiten und durch die gesteigerten Möglichkeiten einer Rückführungsstruktur (Demand Response) verschiedene Zeitskalen in das System eingebracht werden. Beide Aspekte diktieren eine neue Sichtweise auf die zugrundeliegenden Marktmechanismen; ein regelungstechnischer Standpunkt bietet dabei neuartige Möglichkeiten zur Analyse und Synthese.

In dieser Dissertation werden statische und dynamische Modelle vorgestellt, die verschiedene Dynamiken im System, physikalische und technische Beschränkungen, Unsicherheiten und Preisschwankungen erfassen. Die Gestaltung von Großhandelsmärkten für Elektrizität wurde neu beleuchtet um das Verständnis zu vergrößern, wie Märkte ihre Verlässlichkeit und Effizienz unter Berücksichtigung von periodischen Ressourcen und Schwankungen erhöhen und gleichzeitig stabile Preisprofile sicherstellen können. Dazu wird der Begriff des Marktgleichgewichts in der Gegenwart von erneuerbaren Energien und Nachfragerückführung eingeführt. Die Einflüsse auf das Marktgleichgewicht, die durch Unsicherheiten aufgrund von Vorhersagefehlern bei der Verfügbarkeit erneuerbarer Energiequellen und Veränderungen aufgrund der Nachfragerückführung hervorgerufen werden, werden mithilfe der Störungstheorie untersucht. Anschließend wird der Begriff des Ungleichgewichtsprozesses vorgestellt, ohne den ein Marktgleichgewicht in Gegenwart von Störungen, die von erneuerbargen Energien verursacht werden, und Nachfragerückführung nicht erreicht werden kann. Hierzu gehört auch der Entwurf von dynamischen Mechanismen, deren Rolle umso bedeutender sowohl beim Übergang von day-ahead zu Echtzeitmärkten als auch der stetigen Verbesserung der zugrundeliegenden Vorhersagemodelle für erneuerbare Energien wird. Diese werfen jedoch auch Fragen nach Stabilität auf. Eine systematische Stabilitätsbetrachtung, die das Zusammenspiel von Preistrategien, veränderbarer Nachfrage und Produktion unter Gewährleistung stabiler Preisprofile analysiert, wird untersucht. Darüberhinaus wird ein analytisches Modell einer transaktiven Regelungsarchitektur vorgestellt, das unter Berücksichtigung von erneuerbaren Energiequellen die Wechselwirkungen zwischen Markttransaktionen, Echtzeitpreisen, physikalischen Beschränkungen und Nachfragerückführung beinhaltet. Die transaktive Regelung beinhaltet drei Ebenen: (i) die primäre Regelung des Stroms auf Geräteebene, (ii) die sekundäre Regelung der Frequenz auf Gebietsebene und (iii) die tertiäre Regelung, die die Markttransaktionen zwischen produzierenden und konsu-

mierenden Unternehmen ökonomisch verteilt. Unter der Maßgabe die Frequenzregulierung unter optimaler Aufteilung der Ressourcen in Anwesenheit von Unsicherheiten in den erneuerbaren Energien und der Last sicherzustellen, wird eine hierarchische Regelungsmethodik vorgestellt. Globale asymptotische Stabilität für das Gesamtsystem in Anwesenheit von Unsicherheiten auf allen drei Zeitskalen wird sichergestellt und durch numerische Simulationen wird gezeigt, dass der hierarchische transaktive Regler in Anwesenheit von Produktions- und Lastunsicherheiten effektiv arbeitet.

Contents

Notations

Abbreviations

GenCo	Generating Company
ConCo	Consumer Company
ISO	Independent System Operator
LMP	Locational Marginal Price
LCP	Linear Complementarity Problem
MPEC	Mathematical Program with Equilibrium Constraints
EPEC	Equilibrium Programming with Equilibrium Constraints
AGC	Automatic Generation Control
ACE	Area Control Error
DAM	Day Ahead Market
RTM	Real Time Market
DR	Demand Response
RER	Renewable Energy Resources
DER	Distributed Energy Resources

Variables

P_{Gi}	Power that the generating unit i is producing
P_{Dj}	Power k that the demand j is consuming
P_{Gib}	Power block b that the generating unit i is producing
P_{Djk}	Power block k that the demand j is consuming
P^{w}_{Glb}	Power block b that the renewable generating unit l is producing
δ_n	Voltage angle of bus n
Ω_G	Rotor speed of generation unit
θ_G	Rotor angle of a generating unit
P_m	Mechanical power exerted on a machine by the turbine
P_C	Electrical power output for dispatchable generator
a	Valve position
Ω_C	Reference frequency set by the secondary controls
θ_W	Induction generator rotor angle
θ_T	Turbine rotor angle
ω_W	Rotor speed of the induction generator
ω_T	Rotor speed of the wind turbine
Δ_W	Wind torque

P_W Electrical power output

Dual variables

ρ_n Locational marginal price corresponding to the generating unit i or the demand j that is located at node n
γ_{nm} Dual variable associated with the transmission capacity constraint of line $n-m$
α_i Dual variable associated with the maximum capacity constraint of generating unit i
ϕ_{ib} Dual variable associated with the maximum capacity limit for block b of generating unit i
σ_j Dual variable associated with the minimum demand constraint of demand j
ψ_{jk} Dual variable associated with the maximum capacity limit for block k of demand j

Sets and numbers

N_D Number of demands
N_G Number of generating units
N_{Dj} Number of blocks demanded by demand j
N_{Gi} Number of blocks bid by generating unit i
N_{Gl} Number of blocks bid by renewable generating unit l
N Number of all buses
N_t Number of transmission lines
G_f Set of indices of generating units $\{1,2,\ldots,N_G\}$
G_w Set of indices of renewable generating units $\{1,2,\ldots,N_W\}$
D_q Set of indices of Consumers $\{1,2,\ldots,N_D\}$
Ω_n Set of indices of nodes connected to node n
θ_n Set of indices of generating units at node n
ϑ_n Set of indices of demands at node n

Constants

λ^B_{Djk} Price bid by demand j to buy power block k
$\lambda^B_{G_{ib}}$ Price bid by generating unit i to sell power block b
Δ_{Glb} Uncertainty in block b of wind generating unit l
P^{max}_{Gi} Maximum power output of generating unit i
P^{min}_{Gi} Minimum power output of generating unit i
P^{max}_{Gib} Maximum power output in block b of generating unit i
P^{min}_{Djk} Minimum power supplied to the demand j
P^{max}_{Djk} Maximum power demanded in block k of demand j
$P^{w}_{Glb_{max}}$ Maximum wind power estimation for block b of renewable generating unit l
$P^{w}_{Glb_{min}}$ Minimum wind power estimation for block b of renewable generating unit l
$\bar{P}^{w}_{Glb_{min}}$ Mean wind power for block b of renewable generating unit l

κ_{Dj}	Curtailment Factor by demand j
ΔP_{Dj}	Change of consumption by demand j
$\Delta\rho_{n(j)}$	Change of LMP for demand j
$\lambda^{U}_{D_{jk}}$	Marginal utility associated with block k of demand j
$\lambda^{C}_{G_{ib}}$	Marginal operating cost associated with block b of generator i
B_{nm}	susceptance of line $n-m$
B_{line}	Line admittance matrix with elements B_{nm}
τ_g	Diagonal matrix of generators time constant diag$\{\tau_{Gi}\}$
τ^{R}_{g}	Diagonal matrix of wind generators time constant diag$\{\tau^{R}_{Gi}\}$
τ_d	Diagonal matrix of demand time constant diag$\{\tau_{Dj}\}$
τ_δ	Diagonal matrix of voltage angle time constant diag$\{\tau_\delta\}$
τ_ρ	Diagonal matrix of Locational Marginal Price time constant diag$\{\tau_\rho\}$
τ_γ	Diagonal matrix of congestion price time constant diag$\{\tau_\gamma\}$
c_g	Diagonal matrix of generators cost coefficient diag$\{c_{Gi}\}$
c_d	Diagonal matrix of consumers utility coefficient diag$\{c_{Dj}\}$
b_g	Vector of generators cost coefficient whose elements are$\{b_{Gi}\}$
b_d	Vector of consumers cost coefficient whose elements are$\{b_{Dj}\}$
A	Bus incident matrix$\big(N_t \times N\big)$
A_r	Reduced bus incident matrix$\big(N_t \times N-1\big)$
A_g	Generators incident matrix where $A_{g_{ij}}=1$ if the i^{th} generator is connected to j^{th} bus and $A_{g_{ij}}=0$ if the i^{th} generator is not connected to j^{th} bus$(N \times \mathbb{N}_g)$
A_d	Consumers incident matrix where $A_{d_{ij}}=1$ if the i^{th} consumer is connected to j^{th} bus and $A_{d_{ij}}=0$ if the i^{th} consumer is not connected to j^{th} bus
P^{max}_{nm}	Transmission capacity limit of line $n-m$
P^{max}	Vector of maximum capacity limit whose elements are P^{max}_{nm}
R	Rotating matrix where $Rx1=[\delta_1 ... \delta_{N-1}]$
U_{Dj}	Utility of demand j
C_{Gi}	Cost of Generator Company i
M	Inertia constant
D	Damping coefficient
T_u	Time constant representing the delay between the control valves and the turbine nozzles
T_g	Time constant of the valve servo motor-turbine gate system
r	Permanent speed droop of the turbine
M_G	Generator inertias
M_T	Turbine inertias
D_m	Mutual damping coefficients
K_s	Spring constant of the tortional spring

List of Figures

List of Tables

"If you deliberately plan on being less than you are capable of being, then I warn you that you'll be unhappy for the rest of your life."
- Abraham Maslow

1 Introduction

Following deregulation in the 1980s, the wholesale electricity market was proposed in order to ensure an efficient and reliable scheduling of power generation. In this structure, organized competitive markets would set the price of wholesale electricity. Ownership of generation would often be separated from the rest of the system, and an independent entity would operate the transmission system and administer the wholesale markets [14]. Overall, markets would take on some of the coordinating and cost-minimizing functions traditionally performed within vertically integrated utilities to provide secure, reliable and affordable electricity for all consumers with a reasonable quality of service.

Competitive electricity market had great appeal to some governments which found themselves owning nationalized power systems including generating plants that could be sold to raise revenue and enable wholesale market competition. In 1982, Chile adopted a version of this new model, and in 1990, the Thatcher government in the United Kingdom followed suit as part of its privatization program [15–17]. In the U.S., as a result of slowing demand growth and significant capacity expansion in some regions, the competitive market became an important issue because it was presumed that prices for electricity would then be below regulated prices [14, 18, 19].

To promote competition, in 1996 the Federal Energy Regulatory Commission (FERC) issued Order No. 888, which required transmission owners to provide wholesale customers open, non-discriminatory access to their systems under a regulated Open Access Transmission Tariff [14, 19]. This order effectively granted equal access to both utility and non-utility generators. Since then, independent system operators (ISOs) and regional transmission organizations (RTOs) have been created in certain parts of the U.S. As a result of this reform in the U.S. power grid, ISOs and RTOs organized wholesale electricity markets in which independent decisions of market participants set the price of energy generation, and also respect the requirements of central commands provided by the ISO or RTO.

Furthermore, efforts by the European Union led to a major movement towards deregulation in Europe in the second half of the 1990s [20]. The Nord Pool market, for instance, was established in 1992. Sweden joined this market in 1996, Finland in June 1998, Western Denmark in July 1999, and Eastern Denmark in October 2000 [20]. Germany brought in deregulation in 1998 when its new energy law became effective. As a consequence, the first German power exchange in Leipzig started operations in June 2000 [21].

Beginning in the summer of 2000 and continuing through the summer of 2001, wholesale power prices in California increased significantly, forcing the federal government to subsidize power for low-income families in San Diego and bankrupting one of the state's three major utility companies [18]. At the same time, huge shortages in available generation capacity forced state-wide blackouts. The energy crisis in California may have cost the state as much as $45 billion from increased electricity costs, lost business due to blackouts, and a slowdown in economic growth [22, 23]. The official explanation for California's power crisis [23] was

that flaws in the restructuring agreement, combined with poor federal oversight, made it possible for companies to artificially drive up prices.

A more recent example happened in ERCOT, the Texas market, for two days in 2011. January 31 was a typical day, with prices ranging from a high near $80/MWh, and a low just below zero. Two days later on February 2, 2011, unusually cold weather in Texas resulted in real-time prices hitting the cap of 3,000 $/MWh, about 100 times the average [93]. In another example, in March 2011 in New Zealand, electricity prices exceeded $20,000/MWh in one region of the country, and remained near this extraordinary level for about six hours.

Economists and engineers agree that the unique physical attributes of electricity make the design of efficient power markets a challenge [18, 24]. One of the significant challenges is that power must be produced as it is needed because of the prohibitively high cost of storage. Since demand for power is difficult to predict, some power plants are kept on reserve and ready to begin production on short notice. However due to physical constraints, there is a lag time before additional power can be generated. Because of capacity constraints in power lines and other equipment, it can also be a challenge to deliver electricity where it is needed. These technical issues make power dispatch a significant challenge.

As a result, models that capture the various dynamics in the system, the physical and technical constraints, the uncertainty and volatility are needed, to shed new light on wholesale electricity market design and gain an understanding of how to create markets to enhance reliability and efficiency, with stable price profiles, in the presence of uncertain and intermittent resources and demand. Many of these challenges are discussed at length in the following chapters of this dissertation.

1.1 Motivation

Smart grids introduce revolutionary changes to the generation, operation, scheduling, and use of electricity. The emerging smart grid will be more dynamic, flexible, reliable, and robust. Dynamic modeling and identification, estimation and optimization, feedback and adaptation, and other control technologies and concepts will be key enablers for smart power grids. The smart power grids will have four significant characteristics:

1. *A tremendous number of sensing devices:* Sensors, actuators, and communication devices will be deployed at generators, along transmission lines, at substations, in transformers, in distributed energy resources such as photovoltaics, wind turbines, inverters, storage devices, electric vehicles, and smart appliances in distribution networks, and microgrids.

2. *A significant number of active agents:* Active agents in the operation of the new smart grid include industrial, commercial and residential customers together with microgrids, utilities, and power generating companies. Since these stakeholders are profit seeking, their objectives are not perfectly aligned.

3. *The penetration of Renewable Energy Resources (RERs):* The power output from renewable energy resources, such as wind and solar is intermittent and less predictable than

the output from fossil fuel generators. Information exchange is required for rapid adaptation to unpredicted fluctuations in power supply, voltage, and frequency.

4. *Advanced power electronics:* Substantial advances are being made in smart components such as DC/AC inverters, smart batteries, flexible AC transmission system (FACTS) devices, and storage devices. Such advanced power electronics will not only enable more effective use of existing power system assets, but, more importantly, they will provide the means to implement control and optimization algorithms.

These characteristics of smart power grids pose several challenges. Among these challenges, jointly optimizing control structure and information and communication technologies to manage hundreds of millions of active endpoints, designing economic mechanisms to align incentives and market forces to reach desired global outcomes are the most significant challenges. Furthermore, a systematic methodology is necessary in order to design the control architectures and algorithms, to balance supply and demand, and regulate frequency in the presence of volatile supply.

An interconnected system of billions of RERs introduces rapid, large, and random fluctuations in power supply and demand, voltage and frequency Introducing huge intermittency and uncertainty in a smart grid will demand a dynamic framework to address the operation, scheduling and financial settlements in the dynamic and uncertain environment. The temporal components are necessary due to increasing penetration of renewable sources in scheduling generation, and increasing potential of adjustable demand via Demand Response. The former brings issues of strong intermittency and uncertainty, and the latter brings a feedback structure, where demand can be modulated over a range of time-scales. Both of these components are dictating a new look at market mechanisms, with a controls viewpoint enabling a novel framework for analysis and synthesis.

Following this new look at market mechanisms, modeling of the wholesale electricity market dynamics in an accurate manner is becoming increasingly important as new time-scales and uncertainties enter the picture. These models must capture the behavior of the dominant market players such as Generators Company (GenCo), Consumers Company (ConCo), and Independent System Operator (ISO), real-time prices, diverse dynamic drivers (e.g., weather, load, fuel prices, and wind supply), and physical constraints (e.g., ramping, transmission congestion). These market models, as well as an analysis of the market equilibrium, directly help to identify various sources of price volatility, and can help to quantify sensitivity to uncertainties and intermittencies in Renewable Energy Resources (RER) and variations in real-time prices due to Demand Response (DR).

Furthermore, dynamic market mechanisms will become increasingly important as we move from a day-ahead to a real time market and the underlying forecast models of renewables and consumer and load control behavior become more accurate. The dynamic market mechanism is entwined with the notion of a *disequilibrium* process, which is indispensable in the current context of market mechanisms to attain market equilibrium in the presence of perturbations due to the uncertainty and intermittency of RERs . The real-time price can be viewed as a state of this dynamic framework, since it is determined through financial transactions of various market entities, and also as a feedback control variable, since it can affect consumption. Introduction of dynamics and feedback brings in questions of stability. A systematic stability framework to analyze the interplay between pricing strategies, adjustable

demand, and generation, while guaranteeing stable behavior, is highly warranted. Needless to say, this framework must include multiple time-scales, latencies leading to time-delays, nonlinearities, distributed systems, learning, and adaptation. It should also be noted that because of the flexibility in selecting price strategies and their underlying information infrastructure, the market design can be viewed as a control problem. The inter-relationships between demand, real-time pricing strategies, and financial transactions, grouped under the rubric of *Transactive Control*, necessitate a dynamic framework of study, in order to enable integration of renewables and DR-compatible devices, social efficiency, and stability.

1.2 Related Work

The seminal papers of Fred Schweppe and his co-workers can be considered as the first studies that systematically investigated and established the notion of spot pricing in the wholesale electricity market [25]. Ever since, there has been a tremendous amount of research devoted to different aspects of electricity market. For a detailed introduction and an overview, the interested reader is to referred to many books on the subject, e.g., [26–31]. In particular, for a detailed overview and some recent results concerning different modeling approaches of the wholesale electricity market, market equilibrium, and congestion management of transmission systems, we refer to [32, 33, 35–37].

Various methods have been proposed in the literature to determine market models [38–40]. Given the primary purpose of balancing supply and demand in the market, these methods are primarily focused on the analysis of market equilibrium. Methods in [38, 39] model the electricity market participants, subject to spot market equilibrium and their own constraints, leading to a method termed Equilibrium Programming with Equilibrium Constraints (EPECs). In such models, each agent solves a Mathematical Program with Equilibrium Constraints (MPEC) [40], and by using stationarity theory for MPECs, a standard linear mixed complementarity problem (LMCP) is shown to lead to equilibrium [41].

Another approach to market modeling is the use of a variational and linear complementarity problem (LCP) formulation (see [42–45]). A single-settlement framework based on a LCP is proposed in [46], which leads to a strategic game in which players have coupled constraints. Starting from the framework proposed in [46] and [47], the approach based on LCP is used in Chapter 3 to delineate the underlying market model. Representing the effect of forecast errors in renewable energy as an uncertain parameter, we evaluate its effect on the market equilibrium.

One of the most promising approaches to understanding and studying competition in deregulated electricity markets is game theory [36, 48–55]. Game theory has long been a discipline within the broader field of industrial organization, and is now finding applications in the study of strategic behavior in the wholesale electricity markets. In particular, the notion of Nash equilibrium, which specifies strategies such that competing firms maximize their profits in the absence of collusion, can be applied to understand the likely behavior of rational firms in the electricity markets.

According to Hobbs et al. [36], a crucial difference among various game-theoretical studies of wholesale electricity markets is the economic model used to characterize interactions between competing generating companies. These models usually range from Bertrand com-

petition (see [48]) to the more commonly used Cournot competition (see for example [18]). Bertrand competition usually results in electricity prices equal to short-run marginal costs of generating power, referred to as perfectly competitive equilibrium. Cournot competition, however, results in prices exceeding short-run marginal costs due to some (often significant) withholding of capacity from the market by generation owners. However, neither of these sets of models appears realistic enough to capture the details of electricity markets but these models are very useful for shedding light on the interaction of essential elements of the market. Indeed, in order to achieve a perfectly competitive outcome of the Bertrand competition, one would have to assume that in each hour, generators first use all their capacity to generate electricity, and then compete for revenues by setting a price which is low enough to ensure that all generated power is sold, but high enough to recover all generation costs incurred. No real electricity market operates this way, largely because electricity cannot be stored in large quantities and, therefore, generators would have to set prices for their output before, not after, committing for producing certain level of power. Given this sequence of actions, generators are not pressed to set prices as low as the marginal cost of production, and thus unlikely to achieve the Bertrand equilibrium in the market. On the one hand, under Cournot competition, generators would commit to production only after establishing price requirements; on the other hand, generators are assumed to have a perfectly flexible real-time control of the level of generation they can offer to the market. By using this control, generators can instantaneously change their commitments and influence market clearing prices. In doing so, generators can maximize their profits through the trade-off between reduced market shares and increased prices. However, in reality, generators neither have the full real-time control of their units, nor the ability to perfectly maximize their profits, due to the lack of precise information required to reach such an equilibrium on an hourly basis (see [43, 45, 53, 54]).

The results presented in Chapter 4 are mainly based on Cournot competition, inspired by the work of Alvarado and his co-workers [32, 33, 53, 56–58]. In [33], the authors investigated how an independent system operator (ISO) could use electricity prices for congestion management, without having a priori knowledge about the cost functions of the generators in the system. The authors illustrated how a sequence of market observations could be used to estimate the parameters in the cost function of each generator. Based on these estimates, and by solving a suitably defined optimization problem, an ISO could issue the nodal prices causing congestion mitigation. In [32, 53, 56] the results of [33] were extended by addressing a dynamical process for congestion management in the wholesale market. The usage of price as a dynamic feedback control signal for power balance control was investigated in [56]. There, the effects of interactions of price update dynamics and the dynamics of an underlying physical system (e.g., generators) on the stability of the overall system were investigated. However, no congestion constraints were considered and therefore only one, scalar valued, price signal was used to balance the power system.

In contrast to the papers above, our proposed model introduces a state-space structure in the static strategic form games while acknowledging the fact that the generators are limited in their ability to instantaneously change their commitment level. Our proposed market model includes information exchange pertaining to the state between the dominant players, such as real time price, congestion price, generation and consumption level in order to arrive

at the desired equilibrium, and is dynamic in nature. Furthermore, our proposed model is directly linked with the standard market clearing structure, so that the relation between the state-variables of the dynamic model and the primal variables of the power dispatch model is transparent. Several constraints that are inevitable in power systems such as those due to capacity limits on power generation and transmission as well as balance equations are explicitly included. Using this model, in Chapter 4 we show the conditions under which the dynamic model will result in asymptotic stability to the unique equilibrium.

A recent addition to the list of market players is generation due to RER. The integration of RER into market dispatch poses the challenge of intermittency and uncertainty, both of which can affect the economic planning and operation of the overall power system. The results of [59–64] deal with a perturbed market due to RER by employing a stochastic framework to capture both overestimation and underestimation of available wind power, and show the effect on the optimal expected profit of wind power producer, overall market efficiency, and overall operation cost. The model that we propose in Chapters 3 and 4 can be viewed as a deterministic version of the model developed in [63].

Furthermore, the need for increased penetration of RERs has spurred significant interest in the design of a Smart Grid. Another dominant feature of a smart grid is an information layer. This layer helps to gather information from a variety of sources, at multiple time-scales, and at distributed locations, and enables accurate decision and control by incorporating all available information about generation and load.

In the classical power system problem, all control actions are grouped under the rubric of Automatic Generation Control (AGC). AGC has been studied extensively in the power systems literature, with focus on topics such as parameter uncertainties, load characteristics, excitation control, self-tuning regulator, and adaptive AGC regulator design [65–73]. The focus of the control actions, by and large, has been on primary control where power is regulated at a unit level (with time-scales of the order of milliseconds), and on secondary control, where frequency is regulated at an area-level (with time-scales of the order of seconds) [65, 74]. Signals from economic dispatch are used to determine the participation factor that allows minimal resources to be utilized while satisfying all constraints [65].

Wind intermittency requires a new way of looking at economic dispatch that accurately captures the underlying dynamics and uncertainty. Due to the huge volatility and uncertainty of the dynamic drivers such as wind and solar energy sources, and Demand Response, the continued exchange of information is needed in order to mitigate costs imposed due to intermittency and uncertainty [8, 10]. Moreover, market mechanisms are the most successful way to incentivize and organize large distributed control policies. Therefore, control and economic mechanisms must be jointly designed. A hierarchical Transactive control architecture, which combines market transactions with the conventional AGC, is presented in Chapter 5. This architecture enables us to incorporate the interaction between real-time pricing, physical constraints, and Demand Response(DR) compatible loads in the presence of uncertainty of RERs.

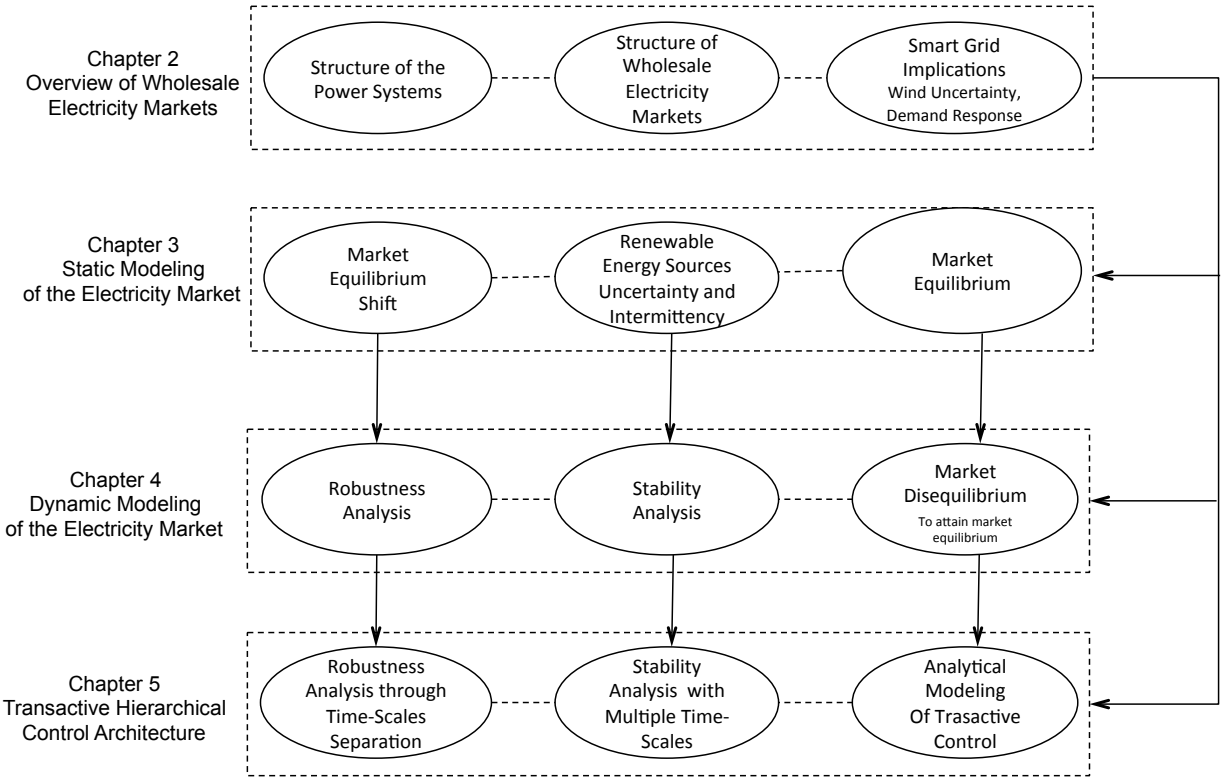

Figure 1.1: Outline of the thesis, "Wholesale Energy Market in a Smart Grid: Dynamic modeling, stability, and robustness" .

1.3 Thesis Outline

This thesis covers three major aspects of the Smart Grid: Static modeling of the wholesale electricity market, dynamic modeling of the wholesale electricity market and finally Transactive control. Figure 1.1 illustrates the outline of this thesis. Chapter 2 provides an overview of wholesale electricity markets, emphasizing the tight coupling between physical properties of power systems and economics of power systems. This chapter explains how an electricity market based on a pool operates, and finally introduces the concept of a Locational Marginal Price as a main mechanism which is currently implemented in many markets around the world.

In Chapter 3, we discuss the equilibrium of an electric energy market in the presence of RER and DR . The market framework proposed in this chapter consists of three main participants:

- *Generating companies (GenCos)*: GenCos are entities that own generating units. GenCos sell their electricity either through the electricity market, or through bilateral contracts to the consumer. GenCos are responsible for the operation and maintenance of their generating units.

- *Consumer companies (ConCos)*: ConCos are entities that purchase electricity to supply consumption, either through the electricity market, or through bilateral contracts directly from the GenCos.

- *Independent System Operator (ISO)*: Independent entity that clears the market by maximizing social welfare based on power systems security and reliability.

The overall market equilibrium is first evaluated in the absence of uncertainties, and sufficient conditions are established for the proposed market equilibrium to be identical to the Nash equilibrium. The effects of uncertainties, due to forecast errors in RER, and variations, due to DR on the market equilibrium are analyzed using perturbation analysis. A parametric characterization of the equilibrium shift is provided. In both the nominal and perturbed markets, the equilibria are derived using the LCP approach based on Karush-Kuhn-Tucker (KKT) conditions. We characterize the closeness of two strategic games corresponding to the nominal market and the perturbed market, using the notion of $\alpha-$approximation and $\epsilon-$equilibrium. An IEEE 30-bus system is used to evaluate the results of uncertainties in both renewable energy and in demand curtailment.

In Chapter 4 of this thesis, we develop a new market model with an interactive framework which introduces a state-space structure to the problem. Our market model uses an information exchange pertaining to the state between the dominant players, such as real time price, congestion price, generation and consumption level, to arrive at the desired equilibrium and is dynamic in nature. The dominant players in this model include GenCos, ConCos, and ISO. Our proposed dynamic model is directly linked with the standard market clearing structure so that the relation between the state variables of the dynamic model and the primal variables of the power dispatch model is transparent. Several constraints that are inevitable in a power systems, such as those due to power balance as a result of kirchoff's law, capacity limits on power generation and transmission are explicitly included. Using this model, it is shown in this chapter that the dynamic model will result in asymptotic stability for all initial conditions in the region of attraction. Finally, the effects of two main features of a smart power grid, uncertainties in renewable energy sources and changes in the demand due to changes in real-time pricing are analyzed using this model. In both the unperturbed dynamic model and the perturbed model, conditions of stability and asymptotic stability are explicitly derived. Numerical studies of an IEEE 30-bus are reported to illustrate the dynamic model, its stability properties, and the effect of perturbations.

The wind power fluctuation, together with total average power variation, contributes to the power imbalance and frequency deviation should be taken into account in the AGC control scheme. An overall framework that shows the interconnection between the dynamic market mechanism, mainly based on a dynamic economic dispatch and AGC is needed. In Chapter 5, the analytical framework is presented by including models at a unit-level of dispatchable, non-dispatchable and cyber physical load, tie-line flows between areas, and Area Control Error (ACE), which includes a weighted combination the system frequency and tie-line power deviations. Starting with models of pertinent dynamics at the primary, secondary, and tertiary levels, we introduce uncertainties in generation and load. We include controllers at the secondary level that utilize ACE, and controllers at the tertiary level that include a dynamic information exchange between the generating and consumer companies, as well as a real-time price transaction. This overall *hierarchical Transactive controller* is then shown to be stable in the presence of generation and load uncertainties, and tie-line error. Numerical studies of a 4-bus power system are reported to illustrate the effectiveness of the proposed Transactive controller in the presence of wind uncertainty.

1.4 Contributions

The groundwork for the proposed analysis was laid in my recent papers [6–13].

Equilibrium of Electricity Market Under Perturbation of Renewable Energy Sources

The integration of RER into market dispatch poses the challenge of intermittency and uncertainty, both of which can affect the market equilibrium and operation of the overall power system. The main contributions of Chapter 3 are the introduction of an analytical framework to evaluate the electricity market equilibrium, and the provision of a computable upper bound for market equilibrium shift with wind uncertainty and Demand Response. The analytical framework introduced in this chapter consists of an overall model of the energy market including Generation Companies (GenCos), Consumers Companies (ConCos) as well as Independent System Operator (ISO), which allows the analysis of the market under normal conditions and perturbed conditions.

Furthermore, game theory interpretation of market equilibrium is presented and sufficient conditions for the existence of a unique Pure Nash Equilibrium for the nominal market is established. The perturbed market in the presence of wind uncertainty is analyzed using the concept of closeness of two strategic games and the equilibria of close games based on the notion of α-approximation and ϵ-equilibrium. The material presented in this chapter has been published in [13], and the journal version of this chapter has been edited and submitted for publication in *IEEE Transaction on Smart Grid* [6].

Disequilibrium of Electricity Market, Stability and Robustness

Wind intermittency requires a new way of looking at market mechanism that accurately captures the underlying dynamics and uncertainty. Due to the huge volatility and uncertainty of the dynamic drivers such as wind and solar energy sources, and Demand Response, continued exchange of information is needed in order to mitigate costs imposed due to intermittency and uncertainty. In Chapter 4, a dynamical framework to incorporate these challenges is developed. The main contribution of this chapter is the notion of disequilibrium process [7–10].

Disequilibrium process, often used in econometrics, can prove to be indispensable in the current context of market mechanisms to attain market equilibrium in the presence of perturbations due to renewables and Demand Response. Associated with this notion is the design of dynamic mechanisms, whose role becomes more crucial as one moves from a day-ahead to a real time market and the underlying forecast models of renewables become more accurate. Introduction of dynamics and feedback, both of which take a more prominent position in all of the approaches suggested above, also brings in questions of stability. A systematic stability framework which analyzes the interplay between pricing strategies, adjustable demand, and generation, while guaranteeing stable behavior is studied in Chapter 4. In this chapter, a dynamic model of the wholesale energy market that captures the effect of uncertainties of RER and real-time pricing with DR is derived. Beginning with a framework that includes real-time pricing as an underlying state, an attempt is made in this model to capture the dynamic interactions between generation, demand, locational marginal price,

and congestion price near the equilibrium of the optimal dispatch. Conditions under which the stability of the market can be guaranteed are derived. Modeling the effect of RER and DR as perturbations, robust stability of the energy market model in the presence of such perturbations are discussed.

This chapter is mainly based on the following published papers. In [8, 10, 11], an empirical dynamic model of the wholesale energy market is proposed where the major market components interact with each other in a distributed manner.

Stability of the Electricity Market in the Presence of Real Time Pricing Latency

The effect of latencies in a smart meter on this dynamic model is evaluated together with real-time pricing, in the presence of congestion constraints due to transmission capacity in [8, 11]. In particular, feedback of real-time pricing is shown to beneficial in alleviating the burden of peak demands but at the same time, if this information is delayed, the overall stability of the dynamic power market can be adversely affected. In [8,10,11], instead of an empirical approach, an optimal power flow-based approach is used to derive the underlying model. This in turn allows the effect of congestion constraints on stability to become more transparent. Chapter 4 is based on these papers and the main contribution of this chapter is the introduction of a dynamical framework for market clearing process based on the notion of disequilibrium process.

Transactive Hierarchical Control, Analytical Modeling, Stability, and Robustness

The introduction of both RER, as well as efforts to integrate them through an information processing layer, brings in dynamic interactions between the major components of a smart grid. In [9, 12], a hierarchical control framework is proposed for the decision and control of the entire grid, with Automatic Generation Control-based approaches used for the lower levels of primary and secondary control, and a dynamic market mechanism developed in Chapter 4 as market-based tertiary control for the higher, supervisory level. Chapter 5 introduces such a Transactive market that makes effective use of the emerging concept of DR, where loads are adjustable in response to economic signals. Noting that flexibility is present in determining price strategies and what information is fed-back and when, the market design can be viewed as a control problem embedded in game theory, where parts of the overall dynamic system can be selected for a given structure of generation, demand and topology, akin to the concept of Transactive Control addressed and formulated in [9, 12], where control actions are tightly integrated with price signals and utilized primarily for end-use optimization.

2 Overview of Wholesale Electricity Markets

Summary. *This chapter provides an overview of electricity market and overall power systems operation and control. The main topics in this chapter are*

- *A description of the electric power systems,*
- *Operation and control of power systems in the current stage,*
- *An introduction to the wholesale electricity market,*
- *Challenges of smart grid implications in the wholesale market.*

2.1 Structure of the Electric Power System

The electric power system consists of generating units where primary energy is converted into electric power, transmission and distribution networks which transport this power, and consumers who use the power. While originally generation, transport, and consumption of electric power were limited to relatively small geographic regions, today these regional systems are connected together by high-voltage transmission lines to form highly interconnected and complex systems spanning wide areas. This interconnection allows economies of scale, utilization of the most economical generators, increased reliability, and an improved ratio of average load to peak load due to load diversity, thus increasing capacity utilization. Interconnection also leads to complexity, however, as any disturbance in one part of the system can adversely impact the entire system. Figure 2.1 illustrates the basic structure of the electric power system. We discuss each of its subsystems in the following sections.

2.1.1 Generation Units

Electric power is produced by generation units, housed in power plants, which convert primary energy into electric energy. Primary energy comes from a number of sources, such as fossil fuel, nuclear, hydro, wind, and solar power. The process used to convert this energy into electric energy depends on the design of the generating unit, which is partly dictated by the source of primary energy. The term "thermal generation" commonly refers to generating units that burn fuel to convert chemical energy into thermal energy, which is then used to produce high-pressure steam. This steam flows and drives the mechanical shaft of an AC electric generator which produces alternating voltage and current at its terminals.

Nuclear generating units use an energy conversion process similar to thermal units, except the thermal energy needed to produce steam comes from nuclear reactions. Hydro power and wind generating units convert kinetic energy of water and wind respectively,

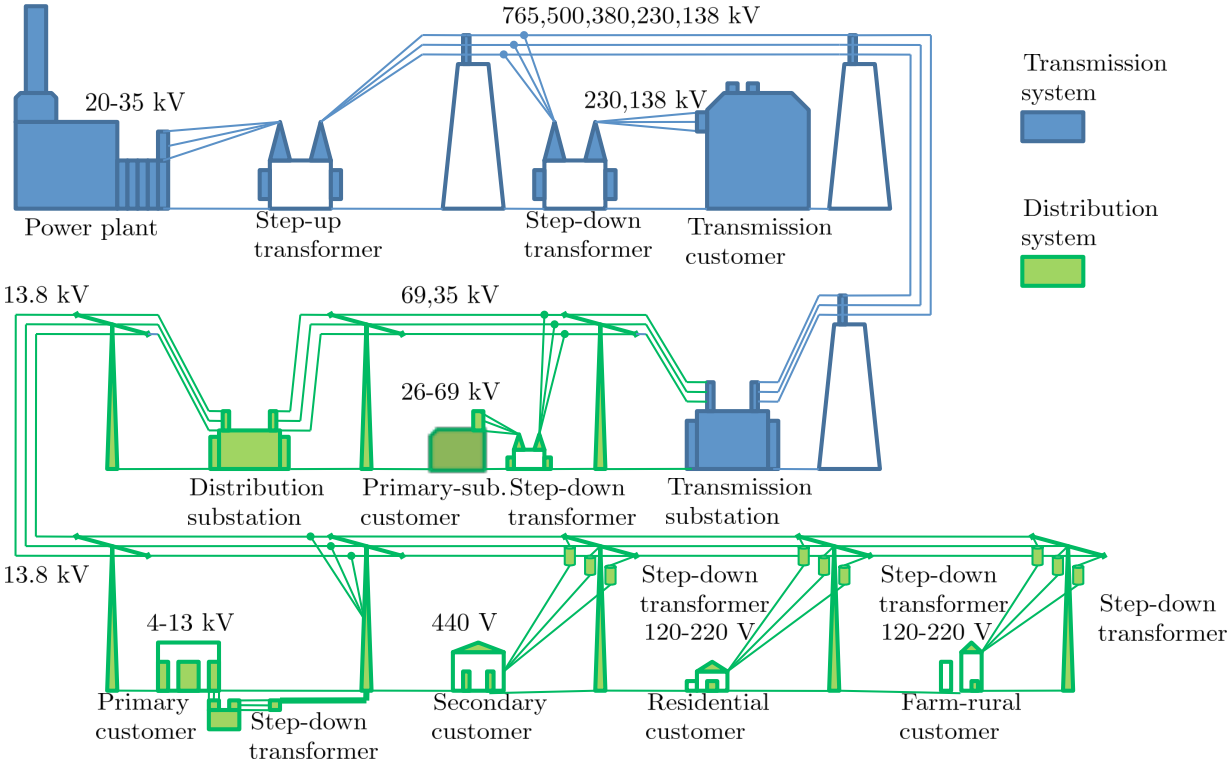

Figure 2.1: Structure of the Electric Power System

directly into rotation of the shaft of the electric generator. Solar-thermal and geothermal generating units use the sun's radiation and the Earth's warmth respectively, to heat a fluid and then follow a conversion process similar to thermal units. Solar photovoltaic generating units are quite different and convert the energy in solar radiation directly into electrical energy. Another common type of generating unit is gas, or combustion, turbine. This burns a pressurized mixture of natural gas and air in a jet engine that drives the electric generator. Combined-cycle gas turbine plants have a gas turbine and a steam turbine. They reuse the waste heat from the gas turbine to generate steam for the steam turbine, and hence achieve higher energy conversion efficiencies.

From the operational perspective of the electric power system, generating units are classified into three categories: baseload, intermediate, and peaking units.

- Baseload units are used to meet the constant, or base, power needs of the system. They run continuously throughout the year, except when they have to be shut down for repair and maintenance. They must therefore be reliable and economical to operate. Because of their low fuel costs, nuclear and coal plants are generally used as baseload units, as are hydroelectric plants. However, nuclear and coal baseload units are expensive to build and have slow ramp rates, i.e. their output power can only be changed slowly (on the order of hours).

- Intermediate units, also called cycling units, operate for extended periods of time, but unlike baseload units, not at a fixed power level continuously. They have the ability to

vary their output more quickly than baseload units. Combined-cycle gas turbine plants and older thermal generating units are generally used as intermediate units.

- Peaking units operate only when the system power demand is close to its peak. They have to be able to start and stop quickly, but they only run for a small number of hours in a year. Gas turbine and hydroelectric plants with reservoirs are generally used as peaking units. Gas turbines are the least expensive of all generation units to build, but have high operating costs.

In addition to the main large generating units, the system typically also has some distributed generation, including combined heat and power units. These and other small generating units, such as small hydroelectric plants, generally operate at lower voltages, and are connected at the distribution system level.

Large generating units generally are located outside densely populated areas, and the power they produce has to be transported to load centers through transmission lines.

2.1.2 Power Transmission

The transmission system carries electric power over long distances from the generating units to the distribution system. The transmission network is composed of power lines and stations/substations. Stations and substations house transformers, switchgear, measurement instrumentation, and communication equipment. Transformers are used to change the level of the transmission voltage, while switchgear includes circuit breakers and other types of switches used to disconnect parts of the transmission network for system protection or maintenance. Measurement instrumentation collects voltage, current, and power data for monitoring, control, and metering purposes. Communication equipment transmits the data to control centers, and also allows switchgear to be controlled remotely.

Topologically, the transmission and subtransmission line configurations are *mesh networks*, as opposed to radial, meaning there are multiple paths between any two points on the network [65,75]. This redundancy in multiple paths allows the system to provide power to the loads even when a transmission line or a generating unit goes offline.

The power flow through a particular transmission line depends on the line's impedance and the amplitude and phase of the voltages at its ends. Predicting these flows requires substantial computing power and precise knowledge of the network voltages and impedances, which are rarely known with high precision.

The power transmission network is modeled as follows. The network consists of n buses, indexed $i = 1,\ldots,n$. To each node are attached generators which supply power and loads that consume power. The voltage at bus i is a sinusoidal waveform, whose instantaneous value at time t is

$$v_i(t) = V_i \sin(\omega t + \delta_i) \tag{2.1}$$

where V_i is the magnitude of the sinusoidal waveform, $\omega = 2\pi \times 60$ is the waveform's frequency in radians per second (for 60 Hz), and δ_i is the voltage phase angle. A line connecting bus i to bus j is characterized by its *electrical admittance*, denoted Y_{ij} where $Y_{ij} = Y_{ji} > 0$. The real power flow over the line from bus i to j is equal to

$$P_{ij} = V_i V_j Y_{ij} \sin(\delta_i - \delta_j) \tag{2.2}$$

measured in kW or MW. Using Eq. (2.2), the net power, P_i, injected into the network at bus i is the algebraic sum of the P_{ij} as

$$P_i = \sum_{j=1}^{n} P_{ij} = \sum_{j=1}^{n} V_i V_j Y_{ij} \sin(\delta_i - \delta_j), \quad i = 1, \ldots, n. \tag{2.3}$$

For the sake of simplicity in this thesis, we assume that the voltage magnitude at bus i, V_i, is constant. With no loss of generality, we can then set $V_i = 1$ for all i. Then the net power, P_{ij} in (2.3), can be simplified as

$$P_i = \sum_{j=1}^{n} Y_{ij} \sin(\delta_i - \delta_j), \quad i = 1, \ldots, n. \tag{2.4}$$

Eq. (2.4) defines the *real power flow equations*. It should be noted that, since $P_1 + \ldots + P_n = 0$, only $n-1$ of these equations are independent, implying that the phase angle differences are dependent. Thus, we set $\delta_n = 0$ and eliminate the nth equation. Bus n is called the reference bus, or swing bus. Given the power injections $P_1, \ldots, P_{n-1}$, we can solve (2.4) for the $n-1$ unknown phase angles $\delta_1, \ldots, \delta_{n-1}$. Then, we can obtain the individual line flows from

$$P_{ij} = Y_{ij} \sin(\delta_i - \delta_j). \tag{2.5}$$

The power that can flow on a transmission line is limited by either thermal, voltage stability, or transient stability constraints. The thermal constraint arises from the resistance of the transmission line, causing excessive power losses and through heating when the power exceeds a certain level. The voltage stability constraint is due to the reactance of the transmission line causing the voltage at the far end of the line to drop below an allowable level (typically 95% of the nominal design voltage level [65]) when the power exceeds a certain level. The transient stability constraint relates to the ability of the transmission line to deal with rapid changes in power without causing the generators to fall out of synchronism with each other.

Generally, maximum power flow on short transmission lines is limited by thermal constraints, while power flow on longer transmission lines is limited by either voltage or transient stability constraints. From Eq. (2.5) we can see that the maximum value of $|P_{ij}|$ is Y_{ij}, since the sine function is bounded by unity. Power flow beyond the limit, C_{ij}, can cause physical damage to the transmission line, with subsequent high probability of power failure [76]. Usually $C_{ij} \leq Y_{ij}$, and so we have the *thermal constraints* on each line

$$P_{ij} = Y_{ij} \sin(\delta_i - \delta_j) \leq C_{ij}. \tag{2.6}$$

The power flow constraints in (2.6) are denoted as *congestion on transmission lines*, and mean the excess capacity in the lowest-cost generating units often cannot be supplied to loads due to the limited capacity of one or more transmission lines.

Some very large consumers take electric power directly from the transmission or subtransmission network. However, the majority of consumers get their power from the distribution network, as is described next.

2.1.3 Power Distribution

Distribution networks carry power for the last few kilometers from transmission or subtransmission to consumers. The power is carried in distribution networks through wires, either on poles or, in many urban areas, underground. Distribution networks are distinguished from transmission networks by their voltage level and topology. Lower voltages are used in distribution networks, typically up to 35 kV are considered part of the distribution network. The connection between distribution networks and transmission or subtransmission occurs at distribution substations, see Figure 2.1. Distribution substations have transformers to step the voltage down to the primary distribution level. Like transmission substations, distribution substations also have circuit breakers and monitoring equipment. However, distribution substations are generally less automated than transmission substations.

Distribution networks usually have a radial topology, referred to as a "star network," with only one power flow path between the distribution substation and a particular load. Distribution networks sometimes have a ring (or loop) topology, with two power flow paths between the distribution substation and the load. However, these are still operated as star networks by keeping a circuit breaker open. The presence of multiple power flow paths in ring and mesh distribution networks allows a load to be serviced through an alternate path by opening and closing appropriate circuit breakers when there is a problem in the original path. When this process is carried out automatically, it is often referred to as *self-healing*. Distribution networks are usually designed assuming power flow is in one direction. However, the addition of large amounts of distributed generation may make this assumption questionable and require changes in design practices.

2.1.4 Power Consumption

Electricity is consumed by a wide variety of loads, including lights, heaters, electronic equipment, household appliances, and motors driving fans, pumps, and compressors. These loads can be classified based on their impedance, which can be resistive, reactive, or a combination of the two. In theory, loads can be purely reactive, and their reactance can be either inductive or capacitive. However, in practice the impedance of most loads is either purely resistive or a combination of resistive and inductive reactance. Heaters and incandescent lamps have purely resistive impedance, while motors have impedance that is resistive and inductive. Purely resistive loads only consume real power. Loads with inductive impedance also draw reactive power. Loads with capacitive impedance supply reactive power. From the power system's operational perspective, the aggregate power demand of the loads in a region is more important than the power consumption of individual loads.

2.2 Operation and Scheduling of Power System

The electric power system is operated through a combination of automated control and a wholesale electricity market conducted by the system operator. The main challenge in operating the electric power system is that there is negligible *electrical storage* in the system. Hence, supply and consumption of electrical power must be balanced at all times. Since

the load changes all the time in ways that cannot be perfectly predicted, generation must follow the load in real time. The balance between supply and demand is maintained using a hierarchical control scheme at multiple timescales.

The objective of real-time operation of the electric power system is to ensure that the system remains stable and protected, while meeting end-user power requirements. This means a precise balance between power generation and consumption is required at all times. If this balance is not maintained the system can become unstable and its voltage and frequency can exceed allowable bounds, resulting in damaged equipment as well as blackouts. If the balance is not restored sufficiently quickly, a local blackout can grow into a cascading blackout similar to those in the U.S. in 1965 and 2003 [77]. Fortunately, the stored kinetic energy associated with the inertia of generators and motors connected to the system helps overcome small imbalances in power, giving enough time for an active control system to take corrective action. This balance between supply and demand at the shortest timescale is maintained actively via *governor control.*

2.2.1 Governor Control: Primary Control

The generators on governor control take the first corrective action as the balance between demand and supply changes. The governor is a device which controls the mechanical power driving the generator, via a valve limiting the amount of steam, water, or gas flowing to the turbine. The governor acts in response to locally measured changes in the generator's output frequency with respect to the established system standard, which is 60 Hz in the U.S and 50 Hz in Europe.

If the electrical load on the generator is greater than the mechanical power driving it, the generator maintains power balance by converting some of its kinetic energy into extra output power, but slows down in the process. On the other hand, if the electrical load is less than the mechanical power driving the generator, the generator absorbs the extra energy as kinetic energy and speeds up. This behavior is known as *inertial response.* The frequency of the ac voltage produced by the generator is proportional to its rotational speed. Therefore, changes in generator rotational speed are tracked by the generator's output frequency. A decreasing frequency is an indication of real power consumption which is greater than generation, while an increasing frequency indicates generation exceeding power consumption. Any changes in frequency are sensed within a fraction of a second, and the governor responds within seconds by altering the position of the valve, increasing or reducing the flow to the turbine.

If the frequency is decreasing, the valve will be opened further to increase the flow and provide more mechanical power to the turbine, hence increasing the generator's output power, bringing demand and supply in balance and stabilizing the speed of the generator at this reduced level. The speed of the generator will stay constant at this level as long as the mechanical power driving it balances its electrical load. While very fast, for stability reasons, governor control is not designed to bring the frequency of the generator back to exactly 60 Hz. Correcting this error in frequency is the job of the slower *automatic generation control (AGC)*, which will be discussed in the next section.

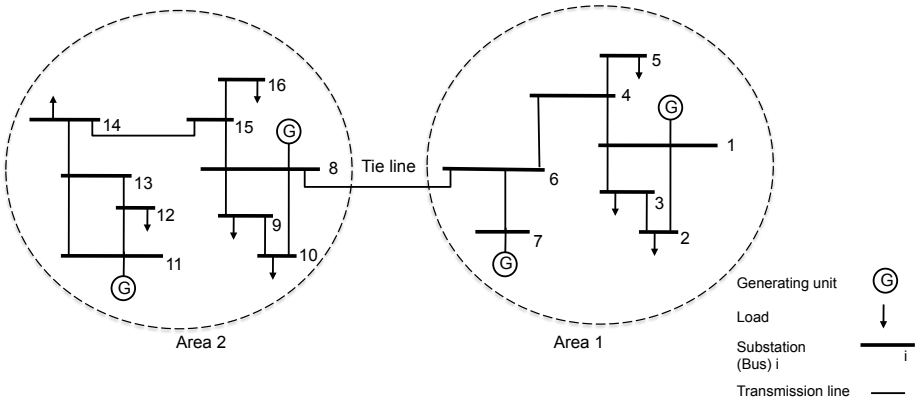

Figure 2.2: Representation of Control Areas

2.2.2 Automatic Generation Control: Secondary Control

While governor control keeps the supply and demand of real power in balance, it results in a small change in system frequency. Furthermore, the governor-based reaction of generators located outside a control area[1] to load changes inside the control area (or vice versa) can alter power flows between control areas from their scheduled levels. As can be seen in Figure 2.2, control areas are connected through *tie lines*.

The errors in frequency and power flows between control areas are corrected by the relatively slower AGC. AGC aims to eliminate the area control error (ACE). Over the control area of interest, the ACE signal is constructed as a weighted sum of an area representative frequency error, and deviations from scheduled values for power flows on a set of monitored transmission tie lines, more details are presented in Appendix A.2. The area control center automatically sends signals to generators equipped with AGC to increase or decrease their output based on the ACE signal.

Beyond a certain level of power imbalance, system operators need to call in generation reserves. These may be additional generating units on standby, or generators already producing power and able to ramp up their output on request. Having adequate reserves in the system is essential for dealing with load uncertainties and contingencies, such as the failure of a generating unit.

Reserves are categorized based on the time taken to start delivering the requested power. Reserves can be either spinning or non-spinning.

- Spinning reserves are generating units with turbines spinning in synchronicity with the grid's frequency without supplying power. They can deliver the requested power within a few minutes.

- Non-spinning reserves are units that are offline but can also be quickly synchronized with the grid.

[1] A control area consists of a collection of generation, transmission, and loads within metered boundaries for which a responsible entity integrates resource plans for that area ahead of time, maintains the area's load-resource balance, and supports the area's interconnection frequency in real time.

In systems with organized markets, reserves are paid not only for the energy, they produce but also for being available on short notice to deliver reserve power.

2.2.3 Economic Dispatch: Tertiary Control

A third level of control is required to ensure that all generators in the area are allocated so that each power source is loaded most economically. The optimal operating point of each generator is usually determined through the *Economic Dispatch (ED)* program running at the control centre. Since system load continually changes over time, ED calculations have to be made at frequent intervals. Through tertiary control, the speed changer settings of generators are adjusted to ensure an economic dispatch order among them. Details of tertiary control will be discussed in Chapter 5.

2.3 Wholesale Electricity Market

Scheduling of generation through the wholesale electricity in the transmission level determines which generation units should operate and at what power level. The objective is to minimize cost, subject to generation and transmission constraints. Scheduling and market mechanisms depend on the market model that will be discussed in Section 2.3.1. However two important tools are widely implemented in the wholesale market. These consist of economic dispatch, which will be introduced in Section 2.3.2, and unit commitment, which will be presented in Section 2.3.3. Section 2.3.4 will provide the basics of the market clearing mechanism and electricity pricing termed as Locational Marginal Price (LMP).

2.3.1 Wholesale Market Model

Pool markets and bilateral markets are two major types of markets in the world. Pool markets require a central coordinator, usually referred to as the Independent System Operator (ISO), who is responsible for both the market and system operation. On the other hand, bilateral markets can be decentralized, requiring far less intervention from the ISO.

Bilateral Markets

Bilateral markets are conceptually simple and treat electricity as a commodity. Market participants are free to enter into whatever trading mechanism they choose. Unlike pool markets, bilateral markets do not require a central market operator. This decentralization means that generator commitment and dispatch decisions are the responsibility of the individual market participants. This is known as self-commitment and may be advantageous in markets where the level of centralized control is to be minimized. There is, however, still a requirement for a central ISO responsible for the operation of the transmission system, i.e. solving transmission congestion and procuring ancillary services. This type of ISO is generally referred to as a Minimal ISO due to the low level of intervention in the market [78].

Due to the stochastic nature of electricity demand, imbalances will occur between bilaterally contracted quantities and actual consumption and generation of electricity. If these

imbalances were allowed to persist, the system frequency would change. The ISO, which is responsible for frequency control, will therefore correct these imbalances in real time. This can be achieved using the *ancillary services markets*, a secondary bilateral market, or most commonly, a *balancing pool*. This balancing pool is similar to the pool market except that only imbalances are traded through it, and will be described in the next section.

Since bilateral contracts can be structured over any time-frame, bilateral markets generally result in *stable prices* for electricity [79]. This is beneficial to both consumers, who are isolated from the risk of unexpected price spikes, and generators, who are assured a steady revenue stream, making investment projects bankable. Examples of bilateral markets include ERCOT (Texas), NETA (Great Britain), and Ontario (pre 1998).

Pool-Based Electricity Market

Generators sell their output into the pool and consumers buy their electricity from it. The pool market structure requires an ISO, who is responsible for matching offers and bids for energy, a process known as market clearing, and then dispatching the generation to meet the demand. This type of market structure follows very neatly from a vertically integrated environment [79]. As in a bilateral market, the ISO is also responsible for procuring ancillary services and ensuring the secure operation of the transmission system. However, in contrast with a bilateral market, the ISO is also responsible for the economic operation of the market through scheduling and dispatching generation and is therefore termed a Maximal ISO [78].

In a pool-based electricity market, the generating companies (GenCos) submit bids to the pool consisting of *energy blocks* and their corresponding minimum selling prices for every hour of the market horizon and every unit. The consumer companies (ConCos) submit energy blocks and their corresponding maximum buying prices for every hour of the market horizon, and every demand. The ISO collects purchase and sale bids and clears the market seeking maximum social welfare and using an appropriate market-clearing procedure. This results in hourly prices, and production and consumption schedules. Figure 2.3 shows a representation of a pool-based electricity market.

A pool market has a number of advantages over a bilateral market. Firstly, if the market is competitive, pool markets, through the market clearing price, will provide the true incremental cost of electricity. Secondly, pool markets provide ease of system operation since the market and system operation functions are within one entity, namely the ISO. Another advantage of the pool market is that it provides a price signal. In the short-term, high prices provide an incentive for generators to increase production and for loads to reduce consumption. Over longer time-frames, the high prices are a signal that investment in additional generation capacity is required.

However, the pool market also has a significant disadvantage. It can exhibit considerable volatility, see Figure 2.4 [2]. When high loads coincide with low generator capacity, consumers are exposed to large price spikes [93]. This phenomenon has been observed on countless occasions in pool markets all over the world. Similarly, when there is excess generation capacity available, prices can fall and generators can have insufficient revenue to recover their fixed costs. While the same capacity considerations will also result in high or low prices in bilateral markets, participants are generally not exposed to such short-term volatility.

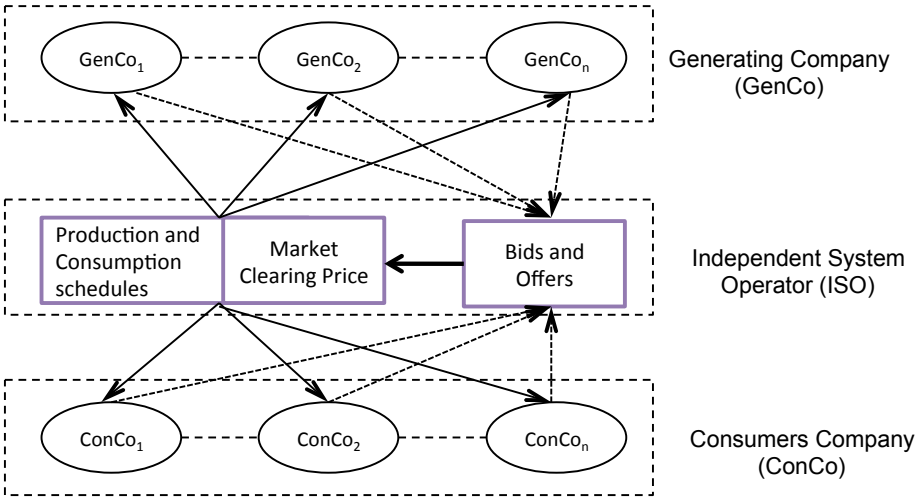

Figure 2.3: Representation of a Pool-based Electricity Market

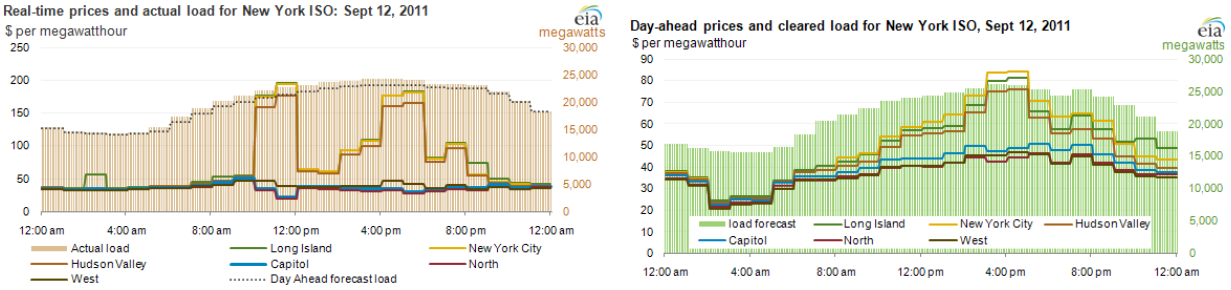

Figure 2.4: Day-ahead Market Price and Price Volatility in RTM [2]

Generator dispatches and the corresponding prices are generally calculated for a fixed length of time (e.g. one hour, thirty minutes, five minutes), known as the dispatch interval. The pool price can be calculated before the dispatch interval, known as *ex ante* pricing, or after the dispatch interval, known as *ex post* pricing. Ex ante pricing has the advantage of providing market participants with a price signal to which they can respond. However, since it is calculated in advance, it is based on forecast quantities so may not be a true reflection of the actual costs. Ex post pricing on the other hand is based on what actually occurred so is more accurate. Its disadvantage is that, since market participants get no price signal, they are not in a position to respond.

One of the first implementations of the pool market structure was in England and Wales, where a power pool was introduced in 1990. Other pool markets include Australia, New Zealand, Greece, and New England.

Hybrid Electricity Market

Finally, some markets are a hybrid of bilateral and pool-based market types. Generators may here enter into physical bilateral contracts with loads, or they may elect to submit bids to the system operator. The ISO will then determine the dispatch for all the generators in the pool

and calculate the prices, while taking into consideration the effect of the bilateral contracts on the transmission system.

Examples of such hybrid markets include NordPool (Scandinavia), Ontario and the PJM (Pennsylvania, New Jersey, Maryland) Interconnection.

2.3.2 Economic Dispatch

The incremental production costs of generating units can be quite different from one another, mostly due to differences in the costs of their fuel (for example, uranium, coal, natural gas), and their efficiencies. Economic dispatch minimizes overall production costs by optimally allocating projected demand to generating units that are online. Computers at control centers run optimization algorithms, typically every 5 or 10 minutes, to determine the dispatch for the next hour, and send these economic dispatch signals to all the generators. Sometimes, power cannot be dispatched from the lowest-cost generating unit due to the physical limits of the system, or security constraints associated with maintaining secure operation under contingencies. Physical restrictions include transmission lines' thermal and stability constraints, and limitations on generating units' output power and ramp rates. The cost and benefit of the net injection, P_i, is denoted by the increasing convex function $C_i(P_i)$. This means that if i is a generator and $P_i > 0$ then $C_i(P_i)$ is the variable cost of generation and the marginal cost is increasing. The Economic Dispatch problem with Alternative Current (AC) transmission constrains can be represented as

$$\text{minimize}_{P_i,\delta_i} \sum_{i=1}^{n} C_i(P_i) \tag{2.7a}$$

subject to

$$P_i = \sum_{j=1}^{n} Y_{ij} \sin(\delta_i - \delta_j), \quad i = 1, \ldots, n \tag{2.7b}$$

$$P_{ij} = Y_{ij} \sin(\delta_i - \delta_j) \leq C_{ij}. \tag{2.7c}$$

The AC Economic Dispatch is difficult to solve because it is a nonlinear non-convex program [80]. We now make one more simplification assumption.

Assumption 2.1. The phase angle differences, $|\delta_i - \delta_j|$, are small.

Assumption 2.1 follows when the line admittances are large relative to $\sin(\delta_i - \delta_j)$ [76]. Then we can make the approximation $\sin(\delta_i - \delta_j) \approx (\delta_i - \delta_j)$ and end up with a convex programming problem with linear constraints called as DC Economic Dispatch:

$$\text{minimize}_{P_i,\delta_i} \sum_{i=1}^{n} C_i(P_i) \tag{2.8a}$$

subject to

$$P_i = \sum_{j=1}^{n} Y_{ij}(\delta_i - \delta_j), \quad i = 1, \ldots, n \tag{2.8b}$$

$$P_{ij} = Y_{ij}(\delta_i - \delta_j) \leq C_{ij}. \tag{2.8c}$$

Associate Lagrange multipliers ρ_i with the n constraints in (2.8b), and $\gamma_{ij} \geq 0$ with the constraints in (2.8c), the Lagrangian can be written as

$$L = \sum_{i=1}^{n} C_i(P_i) + \sum_{i=1}^{n} \rho_i \left[\sum_{j=1}^{n} Y_{ij}(\delta_i - \delta_j) - P_i \right] + \sum_{i=1}^{n} \sum_{j=1}^{n} \gamma_{ij} \left[Y_{ij}(\delta_i - \delta_j) - C_{ij} \right]. \quad (2.9)$$

The optimal solution of DC Economic Dispatch, denoted as (P^*, δ^*), is characterized by the existence of Lagrange multipliers such that

$$\frac{\partial C_i(P_i^*)}{\partial P_i^*} = \rho_i^*, \quad i = 1, \ldots, n \quad (2.10a)$$

$$\sum_{j=1}^{n} Y_{ij}(\rho_i^* - \rho_j^* + \gamma_{ij}^* - \gamma_{ji}^*) = 0, \quad i = 1, \ldots, n \quad (2.10b)$$

$$\gamma_{ij}^* \left[Y_{ij}(\delta_i^* - \delta_j^*) - C_{ij} \right] = 0, \quad i, j = 1, \ldots, n. \quad (2.10c)$$

Equations (2.10a)-(2.10c) follow from the Karush-Kuhn-Tucker (KKT) criteria (See Appendix A.1.5.)

2.3.3 Unit Commitment

In addition to determining the level of power each generating unit should be producing when it is online, system operators must also determine when each generating unit should start up and shut down. This function is known as "unit commitment." Although significant costs are associated with the startup and shutdown of generating units, it is not practical to keep all of them online all the time. There are large fixed costs associated with running generating units, and some units have a minimum power they must produce when they are online. Unit commitment determines the economically optimal time when generating units should start up and shut down and how much power they should produce while they are online. This optimization is more complex and time consuming than economic dispatch. Unit commitment is typically done one day ahead and covers dispatch for periods ranging from one to seven days. It should be noted that only scheduling and control in real time through economic dispatch are the main focuses of this thesis, thus with no loss of generality, we assume that specific generators have been committed through unit commitment. Unit commitment has been widely studied in [81, 82] and the references therein.

2.3.4 Market Clearing Mechanism: Locational Marginal Prices

The process of trading wholesale energy begins with a bidding process, where generators offer an amount of energy for sale during specific periods of the day at a specific price. These offers are arranged by the System Operator in ascending order, called the "bid stack," and the generators are dispatched in the merit order until generation matches expected load. Large loads also sometimes submit bids for the purchase of energy in the market.

In clearing the market, the ISO may require simple or complex offers and bids. A complex offer consists of an incremental cost function, as well as other costs including start-up costs

and idling (no-load) costs; a simple offer consists of only an incremental cost function. The ISO may also allow generators to submit operational constraints applicable to their units, including ramp rates, minimum up- and down-times, start-up times and minimum loading levels. A market that incorporates complex offers and bids, and the various operational constraints, will require a complex unit commitment solver for market clearing but it will have the advantage that the solution (i.e. dispatch) will be more optimal, subject to participants providing bids which are a true reflection of their costs. The solution will be feasible with respect to those constraints. Conversely, a market that allows only simple bids and offers will be more transparent to the casual observer, but it requires the participants to internalize their fixed costs and operational constraints. As a consequence, it may in fact result in infeasible and/or sub-optimal dispatches.

The goal of the Independent System Operator (ISO) is to determine the dispatch that minimizes total cost, as measured by generators' bids, subject to security constraints. The ISO's task is to select the operating point that satisfies Eqs. (2.10a)-(2.10c). This process determines the marginal cost of meeting an increment of load at each bus in the transmission system to which load or generation is connected. Following [25] these costs are termed *locational marginal prices* (LMPs) because they enable the ISO to fix the LMP ρ_i at the Lagrangian multipliers corresponding to the balance equation denoted in (2.8b). The attractive feature of LMP is that it forces the system to operate at the unique, efficient equilibrium that will be discussed in Chapter 3.

Distribution companies or large customers pay the applicable LMP for energy consumed. Similarly, generation is paid the LMP at the point at which it is located. The LMP pricing structure used in modern markets ensures that the profitable choice for generators and loads is to follow the instructions of the economic dispatch.

Generators are only dispatched when their offer to sell is at a price no greater than LMP at their location. Likewise, generators are not dispatched when the market price is less than their offer to sell. The use of LMPs exploits the natural definition of an efficient equilibrium for a market, (discussed in Chapter 3), utilizes the crucial central coordination, and avoids the need for market participants to track transmission flows or understand the many constraints and requirements of the power system.

The Effect of Congestion on LMP

LMP reflects the market clearing price (MCP) at each location. In other words, ConCos pay the ISO based on their LMP for dispatched energy. The ISO in turn pays GenCos based on their respective LMPs. When the line flow constraints are not congested, LMPs at all locations will be the same as the MCP the marginal bidding price of the most expensive dispatched generation unit. However, when transmission flows are constrained, LMPs will vary among buses. In this case, constrained flows could prevent the economic supply of energy from serving bus demands at a certain location. As a result, the demand has to be supplied by more expensive units via other transmission lines, which could result in LMP differences. The LMP difference between two adjacent buses is the congestion cost defined in the following definition.

Definition 2.1. [76] Let ρ_i^* and γ_{ij}^* be the associated Lagrangian variables corresponding

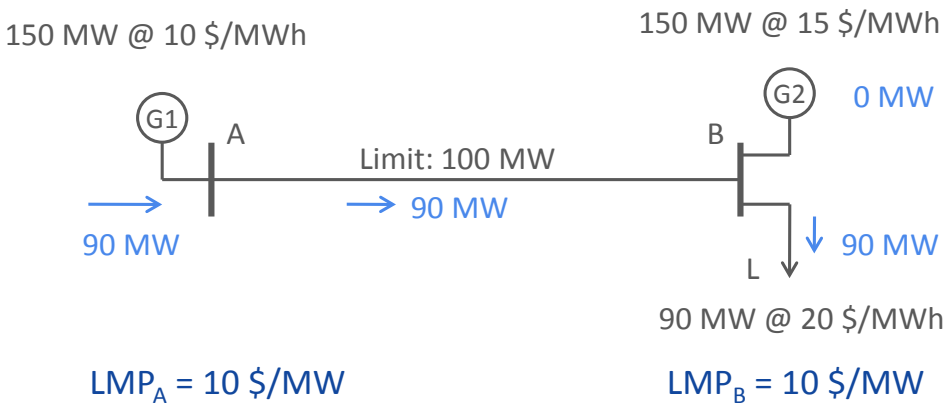

Figure 2.5: LMP calculation: system with no congestion

to the optimal solution of DC Economic Dispatch (P_i^*, δ_i^*). Then γ_{ij}^* is the congestion price for the constraint $Y_{ij}(\delta_i^* - \delta_j^*) \leq C_{ij}$, and $\sum_i \sum_j \gamma_{ij}^* C_{ij}$ is the congestion rent.

Transmission losses impact LMP differences as well. Marginal losses are the incremental changes in system losses due to incremental demand changes. Incremental losses yield additional costs which are referred to as the cost of marginal losses. However in this thesis, we ignore ohmic losses and only focus on congestion constraints. To clarify the effect of congestion in LMP, let us consider a n-bus network where the flow on link $1-n$ is congested, i.e. in Eq. (2.8c), $P_{1n} = C_{1n}$ and all other flows are not congested. From (2.10c), this implies that $\gamma_{ij} = 0$ for all $i, j \neq 1n$ since the constraints are not active [76]. We can then write Eq. (2.10b) in matrix form as

$$\begin{bmatrix} \sum_j Y_{1j} & -Y_{12} & . & -Y_{1n} \\ -Y_{21} & \sum_j Y_{2j} & . & -Y_{2n} \\ . & . & . & . \\ -Y_{n1} & -Y_{n2} & . & \sum_j Y_{nj} \end{bmatrix} \begin{bmatrix} \rho_1 \\ \rho_2 \\ . \\ \rho_n \end{bmatrix} = \begin{bmatrix} -Y_{1n} \\ 0 \\ 0 \\ Y_{n1} \end{bmatrix} \gamma_{1n}. \tag{2.11}$$

These equations are linearly dependent [76]. We choose to eliminate the last equation. Dividing throughout by λ_n and defining $\pi_i = \rho_i/\rho_n$ for all $i = 1, \ldots, n-1$ and $m = \gamma_{1n}/\rho_n$, we obtain

$$\begin{bmatrix} \sum_j Y_{1j} & -Y_{12} & . & -Y_{1n-1} \\ -Y_{21} & \sum_j Y_{2j} & . & -Y_{2n-1} \\ . & . & . & . \\ -Y_{n-11} & -Y_{n-12} & . & \sum_j Y_{n-1j} \end{bmatrix} \begin{bmatrix} \pi_1 \\ \pi_2 \\ . \\ \pi_{n-1} \end{bmatrix} = \begin{bmatrix} -Y_{1n} \\ 0 \\ 0 \\ 0 \end{bmatrix} m + \begin{bmatrix} Y_{1n} \\ Y_{2n} \\ 0 \\ Y_{n-1n} \end{bmatrix}. \tag{2.12}$$

We can compactly write (2.12) as

$$Y\pi = gm + h \tag{2.13}$$

where $g = \begin{bmatrix} -Y_{1n} & 0 & 0 & 0 \end{bmatrix}^T$, $h = \begin{bmatrix} Y_{1n} & Y_{2n} & 0 & Y_{n-1n} \end{bmatrix}^T$, and

$$Y = \begin{bmatrix} \sum_j Y_{1j} & -Y_{12} & . & -Y_{1n-1} \\ -Y_{21} & \sum_j Y_{2j} & . & -Y_{2n-1} \\ . & . & . & . \\ -Y_{n-11} & -Y_{n-12} & . & \sum_j Y_{n-1j} \end{bmatrix}.$$

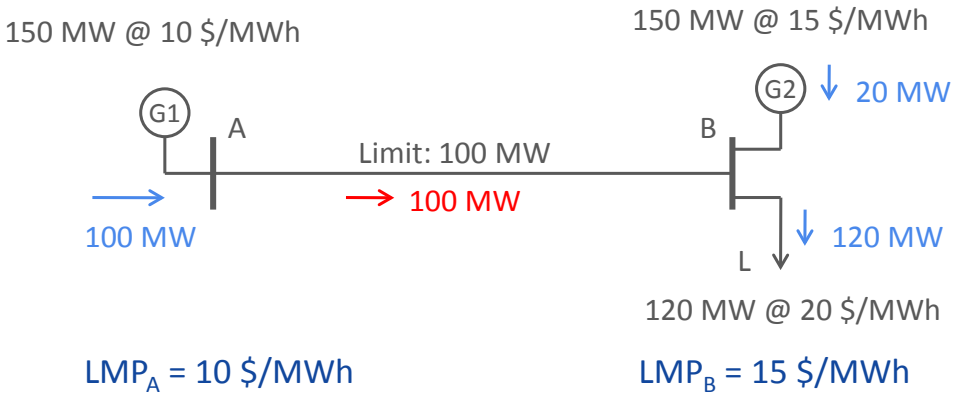

Figure 2.6: LMP calculation: system with congestion

By inspection it follows that $h = Y\mathbf{1}$ where $\mathbf{1}$ is a vector with all elements equal to unity (see [76]). Then it follows that

$$\rho_i = \rho_n - \alpha_i \gamma_{1n} \tag{2.14}$$

where $\alpha = -Y^{-1}g$ and α_i is the ith element of δ. As can be seen in Eq. (2.14), congestion at link $1-n$ causes the difference between ρ_i and ρ_n. It can be seen from Eq. (2.14) that if $\gamma_{1n} = 0$, all LMPs are equal which corresponds to the uncongested case.

Example 2.1. Consider a 2-bus system connected through a transmission line with maximum capacity equal to 100 MW. A GenCo located in bus A offers to produce 150 MW at 10 $\$/MWh$ and another GenCo at bus B offers to produce 150 MW at 15 $\$/MWh$. A ConCo located at bus B submits a bid to consume 90 MW at 20 $\$/MWh$. Figure 2.5 represents the configuration of our example. As can be seen in this figure, $G1$ serves the incremental megawatt of ConCo located in bus B and therefore LMP at bus B will be 10 $\$/MWh$, equal to the offer of $G1$. We denote $G1$ as the marginal asset that would supply the next increment of load at either location A or B. Since the limit of the transmission line connecting bus A to bus B is 100 MW, congestion does not occur, and therefore LMP at bus A is equal to LMP at bus B and equal to the offer price of marginal asset $G1$ at both locations.

Example 2.2. Now consider that in Example 2.1 ConCo located in bus B submits a bid to consume 120 MW at 20 $\$/MWh$. As can be seen in Figure 2.6, the transmission line connecting bus A to bus B is congested. In this example, there are two marginal assets G1 and G2. G1 would supply the next increment of load at location A and G2 would supply the next increment of load at location B. Therefore, there are two different LMPs at different locations, LMP in bus A is 10 $\$/MWh$ that is equal to the offer price of marginal asset G1 and LMP in bus B is 15 $\$/MWh$ that is equal to the offer price of marginal asset G2.

Electric Energy Supply Offers and Demand Bids

The offers made by GenCos, and the bids due to ConCos determine the LMPs. Production costs and supplier operating characteristics influence the offers by GenCos. Generating units submit three-part supply offers for their output including start-up, no-load, and incremental energy offers. Start-up offers reflect the costs associated with bringing a unit from an off-line

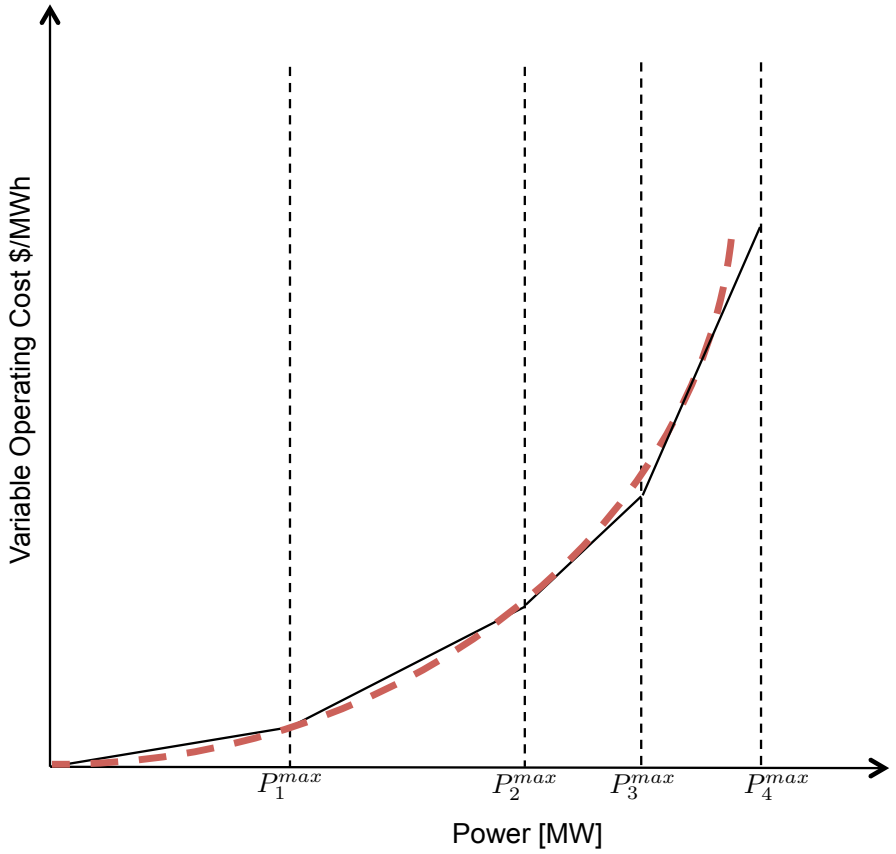

Figure 2.7: Quadratic (dashed line) and piece-wise linear (solid line) cost function

state to the point of synchronization with the grid. No-load offers reflect the hourly cost of operating that does not depend on the megawatt level of output. Incremental energy offers represent the willingness of participants to operate a resource at a higher output level for a higher price. The first two costs should be considered in unit commitment and the last is an essential cost for the economic dispatch problem.

The bids for electric energy reflect a participant's load-serving requirements and the accompanying uncertainty, its tolerance for price volatility, and its expectations about congestion on the system caused by transmission constraints. Participants may bid for a fixed demand- i.e., they would buy at any price- and for price-responsive demand adjusting their demand in response to the price signal.

Piecewise linear or quadratic functions are two general methods to represent costs and bids. These two methods are illustrated in Figure 2.7. Generators with multiple units are well approximated by piecewise linear curves, since there is a jump in cost each time a unit is turned on or off, and then a gradual increase as individual units are ramped up or down. Piecewise linear bid curves lead to jumps in the dispatch results, and volatility in revenue and profit curves [34]. Quadratic cost curves lead to smooth dispatch, revenue, and profit curves when none of the system constraints is active (transmission congestion, generator capacities). While quadratic curves facilitate analysis, they are not a perfect characterization of a generator's cost structure. In Chapter 3, a piecewise linear bidding curve is considered, and for the sake of analysis, a quadratic bidding curve is assumed in Chapter 4.

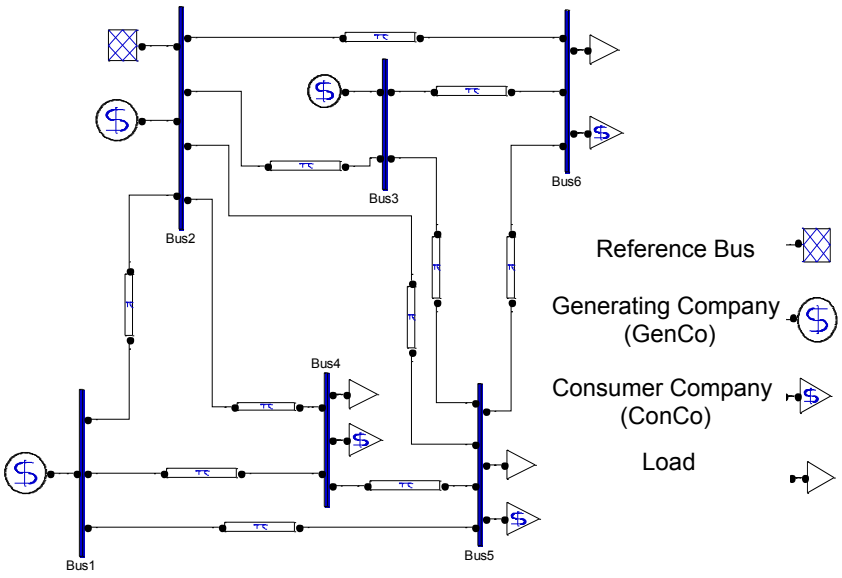

Figure 2.8: IEEE 6-bus case study for Example 2.3

Example 2.3. Figure 2.8 shows a 6-bus system [5] with three GenCos. The maximum capacity of the GenCo at bus 2, the reference bus, is 0.25 per-unit (p.u.) based on 100 MVA. The maximum capacities of the GenCo at bus 1 and 3 are 0.2 $p.u.$ and 0.22 $p.u.$, respectively. A quadratic cost function is assumed to model the variable cost for each generator as

$$C_i(P_i) = a_i + b_i P_i + c_i P_i^2 \tag{2.15}$$

Table B.1 in Appendix B provides cost coefficients a_i, b_i, and c_i. The same as GenCos, we consider the quadratic utility function for ConCos located at buses 4, 5, and 6. Table B.1 provides utility coefficients for each of theConCos.

Transmission lines are modeled with reactance equal to 0.2 $p.u.$ and ohmic losses are ignored. The maximum capacity of all transmission lines is the same and equal to 0.914 $p.u.$

PSAT toolbox [5] was used to simulate this example. LMP at each node is shown in Figure 2.9. As can be seen, in this example LMP at bus 1 is lower than the LMPs at all other buses due to the congestion of transmission lines. Fig 2.10 presents the flow of transmission lines. Except for the line connecting buses 1 and 2, all lines connecting bus 1 to other buses are congested. Therefore LMP at bus 1 is lower than other LMPs.

2.4 Structure of the Wholesale Electricity Market

ISOs are responsible for overseeing and administering competitive wholesale electricity markets. These markets work together to ensure the constant availability of electricity. In this

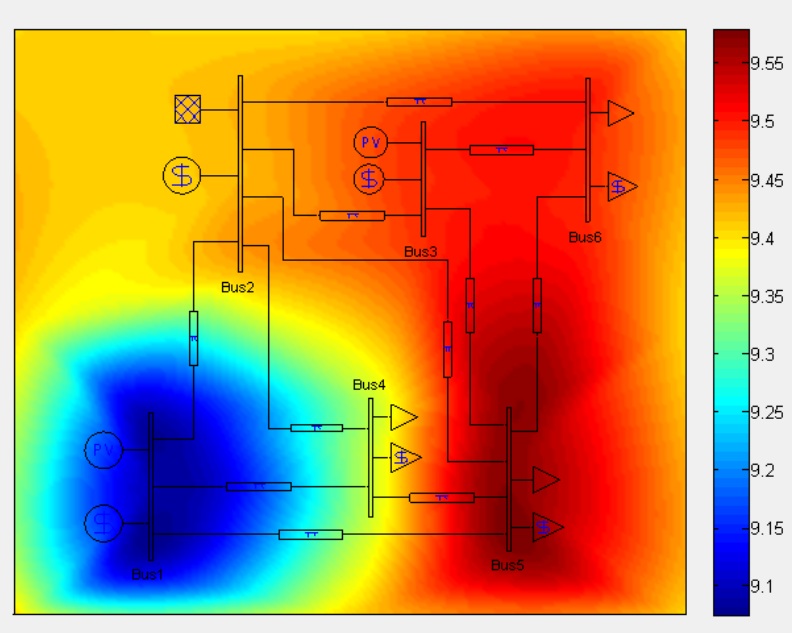

Figure 2.9: Locational Marginal Price in $\$/MWh$ at each bus

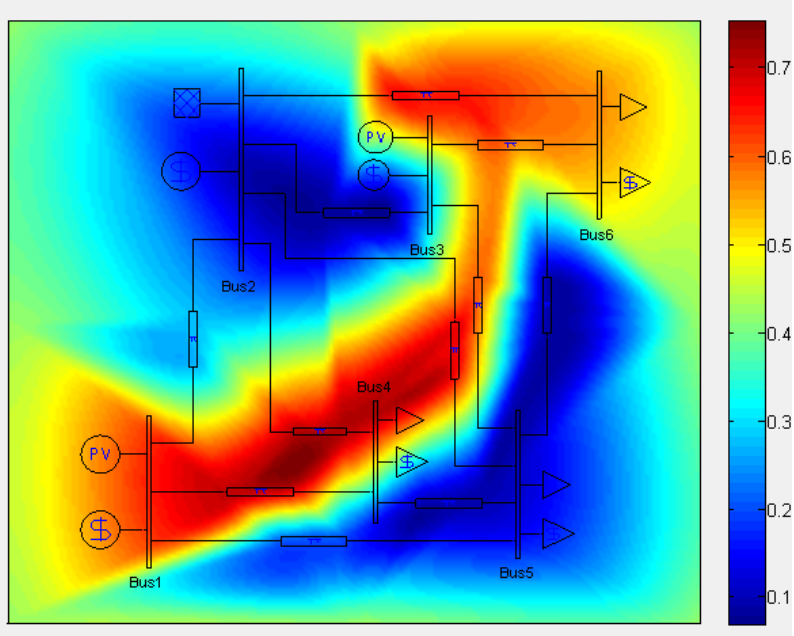

Figure 2.10: Line Flow[p.u.]

section, the structure of the wholesale electricity market is presented. It should be noted that the following structure of the wholesale markets is based on the current practice of ISO New England [1], however different regions or countries might have modified structures, based on their own energy policy. In particular, the wholesale electricity markets consist of the following markets [3]:

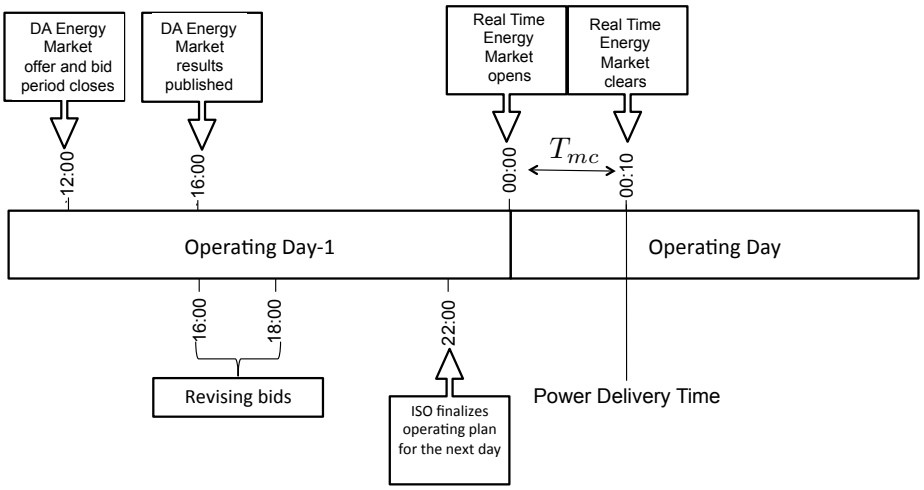

Figure 2.11: Day-ahead and Real-Time Markets Time Line

2.4.1 Day-Ahead Energy Market (DAM)

DAM allows market participants to hedge against price fluctuations which occur in real time. The primary objective of the electricity markets operated by any ISO is to ensure a reliable and economic supply of electricity to the high-voltage power grid. The day-ahead market is a forward market, in which hourly clearing prices are calculated for each hour of the next operating day, based on generation offers, demand bids, virtual supply offers, virtual demand bids, and bilateral transaction schedules submitted into the day-ahead market.

All of the transactions between participants in the day-ahead market are settled at the day-ahead prices. Figure 2.11 shows the time line of DAM. After the day-ahead market bid period closes at 12:00, ISO calculates the day-ahead schedule based on the GenCo offers and ConCo bids, and schedules the dispatch plan for each hour of the next operating day based on a least-cost, security-constrained unit commitment. The day-ahead market clearing process incorporates reliability requirements and reserve obligations into the analysis. Generators that are available but not selected in the day-ahead scheduling may revise their bids for use in the Real-Time Market (RTM), discussed in Section 2.4.2, during the generation rebidding period from 16:00 to 18:00; otherwise the original day-ahead market bids remain in effect for the real-time energy market. At 22:00, the ISO finalizes the operating plan for the next day. To economically meet actual real-time load, RTM needs to balance energy and reserves in the grid, while accounting for transmission system limits and providing contingency coverage.

2.4.2 Real-Time Energy Market (RTM)

The Real-Time Energy Market is a physical delivery market rather than a financial forward market like the day-ahead energy market. The RTM is the environment in which the ISO control room commits and dispatches physical resources to meet actual real-time load, including the minute-to-minute balancing of energy and reserves, while accounting for transmission system limits and the need to provide contingency coverage. The financial schedules

produced by the Day-Ahead Energy Market clearing process provide a starting point for the operation of the RTM. At each location, the power required, and available, can increase or decrease for a number of reasons, including generator re-offers of their supply into the market, real-time hourly self-schedules (i.e., generators' choosing to be on line and operating at a fixed level of output regardless of the price of electric energy), transmission or generation outages, and unexpected real-time system conditions.

Physically, real-time operations balance instantaneous changes in supply and demand, and ensure that adequate reserves are available to operate the transmission system within its limits. Financially, the Real-Time Energy Market settles the differences between the day-ahead scheduled amounts of load and generation and the actual real-time load and generation. Participants either pay or are paid the real-time locational marginal price (LMP) (see Section 2.3.4) for the load or generation in megawatt-hours (MWh) that deviates from their day-ahead schedule.

In the real-time energy market, the ISO meets the energy demand while respecting the transmission security constraint using the least-cost security constrained Economic Dispatch (ED) (see Section 2.3.2). The ED is an *ex-ante* dispatch that is based on the projected system conditions within the next 5 minutes. The LMP calculations are *ex-post* and are based on the actual generation response to the *ex-ante* dispatch that was sent 5 min earlier. The LMP calculation will take into account the current transmission and generation outages as well as transmission limitations through the ISO state estimator.

The sequential process of DAM and RTM is expressed in Figure 2.12. First, all generators have the flexibility to revise their incremental energy supply offers during the re-offer period as discussed in Section 2.4.1. The ISO also may be required to commit additional generating resources to support local-area reliability, or to provide contingency coverage. This additional generating resources ensure that the system reliably serves actual demand, the required operating-reserve capacity is maintained, and finally transmission line loadings are safe. For these processes, the ISO evaluates the set of generator schedules produced by the DAM solution, any self-schedules submitted during the re-offer period, and the availability of resources for commitment near real time. The ISO will commit additional generation if the DAM generation schedule, plus the self-scheduled resources and available fast-start generation, does not meet the real-time forecasted demand and also reserve requirements that ensure system reliability. In addition, generating-unit and transmission line outages, along with unexpected changes in demand, can cause the ISO to call on additional generating resources to preserve the balance of supply and demand. All the circumstances which affect the level of generator dispatch, such as changes in the level of demand, actual generator availability, and system operating conditions, affect the real-time LMPs. RTM prices are inherently volatile in the competitive equilibrium due to physical constraints and uncertainty. Recent work shows that volatility and uncertainty can have tremendous impact on system operations and market outcomes [92]. As the penetration of wind and other renewable energy resources increases, power systems are facing additional volatility. For this reason, it is expected that many of the difficulties observed in today's RTM might increase without proper design.

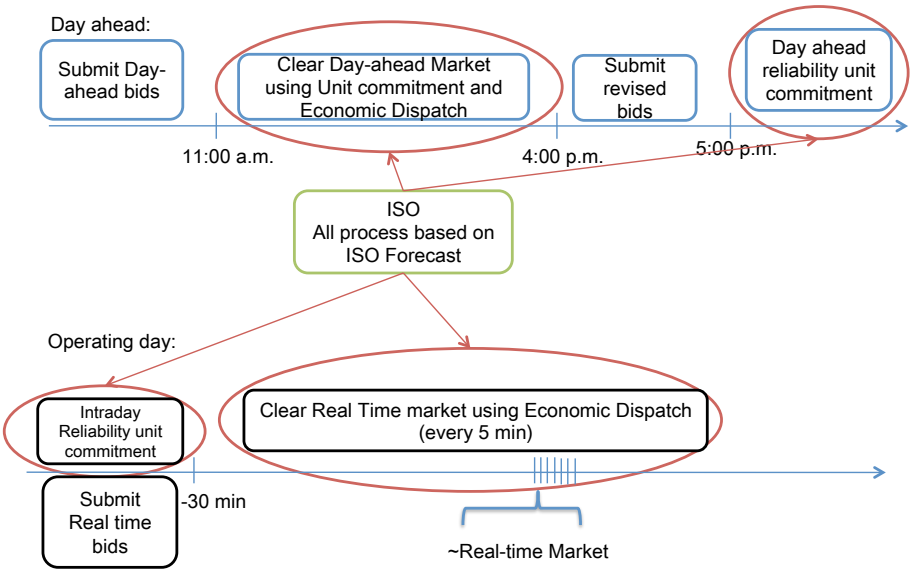

Figure 2.12: Pool-based market time line

2.4.3 Reserve Market

To maintain system reliability, all power systems need reserve capacity to be able to respond to contingencies, such as those caused by unexpected outages. Operating reserves are the unloaded capacity of generating resources, either off line or on line, which can deliver electric energy within 10 or 30 minutes.

The ISO's operating procedures require reserve capacity to be available within 10 minutes to meet the largest single system contingency. Additional reserves must be available within 30 minutes to meet one-half of the second-largest system contingency. The ISO also identifies local second-contingency-protection resources (LSCPRs) to meet the second-contingency requirements in the constrained areas. In general, capacity equal to between one-fourth and one-half of the 10-minute reserve requirement must be synchronized to the power system, or be 10-minute spinning reserve (TMSR), while the rest of the 10-minute requirement may be 10-minute nonspinning reserve (TMNSR). The entire 30-minute requirement may be served by 30-minute operating reserve (TMOR) or the higher-quality 10-minute spinning reserve or nonspinning reserve. In addition to the system-wide requirements, 30-minute reserves must be available to meet the local second contingency in constrained areas.

The Forward Reserve Market (FRM) obliges participants to provide reserve capacity in real time through a competitive, intermediate-term forward-market auction. Then, the ISO dispatches resources in real time, and the use of resources for providing electric energy and real-time reserves will be co-optimized. When resources are dispatched to a lower level in real-time to provide reserve capacity rather than electric energy, a positive real-time reserve price for the product is assigned, recognizing the resource's opportunity cost of providing reserve rather than energy. The real-time reserve prices also reflect additional costs to the system of dispatching more expensive resource to provide electric energy in order to replace the output of the resource which was dispatched down.

In particular, the reserve market consists of a regulation market, a forward reserve market

and a voltage support market. Brief details of each of these markets are now discussed.

Regulation Market

Regulation is the capability of specially equipped generators and other energy sources to increase or decrease their output *every four seconds* in response to signals they receive from the ISO to control slight changes on the system. This capability is necessary to balance supply levels with the rapid variations in demand and to assist in maintaining the frequency of the entire interconnected power network.

The primary objective of the Regulation Market, which is the mechanism for selecting and paying resources needed to manage system balancing, is to ensure that the ISO meets the Real Power Balancing Control Performance Standard assigned by *North American Electric Reliability Corporation (NERC)*. According to this standard each balancing authority shall operate such that its average area control error (ACE) for at least 90% of clock-10-minute periods (six non-overlapping periods per hour) during a calendar month is within a specified limit. The regulation clearing price (RCP) is calculated in real time and is based on the regulation offer of the highest-priced generator providing the service.

Forward Reserve Market (FRM)

The Forward Reserve Market is designed to attract investments in the type of resources that provide the long-run, least-cost solution to satisfying the reserve requirements. The ISO conducts two FRM auctions, one each for the summer and winter reserve periods (June through September and October through May, respectively), which acquire obligations to provide pre-specified quantities of each reserve product. Forward-reserve auction clearing prices are calculated for each reserve product in each reserve zone. To attract and maintain resources which are normally expected to provide reserves instead of electric energy, the FRM requires the resources designated as forward-reserve resources to offer the megawatt. When enough supply is offered under the price cap to meet the requirement for a product in a particular zone, the auction clearing price for that product is set equal to the price of the marginal supply offer.

Voltage support

This allows ISO to maintain transmission voltages within acceptable limits through facilities to produce Reactive Power. Thus, Reactive Supply and Voltage Control Services, called Voltage Support Services, must be provided to support voltage level in the transmission level. The amount of Voltage Support Service that must be supplied will be determined based on the Reactive Power support necessary to maintain transmission voltage within the limits that are accepted in the region by the ISO.

2.4.4 Summary of Scheduling Process through Wholesale Market

As we discussed in the previous section, the ISO runs different generation schedules in its day-ahead market and real-time market, to make sure that the energy and reserve re-

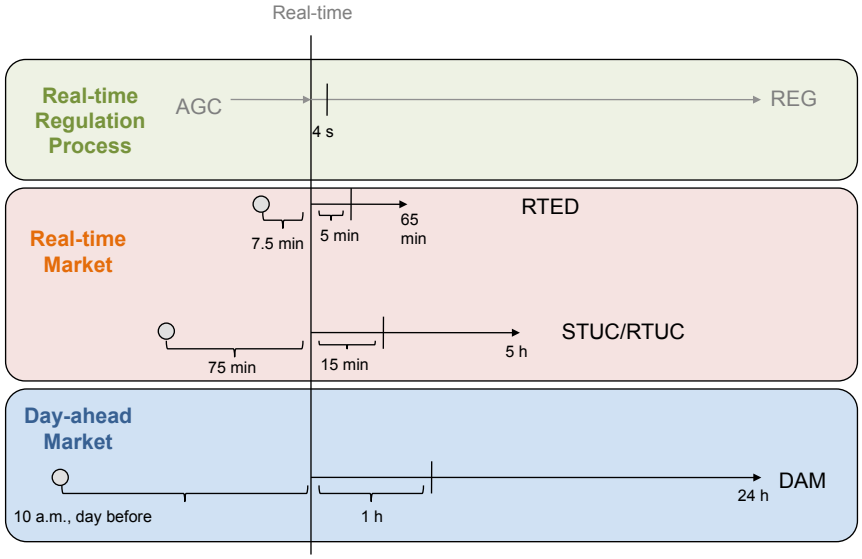

Figure 2.13: Granularity of dispatch in the wholesale market, adopted from [110]

quirements, including regulating up, regulation down, and ramping requirements are ultimately met in real-time operation. Figure 2.13 shows the typical market timeline. The ISO scheduling process includes day-ahead market (DAM), real-time unit commitment (RTUC), short-term unit commitment (STUC), and real-time economic dispatch (RTED). Although regulation (REG) capacity is procured in the day-ahead market, it is controlled by the AGC system which is discussed in details in Chapter 5 and Appendix A.2. The RTM consists of several applications, of which STUC, RTUC, and RTED work together. The STUC and RTUC applications ensure there is enough on-line capacity to meet a 5-minute demand. The STUC is performed in the RTM to commit units, and balance the system resource and demand, while enforcing transmission constraint. STUC is run once an hour, and looks ahead 5 hours to commit resources that have start up times greater than 90 minutes. The RTUC application runs every 15 minutes and looks ahead between 60 minutes to 75 minutes intervals to determine if short-start and fast-start units need to be committed or de-committed.

The RTED process runs every 5 minutes to meet the imbalance energy requirements of the system. This process looks ahead 65 minutes to ensure that enough capacity is on-line to meet real-time demand. It is expected that wind variability and the lack of accurate wind forecast could create challenges for the RTED application. RTED is the lowest granularity of dispatch in the overall hierarchical electricity market. Then regulating reserves is dispatched through the EMS AGC system every 4 seconds to follow the remaining uncertainties.

Figure 2.14 represents the components of generation dispatch in the presence of uncertainty. In the day-ahead timeframe, wind and solar resources are not required to bid directly into the markets. This fact can significantly impact the unit commitment process in the DAM timeframe because the ISO must forecast the expected hourly production in the DAM to ensure that enough resources are committed for the next day's operation. Similarly, the ISO load forecast is done in the DAM and RTM timeframes. RTED is provided 7.5 minutes before the dispatch operating target (DOT) and is based on real-time forecasts. In the RTM, the ISO automatic load forecasting system provides a load forecast for each 15-minute and 5-

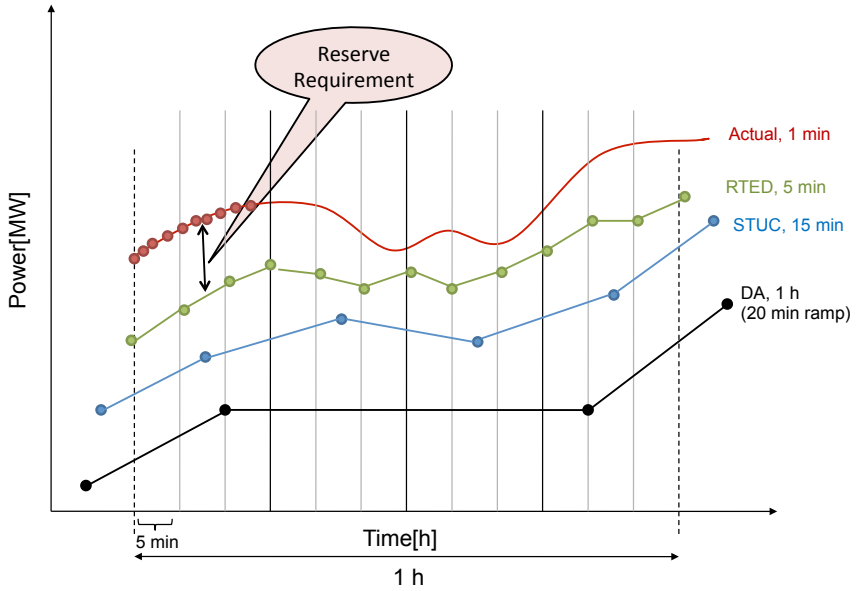

Figure 2.14: Components of Generation Dispatch in the Presence of Uncertainty, adopted from [110]

minute interval. Load and wind forecasting errors can cause the RTM application to dispatch incorrect amounts of imbalance energy needs. Because of the load and wind (as well as solar) forecast errors, there are uncertainties in the ranges of regulation and load following requirements.

Greater volatility means increased reserves, which reduces the value of wind power. With sufficient storage and Demand Response (DR) we can reduce the impact of volatility and increase the value of wind power. DR is discussed further in Section 2.5.2, and its effect on market equilibrium is quantified in Chapters 3 and 4. It is also hoped that smart meters will reduce the negative impacts of volatility, bringing a feedback structure where demand can be modulated over a range of time-scales. In Chapter 4, we will develop a dynamic framework for addressing the financial settlement, and will study the effects of wind uncertainty and demand elasticity on the overall market stability.

2.5 Smart Grid Implications

One of the main foundations of the emerging Smart Grid is the integration of renewable energy resources (RER). Particularly integration of wind and solar energy (two of the most rapidly growing resources) into the electric power infrastructure presents significant challenges. At the heart of this challenge lies the inherent variability (often referred to as intermittency) of wind and solar. An interesting concept that is being explored for mitigating the integration cost of RERs is DR, the concept of controlling loads via economic signals. In the following subsections, the challenges of Smart Grid implications, in terms of wind power uncertainty and DR , will be discussed. There are other implications of Smart Grid such as PHEVs, micro-grids, direct load control, and smart meters. These aspects of Smart Grid are

beyond the scope of this thesis, but can be found in [109].

2.5.1 Wholesale Electricity Market Under Wind Uncertainty

Wind power cannot be dispatched in a traditional sense, due to the inherent intermittency and uncertainty of wind. Therefore large-scale integration of wind power into a power system constitutes a challenge for system operators and planners [83]. In particular, the management of uncertainties in a power system has already been observed in current practice. Demand is also variable and uncertain, and system operators have been coping with the natural variability and stochasticity of demand since the dawn of the power industry. However, the integration of wind generation into a power system entails the consideration of additional uncertainty and variability in the operation of the system. Specially for the case that wind penetration is significant, uncertainty poses the significant challenge that needs to be taken into account . Part of this variability can be predicted some hours or days ahead. The uncertain part of the variability is managed with reserves in the power system. As the level of wind power generation increases, the need for spinning and non-spinning reserves increases to maintain system security. Increasing wind penetration requires higher degree of flexibility in order to coordinate the resulting fluctuating of load and the variable output of wind generation. This greater flexibility usually imposes huge integration costs to operate conventional power systems at larger range of production levels in an attempt to accommodate the inherent variability of wind generation by ramping up or down.

Through competition among participants, electricity markets should guarantee the economically efficient operation of electrical systems . However, when wind power comes on stage in high levels, the competitive system can be altered, as the energy transactions settled in these markets may not be implemented in real-time, exactly as agreed due to intermittency and uncertainty.

Therefore, the successful integration of wind generation into power systems relies on economic criteria while maintaining, or even improving, the reliability of the overall power systems. The reliability of power systems is largely dependent on reserve management, which, in turn, depends on the penetration of wind power [83]. All these issues can be tackled suitably by utilizing dynamic information in the form of dynamic mechanism of the market clearing procedure, introduced in Chapter 4. This procedure constitutes a real-time pricing, to reconcile economic efficiency and system security for clearing electricity markets with high levels of uncertainty. In Chapter 5, a hierarchical control methodology based on dynamic information is presented with a goal of ensuring frequency regulation using optimal allocation of resources in the presence of uncertainties in renewables and load.

2.5.2 Demand Response (DR)

Along with adequate supply and robust transmission infrastructure, Demand Response (DR) is an important component in the wholesale energy market. DR consists of the equipment, systems, services, and strategies that enable demand resources to adjust their consumptions in response to power grid needs through economic signals from a competitive wholesale market. DRs can provide relief from capacity constraints and promote more economically efficient uses of electrical energy. In the Forward Capacity Market, some types of DR resources

are paid *capacity payments*, which can compete in the Forward Capacity Auction along with other supply-side resources. For example, some customers can reduce their overall energy usage while maintaining the same level of productivity and comfort by implementing energy-efficiency measures. Other customers can supply capacity by eliminating their consumption on short notice in response to a capacity deficiency. Still others may be able to shift end-use customer load onto an on-site emergency generator in response to system emergencies. The ISO has three basic categories of DR

- Active DRs that reduce load to support system reliability,
- Active DRs that respond to wholesale energy prices,
- Passive DRs that reduce load through energy efficiency and similar measures.

In the subsequent chapters, different concepts of DR are presented. DR has increasingly provided grid operators and utilities with flexibility in order to control power systems in the presence of uncertainty and intermittency of RERs, which is delineated in the following chapters.

2.6 Concluding Remarks

To achieve large-scale use of uncertain and variable renewable generation, it is necessary to move to a new paradigm, where both the consumption and generation have a possibility to suitably adjust in response to the power systems conditions. DR is such a paradigm, and refers to a portfolio of control schemes which modulate and control consumption. In Chapter 3, we analyze the effect of RER uncertainty, and we show that the integration cost of RER in the wholesale market is mitigated by implementing DR. In Chapter 4, robust stability of the wholesale market is presented and we will demonstrate how DR is useful to increase robustness of market dynamics in the presence of wind uncertainty. Finally, in Chapter 5, DR is used as a part of hierarchical Transactive control structure and the effect of DR in power systems control is illustrated.

3 Static Equilibrium Modeling of the Electricity Market

Summary. *The notion of market equilibrium in the presence of Renewable Energy Resources (RERs) and Demand Response (DR) is presented. The main contributions of this chapter are*

- *An analytical framework to determine the market equilibrium shift using a linear complementarity problem (LCP) approach,*
- *Conditions under which the equilibrium of the market exists and is identical to the Nash Equilibrium of the corresponding game, which is provided in Theorem 3.2,*
- *A computable upper bound for market equilibrium shift in the presence of wind uncertainty, which is provided in Theorem 3.3,*
- *Quantifying the deviation of Nash Equilibrium in the presence of wind uncertainty and the effect of perturbation on the payoffs of GenCos and ConCos, which is provided in Proposition 3.1.*

One of the main challenges in the emerging smart grid is the integration of renewable energy resources (RER). The latter introduces both intermittency and uncertainty into the grid, both of which can affect the underlying energy market. An interesting concept that is being explored for mitigating the integration cost of RERs is DR. Beginning with an overall model of the major market participants with RER and DR, together with the constraints of transmission and generation, the energy market in this chapter is analyzed and conditions for global maximum using standard Karush-Kuhn-Tucker (KKT) criteria are derived. The effect of wind uncertainty on the market equilibrium is then quantified. Perturbation analysis methods are used to compare the equilibria in the nominal and perturbed markets. These markets are also analyzed using a game-theoretic point of view. Sufficient conditions are derived for the existence of a unique Pure Nash Equilibrium in the nominal market. The perturbed market is analyzed using the concept of closeness of two strategic games and the equilibria of close games. This analysis is used to quantify the effect of uncertainty of RERs and its possible mitigation using DR. Finally numerical studies are reported using an IEEE 30-bus to validate the theoretical results.

The remainder of this chapter is organized as follows: Section 3.1 describes the model of the three market participants. In Section 3.2, the overall market equilibrium under nominal conditions is formulated. A perturbation analysis is introduced in Section 3.4 to address the effects due to uncertainty. In Section 3.5 numerical simulation results are reported. Section

3.6 includes concluding remarks.

3.1 Modeling of Market Agent Behavior

In this section, we derive the model of the wholesale electricity market. The main components of this market include

1. *Generating companies (GenCos)*: GenCos are entities that own generating units. GenCos sell their electricity either through the electricity market, or through bilateral contracts to the consumer. GenCos are responsible for the operation and maintenance of their generating units.

2. *Consumer companies (ConCos)*: ConCos are entities that purchase electricity to supply consumption, either through the electricity market, or through bilateral contracts directly from the GenCos.

3. *Independent System Operator (ISO)*: Independent entity that clears the market by maximizing social welfare based on power systems security and reliability.

A deterministic framework is used to capture interactions between these players. The underlying goal is the determination of the power production of the generating units and the power demanded by the consumers such that power is balanced at all network nodes and social welfare is maximized while meeting capacity limits. The solution of the resulting optimization problem not only determines the optimal dispatch but also the optimal Local Marginal Price which is determined as the corresponding shadow price. In what follows, we model each of the components 1-3 together with their constraints and the optimization goals.

3.1.1 Generating Company

It is assumed that the generating company consists of N_G generating units, and that the production of each generating unit i, $i = 1,\ldots,N_G$ is divided into b power blocks, where $b = 1,\ldots,N_{G_i}$, and is denoted as P_{Gib}. The associated linear marginal operating cost is denoted as $\lambda^C_{G_{ib}}$. These costs are due to fuel consumption, and to operation and maintenance. A precise model of the operation costs could require the use of non-differentiable and non-convex functions [28, 74]. In practical applications, several approximations are used to model operating costs. In this chapter, a piecewise linear approximation of the variable cost is used. As can be seen in Figure 3.1, each power variable has a minimum value equal to zero and a maximum value equal to the size of the corresponding block denoted as P_{Gib}. The slope of the linear approximation for each block corresponds to the marginal cost of this block and is represented by $\lambda^C_{G_{ib}}$.

The goal of the company is to maximize its overall profit, and is stated as

$$\text{maximize}_{P_{Gib}} \sum_{i\in G_f}\sum_{b=1}^{N_{Gi}} (\rho_{n(i)} - \lambda^C_{G_{ib}}) P_{Gib} \tag{3.1}$$

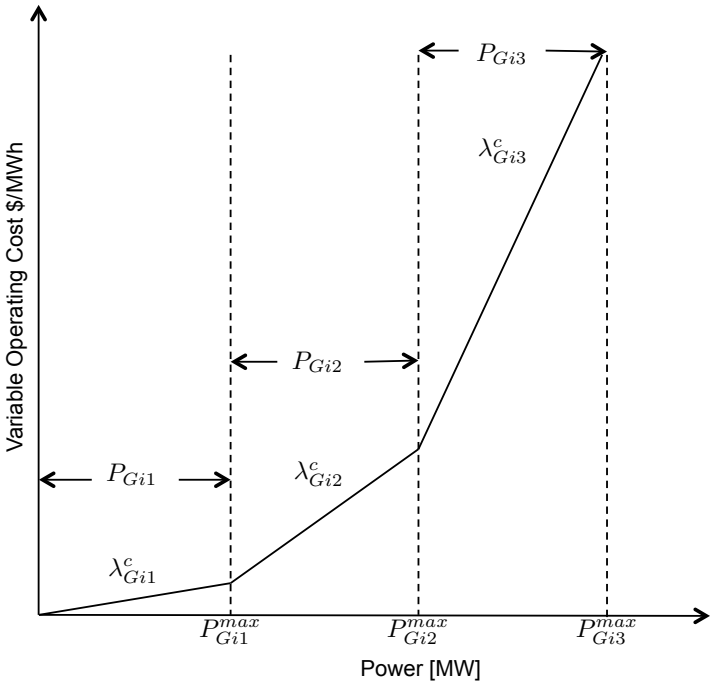

Figure 3.1: Piecewise linear variable operating cost function, adopted from [46].

where $\rho_{n(i)}$ denotes the Locational Marginal Price (LMP) of unit i at node n in the network. The power production is subject to the following constraints:

$$\sum_{b=1}^{N_{Gi}} P_{Gib} \leq P_{Gi}^{max} : \alpha_i; \forall i \in G_f \tag{3.2a}$$

$$P_{Gib} \leq P_{Gib}^{max} : \phi_{ib}; \forall i \in G_f; b = 1, \ldots, N_{Gi} \tag{3.2b}$$

$$P_{Gib} \geq 0; \forall i \in G_f; b = 1, \ldots, N_{Gi} \tag{3.2c}$$

where α_i and ϕ_{ib} are the corresponding shadow prices. The decision variables of this problem are the amounts of power P_{Gib} to be generated by each unit i in each block b. While $\rho_{n(i)}$ are dual variables in the ISO problem in (3.14a)-(3.14e), they can be viewed as fixed values with respect to the optimization of (3.1).

Assumption 3.1. The associated marginal cost of block b for GenCo i denoted as $\lambda^C_{G_{ib}}$ is nondecreasing with respect to $P_{G_{ib}}$.

Using Assumption 3.1, necessary and sufficient conditions for the optimization of (3.1) subject to (3.2a) - (3.2c) are enumerated below, using dual variables α_i and ϕ_{ib}, which correspond to the KKT conditions (see Appendix A.1.5 for more details about KKT conditions.)

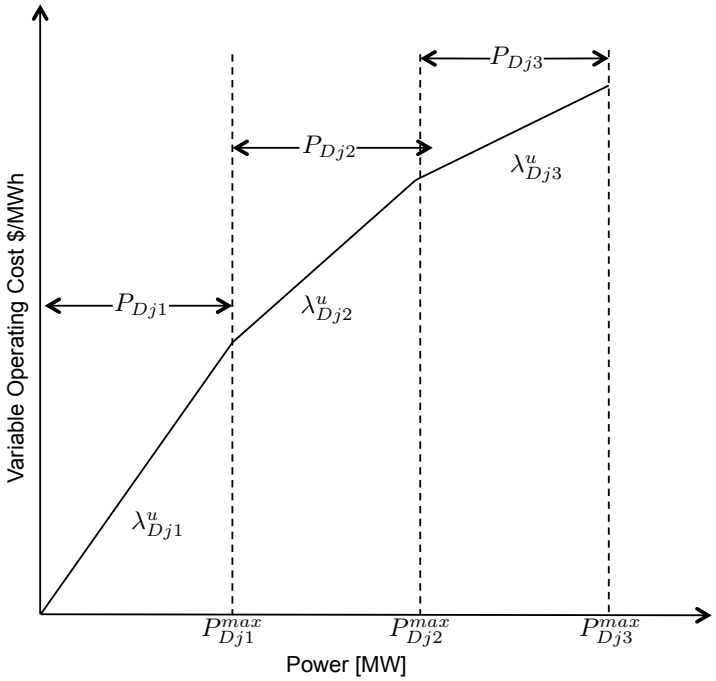

Figure 3.2: Piecewise linear utility function, adopted from [46].

$$0 \leq P_{Gib} \perp \left(-\rho_{n(i)} + \lambda^C_{G_{ib}} + \alpha_i + \phi_{ib} \right) \geq 0 \; \forall i \in G_f; \quad b = 1, \ldots, N_{Gi} \tag{3.3a}$$

$$0 \leq \alpha_i \perp \left(-\sum_{b=1}^{N_{Gi}} P_{Gib} + P^{max}_{Gi} \right) \geq 0; \forall i \in G_f \tag{3.3b}$$

$$0 \leq \phi_{ib} \perp \left(P^{max}_{Gib} - P_{Gib} \right) \geq 0; \forall i \in G_f; b = 1, \ldots, N_{Gi} \tag{3.3c}$$

where the symbol $0 \leq x \perp y \geq 0$ denotes the complementarity condition for optimality and is equivalent to $x^T y = 0$, $0 \leq x$ and $y \geq 0$.

3.1.2 Consumer Modeling

A consumer company (ConCo) is assumed to consist of N_D units, and the demand of each unit j, $j = 1, \ldots, N_D$, is divided into several blocks N_{D_j}, with a block-index $k = 1, \ldots, N_{D_j}$. The associated linear marginal utility function is denoted as $\lambda^U_{D_{jk}}$ which represents the value of using electricity for the consumer. The consumer is assumed to have a rational behavior and the utility function representing that behavior is nonlinear. Utility is linearized by blocks using marginal utilities denoted by $\lambda^U_{D_{jk}}$. The marginal utility represents the satisfaction increase for consuming an additional MWh. The utility function for ConCo j is shown in Figure 3.2. The goal of a ConCo is to maximize the total profit while consuming electricity. The overall profit, for a unit j in block k connected to node n, is determined as the difference between the utility $\lambda^U_{D_{jk}}$ and the corresponding LMP, $\rho_n(j)$. Assuming that the corresponding

power consumed is denoted as P_{Djk}, the maximization problem can be posed as

$$\text{maximize}_{P_{Djk}} \sum_{j \in D_q} \sum_{k=1}^{N_{Dj}} \left(\lambda^{U}_{D_{jk}} - \rho_{n(j)}\right) P_{Djk} \tag{3.4}$$

As before, this is subjected to the constraints

$$P_{Djk} \leq P^{max}_{Djk} : \sigma_j; \forall j \in D_q; k = 1, \ldots, N_{Dj} \tag{3.5a}$$

$$\sum_{k=1}^{N_{Dj}} P_{Djk} \geq P^{min}_{Djk} : \psi_{jk}; \forall j \in D_q; k = 1, \ldots, N_{Dj} \tag{3.5b}$$

$$P_{Djk} \geq 0; \forall j \in D_q; k = 1, \ldots, N_{Dj} \tag{3.5c}$$

where σ_j and ψ_{jk} are the corresponding dual variables for (3.5a) and (3.5b). While the constraint (3.5c) is almost always satisfied in current-day markets, this may not be the case in micro-grid topologies.

The decision variables of this problem are P_{Djk}, the amounts of power to be consumed by each demand j in each block k. While $\rho_{n(j)}$ are dual variables in the ISO problem denoted in (3.14a)-(3.14e), they can be viewed as fixed values, as before, with respect to the optimization of (3.4).

Assumption 3.2. The associated marginal utility of block k for ConCo j denoted as $\lambda^{u}_{D_{jk}}$ is non-increasing with respect to $P_{D_{jk}}$.

Under Assumption 3.2, necessary and sufficient conditions for the optimization of (3.4) subject to (3.5a) and (3.5b) are enumerated below, using dual variables σ_j and ψ_{jk}, which correspond to the KKT conditions [46]:

$$0 \leq P_{Djk} \perp \left(\rho_{n(j)} - \lambda^{u}_{D_{jk}} - \sigma_j + \psi_{jk}\right) \geq 0 \tag{3.6a}$$
$$\forall j \in D_q; k = 1, \ldots, N_{Dj}$$

$$0 \leq \psi_j \perp \Big(\sum_{k=1}^{N_{Dj}} P_{Djk} - P^{min}_{Djk}\Big) \geq 0; \forall j \in D_q; k = 1, \ldots, N_{Dj} \tag{3.6b}$$

$$0 \leq \sigma_{jk} \perp \left(-P_{Djk} + P^{max}_{Djk}\right) \geq 0; \forall j \in D_q; k = 1, \ldots, N_{Dj} \tag{3.6c}$$

3.1.3 Effect of Uncertainties and Demand Response

The most dominant impact of the introduction of distributed energy resources is due to uncertainties, which can directly alter the power generated. This in turn can affect the overall market equilibrium as well as the corresponding LMP. A first step in this direction is taken by introducing uncertainties in the decision variables introduced in Section 3.1.1. First the family of P_{Gib} is separated into P^{C}_{Gib}, $i = 1, \ldots, N_G$, and P^{W}_{Glb}, $l = 1, \ldots, N_W$, where N_G denotes the conventional dispatchable generating units, and N_W denotes distributed energy resources such as those based on wind and solar energy, which are non-dispatchable. At each node, both conventional generators and wind generators may be committed for production. We assume that the wind GenCo are competitive and that they submit their bids to the market as other conventional GenCo, and not modeled as a negative demand [62, 63].

Using the above discussion, the objective function defined in (3.1) is modified as

$$\text{maximize}_{P^w_{Glb}} \sum_{l\in G_w}\sum_{b=1}^{N_{Gl}} \left(\rho_{n(l)} - \lambda^C_{G^w_{lb}} - C^r_{G_r}(\Delta_{w_{lb}})\right) P^w_{Glb} \tag{3.7}$$

where P^w_{Glb} is the wind power from the l^{th} wind generator, and assumed to lie in the interval $\left[P^w_{Glb_{min}}, P^w_{Glb_{max}}\right]$. $\Delta_{w_{lb}}$ is due to wind uncertainty, given by

$$\Delta_{w_{lb}} = P^w_{Glb}\Delta_{Glb} \;\forall\; \Delta_{Glb} \in (-1, 1). \tag{3.8}$$

It should be noted that $\lambda^C_{G^w_{lb}}$ is the marginal cost function for the l^{th} wind generator which is close to zero. Finally, $C^r_{G_r}(\Delta_{w_{lb}})$ is a cost incurred by committing specific generators as reserves [64], due to the wind uncertainty $\Delta_{w_{lb}}$, and is modeled as

$$C^r_{G_r}(\Delta_{w_{lb}}) = \lambda^C_{G_r}\Delta_{w_{lb}} \tag{3.9}$$

where $\lambda^C_{G_r}$ is the associated linear operating cost of reserve for the generator that is committed by ISO as a reserve unit. $\lambda^C_{G_r}$ is determined using an independent procedure involving reserve markets [64]. The available wind energy is overestimated when $0 < \Delta_{Glb} < 1$ which implies that if the assumed power is not available, power can be purchased from an alternate source or that loads can be shed. We furthermore assume that the overestimation is only due to wind uncertainty and not because of strategic behavior of wind provider. The available wind energy is underestimated if $-1 < \Delta_{Glb} < 0$ which implies that surplus power is either sold to adjacent utilities, or consumed through fast redispatch and automatic gain control, or reduced through reduction of conventional generation.

The percentage of wind penetration is defined using a variable x^w as

$$x^w = \frac{\sum_{l\in G_w}\sum_{b=1}^{N_{Gl}} P^w_{Glb}}{\sum_{j\in D_q}\sum_{k=1}^{N_{Dj}} P^{max}_{Djk}} \tag{3.10}$$

where P^{max}_{Djk} is the maximum power demanded by consumer j in block k defined in (3.5a). We note that the impact of wind power on the market equilibrium is small if x^w is small, i.e., if wind penetration is low.

To include the effect of DR, we divide all ConCo units into dispatchable and non-dispatchable ones, we consider a dispatchable load P_{Djk}. This effect is modeled using a control parameter κ_{Djk}, and denotes the response of the consumers to a change in the Real Time Price (RTP) as

$$\bar{P}_{Djk} = P_{Djk}\left(1 - \kappa_{Djk}\right) \qquad 0 < \kappa_{Djk} < 1 \tag{3.11}$$

$\bar{P}_{Djk}$ denotes the consumption incorporated with demand responsiveness into RTP. It is assumed that κ_{Djk} is suitably calibrated to represent the effect of RTP on the consumer behavior, and is synonymous to *elasticity factor* defined in [84]. In contrast to Δ_{Glb} which may be unknown, κ_{Djk} is assumed to be controllable. However, the equilibrium as well as the LMPs are altered due to the presence of the perturbation parameters Δ_{Glb} and κ_{Djk}, the details of which are discussed in Section 3.4.

3.1.4 Modeling of Independent System Operator

In addition to GenCo and ConCo, a competitive electricity market also includes a coordinator such as the ISO, who is independent of these profit-maximization entities [85]. The responsibilities of the ISO are to enforce transmission capacity limits, to maintain independence from the market participants, to avoid discrimination against the market participants, and to promote the efficiency of the market.

In this paper we include network constraints in the underlying market model and the resulting prices are therefore the Locational Marginal Prices [25]. For ease of exposition, ohmic losses are not modeled in this paper. The standard market-clearing procedure is based on Social Welfare, S_w, defined as

$$S_W = \sum_{j \in D_q} \sum_{k=1}^{N_{Dj}} \lambda^B_{Djk} P_{Djk} - \sum_{i \in G_f} \sum_{b=1}^{N_{Gi}} \lambda^B_{G_{ib}} P_{Gib} \tag{3.12}$$

where the first and second terms denote the revenue due to surpluses stemming from bids from GenCo and ConCo, respectively. The market-clearing procedure is then given by

$$\text{maximize } S_W \tag{3.13a}$$

subject to

$$\sum_{i \in \theta_n} \sum_{b=1}^{N_{Gi}} P_{Gib} - \sum_{j \in \vartheta_n} \sum_{k=1}^{N_{Dj}} P_{Djk} - \sum_{m \in \Omega_n} B_{nm}\left[\delta_n - \delta_m\right] = 0; \rho_n \forall n \in N \tag{3.13b}$$

$$B_{nm}\left[\delta_n - \delta_m\right] \leq P^{max}_{nm}; \gamma_{nm} \forall n \in N; \forall m \in \Omega_n \tag{3.13c}$$

The constraints (3.13b) and (3.13c) are due to power balance and capacity limits, respectively. It can be seen that the associated Lagrange multipliers, ρ_n and γ_{nm}, are indicated in each constraint.

The underlying optimization problem of the ISO can therefore be defined as the optimization of (3.13a) subject to constraints (3.13b) and (3.13c). This problem can be restated as the solutions of the generation power blocks levels P_{Gib}, the demand power blocks levels P_{Djk}, the voltage angle δ_n, and dual variables ρ_n and γ_{nm} such that

$$0 \leq P_{Gib} \perp \left(\lambda^B_{Gib} - \rho_{n(i)}\right) \geq 0 \tag{3.14a}$$

$$0 \leq P_{Djk} \perp \left(\rho_{n(j)} - \lambda^B_{Djk}\right) \geq 0 \tag{3.14b}$$

$$0 \leq \delta_n \perp \Big(\sum_{m \in \Omega_n} B_{nm}\left[\rho_n - \rho_m\right] + \sum_{m \in \Omega_n} B_{nm}\left[\gamma_{nm} - \gamma_{mn}\right] \Big) \geq 0 \; \forall n \in N \tag{3.14c}$$

$$0 \leq \rho_n \perp \Big(-\sum_{i \in \theta_n} \sum_{b=1}^{N_{Gi}} P_{Gib} + \sum_{j \in \vartheta_n} \sum_{k=1}^{N_{Dj}} P_{Djk} + \sum_{m \in \Omega_n} B_{nm}\left[\delta_n - \delta_m\right] \Big) \geq 0 \; \forall n \in N \tag{3.14d}$$

$$0 \leq \gamma_{nm} \perp \left(P^{max}_{nm} - B_{nm}\left[\delta_n - \delta_m\right]\right) \geq 0 \tag{3.14e}$$

The decision variables of this problem are the amounts of power to be generated by each generating unit i in each block b, i.e., P_{Gib}; the amounts of power to be consumed by each demand j in each block k, i.e., P_{Djk}; and the locational marginal prices, $\rho_{n(j)}$. It should be noted that (3.14d) is arrived at using the balance equation, which implies that the term in the corresponding parenthesis is zero, and by multiplying this term by ρ_n, which is positive.

In summary, the market model that we consider in this paper includes optimization goals of GenCo discussed in Section 3.1.1 and formulated in Eqs. (3.1)-(3.2c), optimization goals of ConCo, (3.4)-(3.5c) and formulated in Section 3.1.2, and optimization of the ISO discussed in Section 3.1.4 and formulated in Eqs (3.12)-(3.13c). The corresponding equilibrium point is therefore defined as that which satisfies the following criteria:

1. maximum profit for every individual generating company

2. maximum utility for every individual consumer

3. maximum net social welfare for the ISO.

3.2 Market Equilibrium

We now discuss the overall market equilibrium. In the GenCo and ConCo optimization problems, given in (3.1)-(3.2c) and (3.4)-(3.5c), respectively, the Locational Marginal Prices appear as inputs. On the other hand, these LMPs appear in the optimization problem of the ISO in (3.12)-(3.13c) as dual prices corresponding to the balance equations, causing a tight link between the three families of optimization problems, thereby making the overall problem nontrivial.

It should be noted that under Assumptions 3.1 and 3.2, each of these three sets of optimization problems are convex programming problems. Thus, the Karush-Kuhn-Tucker (KKT) optimality conditions are both necessary and sufficient for describing the optimal solutions. The optimality conditions of the three sets of problems result in a Linear Complementarity Problem (LCP) which correspond to the market equilibrium for all $i \in G_f$, $b = 1, \ldots, N_{Gi}$, $j \in D_q$, $k = 1, \ldots, N_{Dj}$, and $m \in \Omega_n$ can be compactly stated as the solution of the following LCP:

$$0 \leq x \perp \left(Mx + q\right) \geq 0 \tag{3.15}$$

where x is defined as

$$x = \left[\mathbf{P_G} \quad \bar{\alpha} \quad \mathbf{\Phi} \quad \mathbf{P_D} \quad \mathbf{\Psi} \quad \mathbf{\Sigma} \quad \mathbf{\Delta} \quad \bar{\rho} \quad \mathbf{\Gamma}\right]^T, \tag{3.16}$$

with the following vector notations:

$$\mathbf{P_G} = \left[P_{G_{1b}}^T, P_{G_{2b}}^T, ..., P_{G_{N_G b}}^T\right]^T, \qquad \mathbf{\Lambda_D^u} = \left[\lambda_{D_{1k}}^{u^T}, \lambda_{D_{2k}}^{u^T}, ..., \lambda_{D_{N_D k}}^{u^T}\right]^T,$$
$$\mathbf{P_D} = \left[P_{D_{1k}}^T, P_{D_{2k}}^T, ..., P_{D_{N_D k}}^T\right]^T, \qquad \mathbf{\Psi} = \left[\psi_{1k}^T, \psi_{2k}^T, ..., \psi_{N_D k}^T\right]^T,$$
$$\mathbf{\Delta} = \left[\delta_1, ..., \delta_{N-1}\right]^T, \qquad \bar{\rho} = \left[\rho_1, ..., \rho_N\right]^T,$$
$$\mathbf{\Lambda_G^C} = \left[\lambda_{G_{1b}}^{C^T}, \lambda_{G_{2b}}^{C^T}, ..., \lambda_{G_{N_G b}}^{C^T}\right]^T, \qquad \mathbf{\Lambda_G^B} = \left[\lambda_{G1b}^{B^T}, \lambda_{G2b}^{B^T}, ..., \lambda_{GN_G b}^{B^T}\right]^T,$$
$$\bar{\alpha} = \left[\alpha_{1b}^T, \alpha_{2b}^T, ..., \alpha_{N_G b}^T\right]^T, \qquad \mathbf{\Lambda_D^B} = \left[\lambda_{D1k}^{B^T}, \lambda_{D2k}^{B^T}, ..., \lambda_{DN_D k}^{B^T}\right]^T,$$
$$\mathbf{P_G^{max}} = \left[P_{G1}^{max^T}, P_{G2}^{max^T}, ..., P_{GN_G}^{max^T}\right]^T, \qquad \mathbf{P_D^{min}} = \left[P_{D1}^{min^T}, P_{D2}^{min^T}, ..., P_{DN_D}^{min^T}\right]^T,$$
$$\mathbf{P_D^{max}} = \left[P_{D1k}^{max^T}, P_{D2k}^{max^T}, ..., P_{DN_D k}^{max^T}\right]^T, \qquad \mathbf{P_{Gb}^{max}} = \left[P_{G1b}^{max^T}, P_{G2b}^{max^T}, ..., P_{GN_G b}^{max^T}\right]^T,$$
$$\mathbf{P^{max}} = \left[P_{1m}^{max^T}, ..., P_{Nm}^{max^T}\right]^T, \qquad \mathbf{\Gamma} = \left[\gamma_{1m}, ..., \gamma_{Nm}\right]^T,$$
$$\mathbf{\Sigma} = \left[\sigma_{1k}^T, \sigma_{2k}^T, ..., \sigma_{N_D k}^T\right]^T, \qquad \mathbf{\Phi} = \left[\phi_{1b}^T, \phi_{2b}^T, ..., \phi_{N_G b}^T\right]^T.$$

M is defined as

$$M = \begin{bmatrix} 0 & I & I & 0 & 0 & 0 & 0 & -A_g & 0 \\ -\mathbf{1} & 0 & 0 & 0 & 0 & 0 & 0 & 0 & 0 \\ -I & 0 & 0 & 0 & 0 & 0 & 0 & 0 & 0 \\ 0 & 0 & 0 & 0 & I & -I & 0 & A_d & 0 \\ 0 & 0 & 0 & \mathbf{1} & 0 & 0 & 0 & 0 & 0 \\ 0 & 0 & 0 & -I & 0 & 0 & 0 & 0 & 0 \\ 0 & 0 & 0 & 0 & 0 & 0 & 0 & -A_g & 0 \\ 0 & 0 & 0 & 0 & 0 & 0 & 0 & -A_d & 0 \\ 0 & 0 & 0 & 0 & 0 & 0 & 0 & Y_{bus} & A_r^T B_{line} \\ -A_g & 0 & 0 & A_d & 0 & 0 & Y_{bus} & 0 & 0 \\ 0 & 0 & 0 & 0 & 0 & 0 & B_{line} A_r & 0 & 0 \end{bmatrix} \tag{3.17}$$

where B_{line} denotes the line admittance matrix (N_t by N_t diagonal matrix) with elements B_{nm} and A denotes the $N_t \times N$ bus incidence matrix. The reduced bus incidence matrix denoted as A_r is a $(N_t \times N - 1)$ matrix which is equal to A with the column corresponding to the reference bus removed. $Y_{bus} = A_r^T B_{line} A$ denotes the nodal admittance matrix. $\mathbf{1}$ is a $m \times n$ matrix with all elements equal to unity. A_g is generators incidence matrix where $A_{g_{ij}} = 1$ if the i^{th} generator is connected to j^{th} bus and $A_{g_{ij}} = 0$ if the i^{th} generator is not connected to j^{th} bus. A_d is a load incident matrix where $A_{d_{ij}} = 1$ if the i^{th} consumer is connected to j^{th} bus and $A_{d_{ij}} = 0$ if the i^{th} consumer is not connected to j^{th} bus. And finally, q is defined as follows:

$$q = \left[\mathbf{\Lambda_G^C}\ \mathbf{P_G^{max}}\ \mathbf{P_{Gb}^{max}}\ -\mathbf{\Lambda_D^u}\ -\mathbf{P_D^{min}}\ \mathbf{P_D^{max}}\ \mathbf{\Lambda_G^B}\ \mathbf{\Lambda_D^B}\ 0\ \mathbf{P^{max}}\right]^T \tag{3.18}$$

The corresponding solution x^* of (3.15), which determines the market equilibrium and is dependent on M and q, is denoted as

$$x^* \triangleq LCP(M, q). \tag{3.19}$$

Definition 3.1. A matrix $M \in R^{n\times n}$ is called a P-matrix if its all principal minors are positive.

The following theorem is useful for connecting the LCP solution with the properties of matrix M.

Theorem 3.1. *[86] Assume that for all GenCos and ConCos, Assumptions 3.1 and 3.2 hold. In (3.15), M is a P-matrix if and only if the $LCP(M,q)$ has a unique solution for any $q \in R^n$.*

Theorem (3.1) sets the stage for connecting the market equilibrium denoted as x^* as the LCP solution with the Nash equilibrium of the corresponding game in the following section.

3.3 A Game-Theoretic Framework for Wholesale Energy Market Equilibrium

Game theory is highly useful to establish market properties in a systematic manner and thus provide more comprehensive predictive capabilities and possible challenges in electricity markets. Game theoretical models are typically static in the sense that they assume some sort of steady-state behavior of the fundamental market drivers. In the following sections electricity market equilibrium is delineated using game theoretical methods.

3.3.1 Game Theory and NASH Equilibrium

A game is a representation of a situation in which a number of individuals interacts with each other in a setting of strategic interdependence. To describe a game, there are four things to consider: 1) the players, 2) the rules of the game, 3) the outcomes and 4) the payoffs and the preferences (utility functions) of the players. A player plays a game through actions. An action is a choice or election that a player takes, according to his (or her) own strategy. Since a game sets a framework of strategic interdependence, a participant should be able to have enough information about its own and other players' past actions. This is called the information set. A strategy is a rule that tells the player which action(s) it should take, according to its own information set at any particular stage of a game. Finally, a payoff function expresses the utility that a player obtains given a strategy profile for all players.

Game-theoretical analyses of the wholesale electricity markets follow a certain logic employed by the game-theorist. Specifically, the game-theoretical description of competition in these markets is usually based on several typical informational assumptions such as:

- A subset of information is available to all players (common knowledge);
- A subset of information is available to each individual player but not to other players;
- All the above information is available to the game-theorist for being able to analyze the game.

Based on these informational assumptions and on the formal mathematical description of the game (e.g., definition of strategies, constraints, objectives, order of moves, and definition of equilibrium) the game-theorist analyzes the game where the following questions are usually

posed and answered: (i) Does any equilibrium exist? (ii) If it exists, is it unique? (iii) How can this equilibrium (or equilibria) be computed? (iv) What are the economic and policy implications of the equilibrium (or equilibria)?

In electricity market, particularly, it is assumed that LMP is available to all players, and cost function and utility function is only available to each individual player but not to other players. The game-theoretical studies imply that the equilibrium found by solving a particular game is a likely outcome of the market which the game in question intends to model. In the subsequent sections, the posed questions (i)-(iv) are answered.

3.3.2 Electricity Market Equilibrium and Nash Equilibrium

Let a strategic form game $G = \langle \mathscr{I}, (S_p)_{p\in\mathscr{I}}, (u_p)_{p\in\mathscr{I}} \rangle$ with a finite set of players in the wholesale market, i.e. $\mathscr{I} = G_f \bigcap G_w \bigcap D_q$ represents the game theoretical description of competition in the wholesale market modeled in Section 3.1. We denote $s_p \in S_p$ as an action for player p where S_p is the set of feasible actions for player p. For example if $p \in G_f$, then $S_p := \{s_p \in \mathbb{R}^+ | (3.2a) \text{ and } (3.2b) \text{ hold}\}$. We denote $S = \prod_p S_p$ as the set of all action profiles. $u_p : S \to R$ is the payoff function of player p defined in Eq. (3.1) for all $p \in G_f$ and in Eq. (3.4) for all $p \in D_q$. In addition, we use the notation $s_{-p} = [s_q]_{q\neq p}$ as a vector of actions for all players except p, and $S_{-p} = \prod_{q\neq p} S_q$ as the set of all action profiles for all players except p. $(s_p, s_{-p}) \in S$ denotes a strategy profile of the game.

The electricity market represented as the game $G = \langle \mathscr{I}, (S_p)_{p\in\mathscr{I}}, (u_p)_{p\in\mathscr{I}} \rangle$ can be viewed as a class of constrained noncooperative games, which has been widely studied in [89]. Informally, a set of power generation profile $\mathbf{P_G}^*$ and consumption profile $\mathbf{P_D}^*$ is a Nash equilibrium if no player can do better by unilaterally changing his or her strategy. A precise definition of Nash equilibrium is provided below.

Definition 3.2. A Pure Strategy Nash Equilibrium of a strategic game $G = \langle \mathscr{I}, (S_p)_{p\in\mathscr{I}}, (u_p)_{p\in\mathscr{I}} \rangle$ is a strategy profile $s^* \in S$ such that for all $p \in \mathscr{I}$

$$u_p(s_p, s^*_{-p}) \leq u_p(s^*_p, s^*_{-p}) \; \forall s_p \in S_p. \tag{3.20}$$

In the following theorem, the connection between market equilibrium, x^*, and Pure Strategy Nash Equilibrium is presented.

Theorem 3.2. *Assume that for all GenCos and ConCos Assumptions 3.1 and 3.2 hold. If M is a P-matrix, then the equilibrium of the market denoted as $x^* \triangleq LCP(M,q)$ exists and is identical to a unique Pure Strategy Nash Equilibrium.*

Proof. A proof by contradiction follows. That is, we assume Assumptions 3.1 and 3.2 hold, that M is a P-matrix and that $x^* \triangleq LCP(M,q)$ is not a Pure Strategy Nash Equilibrium. Since M is a P-matrix and Assumptions 3.1 and 3.2 hold, then Theorem 3.1 implies that $x^* \triangleq LCP(M,q)$ exists and is the unique maximizer of the GenCo problem denoted in (3.1) - (3.2b), ConCo problem denoted by (3.4) - (3.5b), and ISO problem denoted by (3.13a) - (4.8c). That is

$$u_p(x_p, x^*_{-p}) \leq u_p(x^*_p, x^*_{-p}) \; \forall x_p \in S_p. \tag{3.21}$$

Now let us denote a Pure Strategy Nash equilibrium by ${x_N}^*$. Using the Nash Equilibrium definition in (3.20), it follows that

$$u_p(x_p, x^*_{-p}) \leq u_p(x^*_{N_p}, x^*_{N_{-p}}) \; \forall x_p \in S_p. \tag{3.22}$$

Since we assume that $x^* \triangleq LCP(M,q)$ is not a Pure Strategy Nash Equilibrium, it implies that both x^* and x^*_N maximize the payoffs which contradicts the uniqueness of $x^* \triangleq LCP(M,q)$ and therefore completes the proof. □

Remark 3.1. Theorem 3.2 provides conditions under which the market has a unique equilibrium that is identical to the Nash equilibrium of each player, i.e. no degeneracy can occur in the market if M is a P-matrix and Assumptions 3.1 and 3.2 hold [46]. Assumptions 3.1 and 3.2 essentially imply that the underlying cost functions are convex and that the utility functions are concave.

3.4 Perturbation Analysis of Market Equilibrium

Using the results in the previous section, we now present a perturbation bound for the equilibrium of the electrical market. As we discussed above, the market equilibrium x^* is the solution of $LCP(M,q)$ and given in Eq. (3.15). As we discussed in Section 3.1.3, the wind forecast error parametrized by Δ_{Glb} in (3.8), and DR parametrized by κ_{Djk} in (3.11), are considered as two sources of perturbations. These components can affect M and q as $M + \Delta M$ and $q + \Delta q$, respectively. Therefore the underlying LCP problem is altered as

$$\begin{aligned} & x^T \left((M + \Delta M)x + (q + \Delta q) \right) = 0 \\ & x \geq 0 \\ & (M + \Delta M)x + (q + \Delta q) \geq 0 \end{aligned} \tag{3.23}$$

This in turn leads to a corresponding equilibrium

$$x^*_\Delta \triangleq LCP(M + \Delta M, q + \Delta q). \tag{3.24}$$

In the rest of this section, the effects that cause x^*_Δ to deviate from x^* are analyzed . The following definitions are useful.

Definition 3.3. Define non-dimensional perturbation parameters ϵ_M and ϵ_q as

$$||\Delta M|| \leq \epsilon_M \parallel M \parallel, \tag{3.25}$$

$$||\Delta q|| \leq \epsilon_q \parallel q \parallel, \tag{3.26}$$

a constant η as

$$\eta = \epsilon_M \beta(M) \parallel M \parallel, \tag{3.27}$$

where

$$\beta(A) = max_{d \in [0,1]} ||(I - D + DA)^{-1} D||, \tag{3.28}$$

and a diagonal matrix $D = \text{diag}(d_i)$ with $0 \leq d_i \leq 1$, $i = 1, 2, \ldots, n$.

Theorem 3.3. *If the nominal market (3.15) has a unique solution and $\eta < 1$, then the perturbed market in (3.23) has a unique solution x^*_Δ and satisfies the following inequality*

$$\frac{\| x^* - x^*_\Delta \|}{\| x^* \|} \leq \mu(\Delta_{Glb}, \kappa_{Djk}) \tag{3.29}$$

where $\epsilon_0 = max\{\epsilon_M \| M \|, \epsilon_q \| q \|\}$, and

$$\mu(\Delta_{Glb}, \kappa_{Djk}) = \frac{2\epsilon_0}{1-\eta}\beta(M). \tag{3.30}$$

In order to prove Theorem 3.3, we need to characterize the dependence of $x(M,q)$ on the market parameters. This is characterized in the following theorem.

Theorem 3.4. *(Lemma 2.1 and Theorem 2.2 in [91]) Matrix A is a P-matrix if and only if $(I - D + DA)$ is nonsingular for any diagonal matrix $D = diag(d_i)$ with $0 \leq d_i \leq 1$, $i = 1, 2, \ldots, n$. Furthermore, if $x(A,q)$ and $x(B,p)$ are the solutions of the corresponding $LCP(A,q)$ and $LCP(B,p)$ respectively, we have:*

$$\frac{\| x(B,p) - x(A,q) \|}{\| x(B,p) \|} \leq \beta(A) \| (A-B)x(B,p) + q - p \| . \tag{3.31}$$

Now the proof of Theorem 3.3 is provided as follows.

Proof. If the nominal electrical market (3.15) has a unique solution according to Theorem 3.1, the matrix M is P-matrix. This in turn, according to Theorem 3.4, implies that $(I - D + DM)$ is nonsingular for any diagonal matrix $D = \text{diag}(d_i)$ with $0 \leq d_i \leq 1$, $i = 1, 2, \ldots, n$. We have the following equality

$$\big(I - D + D(M + \Delta M)\big) = (I - D + DM)\big(I + M_0 \Delta M\big) \tag{3.32}$$

where

$$M_0 = (I - D + DM)^{-1} D. \tag{3.33}$$

Noting the definition of $\beta(M)$ in (3.28), it follows that

$$||M_0 \Delta M|| \leq \beta(M)||\Delta M|| \leq \eta, \ \forall \Delta M \in \mathscr{M} \tag{3.34}$$

where the set $\mathscr{M}$ is defined as

$$\mathscr{M} : \{\Delta M \big| \beta(M)||\Delta M|| \leq \eta\}.$$

Since $\eta < 1$ according to theorem 3.3, it follows that $I + M_0 \Delta M$ is nonsingular for all $\Delta M \in \mathscr{M}$. We therefore conclude from (3.32) that $\big(I - D + D(M + \Delta M)\big)$ is a P-matrix and thus the market in (3.23) has a unique solution for all $\Delta M \in \mathscr{M}$ and $\eta < 1$.

We now show that x^*_Δ satisfies (3.29). Using (3.31) in Theorem 3.4, we have that:

$$\frac{\| x^* - x^*_\Delta \|}{\| x^* \|} \leq \beta(M + \Delta M)||\Delta M x^* + \Delta q||. \tag{3.35}$$

We rewrite the argument of $\beta(M+\Delta M)$ as

$$\begin{aligned}&\big(I-D+D(M+\Delta M)\big)^{-1}D=\\&\big(I+M_0(\Delta M)\big)^{-1}(I-D+DM)^{-1}D.\end{aligned}\tag{3.36}$$

Using Appendix 1 in [13], we have that

$$||\big(I+M_0(\Delta M)\big)^{-1}|| \leq \frac{1}{1-\beta(M)||\Delta M||} \leq \frac{1}{1-\eta}.\tag{3.37}$$

Taking norms on both sides of (3.36), we obtain that

$$\beta(M+\Delta M) \leq \frac{1}{1-\eta}\beta(M).\tag{3.38}$$

Therefore (3.35) can be rewritten as

$$\frac{\parallel x^*-x^*_\Delta \parallel}{\parallel x^* \parallel} \leq \frac{1}{1-\eta}\beta(M)||\Delta M+\Delta q||.\tag{3.39}$$

Considering the definition of ΔM in (3.25) and Δq in (3.26), we obtain, in turn,

$$\frac{\parallel x^*-x^*_\Delta \parallel}{\parallel x^* \parallel} \leq \frac{2\epsilon_0}{1-\eta}\beta(M)\tag{3.40}$$

where $\epsilon_0 = max\{\epsilon_M \parallel M \parallel, \epsilon_q \parallel q \parallel\}$ which is the desired bound. □

Remark 3.2. Theorem 3.3 implies that the uncertainty in market can lead to a maximum shift in the equilibrium by an amount $\mu(\Delta_{Glb}, \kappa_{Djk})$. As this function is nonlinear, determining an analytical relationship between $\mu(\Delta_{Glb}, \kappa_{Djk})$, Δ_{Glb} and κ_{Djk} is exceedingly difficult. As will be shown in the next section, simulation studies show that as κ_{Djk} increases, μ decreases. This in turn brings the perturbed equilibrium closer to the nominal equilibrium.

3.4.1 Game Theoretic Interpretations of Wind Uncertainty

We now evaluate the perturbed market using tools from game theory. Consider two strategic games defined by two profiles of utility functions as $G = \langle \mathscr{I}, (S_p)_{p\in\mathscr{I}}, (u_p)_{p\in\mathscr{I}}\rangle$ and $\tilde{G} = \langle \mathscr{I}, (S_p)_{p\in\mathscr{I}}, (\tilde{u}_p)_{p\in\mathscr{I}}\rangle$. If s^*_p is a Nash equilibrium of G, then s^*_p need not be a Pure Strategy Nash Equilibrium of $\tilde{G}$. The equilibria of the strategic games G and $\tilde{G}$ may be far apart, even if $(u_p)_{p\in\mathscr{I}}$ and $(\tilde{u}_p)_{p\in\mathscr{I}}$ are very close to each other.

Definition 3.4. Given $\epsilon \geq 0$, a Pure Strategy Nash Equilibrium $s^* \in S$ is called an $\epsilon-$ equilibrium if for all $p \in \mathscr{I}$ and $s_p \in S_p$,

$$u_p(s_p, s^*_{-p}) \leq u_p(s^*_p, s^*_{-p}) + \epsilon \ \forall s_p \in S_p.\tag{3.41}$$

Obviously in Definition 3.4, when $\epsilon = 0$, the $\epsilon-$ equilibrium is a Pure Strategy Nash Equilibrium in the sense of Definition 3.2. The following definition formally defines the closeness of two strategic form games.

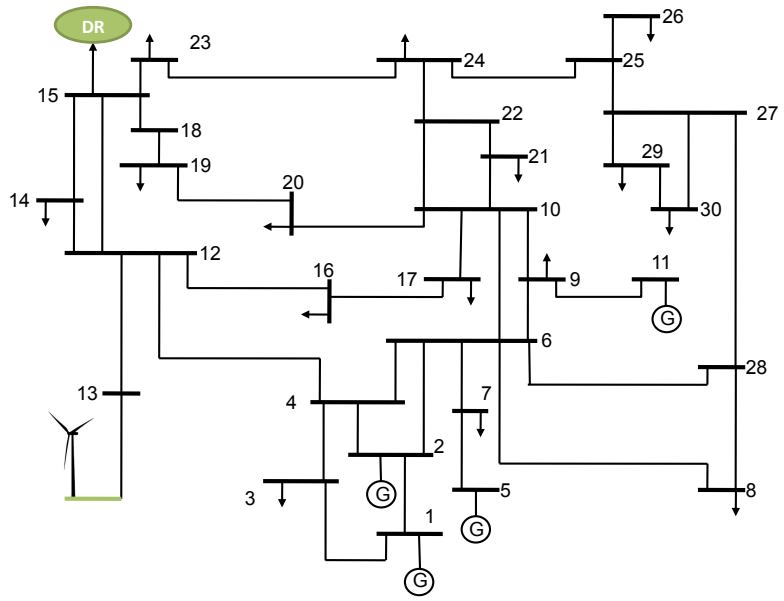

Figure 3.3: IEEE 30-bus case study

Definition 3.5. Let $G = \langle \mathscr{I}, (S_p)_{p\in\mathscr{I}}, (u_p)_{p\in\mathscr{I}} \rangle$ and $\tilde{G} = \langle \mathscr{I}, (S_p)_{p\in\mathscr{I}}, (\tilde{u}_p)_{p\in\mathscr{I}} \rangle$ be two strategic form games, then $\tilde{G}$ is a $\alpha -$ approximation of G if for all $p \in \mathscr{I}$,

$$|u_p(s) - \tilde{u}_p(s)| \leq \alpha \; \forall s \in S. \tag{3.42}$$

The next proposition relates the $\epsilon -$ equilibrium of close games as defined in 3.5.

Theorem 3.5. *If $\tilde{G} = \langle \mathscr{I}, (S_p)_{p\in\mathscr{I}}, (\tilde{u}_p)_{p\in\mathscr{I}} \rangle$ is an $\alpha -$ approximation to $G = \langle \mathscr{I}, (S_p)_{p\in\mathscr{I}}, (u_p)_{p\in\mathscr{I}} \rangle$ and $s^* \in S$ is an equilibrium of $\tilde{G}$, then $s^* \in S$ is a $(2\alpha) -$ equilibrium of G.*

Proof. For all $p \in \mathscr{I}$ and all $s_p \in S_p$, we can write

$$\begin{aligned} u_p(s_p, s^*_{-p}) - u_p(s^*_p, s^*_{-p}) = u_p(s_p, s^*_{-p}) - \tilde{u}_p(s_p, s^*_{-p}) + \\ \tilde{u}_p(s_p, s^*_{-p}) - \tilde{u}_p(s^*_p, s^*_{-p}) + \\ \tilde{u}_p(s^*_p, s^*_{-p}) - u_p(s^*, s^*_{-p}). \end{aligned} \tag{3.43}$$

Since s^* is a Pure Nash Equilibrium of $\tilde{G}$, then $\tilde{u}_p(s_p, s^*_{-p}) - \tilde{u}_p(s^*_p, s^*_{-p}) \leq 0$. This in turn implies that

$$\begin{aligned} u_p(s_p, s^*_{-p}) - u_p(s^*_p, s^*_{-p}) \leq |u_p(s_p, s^*_{-p}) - \tilde{u}_p(s_p, s^*_{-p})| + \\ |\tilde{u}_p(s^*_p, s^*_{-p}) - u_p(s^*, s^*_{-p})|. \end{aligned} \tag{3.44}$$

Using Definitions 3.4 and 3.5, it follows that

$$u_p(s_p, s^*_{-p}) - u_p(s^*_p, s^*_{-p}) \leq 2\alpha \tag{3.45}$$

which in turn implies that $s^* \in S$ is a $(2\alpha) -$ equilibrium of G. □

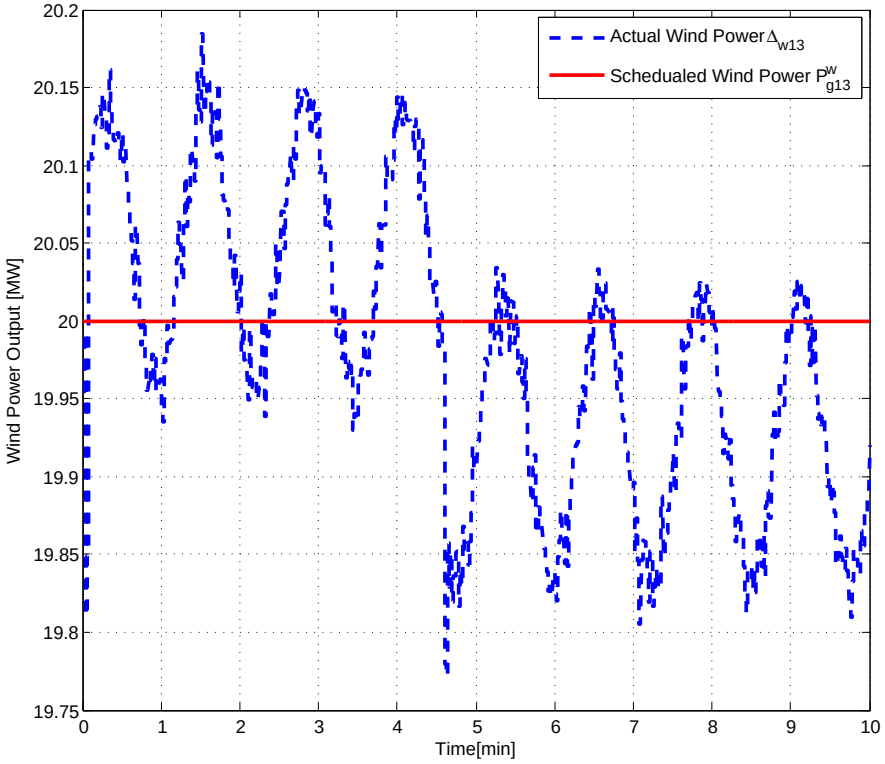

Figure 3.4: Actual wind power and scheduled wind output

Proposition 3.1. *Assume that the perturbed market denoted by the strategic game $\tilde{G}$ under uncertainties Δ_{Glb} and κ_{Djk} is an $\alpha-$approximation of the nominal market denoted by G. If x^*_Δ is an equilibrium of the perturbed market $\tilde{G}$, then x^*_Δ is a $(2\alpha)-$equilibrium of the nominal market G.*

Remark 3.3. If the wind uncertainty due to forecast error Δ_{Glb} increases, from Definition 3.5, it follows that α will increase as the relative payoffs of the corresponding generators will have an increased error. Proposition 3.1 implies that in such a case, the equilibrium of the perturbed game $\tilde{G}$ is correspondingly far away from the nominal market G. It should be noted that as the forecast error increases, the corresponding cost of deploying ancillary services increases as well. If a DR program is in place, this cost increase is conveyed to the consumer, leading to a decrease in the load quantified by the demand curtail factor κ_{Djk} as in (3.11). Similar to our observation in Remark 3.2, it should be noted that the exact impact of an increasing κ_{Djk} on α is difficult to quantify due to its nonlinearity. However, simulation studies show, as discussed in Section 3.5, that as κ_{Djk} increases, α decreases.

3.5 Case Study

An IEEE 30-bus case is used for simulation studies, whose interconnections are shown in Figure 3.3. The size and price of each block of each GenCo are shown in Table B.2. Generator 2 is assumed to function partially in the energy market and partially in the reserve market. The bids associated with all generators in these markets are indicated in Table B.2. The linear

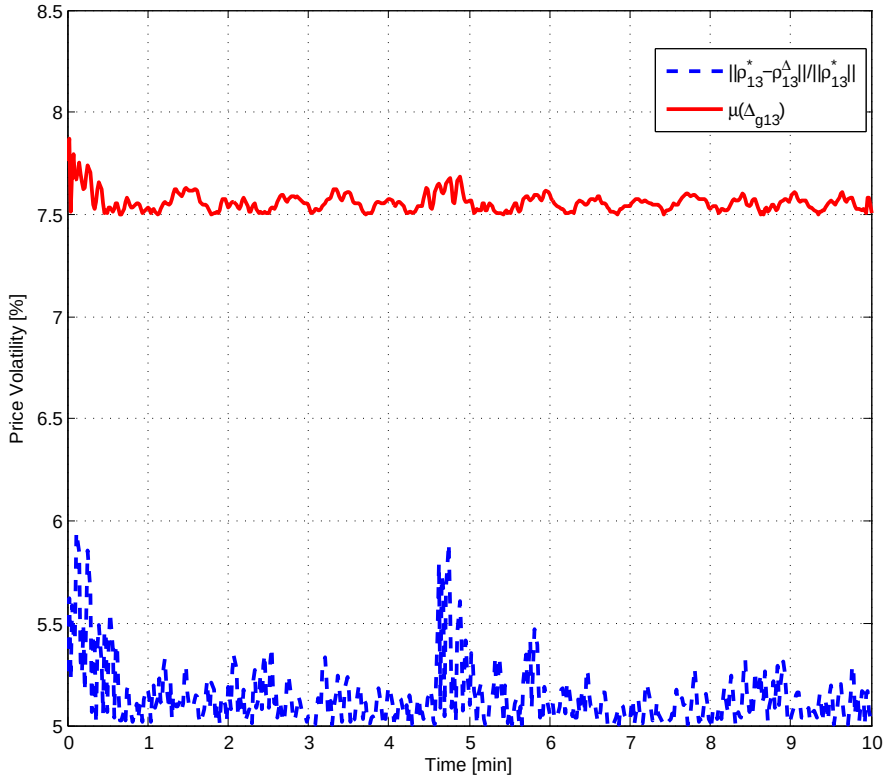

Figure 3.5: Price volatility and market equilibrium shift due to the wind uncertainty

operating costs of Generator 2 are assumed to be the same in both the energy and reserve market. For the sake of simplicity, we assume that each GenCo bids its marginal cost. The minimum power requirement of each demand and the size and price of each block of each demand are shown in Table B.3. We assume that only some of the loads are participating in the market, with the rest remaining fixed and are shown in Table B.4. The reactance B_{nm} of the line connecting bus n and bus m can be found in Table B.5. The transmission capacity limits of all lines are chosen to be 100 MW. The line parameters are per-unit with three-phase base of 230 kV and 10 MVA.

3.5.1 Nominal Market Equilibrium

Table 3.1 provides equilibrium results concerning generator output, revenue, and profit for the electric power market if no wind shortfalls are imposed to the system. These results are obtained by solving the LCP problem in (3.14a)-(3.14e). Table 3.2 shows the power consumed and the corresponding demand payments. The Locational Marginal Price in all of the buses is 23.62 $\$/MWh$ and is uniform due to the fact that transmission lines are not congested.

3.5.2 Perturbed Market Equilibrium with Wind Uncertainty

It is assumed that GenCo at bus 13 is wind based, committed to produce 20 MW as can be seen in Table 3.1, row 5, and subjected to an uncertainty Δ_{G13} whose profile was adopted

Tabular 3.1: Results of market equilibrium for GenCo, no wind uncertainty

Name	Power outputMW	Revenues$\$/h$	Cost$\$/h$	Total Profit$\$/h$
P_{g_1}	30	708.6	660	48.6
P_{g_2}	11.64	274.93	274.76	0.18
P_{g_5}	80	1889.6	1000	889.6
$P_{g_{11}}$	80	1889.6	1000	889.6
$P_{g_{13}}$	20	472.4	8	464.4

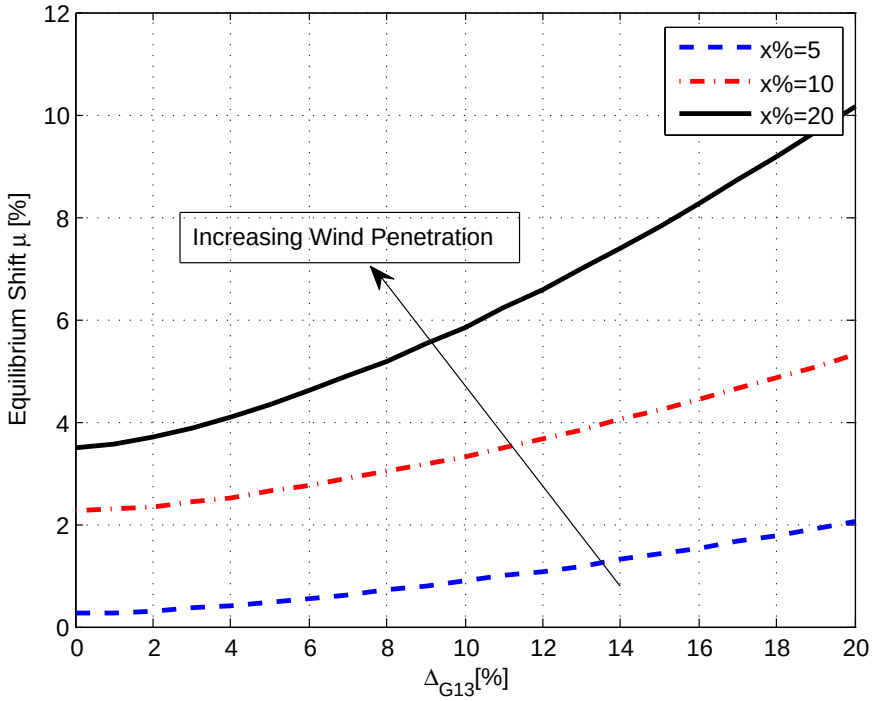

Figure 3.6: Market equilibrium shift as a function of uncertainty and wind penetration

from [4] and is shown in Figure 3.4 over a 10-minute window. This duration was chosen as it corresponds to a typical market clearing period. Using this wind profile, the resulting perturbed market was simulated. In particular, at each instant t over the 10-minute window, the corresponding solutions of the LMP of the ideal and perturbed market equilibrium as ρ^* and ρ^*_Δ, were determined using (3.19) and (3.24), respectively. Also, using the corresponding matrices M, q, ΔM and Δq, the market equilibrium shift μ defined in (3.30) was computed. These are shown in Figure 3.5, which confirms that μ is an upper bound on the equilibrium. This, together with (3.9), implies therefore that μ can be used as a metric for assessing reserve costs that accompany wind uncertainties. Figure 3.5 also illustrates that the volatility of this equilibrium is a function of the wind uncertainty, as also has been pointed out in [92].

The effect of changes in Δ_{G13} on μ is quantified further in Figure 3.6. Also shown in this figure is the change in μ as x_w, the wind penetration, is changed. It can be seen that μ is a

Tabular 3.2: Results of market equilibrium for ConCo, no wind uncertainty

Name	Power consumed MW	Total Payment $\$/h$
P_{d_7}	11	259.82
$P_{d_{15}}$	12	283.44
$P_{d_{30}}$	10	236.2
P_{d_9}	15.5	366.1
$P_{d_{26}}$	9.5	224.4
$P_{d_{27}}$	12.0	283.44

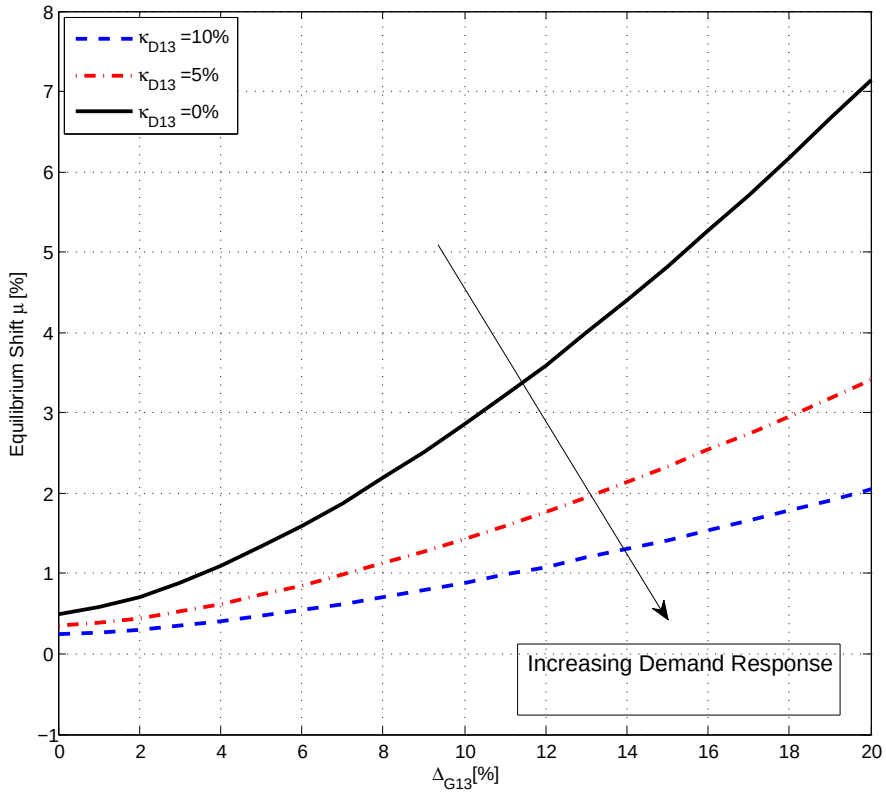

Figure 3.7: Market equilibrium shift as a function of uncertainty and demand curtailment factor

monotonically increasing function of both Δ_{G13} as well as x_w.

3.5.3 Measure of Uncertainty Incorporating Wind Uncertainty With Demand Response

We now introduce a perturbation κ_{D15} into the picture to represent a DR-compatible consumer at bus 15. We numerically evaluate the effect of κ_{D15} on μ for various values of Δ_{G13}. Figure 3.7 shows the corresponding results which clearly demonstrate that κ_{D15} can reduce the equilibrium shift and therefore the cost of uncertainty in the presence of a wind forecast

error.

3.6 Concluding Remarks

The current energy crisis has created an urgent need in integrating renewable energy resources into the power grid. The latter in turn can introduce intermittency and uncertainty into the picture, thereby introducing a prohibitive integration cost. The main contributions of this chapter are the introduction of an analytical framework to evaluate the integration cost and providing a computable upper bound for market equilibrium shift with wind uncertainty and DR.

The analytical framework introduced in this chapter consists an overall model of the energy market including GenCo, ConCo as well as ISO, which allows the analysis of the market under normal conditions and perturbed conditions. Game theory is used to establish sufficient conditions for the existence of a unique Pure Nash Equilibrium for the nominal market. The perturbed market in the presence of wind uncertainty is analyzed using the concept of closeness of two strategic games and the equilibria of close games based on the notion of $\alpha-$approximation and $\epsilon-$equilibrium. This analysis is used to quantify the effect of wind uncertainty and its possible mitigation using DR in the form of a parameter denoted as Curtailment Factor. Finally, numerical results are included that validate the theoretical results, using an IEEE 30-bus network.

4 Dynamic Modeling of the Electricity Market

Summary. *The notion of market disequilibrium is provided in this chapter as a market mechanism to attain market equilibrium in the presence of uncertainties. The main contributions of this chapter are*

- *The notion of disequilibrium process to attain efficient equilibrium,*
- *Conditions under which the competitive equilibrium exists and it is unique,*
- *Stability of the disequilibrium process, which is provided in Theorem 4.5 and it is a direct connection with consumer's elasticity in response to the real time price and the latency of market real time pricing,*
- *Robust stability of the wholesale market in the presence of wind uncertainty, which is discussed in Theorem 4.6.*

The recent paradigm shift in the architecture of a smart grid is driven by the need to integrate Renewable Energy Resources (RERs), the availability of information via advanced metering and communication, and an emerging policy of a demand structure that is intertwined with pricing. The introduction of both RERs as well as efforts to integrate them through an information processing layer brings in dynamic interactions between the major components of a smart grid. In this chapter, a dynamic model of the wholesale energy market that captures the effect of uncertainties of RERs and real-time pricing with Demand Response (DR) is derived, and linked to the notion of a *disequilibrium process*. Beginning with a framework that includes real-time pricing as an underlying state, an attempt is made in this model to capture the dynamic interactions between generation, demand, locational marginal price, and congestion price near the equilibrium of the optimal dispatch. Conditions under which stability of the market can be guaranteed are derived. Modeling the effect of RERs and DR as perturbations, robust stability of the energy market model in the presence of such perturbations is discussed. Numerical studies of an IEEE 30-bus are reported to illustrate the dynamic model, its stability properties, and the effect of perturbations.

This chapter has been organized as follows: In Section 4.1, wholesale energy market is introduced, and the underlying dynamic model of the wholesale market is presented in Section 4.2 and its stability properties are derived in Section 4.3. In Section 4.4, the model is expanded to include the effect of uncertainties and the stability of the uncertain wholesale market is studied and the region of attraction is established. Finally in Section 4.5, numerical studies of an IEEE 30-bus are reported. In Section 4.6, summary and concluding remarks are provided.

4.1 Dynamic Modeling of Market Agent Behavior

The electricity market that is considered in this chapter is wholesale and is assumed to function as follows: First, each generating company (GenCo) submits the bidding stacks of each of its units to the pool. Similarly, each consumer (ConCo) submits the bidding stacks of each of its demands to the pool. Then, the ISO clears the market using an appropriate market-clearing procedure resulting in prices and production and consumption schedules. In what follows, the models for each of the components (GenCo, ConCo, and ISO) together with their constraints and the optimization goal are presented.

4.1.1 Generating Company

It is assumed that the generating company $i \in G_f = \{1, 2, \ldots, N_G\}$ consists of only one generating unit, and that the production of each generating company is denoted as P_{Gi}. In contrast to Chapter 3 that piece-wise linear cost function is used, in this chapter quadratic cost function is implemented. The associated operating cost is denoted as $C_{G_i}(P_{Gi})$

$$C_{G_i}(P_{Gi}) = b_{Gi}P_{Gi} + \frac{c_{Gi}}{2}P_{Gi}^2 \tag{4.1}$$

where b_{Gi}, and c_{Gi} are generators cost coefficients. The goal of the company is to maximize its overall profit, π_{Gi}, and is stated as

$$\text{maximize}_{P_{Gi}} \pi_{Gi} = \text{maximize}_{P_{Gi}} \left[\rho_{n(i)}P_{Gi} - C_{G_i}(P_{Gi})\right] \tag{4.2}$$

$$\text{subject to } P_{Gi} \in X_{G_i} \tag{4.3}$$

where $\rho_{n(i)}$ denotes the LMP of unit i at node n in the network, and $X_{G_i} := \{x | P_{Gi}^{min} \leq x \leq P_{Gi}^{max}\}$ is the closed convex set in $\mathbb{R}^{N_G}$ that P_{Gi}^{min} and P_{Gi}^{max} are lower and upper bounds for the production of GenCo i.

4.1.2 Consumer Modeling

A consumer company (ConCo) $j \in D_q = \{1, 2, \ldots, N_D\}$ is assumed to aggregate to one unit, and the demand of each ConCo is denoted as P_{Dj}. The associated quadratic utility function is denoted as $U(P_{Dj})$ which represents the value of using electricity for the consumer and is defined as

$$U(P_{Dj}) = b_{Dj}P_{Dj} + \frac{c_{Dj}}{2}P_{Dj}^2 \tag{4.4}$$

where b_{Dj}, and c_{Dj} are consumers utility coefficients. The goal of the ConCo is to maximize the total profit, π_{Dj}, while consuming electricity. This profit, for a unit j connected to node n, is determined as the difference between the utility $U(P_{D_j})$ and the corresponding cost of electricity $\rho_{n(j)}P_{Dj}$ where $\rho_{n_(j)}$ is LMP of ConCo j at node n in the grid. Assuming that the corresponding power consumed is denoted as P_{Dj}, the maximization problem can be posed as

$$\text{maximize}_{P_{D_j}} \pi_{Dj} = \text{maximize}_{P_{D_j}} \left[U(P_{Dj}) - \rho_{n(j)}P_{Dj}\right] \tag{4.5}$$

$$\text{subject to } P_{Dj} \in X_{D_j} \tag{4.6}$$

where $X_{D_j} := \{x | P_{Dj}^{min} \leq x \leq P_{Dj}^{max}\}$ is the closed convex set in $\mathbb{R}^{N_D}$ that P_{Dj}^{min} and P_{Dj}^{max} are lower and upper bounds for the production of ConCo j. The decision variables of this problem are P_{Dj}, the amounts of power to be consumed by each demand j.

4.1.3 ISO Market-Clearing Model

The market-clearing procedure consists of optimizing a cost function, subject to various network constraints. The most dominant network constraints are due to line capacity limits [40] and network losses [46]. The power flow through any line is often limited due to technical constraints and is said to be congested when it approaches its maximum limit. This constraint is explicitly included in our model below. The second constraint is due to losses, most of which are due to the heat loss in the power lines. For ease of exposition, such ohmic losses are not modeled in this thesis.

The cost function that is typically used in market clearing mechanism is referred to as Social Welfare. Denoted as S_w, Social Welfare is defined as

$$S_W = \sum_{j \in D_q} U_{Dj}(P_{Dj}) - \sum_{i \in G_f} C_{G_i}(P_{Gi}) \tag{4.7}$$

where the first and second terms denote the revenue due to surpluses stemming from bids from GenCo and ConCo, respectively. $U_{Dj}(P_{Dj})$ and $C_{G_i}(P_{Gi})$ correspond to utility of consumers and cost of generators company and are defined in (4.1), and (4.4). In summary, the market-clearing procedure is given by

$$\text{maximize } S_W = \text{minimize } -S_W \tag{4.8a}$$

subject to

$$-\sum_{i \in \theta} P_{Gi} + \sum_{j \in \vartheta} P_{Dj} + \sum_{m \in \Omega} B_{nm}\left[\delta_n - \delta_m\right] = 0;\ \rho_n, \tag{4.8b}$$

$$B_{nm}\left[\delta_n - \delta_m\right] \leq P_{nm}^{max};\ \gamma_{nm}, \forall n \in N; \forall m \in \Omega \tag{4.8c}$$

$$P_{G_i} \in X_{G_i}\ P_{D_j} \in X_{D_j} \tag{4.8d}$$

The constraints (4.8b) and (4.8c) are due to power balance and capacity limits, respectively. It can be seen that the associated Lagrange multipliers, ρ_n and γ_{nm}, are indicated in each constraint. The underlying optimization problem of the ISO can therefore be defined as the optimization of (4.8a) subject to constraints (4.8b), (4.8c), and (4.8d).

Definition 4.1. A competitive equilibrium is a vector denoted as $\mathbf{P_G^e} = \left[P_{G_1}^e, ..., P_{G_{N_G}}^e\right]^T$ where $P_{Gi}^e \in X_{G_i}$, the amounts of power to be generated by each generating unit i, $\mathbf{P_D^e} = \left[P_{D_1}^e, ..., P_{D_{N_D}}^e\right]^T$ where $P_{Dj}^e \in X_{D_j}$, the amounts of power to be consumed by each consumer j, the voltage phase angles $\mathbf{\Delta^e} = \left[\delta_1^e, ..., \delta_{N-1}^e\right]^T$, the locational marginal prices, $\rho^{\mathbf{e}} = \left[\rho_1^e, ..., \rho_N^e\right]^T$, and congestion price $\mathbf{\Gamma^e} = \left[\gamma_{1m}^e, ..., \gamma_{Nm}^e\right]^T$ that satisfies the following

conditions:

$$\mathbf{P_G^e} \text{ solves the GenCo problem in (4.3)}$$
$$P_{Gi}^e \in \arg\max_{P_{G_i} \in X_{G_i}} \pi_{G_i} \tag{4.9a}$$
$$\mathbf{P_D^e} \text{ solves the ConCo problem in (4.6)}$$
$$P_{Dj}^e \in \arg\max_{P_{D_j} \in X_{Dj}} \pi_{D_j} \tag{4.9b}$$
$$(\mathbf{P_G^e}, \mathbf{P_D^e}, \mathbf{\Delta^e}) \text{ with a competitive prices } (\rho^e, \mathbf{\Gamma^e})$$
$$\text{solves the ISO problem in (4.8a)}$$
$$(P_{Gi}^e, P_{Dj}^e, \delta_n^e, \rho_n^e, \gamma_{nm}^e) \in \arg\max S_W \tag{4.9c}$$
$$\text{Subject to Constraints in (4.8b), (4.8c), and (4.8}d\text{).} \tag{4.9d}$$

Remark 4.1. Current Market Mechanism (CMM) consists of finding a competitive equilibrium $(\mathbf{P_G^e}, \mathbf{P_D^e}, \mathbf{\Delta^e}, \rho^{\mathbf{e}}, \mathbf{\Gamma^e})$ by solving (4.9c) subject to (4.9d) based on the submitted cost function by GenCos and utility function by ConCos. If there exists a competitive equilibrium then ISO can offer an appropriate LMP and Congestion prices such that constraints in (4.9d) are satisfied in the most economical way and each GenCo and ConCo maximizes it own benefit.

The following theorem, known as *first welfare theorem [93]*, provides the connection between competitive equilibrium and efficiency of the market.

Theorem 4.1. *[93] Any competitive equilibrium, if it exists, is efficient, it maximizes the overall social welfare in (3.12) due to the constraints in (4.8b), (4.8d) and (4.8c).*

Existence of the competitive equilibrium plays a crucial rule in our analysis. Theorem 4.1 is a direct result of Definition 4.1, however Theorem 4.1 emphasizes the fact that a competitive equilibrium is the most appealing outcome of a market. Yet immediate question on the necessary and sufficient conditions for existence of competitive equilibrium stems from Theorem 4.1. The next theorem characterizes the conditions for the competitive equilibrium to exists.

Theorem 4.2. *[93] A competitive equilibrium exists if and only if the ISO problem in (4.8a)-(4.8d) satisfies strong duality.*

Theorem 4.2 provides sufficient and necessary conditions for existence of the competitive equilibrium in terms of strong duality condition of the ISO problem. The resulting competitive equilibrium based on Definition 4.1 can be determined as a static solution of the corresponding KKT conditions [10], as P_{Gi}^e, the amounts of power to be generated by each generating unit i, P_{Dj}^e, the amounts of power to be consumed by each consumer j, the locational marginal prices, ρ_n^e, and congestion price γ_{nm}^e that satisfie the following conditions:

$$\frac{d(C_{G_i}(P_{Gi}))}{dP_{Gi}}|_{P^e_{Gi}} - \rho^e_{n(i)} = 0 \ \forall i \in G_f, P^e_{Gi} \in X_{G_i} \tag{4.10a}$$

$$\rho^e_{n(j)} - \frac{d(U_{Dj}(P_{Dj}))}{dP_{Dj}}|_{P^e_{Dj}} = 0 \ \forall j \in D_q, P^e_{Dj} \in X_{D_j} \tag{4.10b}$$

$$\sum_{m\in\Omega_n} B_{nm}\left[\rho^e_n - \rho^e_m + \gamma^e_{nm} - \gamma^e_{mn}\right] = 0 \quad \forall n \in N \tag{4.10c}$$

$$-\sum_{i\in\theta_n} P^e_{Gi} + \sum_{j\in\vartheta_n} P^e_{Dj} + \sum_{m\in\Omega_n} B_{nm}\left[\delta^e_n - \delta^e_m\right] = 0 \ \forall n \in N \tag{4.10d}$$

$$\gamma^e_{nm}\left(B_{nm}\left[\delta^e_n - \delta^e_m\right] - P^{max}_{nm}\right) = 0 \quad \forall n \in N; \forall m \in \Omega_n. \tag{4.10e}$$

Theorems 4.1 and 4.2 set the stage for presenting our dynamic mechanism design in the subsequent section. In contrast to the current practice CMM that ISO solves Eq. (4.8a)-(4.8d) as a static optimization problem, a Dynamic Market Mechanism (DMM) approach is taken in the following sections. The proposed DMM is inspired by the notion of *disequilibrium process* as a sequences of action and state profiles that is needed to attain the competitive equilibrium, defined in (4.10a)-(4.10e) and is characterized in theorems 4.1 and 4.2.

4.2 Dynamic Market Mechanism

Let us denote a finite set of players in the wholesale market as $\mathscr{I} = G_f \bigcap D_q$. An underlying finite state space is denoted as X [95] and $s_p \in S_p$ as an action for player p where S_p is the set of feasible actions for player p. Each agent $p \in \mathscr{I}$ has an action set S_p and a state dependent payoff function $\pi^b_p : X \times S \to R$. For example if $p \in G_f$, then X_{G_p} is the corresponding action set S_p. Let us consider ρ_n, and γ_{nm} as the states then π_{G_i} in (3.1) is the state dependent payoff . Let $S = \prod_p S_p$ denote the set of all action profiles, a deterministic state transition function is defined as $F : X \times S \to X$. In addition, the notation $s_{-p} = [s_q]_{q\neq p}$ is used as a vector of actions for all players except p, and $S_{-p} = \prod_{q\neq p} S_q$ as the set of all action profiles for all players except p.

Repeated play of a DMM produces of action profiles $s(0), s(1), ...$ and a sequence of states $x(0), x(1), ...$ where $s(t) \in S$ is referred to as the action profile at time t and $x(t) \in X$ is state profile at time t. DMM process is summarized as follows:

- At any time $t \geq 0$, each player $p \in \mathscr{I}$ myopically selects an action $s_p(t+1) = A(s_p(t), x(t))$ where $A(.)$ is a myopic decision rule as a function of each player's one-stage payoff function $\pi^b_p(s(t), x(t))$ at time t.
- After all players select their respective action, the state $x(t+1)$ is chosen according to the deterministic state transition function $x(t+1) = F(x(t), s(t))$
- The process is repeated since the equilibrium is reached.

The sequences of action profile and states profile are labeled as a *disequilibrium process* [96]. State dynamics provide a feed-back for entities about the marginal price that they have to pay for deviation of the common constraint denoted in ISO problem (4.8a)-(4.8c).

4.2.1 Dynamic Market Mechanism Design for Wholesale Market

The optimization problem in (4.8a)-(4.8c) can be viewed alternately as a game between the GenCos, ConCos, and the ISO, where each of these three players attempts to maximize their own benefit at the equilibrium. Instead of solving Eq. (4.8a)-(4.8c) as a static optimization problem, a dynamic approach is taken. Now let us define $h = T_{mc}/N$ with

$$h = t_{K+1} - t_K. \tag{4.11}$$

Hence if T_{mc} is chosen as the market clearing time, it follows that N iterations elapse if h is chosen as the sampling interval. The specifics of designing DMM for electricity market are introduced as follows:

State Space:

The underlying state space in this game is denoted by $X \subset \mathbb{R}^{N+N_t}$ where each state $(\rho_n, \gamma_{nm}) \in X$ is the profile of locational marginal prices at each node and congestion prices for each transmission line.

State Dependent Payoff Function:

The state dependent payoff function for GenCo i is defined in Eq. (4.3), ConCo j is defined in Eq. (4.6), and Social Welfare denoted in (4.7).

Actions:

Each GenCo i, ConCo j, and substation at bus n is assigned a state dependent action that permits GenCos and ConCos to change their production and consumption level and substations to change their voltage phase angles. Using gradient play [10, 95], an action for the i th GenCo $\forall i \in G_f$ can be derived as

$$P_{Gi}[K+1] = \mathscr{P}_{X_{Gi}}\left[P_{Gi}[K] + hk_{P_{Gi}}(\rho_{n(i)_k} - c_{Gi}P_{Gi_k} - b_{Gi})\right] \tag{4.12}$$

where $\mathscr{P}_{X_{G_i}}$ denotes the projection on set X_{G_i} and is defined as

$$\mathscr{P}_K[x] = \arg\min_{z \in K} ||x - z|| \tag{4.13}$$

and $||.||$ denotes the Euclidean norm. When K is the box,

$$K = \{k \in \mathscr{R}^n | a_i \leq x_i \leq b_i,\ \forall i\}$$

the projection $\mathscr{P}_K[x]$ is given by

$$\mathscr{P}_K[x] = \begin{cases} a_i & \text{if } x_i < a_i \\ x_i & \text{if } a_i \leq x_i \leq b_i \\ b_i & \text{if } b_i < x_i. \end{cases} \tag{4.14}$$

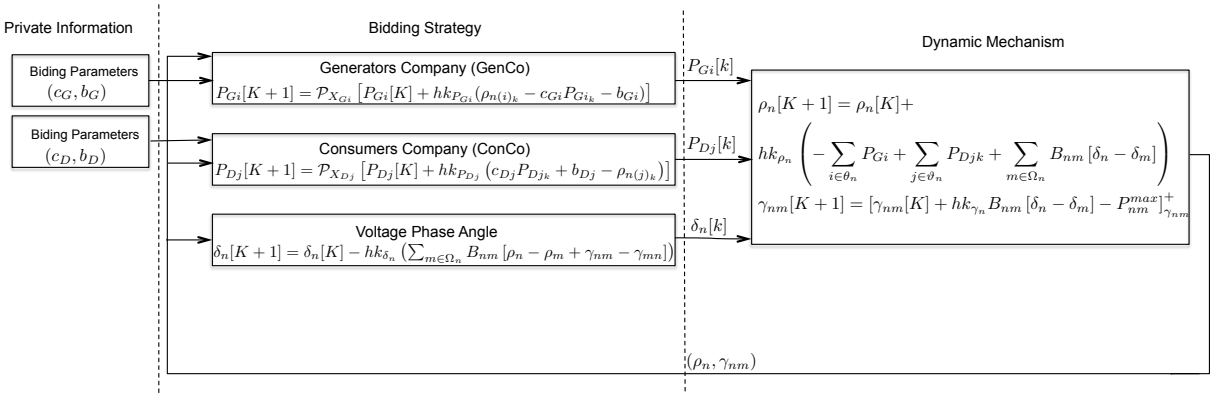

Figure 4.1: Dynamic Market Design for Wholesale Electricity Market

Similarly, using (4.4), a state dependent action can be derived for the jth ConCo $\forall j \in D_q$ as

$$P_{Dj}[K+1] = \mathscr{P}_{X_{Dj}}\left[P_{Dj}[K] + hk_{P_{Dj}}\left(c_{Dj}P_{Dj_k} + b_{Dj} - \rho_{n(j)_k}\right)\right] \tag{4.15}$$

where $k_{P_{Gi}}$ $MW/\$$ and $k_{P_{Dj}}$ $MW/\$$ are representing ramp property of GenCo and price elasticity of ConCo, respectively. For instance, ConCos with higher $k_{P_{Dj}}$ $MW/\$$ can adjust their consumptions faster to the changes of the price. The effect of $k_{P_{Gi}}$ $MW/\$$ and $k_{P_{Dj}}$ $MW/\$$ will be discussed further in Section 4.3.

Finally, the state dependent action for voltage phase angles can be determined as

$$\delta_n[K+1] = \delta_n[K] - hk_{\delta_n}\left(\sum_{m\in\Omega_n} B_{nm}\left[\rho_n - \rho_m + \gamma_{nm} - \gamma_{mn}\right]\right) \tag{4.16}$$

State Dynamics:

A description of how the states evolve as a function of players strategies is provided here. As mentioned earlier, states consist of locational marginal price ρ_n and congestion price γ_{nm}. The state dynamics or pricing mechanism can be derived as

$$\rho_n[K+1] = \rho_n[K] + hk_{\rho_n}\left(-\sum_{i\in\theta_n} P_{Gi} + \sum_{j\in\vartheta_n} P_{Djk} + \sum_{m\in\Omega_n} B_{nm}\left[\delta_n - \delta_m\right]\right) \tag{4.17}$$

$$\gamma_{nm}[K+1] = \left[\gamma_{nm}[K] + hk_{\gamma_n} B_{nm}\left[\delta_n - \delta_m\right] - P_{nm}^{max}\right]^+_{\gamma_{nm}} \tag{4.18}$$

where $\left[h(x,y)\right]^+_y$ denotes the projection onto non-negative orthant which is equal to $h(x,y)$ if $y > 0$, and $max(0, h(x,y))$ when $y = 0$.

The size of the imbalance in the market reflecting in ρ_n, Locational Marginal Price, is a function of the accuracy of forecast with which market participants meet their schedules. Figure 4.1 represents the overall set-up for the proposed Dynamic Market Mechanism. Equations (4.12)-(4.18) represent a dynamic model of the overall wholesale energy market. These action and state profiles can also be viewed as a disequilibrium process [96] needed to arrive at the equilibrium following a perturbation. In the subsequent sections, first the

notion of equilibrium is discussed. Then the connection of the equilibrium of the disequilibrium process with the competitive equilibrium is presented and finally a proof for uniqueness of the equilibrium is provided.

4.2.2 Equilibrium of Wholesale Market Dynamics

Let us make two simplification assumptions.

Assumption 4.1. Let us assume that generator capacities and load capacities are large enough that $\mathscr{P}_{X_{G_i}}$ and $\mathscr{P}_{X_{D_j}}$ are not activated.

From Assumption 4.1, it follows that action of GenCo i in (4.12) can be simplified as

$$P_{Gi}[K+1] = P_{Gi}[K] + hk_{P_{Gi}}(\rho_{n(i)_k} - c_{Gi}P_{Gi_k} - b_{Gi}) \tag{4.19}$$

and action profile of ConCo j in (4.15) is simplified as

$$P_{Dj}[K+1] = P_{Dj}[K] + hk_{P_{Dj}}\left(c_{Dj}P_{Dj_k} + b_{Dj} - \rho_{n(j)_k}\right). \tag{4.20}$$

Assumption 4.2. Let us assume that iteration elapse N is large such that for any x, and $k_x > 0$

$$\lim_{h\to 0} \frac{x[K+1] - x[k]}{k_x h} = \tau_x \dot{x} \tag{4.21}$$

where $\tau_x = 1/k_x$.

From Assumption 4.2 it follows that the discrete process in (4.12)-(4.18) can be viewed as a continuos process. In [8], the same analysis has been studied using (4.12)-(4.18) as a discrete time system with relaxing transmission lines capacity constraints. Using Assumptions 4.1 and 4.2, the disequilibrium process in (4.12)-(4.18) can be represented as

$$\tau_{G_i}\dot{P_{Gi}} = \rho_{n(i)} - c_{Gi}P_{Gi} - b_{Gi} \tag{4.22a}$$

$$\tau_{D_j}\dot{P_{Dj}} = c_{Dj}P_{Dj} + b_{Dj} - \rho_{n(j)} \tag{4.22b}$$

$$\tau_{\delta_n}\dot{\delta}_n = -\sum_{m\in\Omega_n} B_{nm}\left[\rho_n - \rho_m + \gamma_{nm} - \gamma_{mn}\right] \tag{4.22c}$$

$$\tau_{\rho_n}\dot{\rho_n} = -\sum_{i\in\theta_n} P_{Gi} + \sum_{j\in\vartheta_n} P_{Dj} + \sum_{m\in\Omega_n} B_{nm}\left[\delta_n - \delta_m\right] \tag{4.22d}$$

$$\tau_{\gamma_{nm}}\dot{\gamma}_{nm} = \left[B_{nm}\left[\delta_n - \delta_m\right] - P_{nm}^{max}\right]_{\gamma_{nm}}^{+}. \tag{4.22e}$$

where $1/\tau_{Gi}$ and $1/\tau_{Dj}$ are representing ramp property of GenCo and price elasticity of ConCo, respectively.

Two important points should be made regarding the above model. The solution of this model $P_{Gi}(t)$, $P_{Dj}(t)$, $\delta_n(t)$, $\rho_n(t)$, and $\gamma_{nm}(t)$ converges to the equilibrium in (4.23a)-(4.23e), as $t \to \infty$ if the overall system of equations is stable. At all other transient times, the trajectories $P_{Gi}(t)$, $P_{Dj}(t)$, $\delta_n(t)$, $\rho_n(t)$, and $\gamma_{nm}(t)$ represent the specific path that these variables take, when perturbed, as they converge towards the optimal solution. In other words, $(P_{Gi}(t), P_{Dj}(t), \delta_n(t), \rho_n(t), \gamma_{nm}(t))$ is distinct from the optimal solution $(P_{Gi}^*, P_{Dj}^*, \delta_n^*, \rho_n^*, \gamma_{nm}^*)$ and coincides with it at infinity if the market is stable.

The second point that should be noted about the above dynamic model is its decentralized nature. It can be seen that given the LMP at node i, Equation (4.12) can be assembled and solved completely by GenCo i and Eq. (4.15) by ConCo j using the LMP at node j. That is, GenCo i decides their generation quantities by estimating their own marginal profit, as exemplified by c_{Gi}, and b_{Gi}. At any given iteration, if the marginal profit of the GenCo is greater than zero, Eq. (4.12) implies that the GenCo will increase P_{Gi} to obtain a greater economic benefit; if the marginal profit of the GenCo is less than zero, the GenCo will decrease P_{Gi}. ConCo j updates its consumption using Eq. (4.15) in a similar manner. These players then transmit the information to the ISO, over a communication network with low latencies, which then proceeds to solve Eqs. (4.16) to (4.18). Eq. (4.16) implies that the dynamic of voltage angle of bus n depends on the corresponding locational marginal price and also congestion price. Eq. (4.17) describes the evolution of the locational marginal price, and implies that every ρ_n at a node n is affected by the energy imbalance at that node. Eq. (4.18) describes the evolution of the congestion price, and implies that for each transmission line from bus n to bus m, the congestion price is affected by the empty capacity that is the difference of the line flow denoted by $B_{nm}\left[\delta_n - \delta_m\right]$ and maximum thermal capacity P_{nm}^{max}. If the overall system is stable, such an iterative procedure between the market participants, GenCos, ConCos, and ISO, evolving according to the strategies given by Eqs. (4.12)-(4.18), will guarantee convergence to the competitive equilibrium. Now the connection between the equilibrium of the proposed disequilibrium process in (4.22a)-(4.22e) with the competitive equilibrium presented in (4.10a)-(4.10e) is presented.

Theorem 4.3. *Let strong duality hold. Then the equilibrium of the disequilibrium process in (4.22a)-(4.22e) is identical to the competitive equilibrium denoted in (4.10a)-(4.10e).*

Proof. The equilibrium of the disequilibrium process in (4.22a)-(4.22e) is a solution of the following

$$\rho^*_{n(i)} - c_{Gi}P^*_{Gi} - b_{Gi} = 0 \tag{4.23a}$$

$$c_{Dj}P^*_{Dj} + b_{Dj} - \rho^*_{n(j)} = 0 \tag{4.23b}$$

$$-\sum_{m\in\Omega_n} B_{nm}\left[\rho^*_n - \rho^*_m + \gamma^*_{nm} - \gamma^*_{mn}\right] = 0 \tag{4.23c}$$

$$-\sum_{i\in\theta_n} P^*_{Gi} + \sum_{j\in\vartheta_n} P^*_{Dj} + \sum_{m\in\Omega_n} B_{nm}\left[\delta^*_n - \delta^*_m\right] = 0 \tag{4.23d}$$

$$\left[B_{nm}\left[\delta^*_n - \delta^*_m\right] - P^{max}_{nm}\right]^+_{\gamma^*_{nm}} = 0. \tag{4.23e}$$

Using Theorem 4.2, strong duality implies that a competitive equilibrium exits and satisfies (4.10a)-(4.10e). Now it can be seen that Eq. (4.23a) follows by replacing the cost function for GenCo denoted in (4.1) in (4.10a). Similarly, Eq. (4.23b) follows by replacing the utility function of Conco j denoted as (4.4) into (4.10b). Furthermore, Eqs. (4.23c) and (4.23d) are identical to Eqs. (4.10c) and (4.10d). From the definition of the projection denoted in (4.30), it follows from Eq. (4.23e) that (i) $\left[\delta^*_n - \delta^*_m\right] < P^{max}_{nm}$ which implies that $\gamma^*_{nm} = 0$ and therefore $\gamma^*_{nm}(\left[\delta^*_n - \delta^*_m\right] - P^{max}_{nm}) = 0$, or (ii) $\left[\delta^*_n - \delta^*_m\right] = P^{max}_{nm}$ which implies that $\gamma^*_{nm} > 0$ and therefore $\gamma^*_{nm}(\left[\delta^*_n - \delta^*_m\right] - P^{max}_{nm}) = 0$. Both cases (i) and (ii) are identical to Eq. (4.10e). Therefore the equilibrium point that satisfies conditions (4.23a)-(4.23e)

is identical to the competitive equilibrium denoted in (4.10a)-(4.10e). This completes the proof. □

For the sake of exposition, disequilibrium dynamics in (4.22a)-(4.22e) can be rewritten compactly as

$$\begin{bmatrix} \dot{x}_1(t) \\ \dot{x}_2(t) \end{bmatrix} = \left[\begin{array}{c|c} A_1 & A_2 \\ \hline 0 & 0 \end{array}\right] \begin{bmatrix} x_1(t) \\ x_2(t) \end{bmatrix} + \begin{bmatrix} b \\ f_2(x_1, x_2) \end{bmatrix} \tag{4.24}$$

Let us denote $\mathbf{P_G} = \left[P_{G_1}, ..., P_{G_{N_G}}\right]^T$, the amounts of power to be generated by each generating unit i, $\mathbf{P_D} = \left[P_{D_1}, ..., P_{D_{N_D}}\right]^T$ as the amounts of power to be consumed by each consumer j, the voltage phase angles $\mathbf{\Delta} = \left[\delta_1, ..., \delta_{N-1}\right]^T$, the locational marginal prices denoted as $\rho = \left[\rho_1, ..., \rho_N\right]^T$, and congestion price $\mathbf{\Gamma} = \left[\gamma_{1m}, ..., \gamma_{Nm}\right]^T$.

Then

$$x_1(t) = \begin{bmatrix} \mathbf{P_G} & \mathbf{P_D} & \mathbf{\Delta} & \rho \end{bmatrix}^T, \quad x_2(t) = \begin{bmatrix} \mathbf{\Gamma} \end{bmatrix}^T. \tag{4.25}$$

$$A_1 = \begin{bmatrix} -\tau_g^{-1} c_g & 0 & 0 & \tau_g^{-1} A_g^T \\ 0 & \tau_d^{-1} c_d & 0 & -\tau_d^{-1} A_d^T \\ 0 & 0 & 0 & -\tau_\delta^{-1} A_r^T B_{line} A \\ -\tau_\rho^{-1} A_g & \tau_\rho^{-1} A_d & \tau_\rho^{-1} A^T B_{line} A_r & 0 \end{bmatrix} \tag{4.26}$$

$$A_2 = \begin{bmatrix} 0 & 0 & -B_{line}^T A_r \tau_\delta^{-1} & 0 \end{bmatrix}^T \tag{4.27}$$

B_{line} denotes the line admittance matrix (N_t by N_t diagonal matrix) with elements B_{nm} and let A denote the $N_t \times N$ bus incidence matrix. Let A_r denote the reduced bus incidence matrix ($N_t \times N - 1$) which is A with column corresponding to reference bus removed. A_g is generators incidence matrix where $A_{g_{ij}} = 1$ if the i^{th} generator is connected to j^{th} bus and $A_{g_{ij}} = 0$ if the i^{th} generator is not connected to j^{th} bus, similarly for A_d which is load incident matrix where $A_{d_{ij}} = 1$ if the i^{th} consumer is connected to j^{th} bus and $A_{d_{ij}} = 0$ if the i^{th} consumer is not connected to j^{th} bus. Finally

$$b = \begin{bmatrix} b_g^T \tau_g^{-1} & b_d^T \tau_d^{-1} & 0 \end{bmatrix}^T \tag{4.28}$$

$$f_2(x_1, x_2) = \left[\tau_\gamma^{-1} \left[c x_1 - P^{max}\right]_{x_2}^+\right] \tag{4.29}$$

where $c = B_{line} A_r R$, $R x_1 = [\delta_1 \dots \delta_{N-1}]^T$ and R is rotating matrix ($N - 1 \times N_g + N_d + 2N - 1$) and P^{max} denotes a vector with maximum capacity limit of transmission lines ($N_t \times 1$) whose elements are P_{nm}^{max}.

The n-th row of the projection $\left[c x_1 - P^{max}\right]_{x_2}^+$ is denoted as

$$\left[\left[c x_1 - P^{max}\right]_{x_2}^+\right]_n = \begin{cases} max(0, \left[c x_1\right]_n - P_n^{max}) & \text{if } [x_2]_n = 0 \\ \left[c x_1\right]_n - P_n^{max} & \text{if } [x_2]_n > 0. \end{cases} \tag{4.30}$$

where $\left[c x_1\right]_n = B_{nm}(\delta_n - \delta_m)$. In the following theorem, we prove the uniqueness of the equilibrium of the disequilibrium process in (4.24) converges.

Theorem 4.4. *The equilibrium of the disequilibrium process denoted in (4.24) is unique.*

Proof. A proof by contradiction follows. That is, it is assumed that two equilibria denoted as X^*_{01}, and X^*_{02} exist. Let us denote a set of congested lines as $T_c := \{l|B_{lm}(\delta_l - \delta_m) = P_l^{max} \forall m \in \omega_l\}$ and non-congested lines as $\bar{T}_c := \{l|B_{lm}(\delta_l - \delta_m) < P_l^{max} \forall m \in \omega_l\}$. The first equilibrium point denoted as $X^*_{01} = (x^*_{11}, x^*_{12})$ and satisfies the following

$$A_1 x^*_{11} + b + A_2 x^*_{12} = 0 \tag{4.31}$$
$$[x_{12}]^*_l = 0, \ \forall l \in \bar{T}_c. \tag{4.32}$$

Therefore for all transmission lines in this set, $\left[c x^*_{11}\right]_l < P_l^{max}, \ \forall l \in \bar{T}_c$.

The second equilibrium point denoted as $X^*_{02} = (x^*_{21}, x^*_{22})$ and satisfies the following

$$A_1 x^*_{21} + b + A_2 x^*_{22} = 0 \tag{4.33}$$
$$[x^*_{22}]^*_l = \gamma_{lm}, \forall l \in T_c \tag{4.34}$$

where $\gamma_{lm} > 0$ for all $l \in T_c$. In this equilibrium, $[c x^*_{21}]_l - P_l^{max} = 0, \forall l \in T_c$.

Now let us consider the first, k-th and $k' - th$ rows of $A_1 x^*_{11} + b + A_2 x^*_{12} = 0$ as

$$[A_1]_1 x_1 + [b]_1 = 0 \tag{4.35}$$
$$[A_1]_k x_1 + [A_2]_k x_2 = 0 \tag{4.36}$$
$$[A_1]_{k'} x_1 = 0 \tag{4.37}$$

where the first row corresponds to the GenCo's dynamics in (4.22a), $k - th$ row corresponds to the voltage phase angle dynamics in (4.22c), and finally $k - th$ row corresponds to the price dynamics in (4.22d). Subtracting (4.37) from (4.35), it follows

$$[A_1]_{k'} x_1 - [A_1]_1 x_1 - [b]_1 = 0. \tag{4.38}$$

Let us denote a_{ij} as the corresponding element in A_1, (4.38) can be rewritten as

$$a_{k'k} x_{k'} + a_{k'\hat{k}} x_{\hat{k}} + a_{k'k} x_k - a_{1k} x_k + \sum_{i \neq k', k} (a_{k'i} - a_{1i}) x_i - b_1 = 0. \tag{4.39}$$

Simplifying (4.39), it follows

$$a_{k'k} x_{k'} + a_{k'\hat{k}} x_{\hat{k}} + (a_{k'k} - a_{1k}) x_k + K_1 = 0 \tag{4.40}$$

where $K_1 = \sum_{i \neq k', k} (a_{k'i} - a_{1i}) x_i - b_1$.

Now rewriting element by element of (4.36), it follows

$$a_{kk} x_k + \sum_{i \neq k} a_{ki} x_i + \hat{a}_{kk} \hat{x}_k + \sum_{i \neq k} \hat{a}_{ki} \hat{x}_i = 0 \tag{4.41}$$

where $\hat{a}_{ki}$ denotes the corresponding element of A_2 and $\hat{x}_k$ represents the k-th element of x_2. Now (4.41) can be simplified as

$$x_k = -\frac{\hat{a}_{kk}}{a_{kk}} \hat{x}_k - K_2 \tag{4.42}$$

where $K_2 = \sum_{i \neq k} \frac{a_{ki}}{a_{kk}} x_i + \sum_{i \neq k} \frac{\hat{a}_{ki}}{a_{kk}} \hat{x}_i$.

Now replacing (4.42) in (4.40), it follows

$$a_{k'k} x_{k'} + a_{k'\hat{k}} x_{\hat{k}} = -(a_{k'k} - a_{1k})(-\frac{\hat{a}_{kk}}{a_{kk}} \hat{x}_k - K_2) - K_1. \tag{4.43}$$

Simplifying (4.43), it follows

$$a_{k'k} x_{k'} + a_{k'\hat{k}} x_{\hat{k}} = (a_{k'k} - a_{1k})(\frac{\hat{a}_{kk}}{a_{kk}} \hat{x}_k) + K \tag{4.44}$$

where $K = (a_{k'k} - a_{1k})K_2 - K_1$.

From (4.22a)-(4.22e) for any l connected to bus m, we have $a_{k'k} = -a_{k'\hat{k}} = B_{lm}$, $a_{k'k} = 0, a_{1k} = 1, \hat{a}_{kk} = -B_{lm}$, $a_{k'k'} = -B_{lm}$, $x_{k'} = \delta_l$, $x_{\hat{k}} = \delta_m$, and $\hat{x}_k = \gamma_{nm}$. Finally (4.44), is simplified further as

$$B_{lm}(\delta_l - \delta_m) = -\gamma_{lm} + K. \tag{4.45}$$

Now in equilibrium $X^*_{01} = (x^*_{11}, x^*_{12})$ for any $l \in \bar{T}_c$ from (4.32) it follows that $\gamma_{lm} = 0$, which in turn implies that

$$B_{lm}(\delta_l - \delta_m) = K, \ \forall l \in \bar{T}_c. \tag{4.46}$$

And since $B_{lm}(\delta_l - \delta_m) < P^{max}_l$, for all $l \in \bar{T}_c$ this implies that

$$K - P^{max}_l < 0. \tag{4.47}$$

At the second equilibrium $X^*_{02} = (x^*_{21}, x^*_{22})$, since $B_{lm}(\delta_l - \delta_m) = P^{max}_l$, for all $l \in T_c$, this implies that

$$K - P^{max}_l = \gamma_{lm}, \ \forall l \in T_c. \tag{4.48}$$

Since $\gamma_{lm} > 0$, (4.48) implies that

$$K - P^{max}_l > 0, \ \forall l \in T_c. \tag{4.49}$$

Certain conditions have to be satisfied for X^*_{0i} and X^*_{02} to exist:

$$\text{For } X^*_{01}: \ \left[c x^*_1\right]_l - P^{max}_l < 0, \ \forall l \in \bar{T}_c \text{ since } [\dot{x}_2]_l = 0, \text{ at the equilibrium point} \tag{4.50}$$

$$\text{For } X^*_{02}: \quad [x^*_{22}]_l > 0, \ \forall l \in T_c \tag{4.51}$$

Equation (4.50) implies that for any $l \in \bar{T}_c$, see (4.47),

$$K - P^{max}_l < 0.$$

Equation (4.51) implies that for any $l \in T_c$, see (4.49)

$$K - P^{max}_l > 0.$$

Therefore it follows that only (4.50) or (4.51) is satisfied. That is, only X^*_{01} or X^*_{02} exist, which implies uniqueness of equilibrium of (4.24). □

The proposed DMM is a significant departure from the current practice where information is exchanged only once between the GenCos and the ISO following which the ISO clears the market and provides information regarding the price. Our thesis here is that due to the huge volatility and uncertainty of the dynamic drivers such as wind and solar energy sources, and load in the market, such a single iteration will not suffice, and stability cannot be ensured; continued iteration as suggested by the dynamic model above is needed in order to mitigate volatility in real-time price and ensure a stable market design. In the subsequent sections, guidelines for determining stability with such an iterative exchange of information between the different players are discussed.

4.3 Nominal Stability of Electrical Market

Now the stability property of the equilibrium is established using the Lyapunov approach. In what follows, it is assumed that strong duality holds and there exists (x_1^*, x_2^*) such that Eqs. (4.23a)-(4.23e) hold.

Let us define $y_1 = x_1 - x_1^*$, $y_2 = x_2 - x_2^*$, and the Lyapunov function $V : \mathbb{R}^n \to \mathbb{R}$ as

$$V(y_1, y_2) = y_1^T P_1 y_1 + y_2^T P_2 y_2 \tag{4.52}$$

where $n = N_G + N_D + 2N - 1 + N_t$, $P_1 > 0$ and $P_2 > 0$ are real symmetric matrices. It should be noted that a matrix A_1 is Hurwitz if and only if for any given positive definite symmetric Q there exists a unique positive definite symmetric matrix P_1 that satisfies the Lyapunov equation

$$P_1 A_1 + A_1^T P_1 = -Q. \tag{4.53}$$

Furthermore, a positive vector P^{max} is defined with its orthogonal vectors w_i as

$$P^{max} = \sum_{i=1}^{N_t} \psi_i w_i \tag{4.54}$$

where $\psi_i > 0$, for all $i = 1, .., N_t$, and

$$\beta = ||P_1 A_2 + c^T \tau_\gamma^{-1} P_2||. \tag{4.55}$$

Now let us define the compact set Ω_c as

$$\Omega_{c_0} = \{(y_1, y_2) \mid V(y_1, y_2) \leq c_0\}, \tag{4.56}$$

and a set D as

$$D = \{(y_1, y_2) \mid ||y_2|| \leq d\} \tag{4.57}$$

where

$$d = \frac{2\lambda_{min}(P_2)\psi_{min}\lambda_{min}(Q)}{\tau_{\gamma_{max}}\beta^2}. \tag{4.58}$$

The stability of the disequilibrium process is established in Theorem 4.5.

Theorem 4.5. *Let strong duality hold. Then the equilibrium (x_1^*, x_2^*) of (4.24) is asymptotically stable for all initial conditions in $\Omega_{c_{max}}$ for a $c_{max} > 0$ where $\Omega_{c_{max}} \subsetneq D$, if A_1 is Hurwitz.*

Proof. Since strong duality holds, from Theorems 4.3 and 4.4 it follows that (4.24) has a unique equilibrium point. First stability of this equilibrium point is established and then proceed to its asymptotic stability.

(i) Stability: Differentiating $V(y_1, y_2)$ with respect to time, it follows

$$\begin{aligned}\dot{V}(y_1,y_2) = y_1^T(P_1A_1 + A_1^TP_1)y_1 + y_1^TP_1A_2y_2 + y_2^TA_2^TP_1y_1 + \\ y_2^TP_2\left(\tau_\gamma^{-1}\left[cy_1 - P^{max}\right]_{y_2}^+\right) + \left(\tau_\gamma^{-1}\left[cy_1 - P^{max}\right]_{y_2}^+\right)^T P_2y_2\end{aligned} \tag{4.59}$$

Using the non-expansive property of the projection [97], it follows $y_2^TP_2\left(\tau_\gamma^{-1}\left[cy_1 - P^{max}\right]_{y_2}^+\right) \leq y_2^TP_2\left(\tau_\gamma^{-1}\left[cy_1 - P^{max}\right]\right)$. This in turn implies that

$$\begin{aligned}\dot{V}(y_1,y_2) \leq y_1^T(P_1A_1 + A_1^TP_1)y_1 + y_1^TP_1A_2y_2 + y_2^TA_2^TP_1y_1 + \\ y_2^TP_2\left(\tau_\gamma^{-1}cy_1 - \tau_\gamma^{-1}P^{max}\right) + \left(\tau_\gamma^{-1}cy_1 - \tau_\gamma^{-1}P^{max}\right)^T P_2y_2\end{aligned} \tag{4.60}$$

If A_1 is Hurwitz, for any $Q > 0$, a P in (4.53) exists and is positive definite. Let $\lambda_{min}(Q)$ denote the minimum eigenvalue of Q. Since P_2 is a symmetric positive definite matrices, with a set of N_t orthogonal, real and nonzero eigenvectors $x_1, \ldots x_n$, can be written $P_2 = \sum_{i=1}^{N_t} \lambda_i x_i x_i^T$ where $\lambda_i > 0$ is the eigenvalue corresponding to x_i. Using (4.54), it follows that

$$P^{max^T}\tau_\gamma^{-1}P_2y_2 \geq \frac{\lambda_{min}(P_2)\psi_{min}}{\tau_{\gamma_{max}}}||y_2|| \tag{4.61}$$

where $\tau_{\gamma_{max}} = \max(\tau_{\gamma_{nm}})$, and $\psi_{min} = min(\psi_i), \forall i = 1, .., N_t$.

Using (4.55), it is obtained that

$$y_1^T(P_1A_2 + c^T\tau_\gamma^{-1}P_2)y_2 + y_2^T(A_2^TP_1 + P_2\tau_\gamma^{-1}c)y_1 \leq 2\beta||y_1||||y_2||. \tag{4.62}$$

Using Eqs. (4.61)-(4.62) implies that

$$\dot{V}(y_1,y_2) \leq -\lambda_{min}(Q)||y_1||^2 + 2\beta||y_1||||y_2|| - 2\frac{\lambda_{min}(P_2)\psi_{min}}{\tau_{\gamma_{max}}}||y_2|| \tag{4.63}$$

Equivalently,

$$\dot{V}(y_1,y_2) \leq -\lambda_{min}(Q)\left(||y_1|| - \frac{\beta}{\lambda_{min}(Q)}||y_2||\right)^2 - ||y_2||\left(2\frac{\lambda_{min}(P_2)\psi_{min}}{\tau_{\gamma_{max}}} - \frac{\beta^2}{\lambda_{min}(Q)}||y_2||\right) \tag{4.64}$$

For all $\Omega_{c_{max}} \subsetneq D$, it follows that for all solutions beginning in $\Omega_{c_{max}}$, $\dot{V} \leq 0$. Hence the equilibrium is stable, and $\Omega_{c_{max}}$ is the region of attraction.

(ii) Asymptotic stability: We now show that all solutions beginning in $\Omega_{c_{max}}$ will converge to the equilibrium point. Eq. (4.64) can be rewritten as

$$\dot{V}(y_1,y_2) \leq -a(||y_1|| - b||y_2||)^2 - ||y_2||(e - f||y_2||)$$

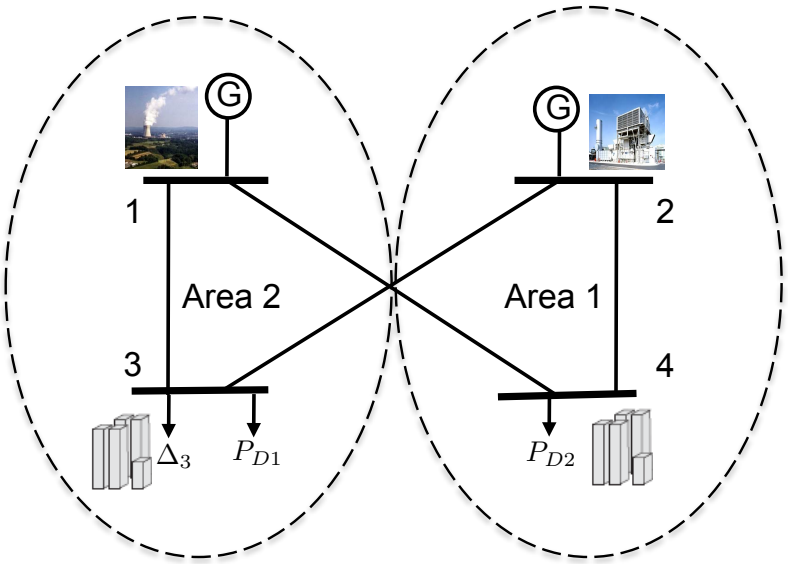

Figure 4.2: 4-bus system example

where $a = \lambda_{min}(Q)$, $b = \frac{\beta}{\lambda_{min}(Q)}$, $e = 2\frac{\lambda_{min}(P_2)\psi_{min}}{\tau_{\gamma_{max}}}$, and $f = \frac{\beta^2}{\lambda_{min}(Q)}$.

That is, $\dot{V}$ can be zero if

$$(||y_1||, ||y_2||) = \left(\frac{be}{f}, \frac{e}{f}\right) \tag{4.65}$$

or if

$$(||y_1||, ||y_2||) = (0, 0) \tag{4.66}$$

Note that $||y_2|| = \frac{e}{f}$ implies that the solution lies on D. However, since the initial conditions start in $\Omega_{c_{max}}$ and the latter is a strict subset of D, y_2 cannot be equal to $\frac{e}{f}$ in $\Omega_{c_{max}}$. This in turn implies that (4.66) is the only invariant set. Hence all solutions (y_1, y_2), starting in $\Omega_{c_{max}}$ converge to the equilibrium point $(x_1, x_2) = (x_1^*, x_2^*)$, which establishes asymptotic stability. □

Remark 4.2. The region of attraction Ω_{max} for which stability and asymptotic stability hold places an implicit bound on the congestion price [97]. In particular, it implies that the congestion price needs to be smaller than d, which is proportional to P_{max}. In Section 4.5, this dependence is explained in more detail through a numerical study.

Corollary 4.1. Let strong duality hold. Then the equilibrium (x_1^*, x_2^*) of (4.24) is asymptotically stable for all initial conditions in $\mathbb{R}^n$, if for any $Q > 0$, there exists $P_1 > 0$, $P_2 > 0$, and diagonal matrix $\tau_\gamma^{-1} > 0$ such that

$$P_1 A_2 + c^T \tau_\gamma^{-1} P_2 = 0 \tag{4.67}$$

$$P_1 A_1 + A_1^T P_1 = -Q. \tag{4.68}$$

Proof. From condition (4.67) and definition (4.55), it follows that $\beta = 0$. This in turn implies that if A_1 is Hurwitz, then $\dot{V}(y_1, y_2)$ in (4.63) can be simplified as

$$\dot{V}(y_1, y_2) \leq -\lambda_{min}(Q)||y_1||^2 - 2\frac{\lambda_{min}(P_2)\psi_{min}}{\tau_{\gamma_{max}}}||y_2||. \tag{4.69}$$

Since P_2 is positive definite, therefore $\lambda_{min}(P_2) > 0$. Eq. (4.54) implies that $\psi_{min} > 0$, and since it is assumed that $\tau_\gamma > 0$ therefore $\tau_{\gamma_{max}} > 0$, which in turn follows that

$$\dot{V}(y_1, y_2) \leq 0. \tag{4.70}$$

Eq. (4.70) implies that the unique equilibrium point (x_1^*, x_2^*) is stable, for all initial conditions in $\mathbb{R}^n$.

Asymptotic stability can be concluded by noting from Eqs. (4.31)-(4.34) that $\dot{x}_1$ and $\dot{x}_2$ are non-zero at all points other than the equilibrium. □

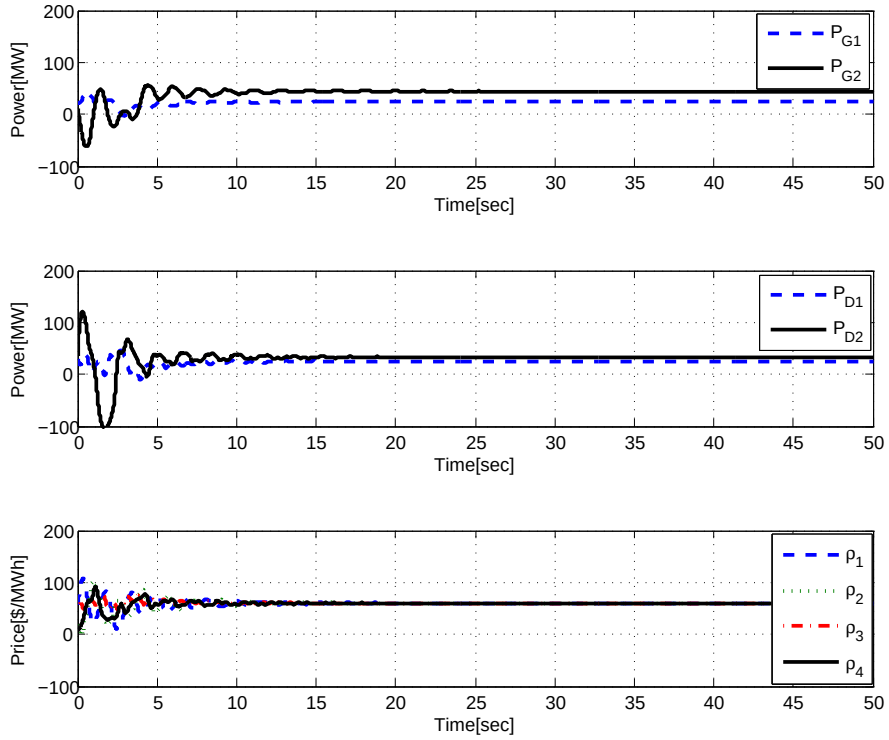

Figure 4.3: Market disequilibrium process for GenCos P_{G1}, and P_{G2}, ConCo P_{D1}, and P_{D2}, and Locational Marginal Prices $\rho_n \forall n = 1, ..., 4$ with initial conditions in Table B.8, Case 1.

4.3.1 Illustrative Example

Now the stability of the equilibrium of the energy market is numerically evaluated using a standard 4-bus network as can be seen in Figure 4.2. The network includes two generating units located at bus 1 which corresponds to a base-load generator and at bus 2 as a peaking generator. The latter can be assumed to be a spinning reserve to compensate for demand fluctuations that may occur in bus 3 denoted as Δ_3. The maximum and minimum power output of each generating unit is shown in Table B.6. There are power consumption at nodes 3 and 4, and their respective minimum demand requirements are indicated in Table B.6.

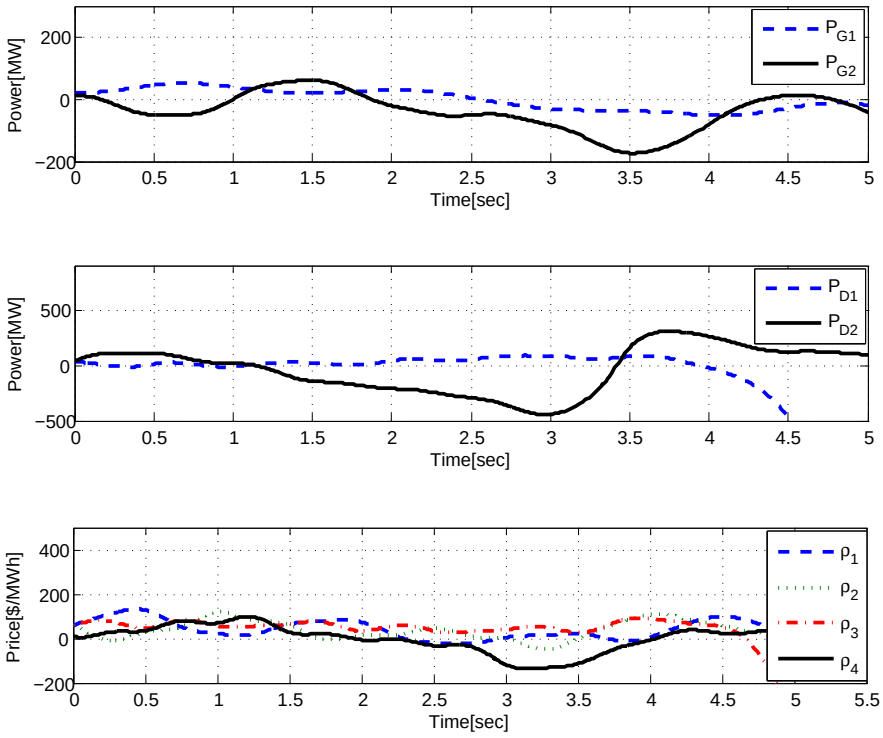

Figure 4.4: Market disequilibrium instability after a sudden increase of load in bus 3 with initial conditions in Table B.8, Case 2.

Price coefficients b_{Gi} and c_{Gi} corresponding to cost functions of generators as well as coefficients b_{Dj} and c_{Dj} of the utility functions of consumers are shown in Table B.6. Transmission line parameters such as B_{nm} and the line capacity limits P_{nm}^{max} are included in Table B.7. The line parameters are per unit with a three-phase base of 230 kV and 10 MVA. It is assumed that the market time constants $\tau_\rho = 5\ MWh^2/\$$, and $\tau_\delta = 5\ \$/MW$.

Region of Attraction

Let us consider two cases, labeled Case 1 and Case 2, different cases with the same parameters given in Tables B.6 and B.7 and all initial conditions being the same except for $\delta_2(0)$ (see Table B.8). Figures 4.3 and 4.4 show responses of the critical state variables, P_{G1}, P_{G2}, P_{D1}, P_{D2}, and ρ_n for the initial conditions in these two cases. It can be seen in Figure 4.3 that P_{G1} supplies the base-load consumption and P_{G2} is dispatched to follow up load fluctuations. Since transmission lines are not congested, Locational Marginal Prices (LMPs), ρ_n, converge to the same value for all n buses, and the wholesale market is stable with the given parameters. However, when $\delta_2(0)$ is increased from 8 deg to 12 deg, the wholesale market exhibits instability, as illustrated in Figure 4.4. The difference in the stable and unstable solutions for Cases 1 and 2 is also illustrated in Figure 4.5 using a projection of the phase-plane.

A more detailed study of the sensitivity to initial conditions was also carried out. Starting with the initial conditions in Case 1, we perturbed each of the fifteen state variables as $x_i + \Delta_i$ while keeping all $j \neq i$ constant, and determined the maximum Δ_{max_i} that led to instability. It follows that larger the Δ_{max_i}, the higher the robustness to perturbations in

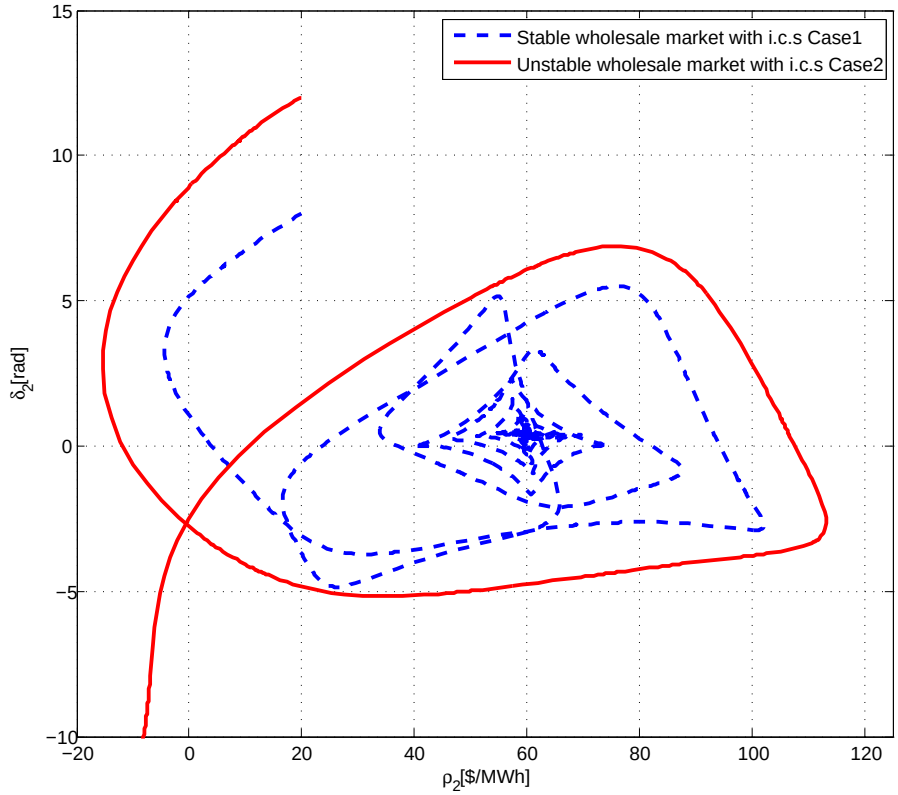

Figure 4.5: Blue curve is stable phase plane, Red curve is unstable phase plane due to the disturbance.

that particular state x_i. The values Δ_{max_i} are shown in Figure 4.6 for each of the fifteen state variables. As Figure 4.6 shows, the most sensitive states, i.e. the states that possess the smallest set Δ_{max_i}'s correspond to the phase angles $\delta_n, \forall n = \{1...4\}$. These sensitivity studies can provide guidance for the design of robust control.

Stability and Volatility

In this section, the results of numerical simulations with only considering changes of τ_{d1} and τ_ρ are presented. It should be noted that $1/\tau_{Dj}$ represents price elasticity of ConCo and τ_ρ represents market time scale for updating prices. A standard 4-bus network as can be seen in Figure 4.2 is considered and the coefficients for GenCos and ConCos are set as represented in Table B.6. An analysis of disequilirbium process in 4.24 showed that the stability is dependent on eigenvalues of A_1. Matrix A_1 is Hurwitz if every eigenvalue of A_1 has strictly negative real part. Figure 4.7 provides the real part of maximum eigenvalue of A_1 by changing demand elasticity τ_{d1} and market adjustment rate denoted by τ_ρ. As can be seen in Figure 4.7, for small τ_ρ because of fast updating of real time price, we expect volatility of prices. Volatility can be mitigated by increasing τ_ρ which in turn implies slower update of prices and therefore market latency is increased. Another important result that can be seen in Figure 4.7 is that by decreasing τ_{d1}, volatility is increased. Decreasing τ_{d1} corresponds to the increase of demand elasticity, and therefore increase of demand elasticity will result in increase of volatility. This observation has been also reported in [94].

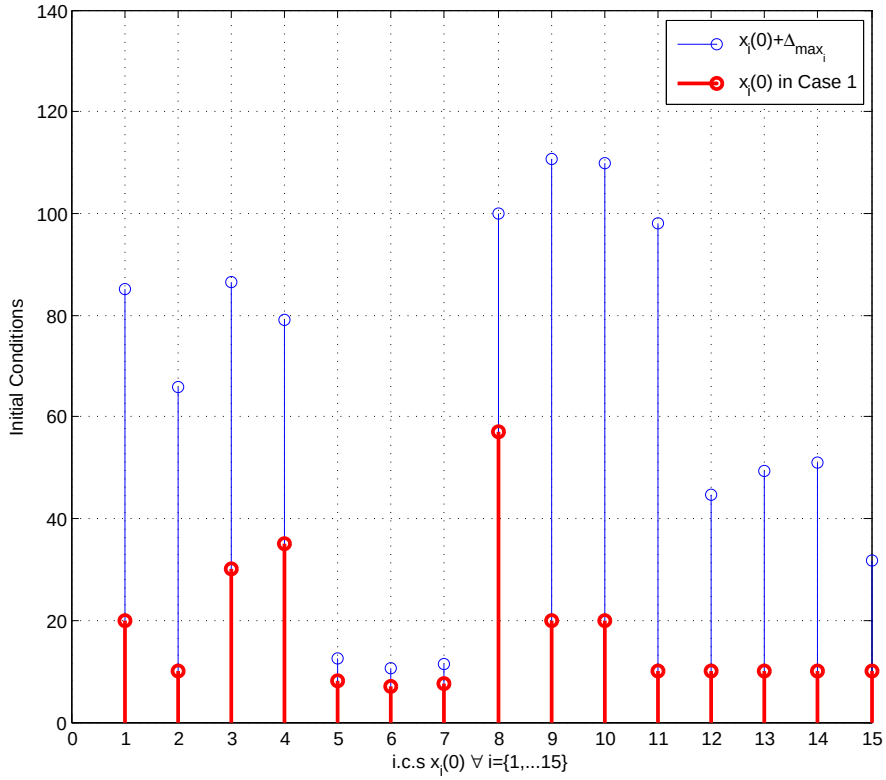

Figure 4.6: Relative size of sensitivity Δ_{max_i} to perturbation in $x_i(0)$ with $x_j(0), j \neq i$ fixed, for $i = \{1, \ldots, 15\}$.

Figure 4.9 compares price profile for 24 in response to the load profile Δ_3 in Figure 4.8 from New England ISO, 1st of June 2012 [1]. As can be seen in Figure 4.9, the price in Case A is extremely volatile under the conditions of $\tau_\rho = 1.5\ MWh^2/\$$, and $\tau_{d1} = 5\ \$/MW$. However by increasing market latency in Case C by keeping τ_{d1} the same as Case A and only increasing τ_ρ from 1.5 $MWh^2/\$$ to 4.5 $MWh^2/\$$, we can see that price profile exhibits oscillations but it is less volatile than Case A. Now in Case B, we keep $\tau_\rho = 1.5\ MWh^2/\$$ and decrease demand elasticity by increasing τ_{d1} from 5 $\$/MW$ to 20 $\$/MW$. We can observe from Figure 4.9 that Case B leads to the stable price profile. As has been pointed out in [94], a large scale use of smart meters by electricity consumers could lead power pricing and demand swings and causes instability in the grid. This result can be delineated from Figures 4.7 and 4.9. As can be seen in Figure 4.9 increasing demand elasticity of Case B, causes huge volatility in Case A. However market designer can adjust market latency denoted by τ_ρ so mitigate the resulting volatility. These observations emphasis that market designer should carefully consider the effect of market time scale and demand elasticity in the stability of wholesale market. Theorem 4.5 provides a guidelines for designing an efficient market with stable price profile.

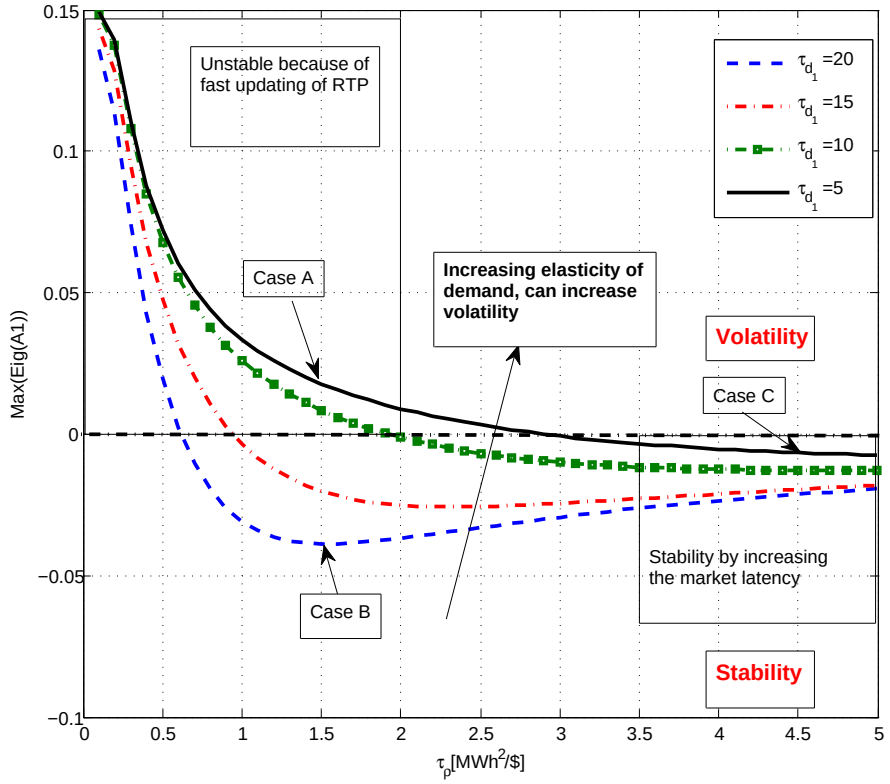

Figure 4.7: Real part of maximum eigenvalue of A_1, stability and volatility regions.

4.4 Robust Stability of The Wholesale Market

The most dominant impact of the introduction of distributed energy resources is uncertainties, which can directly alter the overall market equilibrium. A first step in this direction is taken by introducing uncertainties in the decision variables introduced in Section 4.1.1 in the following section.

4.4.1 Incorporating Wind Power and Demand Response

While modeling of wind power and DR are presented in Chapter 3, some of the concepts and the definitions are introduced here too for the sake of completeness. The family of P_{Gi} is first separated into P^C_{Gi}, $i = 1,\ldots,n_C$, and P^w_{Gl}, $l = 1,\ldots,n_w$, where n_C denotes the conventional dispatchable generating units, and n_w denotes distributed energy resources such as those based on wind and solar energy, which are non-dispatchable. It is assumed that the wind GenCo are competitive and that they submit their bids to the market as other conventional GenCo, and not modeled as a negative demand [13, 62, 63].

Using the above discussion and similar to Chapter 3, the objective function defined in (3.1) is modified as [63]

$$\text{maximize}_{P^w_{Gl}}\, \pi^w_{Gl} = \text{maximize}_{P^w_{Gl}} \left[\rho_{n(l)} P^w_{Gl} - C^w_{G_l}(P^w_{Gl}) - C^r_{w_l}(\Delta_{w_l})\right] \tag{4.71}$$

$$\text{subject to } P^w_{Gl} \in X^w_{G_L} \tag{4.72}$$

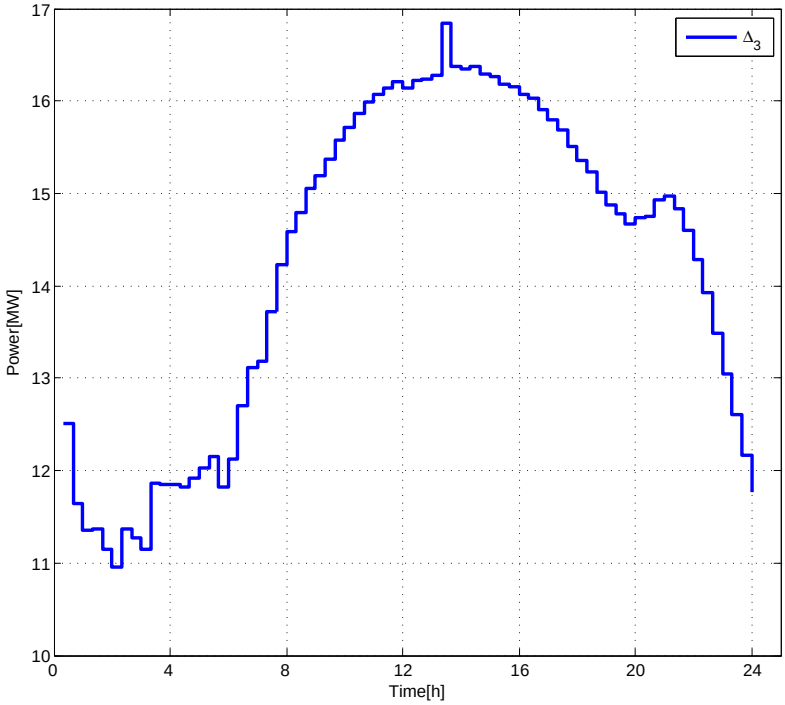

Figure 4.8: Load profile from New England ISO, 1st of June 2012 [1]

where $\rho_{n(l)}$ denotes the LMP of unit l at node n in the network, and $X^w_{G_l} := \{x | x \in [P^w_{Gl_{min}} \; P^w_{Gl_{max}}]\}$ is the closed convex set in $\mathbb{R}^n$ that $P^w_{Gl_{min}}$ and $P^w_{Gl_{max}}$ are lower and upper bounds for the production of wind producer l. Δ_{w_l} is due to wind uncertainty, given by

$$\Delta_{w_l} = P^w_{Gl} \Delta_{Gl}, \; \forall \Delta_{Gl} \in (-1, 1). \tag{4.73}$$

It should be noted that the cost function for the l^{th} wind generator denoted as $C^w_{G_l}(P^w_{Gl})$ is very close to zero. Finally, $C^r_{w_l}(\Delta_{w_l})$ is a cost incurred by committing specific generators as reserves [64], due to the wind uncertainty Δ_{w_l}, and is modeled as a quadratic function

$$C^r_{w_l}(\Delta_{w_l}) = \frac{c_{w_l}}{2} \Delta^2_{w_l}. \tag{4.74}$$

The available wind energy is overestimated when $0 < \Delta_{Glb} < 1$ which implies that if the assumed power is not available, power can be purchased from an alternate source or that loads can be shed. It is furthermore assumed that the overestimation is only due to wind uncertainty and not because of strategic behavior of wind provider. The available wind energy is underestimated if $-1 < \Delta_{Glb} < 0$ which implies that surplus power is either sold to adjacent utilities, or consumed through fast redispatch and automatic gain control, or reduced through reduction of conventional generation. Another quantity x^w which represents the percentage of wind penetration is defined as

$$x^w = \frac{\sum_{l \in G_w} P^w_{Gl}}{\sum_{j \in D_q} P_{Dj}} \tag{4.75}$$

where P_{Dj} is the power demanded by consumer j. It should be noted that the impact of wind

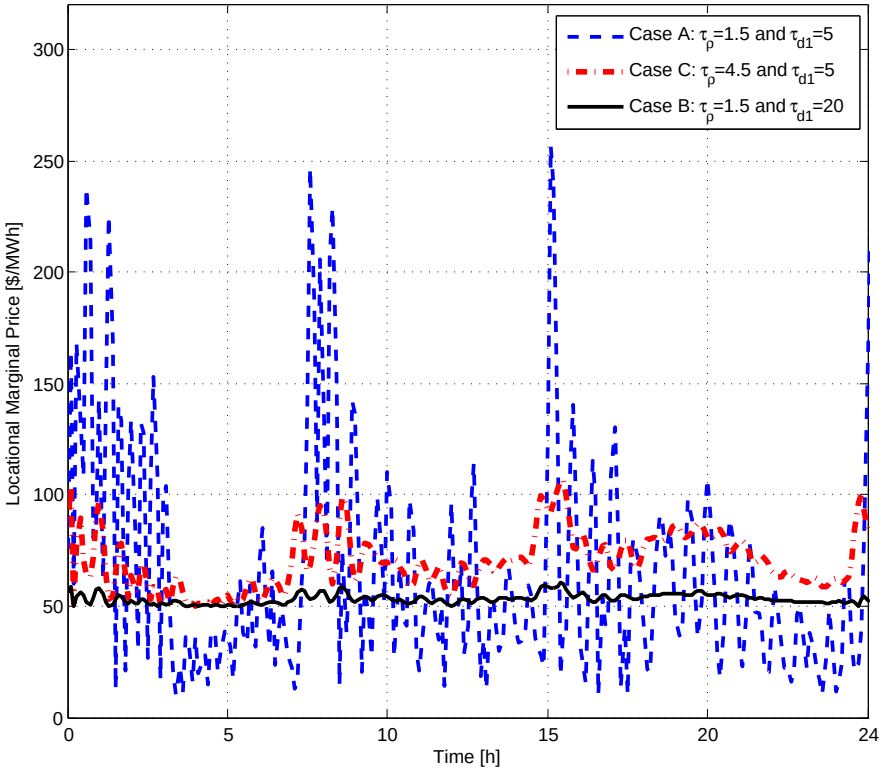

Figure 4.9: Price profile of a dynamic market model in (4.24) with load profile in Figure 4.8.

power on the market equilibrium is much smaller if x^w is small, i.e., if wind penetration is low, than if x^w is large.

To include the effect of DR, we divide all ConCo units into dispatchable and non-dispatchable ones, a dispatchable load P_{Djk} is considered. This effect is modeled using a control parameter κ_{Djk}, and denotes the response of the consumers to a change in the Real Time Price (RTP) as

$$\bar{P}_{Djk} = P_{Djk}(1 - \kappa_{Djk}) \qquad 0 < \kappa_{Djk} < 1 \tag{4.76}$$

where $\bar{P}_{Djk}$ denotes the consumption incorporated with demand responsiveness into RTP. It is assumed that κ_{Djk} is suitably calibrated to represent the effect of RTP on the consumer behavior, and is synonymous to *elasticity factor* defined in [84]. As discussed in Chapter 3, a positive κ_{Dj}, denotes a decrease in the ConCo consumption while a negative κ_{Dj}, denotes an increase. In this section, our attention is restricted to positive κ_{Dj} since our focus is on cases where there is a shortfall in the non-dispatchable GenCo, i.e. $\Delta_{Gl} > 0$. It is assumed that κ_{Dj} is suitably calibrated to represent the effect of RTP on the consumer behavior. The inherent assumption here is that the dispatchable ConCo observes the state signal, i.e. LMP and Congestion price, and suitably adjusts its demand. This adjustment is represented through the curtailment factor κ_{Dj}. The above discussions indicate that the effects of wind uncertainty and DR are represented by three key parameters Δ_{Gl}, x^w, and κ_{Dj}. In Section 4.4.2, it is shown that the stability of the perturbed market is strongly affected by these parameters. In Section 4.5, we explain this dependence in more detail through a numerical study of an IEEE 30-bus.

4.4.2 Robustness of the Electricity Market

Now the dynamic model of the wholesale market is analyzed in the presence of the perturbations due to the wind forecast error defined in (4.73) parametrized by Δ_{Gl} and DR defined in (4.76) parameterized by κ_{Dj}. The same as discussed in Section 4.2.1, the wholesale market dynamic under uncertainty can be written compactly as

$$\begin{bmatrix} \dot{x}_1(t) \\ \dot{x}_2(t) \end{bmatrix} = \left[\begin{array}{c|c} A_1 + \Delta A_1 & A_2 \\ \hline 0 & 0 \end{array}\right] \begin{bmatrix} x_1(t) \\ x_2(t) \end{bmatrix} + \begin{bmatrix} b \\ f_2(x_1, x_2) \end{bmatrix} \tag{4.77}$$

where $\Delta A_1 \in \mathscr{E}$ and $\mathscr{E}$ is defined as

$$\mathscr{E} := \{\Delta_A = \Delta_G - \Delta_D \mid \Delta_G \in \mathscr{E}_G \text{ and } \Delta_D \in \mathscr{E}_D\} \tag{4.78}$$

$$\Delta_G = \begin{bmatrix} \tau_g^{-1} c_g \Delta_g^2 & 0 & 0 & 0 \\ 0 & 0 & 0 & 0 \\ 0 & 0 & 0 & 0 \\ \tau_\rho^{-1} A_g^T (I - \Delta_g) & 0 & 0 & 0 \end{bmatrix} \tag{4.79}$$

$$\Delta_D = \begin{bmatrix} 0 & 0 & 0 & 0 \\ 0 & 0 & 0 & 0 \\ 0 & 0 & 0 & 0 \\ 0 & \tau_\rho^{-1} A_d^T (I - \kappa_d) & 0 & 0 \end{bmatrix} \tag{4.80}$$

$$\mathscr{E}_D := \{\Delta_D \mid ||\Delta_D|| := \sqrt{\lambda_{max}(\Delta_D^T \Delta_D)} \leq \pi_D\} \tag{4.81}$$

and

$$\mathscr{E}_G := \{\Delta_G \mid ||\Delta_G|| := \sqrt{\lambda_{max}(\Delta_G^T \Delta_G)} \leq \pi_G\} \tag{4.82}$$

for a finite π_D and π_G and $\Delta_g = \text{diag}\{\Delta_{Gi}\}$ for all $i \in G_f \cup G_f^w$ as well as $\kappa_d = \text{diag}\{\kappa_{Dj}\}$ for all $j \in D$.

The same as Theorem 4.5, let $y_1 = x_1 - x_1^*$, $y_2 = x_2 - x_2^*$, a positive definite Lyapunov function $V(y_1, y_2) = y_1^T P_1 y_1 + y_2^T P_2 y_2$ and $d_\Delta = d - d_{\Delta G} + d_{\Delta D}$ where d is defined in (4.58) and

$$\begin{aligned} d_{\Delta G} &= \frac{4\lambda_{min}(P_2)\psi_{min}||P_1||\pi_G}{\beta^2} \\ d_{\Delta D} &= \frac{4\lambda_{min}(P_2)\psi_{min}||P_1||\pi_D}{\beta^2}. \end{aligned} \tag{4.83}$$

It should be noted that all three parameters including the wind uncertainty Δ_{Gl}, wind penetration x^w, and demand curtailment factor κ_{Dj} affect π_G and π_D. Denote the latter as $\pi_G(\Delta_{Gl}, x^w)$ and $\pi_D(\kappa_{Dj})$. In the following theorem, the stability of the perturbed market is presented.

Theorem 4.6. *Let A_1 be Hurwitz and strong duality hold. Also let*

$$\pi_G - \pi_D < \frac{\lambda_{min}(Q)}{2||P_1||}. \tag{4.84}$$

Then the equilibrium $(x_1^*, x_2^*) \in E$ is asymptotically stable for all initial conditions in $\Omega_{c_{max}} = \{(y_1, y_2) \mid V(y_1, y_2) \leq c_{max}\}$ for a $c_{max} > 0$ such that $\Omega_{c_{max}} \subsetneq D_\Delta = \{y_2 \mid ||y_2|| \leq d_\Delta\}$.

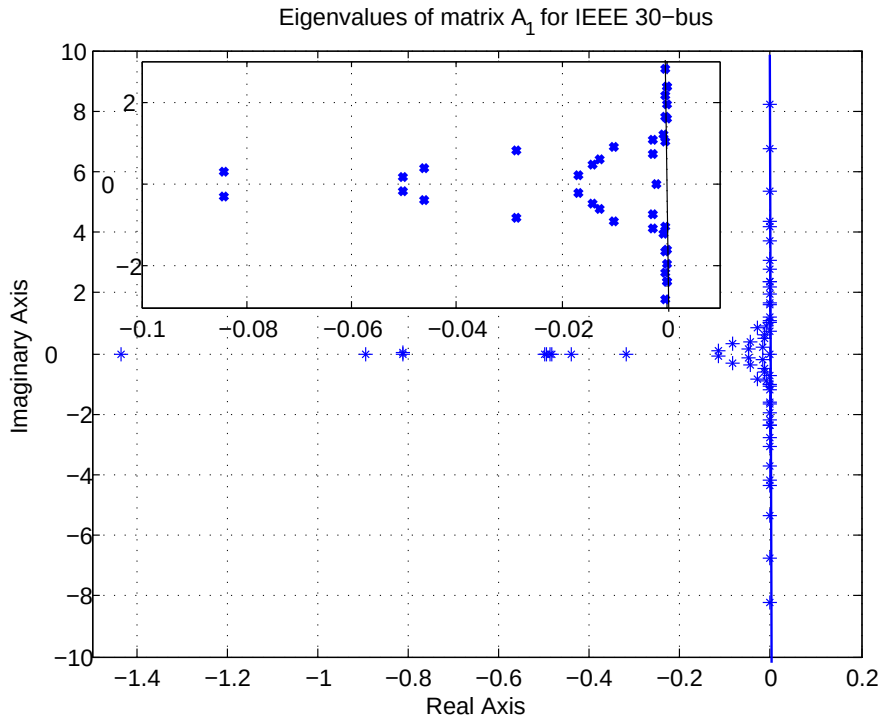

Figure 4.10: Eigenvalues of matrix A_1, for each eigenvalue λ_i of A_1, $Re[\lambda_i] < -2 \times 10^{-5}$

Proof. Differentiating the Lyapunov function $V(y_1, y_2)$ along the trajectories of (4.77), the following is obtained

$$\dot{V}(y_1, y_2) \leq -a_\Delta \left(||y_1|| - \frac{\beta}{a_\Delta}||y_2||\right)^2 - ||y_2||\left(e - \frac{\beta^2}{a_\Delta}||y_2||\right) \tag{4.85}$$

where

$$a_\Delta = \lambda_{min}(Q) - 2||P_1||\pi_G + 2||P_1||\pi_D.$$

From (4.84), it follows that $a_\Delta > 0$. Therefore, Eq. (4.85) implies that for all $\Omega_{c_{max}} \subsetneq D_\Delta$, for all solutions beginning in Ω_Δ, $\dot{V} \leq 0$. Hence the equilibrium is stable, and Ω_Δ is the region of attraction.

Asymptotic stability of the perturbed market can be proved as follows. Since initial conditions start in Ω_Δ and the latter is a strict subset of D_Δ, it can be shown using the same arguments as in Theorem 4.5 that all solutions starting in Ω_Δ converge to the equilibrium point $(x_1, x_2) = (x_1^*, x_2^*)$. □

Remark 4.3. Theorem 4.6 implies that the region of attraction for asymptotic stability, Ω_Δ is determined by D_Δ. D_Δ in turn is a function of d, π_G, and π_D. The relative size of Ω_Δ in relation to $\Omega_{c_{max}}$ in the ideal case is therefore determined completely by $\pi_G - \pi_D$. As the latter increases, the size of Ω_Δ decreases in comparison to $\Omega_{c_{max}}$, and as $\pi_G - \pi_D$ decreases, Ω_Δ increases, and can become larger than $\Omega_{c_{max}}$. That is, the uncertainty of RERs due to forecast errors can reduce the region of attraction, whereas the load curtailment factor can compensate for the effect of RERs and mitigate their effects.

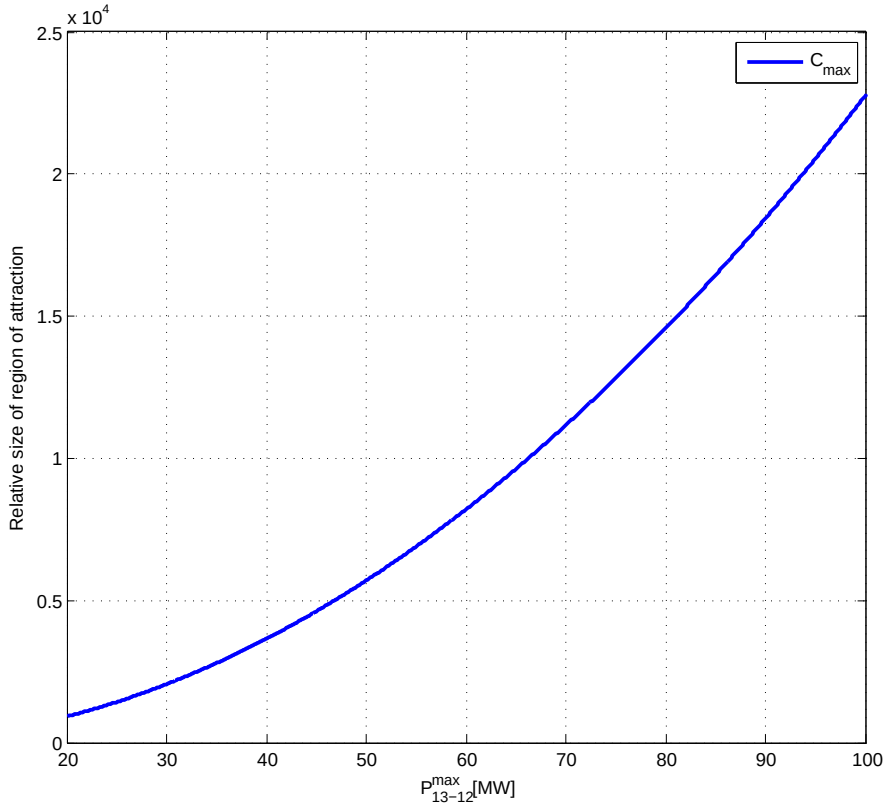

Figure 4.11: Increase of relative size of region of attraction by increase of transmission capacity

4.5 Case Study

An IEEE 30-bus case, whose interconnections are shown in Figure 3.3, is used to demonstrate the properties of the unperturbed and perturbed market models presented in Sections 4.2.1 and 4.4.2. Both a wind generator and a dispatchable load that respond to real-time price changes are introduced, with the former introduced in bus 13, and the latter in bus 15. The effects of these two entities are quantified as Δ_{G13} and κ_{D15} respectively. P_{Gl}^{w} defined in (4.71) is varied so that the effect of wind penetration x^{w}, defined in (4.75), can be analyzed as well. Four scenarios, described below, are simulated and discussed further.

1. Wind generator in bus 13 with $\Delta_{G13} = 0\%$ and penetration $x^{w} = 5.4\%$, without RTP in bus 15, $\kappa_{D15} = 0$ (Base case)

2. Wind generator in bus 13 with $\Delta_{G13} = 5\%$ and penetration $x^{w} = 5.4\%$, without RTP in bus 15, $\kappa_{D15} = 0\%$

3. Wind generator in bus 13 with $\Delta_{G13} = 5\%$ and penetration $x^{w} = 12.5\%$, without RTP in bus 15, $\kappa_{D15} = 0\%$

4. Wind generator in bus 13 with $\Delta_{G13} = 5\%$ and penetration $x^{w} = 12.5\%$, without RTP in bus 15, $\kappa_{D15} = 3\%$

Tabular 4.1: Stability of the wholesale market incorporating wind uncertainty and wind penetration

	Scenario 1	Scenario 2	Scenario 3	Scenario 4
$P^w_{G13_{min}}$	30 MW	30 MW	70 MW	70 MW
$P^w_{G13_{max}}$	30 MW	32 MW	78 MW	78 MW
Δ_{13}	0%	5%	5%	5%
x^w	5.4%	5.4%	12.5%	12.5%
κ_{15}	0	0	0	3%
c_{max}	38.3	37.1	32.5	36.9

Relevant parameters of generators and consumers are shown in Table B.9 and Table B.10, respectively. The transmission capacity limit of all lines is chosen to be $50MW$, the interconnections and the reactance B_{nm} of the line connecting bus n and bus m can be found in Table B.5. It is assumed that GenCo in bus 2, is committed as a reserve generator and start-up and shut-down costs are internalized in its associated cost function C_{G_2}.

4.5.1 Stability of the Ideal Wholesale Market

With the parameters provide in Table B.9, and B.10, d in (4.58) for the scenario 1) is calculated and the corresponding region of attraction $\Omega_{c_{max}}$ such that $\Omega_{c_{max}} \subsetneq D$. It was found that $c_{max} = 38.4$. Eigenvalues of A_1 matrix with the parameters in Table B.9-B.10 is shown in Figure 4.10, and as can be seen, all the eigenvalues of matrix A_1 are in the LHP and matrix A_1 is Hurwitz. Furthermore, as can be seen in Figure 4.11 in the ideal market, by increasing transmission capacity of line 12 to 13 there is an increase in ψ_{min} denoted in (4.54), and therefore c_{max} increases. In the next section, the effect of wind uncertainty will be quantified and robust stability of the market will be studied.

4.5.2 Stability of the Perturbed Wholesale Market

Since the wind generator is introduced in bus 13, the key parameters of interest are Δ_{G13} and x^w. Since a DR entity is introduced in bus 15, the other parameter of interest is κ_{D15}. Now the effects of these parameters on the stability of the perturbed market are examined. The region of attraction c_{max} was computed for different values of Δ_{13}, x^w, and κ_{15}. First, for all values of Δ_{13}, x^w , and κ_{D15}, the condition in (4.84) is satisfied, which implies that the market is stable. As can be seen in Figure 4.12, with $\kappa_{15} = 0$, the region of attraction decreases as the wind uncertainty Δ_{13} is increased. Figure 4.12 also shows that by increasing demand curtailment factor κ_{15}, we can see that the region of attraction is improved. This result indicates the fact that the demand curtailment factor due to real time pricing is an effective way to mitigate the wind volatility in the wholesale market.

Table 4.1 provides a summary of the results obtained in the four scenarios 1) through 4) described above. As can be seen in Table 4.1, the relative size of region of attraction, c_{max} is

reduced in Scenario 2) compared to Scenario 1) due to wind uncertainty. The relative size of region of attraction is reduced with increase in wind penetration as well. Scenario 4) shows the positive effect of κ_{15} on c_{max}.

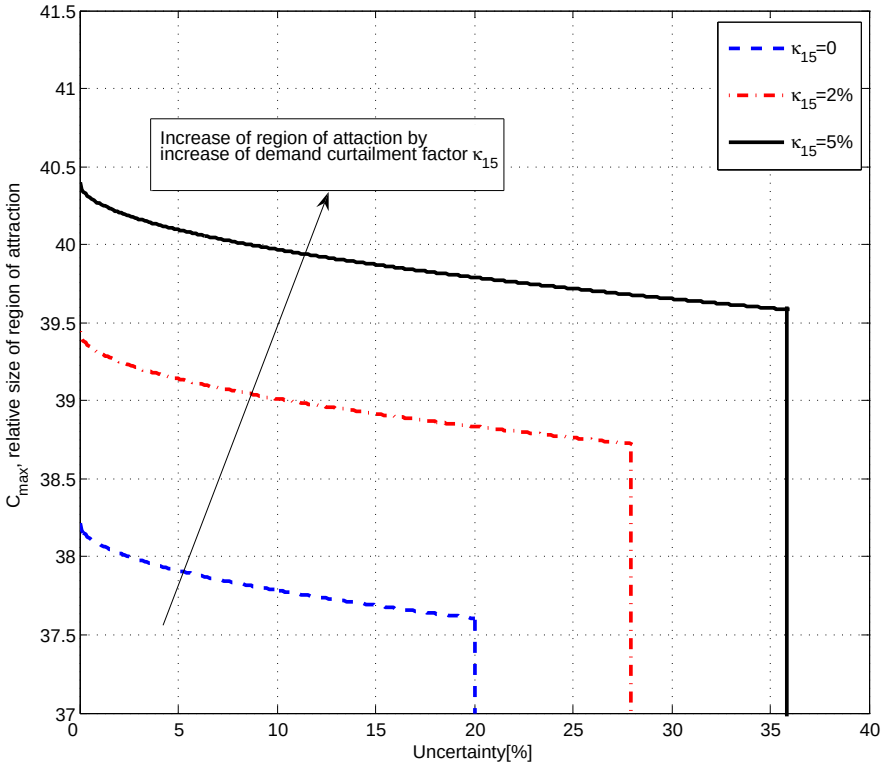

Figure 4.12: Relative size of region of attraction for IEEE 30-bus

4.5.3 Placement of Wind Generations on the Grid

The final point that is made in this section is the placement of a wind generator on the grid. Suppose we wish to add another wind farm with the same characteristics as that located in bus 13 with candidate buses as 12, 10 and 22. Figure 4.13 shows the relative size of region of attraction due to different placement of the new wind farm. As can be seen in this figure, for small uncertainties, it doesn't matter as to where this wind farm is located. However for uncertainties more than 10%, the region of attraction is improved for an installation in bus 10 compared to installation in bus 12, and installation in bus 22 significantly improves the relative region of attraction.

In order to explain this result, $Y_{bus_{ii}}$, self-admittance of bus i is defined, which equals the sum of admittances of all transmission lines that terminate at bus i, with the bus admittance matrix given by $Y_{bus} = A^T B_{line} A_r$, and $Y_{bus_{ii}}$ as its i^{th} diagonal element. That is $Y_{bus_{ii}}$ denotes the strength of all transmission lines that support bus i. For this example, it can be shown that $|Y_{bus_{22-22}}| = 54.6306$, $|Y_{bus_{10-10}}| = 47.3407$ and $|Y_{bus_{12-12}}| = 27.6583$. These indicate that as the self-admittance of a bus increases, the robustness of the perturbed market improves, i.e., the grid integrates wind energy in a better manner at that bus. This may serve as an important guideline to the location of the wind energy in general.

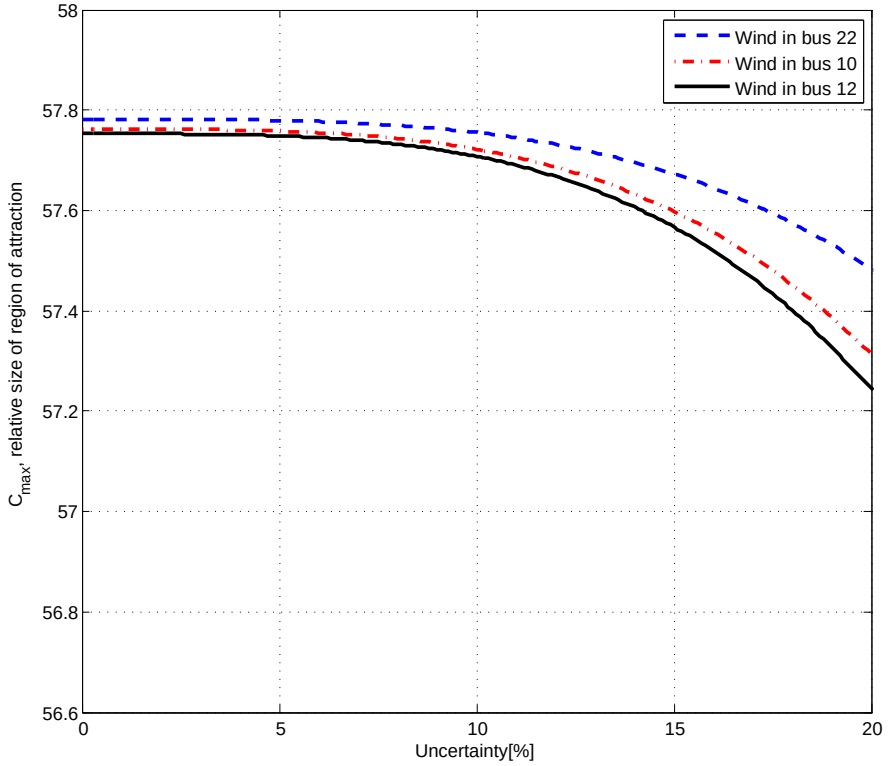

Figure 4.13: Relative size of region of attraction by different placement of the second wind farm

4.6 Concluding Remarks

In this chapter, the model of the players (GenCo, ConCo, and ISO) together with their constraints and the optimization goal are presented and then the dynamics of the real-time market using the notion of disequilibrium process is captured. A gradient play is used to derive the dynamic evolution of the actions for players and underlying states of the game as dual variables to reach the competitive equilibrium of the real-time market. The stability of the resulting dynamical model of the real-time market is investigated and the region of attraction around the equilibrium of interest is established. This region for which the real-time market is asymptotically stable places an implicit bound on the congestion price.

The stability of the underlying market equilibrium in the presence of uncertainty due to renewable energy and the corresponding region of attraction are established. Demand response as a promising tool for improving robustness of the real-time market due to the uncertainty of RERs is illustrated.

Numerical results are included that validate the theoretical results using IEEE 30-bus system. The simulation results show how demand curtailment factor due to the real time pricing can mitigate the wind volatility in the wholesale market. The final point that is presented in this chapter is the placement of a wind generator due to inherent volatility and intermittency. Our simulation studies show that self-admittance of the admittance matrix, $|Y_{bus_{ii}}|$, serves as an important guideline for the location of the wind energy in the power network.

5 Transactive Hierarchical Control Architecture

Summary. *Transactive Control is presented in this chapter which concerns the use of distributed communications to send an incentive signal and receive a feedback signal within the power systems topology. The main contributions of this chapter are*

- *A hierarchical Transactive control architecture that combines market transactions at the higher levels with inter-area and unit-level control at the lower levels,*
- *An analytical model of the overall grid with multiple timescales of primary, secondary, and tertiary levels and the corresponding uncertainties in each level,*
- *Global asymptotic stability of the overall system in the presence of uncertainties at all three time-scales.*

One of the hallmarks of a Smart Grid is the presence of a grid-wise information layer that facilitates decision and control in the presence of intermittencies and uncertainties by gathering and communicating pertinent data from generation, load, and storage distributed across the grid. Given that this information is available at multiple time-scales and from multiple sources, the underlying decision and control algorithms need to necessarily have a hierarchical structure. In this chapter, a hierarchical Transactive control architecture is proposed that combines market transactions at the higher levels with inter-area and unit-level control at the lower levels. A model of the overall grid is introduced, with dynamics at primary, secondary, and tertiary levels. With a goal of ensuring frequency regulation using optimal allocation of resources in the presence of uncertainties in renewables and load, a hierarchical control methodology is presented. Global asymptotic stability of the overall system is established in the presence of uncertainties at all three time-scales and numerically evaluated. Our proposed hierarchical control framework has the following functionalities: (i) Primary Control where fast control actions at a time-scale of T_p ensures stabilization. (ii) Secondary control where frequency stabilization is carried out at a time-scale of T_s at an Area level. (iii) Tertiary control where distributed economic dispatch occurs at a time-scale of T_t. In the subsequent sections, details of (i)-(iii) as well as the information exchange between these levels are presented. The advantage of such a hierarchical control structure is demonstrated through simulation results.

In Section 5.2, we present the models and controllers of the primary, secondary and tertiary dynamics. In Section 5.3, stability of the overall controller is established. In Section 5.4, numerical studies are presented. A summary is presented in Section 5.5.

5.1 Preliminaries on Singular Perturbations Theory

For proving our main result, we will use singular perturbation theorem, which we recall below [102]. Consider the problem of solving the system

$$\Sigma_0 : \begin{cases} \dot{x}(t) = f(t, x(t), u(t), \epsilon), & x(0) = \xi(\epsilon) \\ \epsilon \dot{u}(t) = g(t, x(t), u(t), \epsilon), & u(0) = \eta(\epsilon) \end{cases} \tag{5.1}$$

where $\xi : \epsilon \mapsto \xi(\epsilon)$ and $\eta : \epsilon \mapsto \eta(\epsilon)$ are smooth. Assume that f and g are continuously differentiable in their arguments for $(t, x, u, \epsilon) \in [0, \infty] \times D_x \times D_u \times [0, \epsilon_0]$, where $D_x \subset \mathbf{R}^n$ and $D_u \subset \mathbf{R}^m$ are domains, $\epsilon_0 > 0$. In addition, let Σ_0 be in standard form, i.e. $0 = g(t, x, u, 0)$, has $k \geq 1$ isolated real roots $u = h_i(t, x)$, $i \in \{1, \cdots, k\}$, for each $(t, x) \in [0, \infty] \times D_x$. We choose one particular i, which is fixed. We drop the subscript i henceforth. Let $v(t, x) = u - h(t, x)$.

In singular perturbations theory, the system given by

$$\Sigma_{00} : \dot{x}(t) = f(t, x(t), h(t, x(t)), 0), \; x(0) = \xi(0) \tag{5.2}$$

is called the reduced system, and the system given by

$$\Sigma_b : \frac{dv}{d\tau} = g(t, x, v + h(t, x), 0), \; v(0) = \eta_0 - h(0, \xi_0) \tag{5.3}$$

is called the boundary layer system, where $\eta_0 = \eta(0)$ and $\xi_0 = \xi(0)$, $(t, x) \in [0, \infty) \times D_x$, are treated as fixed parameters. The new time scale τ is related to the original time via the relationship $\tau = (t/\epsilon)$. The following assumptions are needed to present stability of the singular perturbed system [102].

Assumption 5.1. On any compact subset of $D_x \times D_v$, the functions f and g, their first partial derivatives with respect to (x, u, ϵ), and the first partial derivative of g with respect to t are continuous and bounded, $h(t, x)$ and $[(\partial g/\partial u)(t, x, u, 0)]$ have bounded first derivatives with respect to their arguments, $[(\partial f/\partial x)(t, x, h(t, x))]$ is Lipschitz in x, uniformly in t, and the initial condition given by ξ and η are smooth functions of ϵ.

Assumption 5.2. The origin is an exponentially stable equilibrium point of the reduced system Σ_{00} given by (5.2). There exists a Lyapunov function $V : [0, \infty) \times D_x \to [0, \infty)$ that satisfies

$$W_1(x) \leq V(t, x) \leq W_2(x)$$

$$\frac{\partial V}{\partial t}(t, x) + \frac{\partial V}{\partial x}(t, x) f(t, x, h(t, x), 0) \leq -W_3(x)$$

for all $(t, x) \in [0, \infty) \times D_x$, where W_1, W_2, W_3 are continuous positive-definite functions on D_x, and let c be a nonnegative number such that $\{x \in D_x | W_1(x) \leq c\}$ is a compact subset of D_x.

Assumption 5.3. The origin is an equilibrium point of the boundary layer system Σ_b given by (5.3), which is exponentially stable uniformly in (t, x).

Theorem 5.1. *Consider the singular perturbation system Σ_0 given in (5.1), and let $u = h(t,x)$ be an isolated root of $g(t,x,u,0) = 0$. Assume that the Assumptions 5.1-5.3 are satisfied for all $[t,x,u-h(t,x),\epsilon] \in [0,\infty) \times D_x \times D_v \times [0,\epsilon_0]$ such that $D_x \subset \mathbf{R}^n$ and $D_v \subset \mathbf{R}^m$, which contain their respective origins. Let $R_v \subset D_v$ denote the region of attraction of the autonomous system*

$$(dv/d\tau) = g(0,\xi_0, v + h(0,\xi_0), 0). \tag{5.4}$$

Furthermore, let Ω_v be a compact subset of R_v, then for each compact set $\Omega_x \subset \{x \in D_x | W_2(x) \leq \rho c, 0 < \rho < 1\}$, there exists a positive constant ϵ_* such that for all $t \geq 0$, $\xi_0 \in \Omega_x$, $\eta_0 - h(0,\xi_0) \in \Omega_v$, and $0 < \epsilon < \epsilon_*$, Σ_0 has a unique solution x_ϵ on $[0,\infty)$, and

$$x_\epsilon(t) - x_{00}(t) = O(\epsilon) \tag{5.5}$$

holds uniformly for $t \in [0,\infty)$, where x_{00} denotes the solution of the reduced system Σ_{00} in (5.2).

Remark 5.1. Assumption 5.3 can be locally verified by linearization. Let φ denote the map $v \mapsto g(t,\xi,v+h(t,\xi),\epsilon)$. It can be shown that if there exists $\omega_0 > 0$ such that the Jacobian matrix $[(\partial\varphi/\partial v)]$ satisfies the eigenvalue condition $Re(\lambda[(\partial\varphi/\partial v)(t,x,h(t,x),0)]) \leq -\omega_0 < 0$ for all $(t,x) \in [0,\infty) \times D_x$, then Assumption 5.3 is satisfied.

5.2 Modeling of the Transactive Hierarchical Grid

The Primary, Secondary, and Tertiary controllers of the Transactive control architecture, function at three disparate time-scales designed with different purposes. The primary level concerns unit-level time-scales, which includes power balance that occurs instantaneously, and unit dynamics that is of the order of seconds, the secondary level concerns area-level time-scales, where frequency regulation occurs in the order of minutes, and the tertiary level, where economical dispatch occurs, of the order of 5 minutes. Denoting these time scales as t, k, and K, we will show that the primary-level model is of the form

$$\begin{bmatrix} \dot{x}_p \\ \epsilon\dot{z}_p \end{bmatrix} = f(x_p, z_p, \phi_p, \Delta_p) + u[k] \tag{5.6}$$

where Δ_p denotes uncertainties in generation and load, ϕ_p denotes tie-line flow, z_p denotes the faster time scale of power balance, x_p denotes unit states such as mechanical power, valve positions and unit frequencies, ϵ is a small positive scalar and the limit $\epsilon \to 0$ yields the power flow constraint and finally $u[k]$ denotes a desired reference in frequency and load.

In order to accomplish frequency regulation in the presence of a satisfactory economic dispatch, we address the underlying slower dynamics in (5.6), which will be shown to be of the form

$$x_s[k] = g(x_s[k-1], \Delta_s[k-1]) + u[k] \tag{5.7a}$$
$$x_t[K] = h(x_t[K-1], \Delta_t[K-1]) \tag{5.7b}$$

where $\Delta_s[k]$ and $\Delta_t[K]$ are equivalent uncertainties in the slower time scales due to Δ_p and ϕ_p. A hierarchical controller

$$u[k] = C(x_s[k], x_t[K]) \tag{5.8}$$

is proposed, whose goal is to ensure that the overall system with the above multiple time-scales is stable, and satisfactory regulation is maintained even in the presence of the uncertainties Δ_p and ϕ_p. Each of the three levels are described below.

5.2.1 Dynamic Modeling for Primary Control

The purpose of the primary control loop is to regulate real power at a unit level. As mentioned earlier, the underlying time-scale in this level is of the order of T_p. Noting that T_p is significantly small, we represent the dynamics at the primary level using differential equations. Therefore the main components that need to be modeled are Governor-Turbine-Generator (GTG) sets, wind-turbines, and loads that are DR-compatible. We first separate the family of generating units into P_{C_i}, $i = 1,\ldots,N_G$, and P_{W_r}, $r = 1,\ldots,N_w$, where N_G denotes the conventional dispatchable generating units, and N_W denotes non-dispatchable wind energy. Dispatchable generation refers to the generating units that can be dispatched and control at the request of power grid operators. Non-dispatchable generators consist of renewable energy sources that their generation level cannot be fully controlled by system operator because of their uncertainty and intermittency. The dynamics of each of these components are described below:

Reduced-order modeling of non-dispatchable generators

A fixed-speed wind turbine with a squirrel cage induction generator is the simplest electrical topology in a wind turbine technology. The turbine blades convert the kinetic energy of wind into rotational mechanical energy. The squirrel cage induction generator transforms the mechanical energy into electrical energy and delivers the energy directly to the grid. It should be noted that the rotational speed of the generator is relatively high in the order of $1000 - 1500$ rpm for a 50 Hz system frequency. Such rotational speed is too high for the turbine rotor speed with respect to turbine efficiency and mechanical stress. Thus, the generator speed must be stepped down using a multiple-stage gearbox with an appropriate gear ratio [103].

An induction generator consumes a significant amount of reactive power even during zero power production. The reactive power consumption increases along with active power output. Accordingly, compensating capacitor is necessary in order to compensate reactive power consumption in an induction generator. It is possible to include all the dynamics of an induction generator in a highly detailed model. Nevertheless, such a model make stability studies very complicated because it increases complexity and can be computationally prohibitive. More importantly, not all of these dynamics have a significant influence on a stability analysis. A comprehensive discussion of a comparison of different induction generator models can be found in [103].

In our analysis, we consider a two-mass model of a wind turbine discussed in [104]. The mathematical model of the two-mass model was elaborated in more detailed in [105].

In this model the gearbox of a wind turbine is modeled as two inertias that are connected to each other through a spring. The spring represents the low stiffness of the connecting shaft. In addition to shaft stiffness, different damping factors that exist in the two-mass model have been presented in [105]. Three different damping components are present in the model, namely the turbine self damping (D_t), the generator self damping (D_g) and the mutual damping (D_m). The turbine self damping represents the aerodynamic resistance that takes place in the turbine blade. The generator self damping represents mechanical friction and windage. The mutual damping represents balancing dynamics that occur because of different speeds between the generator rotor and the turbine shaft. The mathematical equations of a two-mass drive train model obtained by neglecting the turbine and the generator self dampings are given as

$$\begin{aligned}
\dot{\theta}_W &= \omega_W \\
\dot{\omega}_W &= \frac{D_m}{M_G}\omega_W - \frac{D_m}{M_G}\omega_T + \frac{K_s}{M_G}(\theta_W - \theta_T) - \frac{1}{M_G}P_W \\
\dot{\theta}_T &= \omega_T \\
\dot{\omega}_T &= -\frac{D_m}{M_T}\omega_W + \frac{D_m}{M_T}\omega_T - \frac{K_s}{M_T}(\theta_W - \theta_T) + \frac{1}{M_T}\Delta_W
\end{aligned} \tag{5.9}$$

where θ_W is the generator rotor angle, θ_T is the turbine rotor angle, ω_W is the rotor speed of the induction generator, ω_T is the rotor speed of the wind turbine. Δ_W is the wind torque and is an uncertain input to the system of equations, and P_W is the electrical power output. M_G, M_T are the generator and turbine inertias, respectively. D_m is mutual damping coefficients, K_s is the spring constant of the tortional spring used to model the drive train coupling between the two rotors. Figure A.10 shows the details of dynamic modeling of wind generators with mechanical part of wind turbines and range of the parameters are provided in Appendix A.2.9.

State-space representation of (5.9) can be written as

$$\dot{x}_W = A_W x_W + b_W \Delta_W - c_W P_W \tag{5.10}$$

where $x_W = \begin{bmatrix} \theta_W & \omega_W & \theta_T & \omega_T \end{bmatrix}^T$ is defined as local state variables,

$$A_W = \begin{bmatrix} 0 & 1 & 0 & 0 \\ \frac{K_s}{M_G} & \frac{D_m}{M_G} & -\frac{K_s}{M_G} & -\frac{D_m}{M_G} \\ 0 & 0 & 0 & 1 \\ -\frac{K_s}{M_T} & -\frac{D_m}{M_T} & \frac{K_s}{M_T} & \frac{D_m}{M_T} \end{bmatrix}, b_W = \begin{bmatrix} 0 & 0 & 0 & \frac{1}{M_T} \end{bmatrix}^T, \text{ and } c_W = \begin{bmatrix} 0 & \frac{1}{M_G} & 0 & 0 \end{bmatrix}^T.$$

Reduced-order modeling of dispatchable generators

Steam turbine generator units is one of the most important dispatchable generators. A reduced-order modeling of steam turbine generators is a result of major simplifications that the real power and the corresponding electromechanical variables such as frequency and rotor angle are decoupled from the reactive power and electromagnetic variables including voltage behind the transient reactance of a generator .

A reduced-order model based on these simplifications can be derived as [65, 99]

$$\begin{aligned}
\dot{\theta}_G &= \omega_G - \omega^{ref} \\
M\dot{\omega}_G &= (e_T - D)\omega_G + P_m - P_C \\
T_u\dot{P}_m &= -P_m + k_t a \\
T_g\dot{a} &= -\omega_G - ra + \omega_C
\end{aligned} \tag{5.11}$$

where θ_G is the rotor angle, ω_G is the rotor speed, P_m is the mechanical power, a is valve position, ω_C is the reference frequency set by the secondary controls, and so is assumed constant in the primary dynamics time scale, and finally P_C is the electrical power output for dispatchable generator defined as the system coupling variable. M is the inertia constant, e_T defined by $\frac{\partial P_t}{\partial \omega_G}$ is a coefficient representing the turbine self-regulation, D is the damping coefficient, T_u is the time constant representing the delay between the control valves and the turbine nozzles, k_t is a proportionality factor representing the control valve position variation relative to the turbine output variation, T_g is the time constant of the valve servo motor-turbine gate system, r is the permanent speed droop of the turbine. The block diagram of Stem-Turbine-Generator is shown in Figure A.6. State-space representation of the reduced order steam turbine generator units located in bus i in (5.11) can be written as

$$\dot{x}_C = A_C x_C + b_C \omega_C + c_C P_C \tag{5.12}$$

where $x_C = \begin{pmatrix} \theta_G & \omega_G & P_m & a \end{pmatrix}^T$ denotes local state variables of steam turbine generators,

$$A_C = \begin{bmatrix} 0 & 1 & 0 & 0 \\ 0 & \frac{e_T - D}{M} & \frac{1}{M} & 0 \\ 0 & 0 & -\frac{1}{T_u} & \frac{k_t}{T_u} \\ 0 & -\frac{1}{T_g} & 0 & -\frac{r}{T_g} \end{bmatrix}, b_C = \begin{bmatrix} -1 & 0 & 0 & \frac{1}{T_g} \end{bmatrix}^T, \text{ and } c_C = \begin{bmatrix} 0 & \frac{1}{M} & 0 & 0 \end{bmatrix}^T.$$

Dynamic modeling of hydro-turbine generators, combustion turbine generators, and combined cycle plants are provided in Appendix A.2.6, A.2.7, and A.2.8, respectively.

The overall local physical model of generators can be written compactly as [12, 99]

$$\dot{x}_G = A_G x_G + b_G \omega_{ref} - c_G P_G + \Delta_G \tag{5.13}$$

where the local state as $x_G = \begin{bmatrix} x_W^T & x_C^T \end{bmatrix}^T$, frequency references $\omega_{ref} = \begin{bmatrix} 0 & \omega_C^T \end{bmatrix}^T$, and generator-outputs be defined as , $P_G = \begin{bmatrix} P_W^T & P_C^T \end{bmatrix}^T$, and the local system matrix as $A_G = \text{diag}\{A_W, A_C\}$, $b_G = \text{diag}\{0, b_C\}$, $c_G = \text{diag}\{c_W, c_C\}$, and $\Delta_G = \text{diag}\{b_W \Delta_W, 0\}$.

It should be noted that P_G, the vector of generator power outputs, is the coupling variable which represents interactions with the local dynamics of other generators and loads via a transmission network.

Load Modeling for Demand Response

Conventional methods in power systems control mainly rely on following load fluctuations by adjusting the generation units. However due to huge intermittency and uncertainty, relying on the conventional methods is inefficient and will impose huge cost of ancillary reserves.

Of late, Demand Response (DR) programs have begun to be used as an asset to the power system [100, 101]. Rather than reduce the stress on the power system via peak-load reduction, these programs are targeted to respond to specific reliability events. Some of the loads have been identified as potential AGC signals that can respond on a 1-minute time scale, denoted as Regulation-response DR (RR-DR), while others are classified as Price-response DR (PR-DR) that respond to real-time price signals and move consumption from peak-time to off-peak time [100].

Using the above classification, we express the overall load P_L as

$$P_L = \text{PR-DR} + \text{RR-DR} + \text{uncertain loads} \tag{5.14}$$

Loads with energy storage, such as heaters, air conditioners, refrigerators and PEVs, can be modulated with reasonable disturbance to customer comforts [11]. Equipped with frequency sensors, they can sense the frequency as a measure of supply-demand imbalance, and consequently change the power consumed in less than 1 second [13]. Therefore Eq. (5.14) can be expressed as

$$P_L = \underbrace{P_L^{ref}}_{\text{PR-DR}} + \underbrace{J_L\dot{\omega}_L + D_L\omega_L}_{\text{RR-DR}} + \underbrace{\Delta_L}_{\text{Load Uncertainty}} \tag{5.15}$$

where J_L and D_L refer to the effective moment of inertia and the damping coefficient of the aggregate load, ω_L the frequency measured at the load location, Δ_L represents uncertainty of load, P_L^{ref} is the set point of the electrical energy delivered by the network to the load and is defined based on the real time price as well as local frequency deviation feedback, and finally P_L is the overall demanded power taken by the load and is used for coupling through transmission or distribution lines. It is assumed in (5.15) that the Price-response DR is capable of meeting a specified P_L^{ref} rapidly.

Using Eq. (5.15), we can compactly rewrite the overall cyber-physical load as

$$\dot{x}_L = A_L x_L + b_L P_L^{ref} + c_L P_L + \Delta_L \tag{5.16}$$

where $x_L = \begin{bmatrix}\omega_L\end{bmatrix}^T$ and the local system matrix as $A_L = \text{diag}\{-D_L/J_L\}$, $b_L = \text{diag}\{-1/J_L\}$, and $c_L = \text{diag}\{-1/J_L\}$.

Electrical network coupling

Given that at each node, the generation and demand agents are interconnected, the Kirchhoff current and voltage laws should be satisfied. This requires that the electric power must instantaneously equal the sum of power flow into transmission or distribution lines directly connected to the buses.

Assuming lossless transmission network that consists of n nods or buses, indexed $i, j = 1, \ldots, n$. To each node are attached generators that supply power and load that consume power. A line connecting bus i to bus j is characterized by its electrical admittance, denoted $Y_{ij} > 0$ and $Y_{ij} = Y_{ji}$. As pointed out in Chapter 2.1, the real power flow over the line from bus i to j is equal to

$$P_{ij} = V_i V_j \sin(\delta_i - \delta_j) \tag{5.17}$$

where V_i is the voltage amplitude at bus i, and δ_i is the voltage phase angle at bus i. Using Eq. (5.17), the net power P_i injected into the network at bus i is the algebraic sum of the P_{ij} as

$$P_i = \sum_{j=1}^{n} P_{ij} = \sum_{j=1}^{n} V_i V_j Y_{ij} \sin(\delta_i - \delta_j), \quad i = 1, \ldots, n. \tag{5.18}$$

For the sake of simplicity in this thesis, we assume that the voltage magnitude V_i at bus i is constant and the phase angle differences, $|\delta_i - \delta_j|$, are sufficiently small. With no loss of generality, we can then set $V_i = 1$ for all i. Then the net power P_{ij} in (5.18) can be simplified as

$$P_i = \sum_{j=1}^{n} Y_{ij}(\delta_i - \delta_j), \quad i = 1, \ldots, n. \tag{5.19}$$

As can be seen in Figure 5.1, voltage phase angle δ_i in general is not equal to the rotor phase angle θ_i. Using Thevenin's equivalent, the stator reactance X_s is combined with the

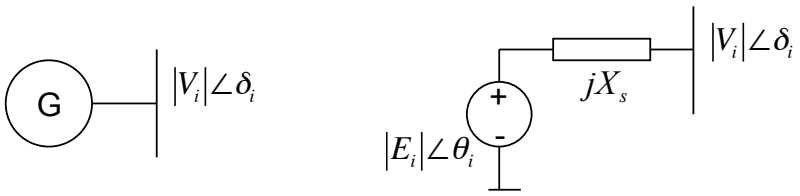

Figure 5.1: Response of the voltage phase angle and rotor phase angle.

transmission line admittance [65], and therefore we can write the real power flow equations as

$$\begin{bmatrix} P_G \\ P_L \end{bmatrix} = \begin{bmatrix} Y_{GG} & Y_{GL} \\ Y_{LG} & Y_{LL} \end{bmatrix} \theta - \begin{bmatrix} \phi_G \\ \phi_L \end{bmatrix} \tag{5.20}$$

where $\theta = \begin{bmatrix} \theta_G^T & \theta_L^T \end{bmatrix}^T$, $Y = A^T B_{line} A_r$ is a bus admittance matrix, B_{line} denotes the line admittance matrix (N_t by N_t diagonal matrix) with elements $B_{nm} + X_{s_n}$ and let A denote the $N_t \times N$ bus incidence matrix. Let A_r denote the reduced bus incident matrix ($N_t \times N - 1$) which is A with column corresponding to reference bus removed. ϕ_G and ϕ_L represent tie-line flows of power from neighbor areas into the area at the generator and load buses, respectively.

Because of line power flow dependence on nodal angles, a general model of power system dynamics comprises both the closed loop dynamics of the generators and loads as defined in (5.13) and (5.16) respectively, and the real power flow constraints in (5.20). Consequently, the general model is given as a differential algebraic equation (DAE) model with two time-scales including the slow dynamics for the generators and loads and the fast dynamics for power flow constraints. For the sake of simplicity, we restrict our attention only on real power. A similar model for voltage control can be derived and analyzed [99].

Using ϵ-embedding techniques [102] and noting that $\theta_G = E_G x_G$ and $\theta_L = E_L x_L$, the algebraic power flow constraint (5.20) changes into fast dynamics as

$$\epsilon \begin{bmatrix} \dot{P_G} \\ \dot{P_L} \end{bmatrix} = \begin{bmatrix} Y_{GG}E_G & Y_{GL} \\ Y_{LG}E_L & Y_{LL} \end{bmatrix} \begin{bmatrix} x_G \\ x_L \end{bmatrix} - \begin{bmatrix} P_G \\ P_L \end{bmatrix} - \begin{bmatrix} \phi_G \\ \phi_L \end{bmatrix} \tag{5.21}$$

where ϵ is a small positive scalar and the limit $\epsilon \to 0$ yields the power flow constraint (5.20).

Reduced Model of Interconnected Grid for Primary Control

Using the dynamical models of generators (5.13), DR-capable loads in (5.16), and interconnections in (5.21) the overall dynamical representation can be rewritten again as follows

$$\begin{bmatrix} \dot{x}_G \\ \dot{x}_L \\ \epsilon\dot{P}_G \\ \epsilon\dot{P}_L \end{bmatrix} = \begin{bmatrix} A_G & 0 & -c_G & 0 \\ 0 & A_L & 0 & c_L \\ Y_{GG}E_G & Y_{GL} & -I & 0 \\ Y_{LG}E_L & Y_{LL} & 0 & -I \end{bmatrix} \begin{bmatrix} x_G \\ x_L \\ P_G \\ P_L \end{bmatrix} - \begin{bmatrix} 0 \\ 0 \\ \phi_G \\ \phi_L \end{bmatrix} + \begin{bmatrix} b_G & 0 \\ 0 & b_L \\ 0 & 0 \\ 0 & 0 \end{bmatrix} \begin{bmatrix} \omega_{ref} \\ P_L^{ref} \\ 0 \\ 0 \end{bmatrix} + \begin{bmatrix} \Delta_G \\ \Delta_L \\ 0 \\ 0 \end{bmatrix}. \tag{5.22}$$

Remark 5.2. As can be seen in Eq. (5.22), both ω_{ref} and P_L^{ref} are set-points provided by the secondary controller, with the former determined by the AGC and the latter by Price-response DR. ΔG and ΔL denote the uncertainties in RER and load, respectively.

Before we proceed to the secondary level, we separate the time-scales in the primary level by defining

$$t_{k+1} = t_k + T_s$$

where $T_s >> T_p$. Denoting $x_p = [x_G^T \; x_L^T]^T$, $z_p = [P_G^T \; P_L^T]^T$, $\Delta_p = [\Delta_G^T \; \Delta_L^T]^T$, $u(k) = [\omega_{ref}^T \; P_L^{ref^T}]^T$ as command inputs, $\phi_p(t) = [\phi_G^T \; \phi_L^T]^T$ as the tie-line flow and $z_s(k) = z_s(t_k)$ for any variable of interest in the secondary level, we can express (5.22) compactly as a singularly perturbed LTI system

$$\dot{x}_p = Ax_p(t) + Bz_p(t) + Fu(k) + \Delta_p \tag{5.23a}$$
$$\epsilon\dot{z}_p = Cx_p(t) + Dz_p(t) + \phi_p(t). \tag{5.23b}$$

5.2.2 Models and Controllers at the Secondary Level

The goal of the secondary level control is to determine the specific set-point u for the primary controllers despite the uncertainties ΔG and ΔL. The primary control acts in response to locally measured changes in the generator's output frequency from the established system standard, which is 60 Hz in the U.S and 50 Hz in Europe. Spontaneous reaction in primary level results in a small change in system frequency. The errors in frequency and flows between control areas are corrected by the relatively slower controller in the secondary level.

Models for Secondary Control

The first step of design is to assume that the primary level variables x_p and z_p denoted in (5.22) have reached steady state and therefore we can rewrite the primary dynamics in (5.23a), and (5.23b) as

$$0 = Ax_{p_{ss}}[k] + Bz_{p_{ss}}[k] + Fu[k] + \Delta_{p_{ss}} \tag{5.24a}$$
$$0 = Cx_{p_{ss}}[k] + Dz_{p_{ss}}[k] + \phi_{p_{ss}}[k] \tag{5.24b}$$

where $*_{p_{ss}}$ denotes the steady-state values of the primary states. Writing Eq. (5.24b) at two successive secondary sampling instants k and $k+1$, we can rewrite (5.24b) compactly as

$$x_s[k+1] = x_s[k] + B_s u_s[k] + C_s \Delta_s[k] \tag{5.25}$$

where $x_s = R_s x_{p_{ss}}$ is the aggregated frequency of the underlying area and R_s denoted as the aggregation matrix, $B_s = R_s(BD^{-1}C - A)^{-1}F$, $u_s[k] = u(k+1) - u(k)$, $C_s = R_s(BD^{-1}C - A)^{-1}$, and finally $\Delta_s[k]$ is an equivalent uncertainty at the secondary level due to Δ_p and ϕ_p, defined as

$$\Delta_s[k] = -BD^{-1}\left(\phi_{p_{ss}}[k+1] - \phi_{p_{ss}}[k]\right) + \left(\Delta_{p_{ss}}[k+1] - \Delta_{p_{ss}}[k]\right). \tag{5.26}$$

Secondary Controller

We now use the model in (5.25) for the design of the secondary controller. The goal of secondary control is to regulate generators frequency $\omega_{G_{ss}}[k]$ and load frequency $\omega_{L_{ss}}[k]$ to reach the desired set point x_t introduced by tertiary control level in the presence of the uncertainty Δ_s. As in the previous section, we introduce a third time-scale

$$t_{K+1} = t_K + T_t \tag{5.27}$$

where $T_t >> T_s$. Let us define the Area Control Error (ACE) compactly as

$$e_s[k+1] = x_s[k+1] - R_t x_t[K] \tag{5.28}$$

where $x_t[K]$ is a reference signal determined by the tertiary level, and is adjusted every K units of time, and $R_t = \text{diag}\{I_{n_s}, 0\}$ is the aggregation matrix for tertiary level. The overall goal of secondary controller is to find the control input $u_s[k]$ such that the following cost function is minimized [99]

$$J = \sum_{k=0}^{N-1} e_s^T[k+1] W e_s[k+1] + u_s^T[k] R u_s[k] \tag{5.29}$$

subject to the equality constraints in (5.25) with the weighting matrices $W \geq 0$, $R \geq 0$. The resulting discrete-time decentralized LQR controller is given by

$$u_s[k] = -L_s e_s[k] = -L_s x_s[k] + L_t x_t[K] \tag{5.30}$$

where $L_t = L_s R_t$, $L_s = (R + B_s^T F_r B_s)^{-1} B_s^T F_r$ and F_r is the solution of discrete finite horizon Riccati equation. The last term in equation (5.30) follows by noting that $x_t[K]$ remains constant between k and $k+1$ for any k. The controller parameters L_s and L_t ensure stability in the absence of the uncertainty Δ_s. In Section 5.3, the robustness of the secondary loop to this uncertainty will be formally discussed.

Using the control input in (5.30), we can write the nominal closed-loop secondary dynamics as

$$x_s[k+1] = \tilde{A}_s x_s[k] + B_s L_t x_t[K] + C_s \Delta_s \tag{5.31}$$

where $\tilde{A}_s = (I - B_s L_s)$. The dynamics of the Area Control Error can be driven as

$$e_s[k+1] = \tilde{A}_s e_s[k] + C_s \Delta_s. \tag{5.32}$$

The controller parameters L_s and L_t ensure stability in the absence of the uncertainty Δ_s. Given the presence of uncertainty, the goal here is to ensure boundedness in the presence of Δ_s and to drive the ACE, $e_s(k)$, to zero. It should be noted that if Δ_s is such that it has a non-zero mean value, then it can change the equilibrium point of $e_s(k)$ which has to be suitably addressed in the analysis of the higher level. This is done in Section 5.2.3.

5.2.3 Models and Controllers at the Tertiary Level

Tertiary control is responsible for the determination of $x_t[K]$ at each K such that the overall system operates in the most economical way and satisfies all stability and reliability criteria. Unlike the current centralized action of the ISO, we propose a dynamic economic dispatch paradigm based on the notion of disequilibrium process where Generating Companies (GenCo), Consumer Companies (ConCo), and ISO exchange information through a communication network with low latencies.

In what follows, we use the model of GenCo presented in Section 4.1.1, and ConCo in Section 4.4. The discussions of wind integration in the market and also the effect of the transmission lines are provided in Chapter 4, here in contrast to what we proposed in Section 4.4 that wind power is one of the main participants in the market, in this chapter we assume that wind power is modeled as a negative load, and for the sake of simplicity we ignore transmission lines capacity constraints.

Following this assumption, ISO problem is defined for all ConCo $j \in D_q$ and GenCo $i \in G_f$ as

$$\text{maximize } \sum_{j \in D_q} U_{Dj}(P_{Dj}) - \sum_{i \in G_f} C_{G_i}(P_{Gi}) \tag{5.33}$$

subject to

$$\Delta_n - \sum_{i \in \theta_n} P_{Gi} + \sum_{j \in \vartheta_n} P_{Dj} + \sum_{m \in \Omega_n} B_{nm} \left[\delta_n - \delta_m\right] = 0;\ \rho_n, \forall n \in N \tag{5.34}$$

where

$$\Delta_n = -\sum_{i \in \theta} \Delta G_i + \sum_{j \in \vartheta} \Delta_{L_j} \tag{5.35}$$

is the aggregation of predicted uncertainties at bus n due to the forecast error of wind generation units and load uncertainty as will be discussed further in Section 5.2.5, and δ_n is the voltage angle of bus n. Set θ_n denotes indices of generating units at node n, ϑ_n set of indices of demands at node n, and finally Ω_n is the set of nodes connected to node n. The constraints (5.34) is due to power balance. It can be seen that the associated Lagrange multiplier, ρ_n, is indicated in each constraint. The underlying optimization problem of the ISO can therefore be defined as the optimization of (4.8a) subject to constraint (4.8b).

The resulting solution can be determined, using KKT conditions [10], as P^*_{Gi}, the amounts of power to be generated by each generating unit i, P^*_{Dj}, the amounts of power to be consumed by each consumer j, the locational marginal prices, ρ^*_n that satisfies the following conditions:

$$\frac{d(C_{G_i}(P_{Gi}))}{dP_{Gi}}|_{P^*_{Gi}} - \rho^*_{n(i)} = 0 \quad \forall i \in G_f \tag{5.36a}$$

$$\rho^*_{n(j)} - \frac{d(U_{Dj}(P_{Dj}))}{dP_{Dj}}|_{P^*_{Dj}} = 0 \quad \forall j \in D_q \tag{5.36b}$$

$$\sum_{m\in\Omega_n} B_{nm}\left[\rho^*_n - \rho^*_m\right] = 0 \quad \forall n \in N \tag{5.36c}$$

$$\Delta_n - \sum_{i\in\theta_n} P^*_{Gi} + \sum_{j\in\vartheta_n} P^*_{Dj} + \sum_{m\in\Omega_n} B_{nm}\left[\delta^*_n - \delta^*_m\right] = 0 \ \forall n \in N \tag{5.36d}$$

5.2.4 Dynamic Market Mechanism Design as a Tertiary Control

The same as Section 4.2.1, instead of solving Eq. (5.33)-(5.34) as a static optimization problem, we take a dynamic approach. Now let us define $h = T_{mc}/N$ with

$$h = t_{K+1} - t_K. \tag{5.37}$$

Hence if T_{mc} is chosen as the market clearing time, it follows that N iterations elapse if h is chosen as the sampling interval. From (5.27), it follows that $h = T_t$. We introduce the specifics of designing DMM for electricity market as follows:

State Space:

The underlying state space in this game is denoted by $X \subset \mathbb{R}^N$ where each state $\rho_n \in X$ is the profile of locational marginal prices at each node and congestion prices for each transmission line.

State Dependent Payoff Function:

The state dependent payoff function for GenCo i is defined in Eq. (4.3), ConCo j is defined in Eq. (4.6), and Social Welfare denoted in (4.7).

Actions:

Each GenCo i, ConCo j, and substation at bus n is assigned a state dependent action that permits GenCos and ConCos to change their production and consumption level and substations to change their voltage phase angle. Using gradient play [10, 95], we can derive an action for the i th GenCo $\forall i \in G_f$ as

$$P_{Gi}[K+1] = P_{Gi}[K] + hk_{P_{Gi}}(\rho_{n(i)_k} - c_{Gi}P_{Gi_k} - b_{Gi}) \tag{5.38}$$

with the goal of driving its solution P_{Gi} to the equilibrium P^*_{Gi} which solves (5.36a). Similarly, using (4.4), a state dependent action can be derived for the jth ConCo $\forall j \in D_q$ as

$$P_{Dj}[K+1] = P_{Dj}[K] + hk_{P_{Dj}}\left(c_{Dj}P_{Dj_k} + b_{Dj} - \rho_{n(j)_k}\right) \tag{5.39}$$

where $k_{P_{Gi}}$ and $k_{P_{Dj}}$ are step sizes that can be adjusted so as to result in an optimal convergence of these solutions to the equilibrium in (5.36a)-(5.36d). Finally, the state dependent action for voltage phase angles can be determined as

$$\delta_n[K+1] = \delta_n[K] - hk_{\delta_n}\left(\sum_{m\in\Omega} B_{nm}\left[\rho_n - \rho_m + \gamma_{nm} - \gamma_{mn}\right]\right) \tag{5.40}$$

State Dynamics:

We now describe how the states evolve as a function of players strategies. As mentioned earlier, states consist of locational marginal price ρ_n. The state dynamics or pricing mechanism can be derived as

$$\rho_n[K+1] = \rho_n[K] + hk_{\rho_n}\left(\hat{\Delta}_n[K+d|K] - \sum_{i\in\theta} P_{Gi} + \sum_{j\in\vartheta} P_{Djk} + \sum_{m\in\Omega} B_{nm}\left[\delta_n - \delta_m\right]\right) \tag{5.41}$$

where $\hat{\Delta}_n[K+d|K]$ is a d-step-ahead prediction of Δ_n.

d-step-head Prediction:

$\hat{\Delta}_n[K+d|K]$ is the d-step ahead predication of $\Delta_n[K]$ such that at each K can be represented based on the actual wind generation uncertainty and load deviation denoted as

$$\hat{\Delta}_n[K+d|K] = \mathscr{F}(\Delta_n(K), \Delta_n(K-1), \ldots, \Delta_n(K-M)), \forall M \in \mathbb{Z}. \tag{5.42}$$

To find the optimal d-step-ahead predictor, consider the ARMA model as

$$A(q^{-1})\Delta_n[K] = C(q^{-1})w[K] \tag{5.43}$$

where

$$A(q^{-1}) = 1 + a_1 q^{-1} + \ldots + a_{na} q^{-na}$$
$$C(q^{-1}) = 1 + c_1 q^{-1} + \ldots + c_{nc} q^{-nc}.$$

Let Y^t denote the information available at the time instant t as $Y^t = \{\Delta_n[K], \Delta_n[K-1], ...\}$. The following assumptions are needed to present the optimal predictor.

Assumption 5.4. Let us assume the followings

- $\{w[K]\}$ is a sequence of uncorrelated and identically distributed Gaussian random variables with zero mean and variance λ^2,
- $A(q^{-1})$ and $C(q^{-1})$ have no common zeros,

- the parameters $\{a_i, c_i\}$ are given,
- $C(q^{-1})$ is asymptotically stable.

The design problem is to determine the mean square optimal d-step predictor of $\Delta_n[K+d]$, i.e. an estimate $\hat{\Delta}_n[K+d|K]$ of $\Delta_n[K+d]$, which is a function of Y^t and is such that the variance of the prediction error

$$\varepsilon_n[K+d] = \Delta_n[K+d] - \hat{\Delta}_n[K+d|K] \tag{5.44}$$

is minimized.

Lemma 5.1. Let for the ARMA model (5.43), Assumption 5.4 holds. Then the optimal d-step-ahead prediction, $\hat{\Delta}[K+d|K]$, of $\Delta[K+d]$ satisfies

$$C(q^{-1})\hat{\Delta}_n[K+d|K] = G(q^{-1})\Delta_n[K] \tag{5.45}$$

where the prediction error has zero mean with variance $(1+f_1^2+\ldots+f_{k-1}^2)\lambda^2$, and $F(q^{-1})$, and $G(q^{-1})$ are the unique polynomials such that for any given $A(q^{-1})$, and $C(q^{-1})$ satisfying

$$C(q^{-1}) = F(q^{-1})A(q^{-1}) + q^{-d}G(q^{-1}) \tag{5.46}$$
$$G(q^{-1}) = g_0 + g_1 G(q^{-1}) + \ldots + g_{k-1}G(q^{1-d}) \tag{5.47}$$
$$F(q^{-1}) = 1 + f_1 F(q^{-1}) + \ldots + f_{k-1}F(q^{1-d}). \tag{5.48}$$

Proof. Since $A(q^{-1})$ and $C(q^{-1})$ are coprime polynomials, it follows that there exists unique F and G such that Bezout's identity in (5.46) for polynomials holds. Inserting (5.46) into (5.43) gives

$$\Delta_n[K+d] = F(q^{-1})w[K+d] + \frac{G(q^{-1})}{C(q^{-1})}\Delta_n[K] \tag{5.49}$$

It should be noted that the first term in the right-hand side of the above relation is independent of Y^t. Thus the variance of the prediction error

$$E\left(\Delta_n[K+d] - \hat{\Delta}_n[K+d|K]\right)^2 = E\left(\frac{G(q^{-1})}{C(q^{-1})}\Delta_n[K] - \hat{\Delta}_n[K+d|K]\right)^2 + E\left(F(q^{-1})w[K+d]\right)^2 \tag{5.50}$$

which shows that the optimal d-step predictor is given by (5.45). The prediction error is obtained as

$$\varepsilon[K+d] = F(q^{-1})w[K+d]. \tag{5.51}$$

Note that since $\{w[K]\}$ is a sequence of Gaussian random variables with zero mean, it implies that the prediction error has zero mean with variance $(1+f_1^2+\ldots+f_{k-1}^2)\lambda^2$. □

Equations (5.38)-(5.42) represent a dynamic model of the overall Transactive tertiary level. These action and state profiles can also be viewed as a disequilibrium process [96] needed to arrive at the equilibrium following a perturbation from lower levels in the hierarchical structure.

Equations (5.38)-(5.42) can be viewed as control strategies adopted by the GenCo, ConCo, and the ISO in order to ensure an optimal market operation. It should also be noted they represent a significant departure from the current practice where information is exchanged only once between the GenCos and the ISO, following which the ISO clears the market and provides information regarding the price. Our thesis here is that due to the huge volatility and uncertainty of the dynamic drivers such as wind and solar energy sources, and load in the market, such a single iteration will not suffice, and stability cannot be ensured; continued iteration as suggested by the dynamic model above is needed in order to mitigate volatility in real-time price and ensure a stable market design. In the subsequent sections, guidelines for determining stability with such an iterative exchange of information between the different players are discussed. Let us denote $\mathbf{P_G} = \left[P_{G_1}, ..., P_{G_{N_G}}\right]^T$, the amounts of power to be generated by each generating unit i, $\mathbf{P_D} = \left[P_{D_1}, ..., P_{D_{N_D}}\right]^T$ as the amounts of power to be consumed by each consumer j, the voltage phase angles $\mathbf{\Delta} = \left[\delta_1, ..., \delta_{N-1}\right]^T$, the locational marginal prices denoted as $\rho = \left[\rho_1, ..., \rho_N\right]^T$. Using Eqs. (5.38)-(5.41), the dynamic model of tertiary level can be written compactly as

$$x_t[K+1] = (I_{n_t} + hA_t)x_t[K] + hk_\rho \hat{\Delta}_t + b \tag{5.52}$$

where

$$x_t(K) = \left[\mathbf{P_G} \quad \mathbf{P_D} \quad \mathbf{\Delta} \quad \rho\right]^T_{(Ng+N_d+2N-1)\times 1}, \tag{5.53}$$

$$A_t = \begin{bmatrix} -k_g c_g & 0 & 0 & k_g A_g^T \\ 0 & k_d c_d & 0 & -k_d A_d^T \\ 0 & 0 & 0 & k_\delta Y^T \\ -k_\rho A_g & k_\rho A_d & k_\rho Y & 0 \end{bmatrix} \tag{5.54}$$

where A_g is generators incidence matrix where $A_{g_{ij}} = 1$ if the i^{th} generator is connected to j^{th} bus and $A_{g_{ij}} = 0$ if the i^{th} generator is not connected to j^{th} bus, similarly for A_d which is load incident matrix where $A_{d_{ij}} = 1$ if the i^{th} consumer is connected to j^{th} bus and $A_{d_{ij}} = 0$ if the i^{th} consumer is not connected to j^{th} bus and the matrix Y is defined in Section 5.2.1. Finally,

$$\hat{\Delta}_t = \left[0 \quad 0 \quad 0 \quad diag\{\hat{\Delta}_n[K+1|K]\}\right]^T,$$

$$b = \left[hb_g^T k_g^T \quad hb_d^T k_d^T \quad 0 \quad 0\right]^T.$$

In the next section, we model the uncertainty in each level and finally in Section 5.3 the stability analysis for the overall hierarchical control system will be presented.

5.2.5 Time Scale Separation of Uncertainties

Main sources of uncertainties that are considered in this paper are correspond to Δ_G and Δ_L in Eqs. (5.13) and (5.14) as well as the uncertainty of the adjacent area in ϕ_p respectively. For the purpose of analysis, we separate the three time-scales in Δ_G and Δ_L, and represent them as Δ_p, Δ_s, and $\hat{\Delta}_t$, defined as in (5.23a), (5.25), and (5.41) respectively.

In the tens of seconds time-scale, generators reflecting automatically to deal with the fast uncertainties in the order of milli-seconds. We denote the uncertainty of this order as Δ_p which is corresponding to the states of primary level x_p and denoted as

$$\Delta_p = E_p x_p \tag{5.55}$$

where E_p is perturbation matrix.

In the tens of minutes time scale, system operators schedule adequate regulation reserves to track minute-by-minute changes in the balance between generation and load. Given that $\Delta_P = E_p x_p$, we can rewrite Δ_s in (5.26) as

$$\Delta_s[k] = -BD^{-1}\left(\Delta\phi_{p_s}[k]\right) + \left(E_p \Delta x_s[k]\right) \tag{5.56}$$

where $\Delta x_s[k] = x_{p_{ss}}[k+1] - x_{p_{ss}}[k]$ and $\Delta\phi_s[k] = \phi_{p_{ss}}[k+1] - \phi_{p_{ss}}[k]$. Change of the steady state variables at time instance k depends directly on the set-point $u_s[k]$ (see Eq. (5.24b)), which in turn depends on the states of the secondary level $x_s[k]$. Due to the presence of uncertainties, this dependency can be denoted as $\Delta x_s[k] = P_s x_s[k]$ where P_s is the perturbation matrix. Using the same logic for the increments in tie line flow denoted as $\Delta\phi_s$, it follows that $\Delta\phi_s = Q_s x_s[k]$ where Q_s is the perturbation matrix for tie line variability. Therefore, we can denote the uncertainties of this order as a multiplicative uncertainty corresponding to the x_s as

$$\Delta_s = E_s x_s \tag{5.57}$$

where $E_s = -BD^{-1}Q_s + E_p P_s$ represents the effect of perturbation on the secondary states in the time scales T_s due to the slow uncertainty of Δ_G and Δ_L and the tie lines flow increments.

In the 5-min to hours time scale, system operators typically change the output of committed units to follow changes in load throughout the day. The aggregated uncertainty was defined as Δ_n in (5.35), whose d-step- ahead prediction in the tertiary time-scale as $\hat{\Delta}_n[K+d|K]$ in (5.42). Using the optimal d-step predictor in (5.45), implies that $\varepsilon[K+d]$ has a zero mean value. In turn, the aggregation of uncertainties at bus n, Δ_n, is directly reflected in the ACE signal. In turn, for the analysis, $\hat{\Delta}_t$ can be expressed as

$$\hat{\Delta}_t = E_t e_s \tag{5.58}$$

where E_t represents the effect of aggregated forecast error on the ACE.

5.2.6 The overall Hierarchical Transactive Model

The overall model, including the primary, secondary, and tertiary level dynamics in the grid is assembled in this section together with the corresponding uncertainties. These can be written by using the primary level dynamics in (5.23a) and (5.23b) denoted by Σ_{Pri}, the secondary level dynamics in (5.30) and (5.32) denoted by Σ_{Sec}, and the tertiary level dynamics in (5.52) denoted by Σ_{Ter} as (see Figure 5.2)

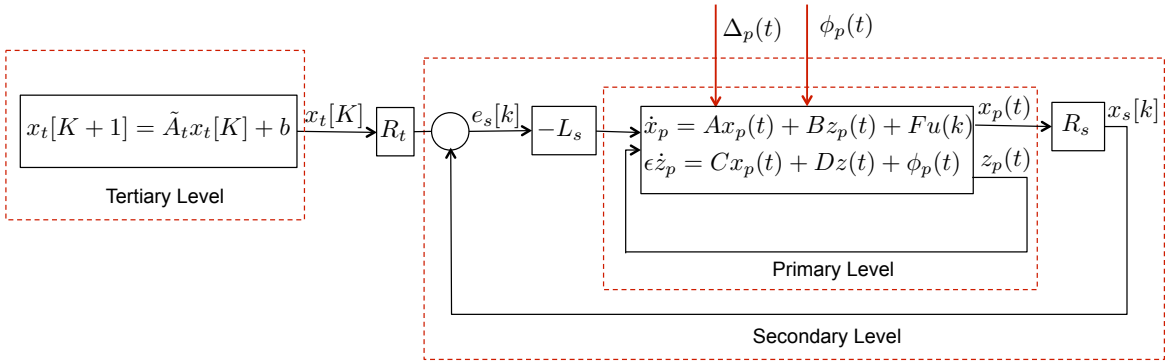

Figure 5.2: Transactive Hierarchical Control Structure

$$\Sigma_{Pri}: \begin{cases} \dot{x}_p = (A+E_p)x_p(t) + Bz_p(t) + Fu(k) & (5.59) \\ \epsilon\dot{z}_p = Cx_p(t) + Dz_p(t) + \phi_p(t) & (5.60) \end{cases}$$

$$\mathscr{I}_{Pri}: \quad u[k+1] = u[k] - L_s x_s[k] + L_t x_t[K] \quad (5.61)$$

$$\Sigma_{Sec}: \quad x_s[k+1] = (\tilde{A}_s + C_s E_s)x_s[k] + B_s L_t x_t[K] \quad (5.62)$$

$$\mathscr{I}_{Sec}: \quad e_s[k+1] = (\tilde{A}_s + C_s E_s)e_s[k] + C_s E_s R_t x_t[K] \quad (5.63)$$

$$\Sigma_{Ter}: \quad x_t[K+1] = \tilde{A}_t x_t[K] + hk_\rho E_t e_s[K] + b \quad (5.64)$$

where $\tilde{A}_t = I_{n_t} + hA_t$. The information exchange between the three levels, from top to bottom, are represented in $\mathscr{I}_{Pri}$ denoted by $u(k)$ in (5.59) from the secondary to the primary level, and $R_t X_t[K]$ from the tertiary to the secondary level represented in $\mathscr{I}_{Sec}$; the terms $x_s[k]$ in (5.62) and $e_s[K]$ in (5.64) represent the aggregated information from the lower levels to the higher levels. Interconnections in $\mathscr{I}_{Sec}$ and $\mathscr{I}_{Sec}$ are necessary for a stable and affordable grid design, as will be shown in Sections 5.3 and 5.4.

5.3 Stability Analysis of Transactive Controller

In this section we present the stability analysis for the overall dynamical system in (5.59)-(5.64). Before we analyze the stability of the dynamic market model in Eqs. (5.59)-(5.64), we evaluate its equilibria. The equilibrium of the primary dynamics is shown in (5.24b). From Eqs. (5.62), (5.63), and (5.64), the equilibrium points of x_s denoted by x_s^* and $e_s[k]$ denoted by e_s^*, and x_t denoted by x_t^* is given as the solution of

$$(I_{n_s} - \tilde{A}_s - C_s E_s)x_s^* - B_s L_t x_t^* = 0 \quad (5.65a)$$

$$(I_{n_s} - \tilde{A}_s - C_s E_s)e_s^* - C_s E_s R_t x_t^* = 0 \quad (5.65b)$$

$$hA_t x_t^* + hk_\rho E_t e_s^* + b = 0. \quad (5.65c)$$

Remark 5.3. It should be noted that the equilibrium of the overall Transactive controller in the absence of uncertainty can be derived from (5.65a)-(5.65c) by letting E_p, E_s, and E_t equal to zero and it follows that $e_s^* = 0$, and $hA_t x_t^* + b = 0$ which is equivalent to the KKT conditions for ISO problem in (4.10a)-(4.10e).

We now state a few assumptions regarding the uncertainties.

Assumption 5.5. Let Δ_p in (5.55) be such that

$$\sigma_{max}(E_p) < \frac{1}{\sigma_{max}(P_p)}$$

where P_p is the unique matrix that satisfies the Lyapunov equation $P_p(A-BC)+(A-BC)^T P_p^T + 2I_{n_s} = 0$.

Assumption 5.6. Let Δ_s in (5.26) be such that

$$\sigma_{max}(C_s E_s) < -\sigma_{max}(\tilde{A}_s) + \left([\sigma_{max}(\tilde{A})]^2 + \frac{1}{\sigma_{max}(P_s)} \right)^{1/2}$$

where $P_s > 0$ is the solution of $\tilde{A}_s^T P_s \tilde{A}_s - P_s + I = 0$.

Assumption 5.7. Let Δ_t in (5.58) be such that

$$\sigma_{max}(\tilde{E}_t) < -\sigma_{max}(\tilde{A}_t) + \left([\sigma_{max}(\tilde{A}_t)]^2 + \frac{1}{\sigma_{max}(P_t)} \right)^{1/2}$$

where $\tilde{E}_t = hk_\rho E_t (I_{n_s} - \tilde{A}_s - C_s E_s)^{-1} C_s E_s R_t$, and $P_t > 0$ is the solution of $\tilde{A}_t^T P_t \tilde{A}_t - P_t + I_{n_t} = 0$.

Theorem 5.2. *Let assumptions 5.5 to 5.7 hold. If the system in (5.59)-(5.64) is such that*

$$Re\left[\lambda_{max}\{A - BC\}\right] < 0 \tag{5.66a}$$
$$|\lambda_i(\tilde{A}_s)| < 1 \text{ for all } i = 1, \ldots n_s \tag{5.66b}$$
$$|\lambda_i(\tilde{A}_t)| < 1 \text{ for all } \; i = 1, \ldots n_t, \tag{5.66c}$$

where λ_i is the i-th eigenvalue of matrix A and $\lambda_{max}(A)$ denoted the largest eigenvalue of the matrix A, then there exists h^*, and ϵ^* such that for all $h \in (0, h^*)$ and $\epsilon \in (0, \epsilon^*)$, the equilibrium $O = (x_{p_{ss}}, x_s^*, e_s^*, x_t^*)$ of the overall hierarchical Transactive control in (5.59)-(5.64) is asymptotically stable.

Proof. The proof is provided in three steps, starting from the stability of the lowest level.
Step 1: Stability of the primary level

Let $u(k) \equiv 0$. Defining $y_p(t) = z_p(t) + D^{-1}Cx_p(t) + D^{-1}\phi_p(t)$, (5.59)-(5.60) can be represented as

$$\frac{dx_p(t)}{dt} = (A - BD^{-1}C)x_p(t) + By_p(t) + \Delta_p \tag{5.67}$$
$$\epsilon \frac{dy_p(t)}{dt} = Dy_p(t) + \epsilon D^{-1}C(A - BD^{-1}C)x_p(t) + \epsilon D^{-1}CBy_p(t) + \epsilon \dot{\phi}_p(t) + \epsilon D^{-1}C\Delta_p. \tag{5.68}$$

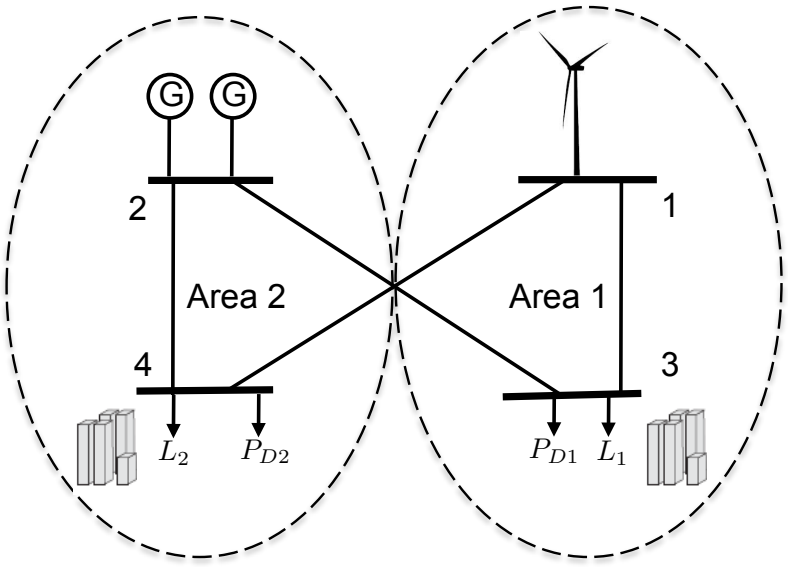

Figure 5.3: 4-bus system example for Transactive control

It follows that the equilibrium of (5.59)-(5.60) is asymptotically stable if and only if the origin of (5.67)-(5.68) is asymptotically stable, see Theorem 5.1. Defining $\tau = t/\epsilon$, we can represent (5.68) in the stretched τ-scale as

$$\begin{aligned}\frac{dy_p(\tau)}{d\tau} = Dy_p(\tau) + \epsilon D^{-1}C(A - BD^{-1}C)x_p(\tau) + \\ \epsilon D^{-1}CBy_p(\tau) + \epsilon\dot{\phi}_p(\tau) + \epsilon D^{-1}C\Delta_p.\end{aligned} \tag{5.69}$$

In order to evaluate the stability of the dynamics in the stretched time-scale of τ, we let ϵ tend to zero in (5.69), which leads to the boundary-layer system, see Theorem 5.1 [102]

$$\frac{dy_p(\tau)}{d\tau} = Dy_p(\tau). \tag{5.70}$$

Since $D = -I$, (5.70) is asymptotically stable, with $y(\tau)$ tending to zero as $\tau \to \infty$. Therefore, it suffices to focus on the reduced system

$$\frac{dx_p(t)}{dt} = (A - BD^{-1}C)x_p(t) + \Delta_p. \tag{5.71}$$

by setting $y_p(t)$ to zero. From Assumption 5.5 and (5.66a), it follows that the origin of (5.71) is asymptotically stable, see Section A.1.2 [102]. This establishes the stability of $x_p = 0$ in (5.59) and (5.60). It therefore follows that for any bounded $u(k) \neq 0$, the solutions of (5.59)-(5.60) are globally bounded.

Step 2: Stability of the secondary level

Let $x_t[K] \equiv 0$ and consider the two lower levels defined by Eqs. (5.59)-(5.63). From (5.26), Eq. (5.62) can be rewritten as

$$x_s[k+1] = (\tilde{A}_s + C_s E_s)x_s[k]. \tag{5.72}$$

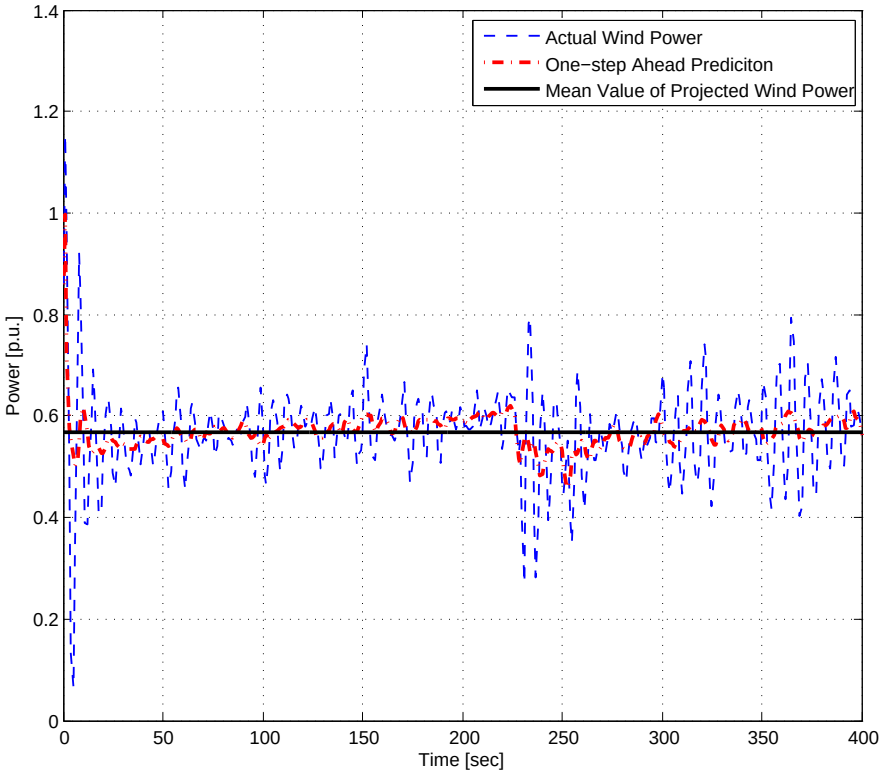

Figure 5.4: Wind power uncertainty and one-step ahead prediction using ARMA(1,1).

Using a Lyapunov function candidate $V(x) = x_s^T P_s x_s$ we obtain

$$\Delta V(k) = x_s^T [-I + (E_s^T C_s^T P_s \tilde{A}_s + \tilde{A}_s^T P_s^T C_s E_s) + E_s^T P_s E_s] x_s. \tag{5.73}$$

From Assumption 5.6 and (5.66b), it follows that $\Delta V(k) \leq 0$. Using Appendix A.1.4, see Eq. (A.29), it follows that (5.72) is asymptotically stable. As before, it follows that for any bounded $x_t[K] \neq 0$, the solutions of (5.72), $u(k)$, and therefore the solutions of (5.59)-(5.60) are bounded for all k.

Step 3: Stability of the tertiary level

We now consider the complete system defined by (5.59)-(5.64). Let us assume that strong duality holds and there exists a regular equilibrium point x_t^*. Let $y_t = x_t - x_t^*$ and $\eta_s = e_s - e_s^*$, the singular perturbed tertiary level in (5.64) together with the Area Control Error dynamics in (5.63) can be represented as

$$y_t(K+1) = \tilde{A}_t y_t(K) + h k_\rho E_t \eta_s(K) \tag{5.74}$$

$$\eta_s(k+1) = (\tilde{A}_s + C_s E_s)\eta_s[k] + (C_s E_s) R_t y_t[K]. \tag{5.75}$$

Using the method of the singular perturbation approach and time scale separation, the tertiary dynamics in (5.74) and ACE dynamics in (5.75) can be transformed into slow and fast subsystems as

$$y_{t_s}(K+1) = (\tilde{A}_t + \tilde{E}_t) y_t(K) \tag{5.76}$$

$$\eta_{s_f}(k+1) = (\tilde{A}_s + C_s E_s)\eta_{s_f}(k) \tag{5.77}$$

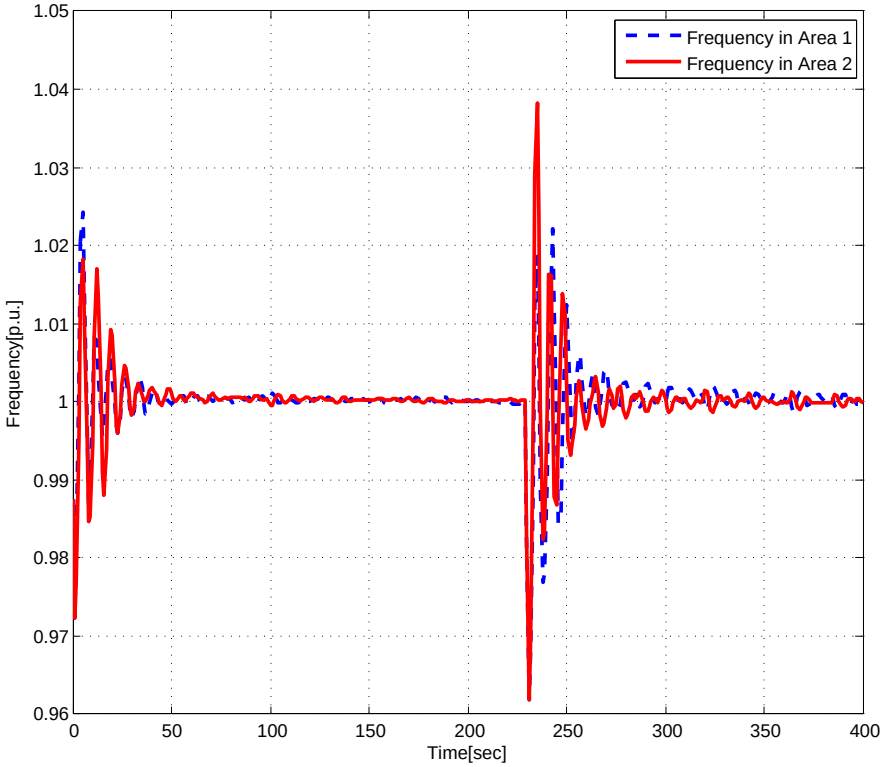

Figure 5.5: Frequency response of Areas 1 and 2.

where y_{t_s}, and η_{s_f} denote the slow and fast decomposition of the original system in (5.74)-(5.75). From assumptions 5.6 - 5.7 and (5.66c) it follows that (5.76) and (5.77) are asymptotically stable. This in turn implies that x_t and e_s are bounded, ensuring the boundedness of the solutions of the secondary level and primary level dynamics in (5.59)-(5.63). □

5.4 Case Study

In this section we study power fluctuations from large scale wind power integration on a power system of 2 interconnected areas, whose interconnection is shown in Figure 5.3. We assume the integration of a wind farm in area 1. Primary, secondary, and tertiary controllers as in Eqs. (5.59)-(5.64) are implemented. Numerical values of the steam units and wind parameters are provided in Appendix A.2.5, A.2.9, and for RR-DR part of the load $J_{L1} = 0.2$, $J_{L2} = 0.1$, $D_{L1} = 0.7$, and $D_{L2} = 0.5$ respectively [12]. The time-scales, as described in Eq. (5.37) are chosen as $T_s = 1s$, $h = 30s$, and $T_t = 5min$. The proposed Transactive control is evaluated in the presence of a wind power shown in Figure 5.4, together with one-step ahead prediction using $ARMA\,(1,1)$ model and mean value of the projected wind power. As can be seen in Figure 5.5, the secondary control responds to the wind power fluctuation and adjusts the set-point of the steam turbine unit in area 1 and regulation response part of load in Area 1. This restores the frequency to its nominal value (60 Hz). Regulation response and price response of DR-compatible load in areas 1 and 2 are shown in Figure 5.6. As can be seen, regulation response components of P_{d1} and P_{d2} adjust their frequency responses

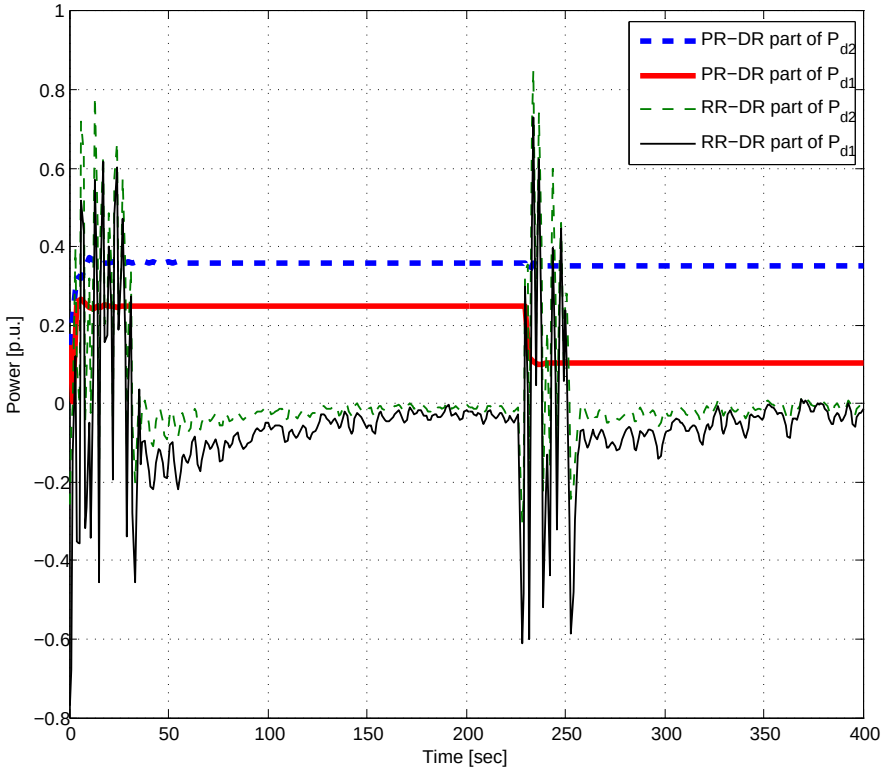

Figure 5.6: RR and PR components of Demand Response load in areas 1 and 2 in response to the wind uncertainty.

following the wind uncertainty and tertiary level adjusts the price response components of demand collectively following the intermittency that happens at 220 seconds .

The performance of the tertiary level in terms of reserve deployment is presented in Figure 5.7. Using Transactive control, less reserve is required to meet the fluctuations of the wind power in Area 1 and the cheaper resources, i.e. demand in area 1 responds since it is assumed to be DR-compatible and changes its set-point as can be seen in Figure 5.6, and the steam turbine unit of area 2, are involved to deal with wind uncertainty. This is mainly due to the coordination between the three levels and the use of one-step ahead prediction in the proposed Dynamic Market Mechanism (DMM) at tertiary level. The efficiency of the proposed hierarchical controller is validated by comparing the corresponding S_w defined in Eq. (5.33) and total generation cost $\sum_{i\in G_f} C_{G_i}(P_{Gi})$ in the case of using our proposed Transactive control with DMM at tertiary level and the case of using Current Market Mechanism (CMM) at tertiary level. As can be seen in Table 5.1, our proposed Transactive hierarchical controller results in a larger S_w following wind-intermittency and less deployment of reserve with lower reserve cost.

Figure 5.8 compares Area Control Error of area 1 when this area is subjected to different wind penetration. As can be seen ACE signal is extremely volatile when the system integrates 30% wind power and at this level of wind penetration our proposed Transactive control is not stable anymore.

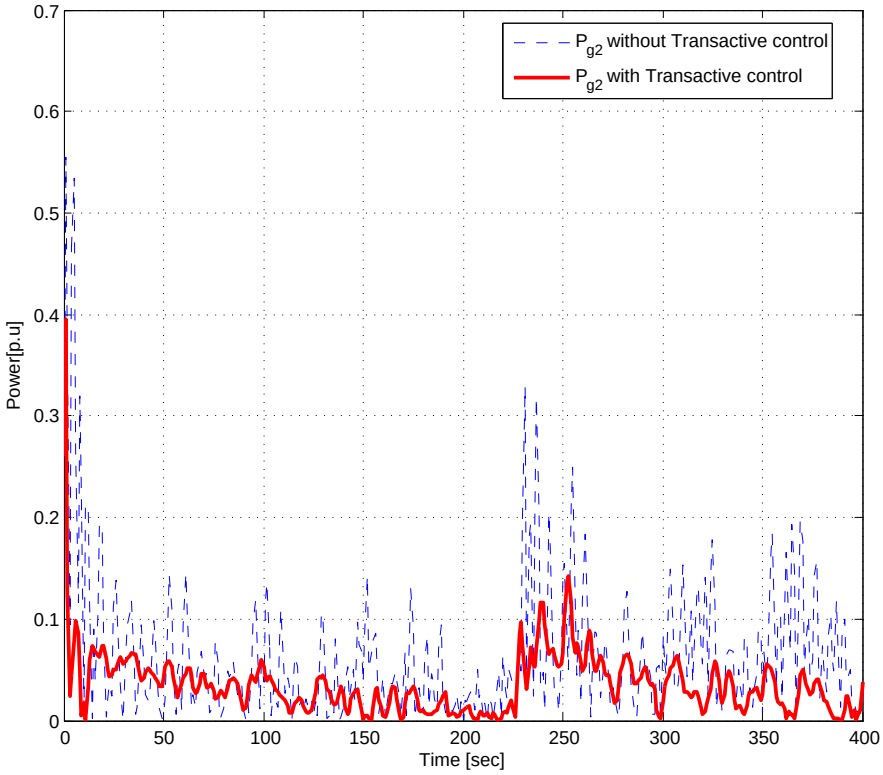

Figure 5.7: Reserve requirement after applying Dynamic Market Mechanism (DMM) at tertiary level.

Tabular 5.1: Comparison of Dynamic Market Mechanism (DMM) and Current Market Mechanism (CMM) for 400 seconds interval

Algorithm	Total Generation Cost $\sum_{i=1}^{2} C_{G_i}(P_{Gi})$ \$/p.u.	Total Reserve Cost $C_{G_2}(P_{G2})$ \$/p.u.	Social Welfare S_W \$
With Transactive Control	120.1	69.2	65.9
Without Transactive Control	152.8	102.5	60.6

5.5 Concluding Remarks

A hierarchical Transactive control architecture is proposed that combines market transactions at the higher levels with inter-area and unit-level control at the lower levels. This architecture consists of a primary, secondary, and tertiary levels, and operates over time-scales that range from seconds to minutes. A dynamic market mechanism inspired by the notion of disequilibrium is introduced into the traditional AGC architecture to develop the hierarchical models and controllers. Global asymptotic stability of the overall hierarchical system is established in the presence of uncertainties at all three time-scales. Finally the resulting

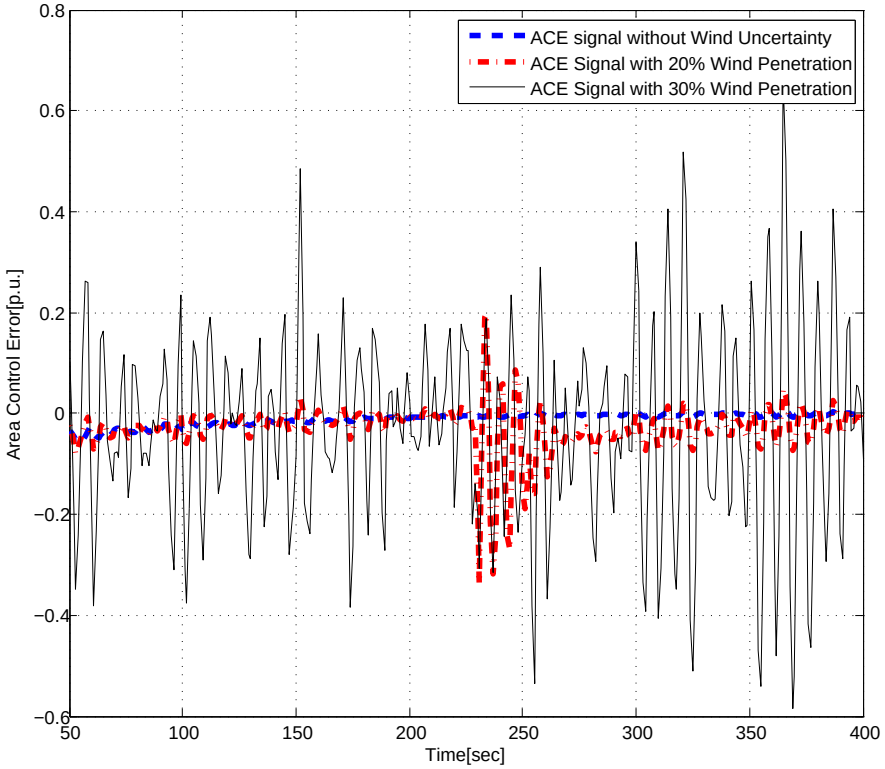

Figure 5.8: Area Control Error as wind penetration is increased.

controller is shown to satisfactorily accommodate perturbations in the wind generation, and results in the desired frequency regulation as well as increased Social Welfare.

6 Conclusions and Future Directions

6.1 Concluding Remarks

The current energy crisis has created an urgent need in integrating renewable energy resources into the power grid. The latter in turn can introduce intermittency and uncertainty into the picture, thereby introducing a prohibitive integration cost. The focus of this dissertation is on introducing an analytical framework to evaluate and mitigate the integration cost of Renewable Energy Resources (RERs).

Beginning with an overall model of the energy market including GenCo, ConCo as well as ISO in Chapter 3, the equilibrium of an electric energy market has been discussed in the presence of RERs and Demand Response (DR). The underlying market equilibrium was analyzed using game theory and sufficient conditions for the existence of a unique Pure Nash Equilibrium for the nominal market are established. The perturbed market in the presence of uncertainty due to renewable energy is analyzed using the concept of closeness of two strategic games and the equilibria of close games using the notion of $\alpha-$ approximation and $\epsilon-$ equilibrium. This analysis is used to quantify the effect of uncertainty of RERs and its possible mitigation using DR in the form of a parameter denoted as Curtailment Factor. Finally, numerical results are included that validate the theoretical results, using an IEEE 30-bus network.

In Chapter 4, dynamic market mechanism is proposed as a significant departure from the current practice where information is exchanged only once between the GenCos and the ISO following which the ISO clears the market and provides information regarding the price. Our thesis here is that due to the huge volatility and uncertainty of the dynamic drivers such as wind and solar energy sources, and load in the market, such a single iteration will not suffice, and stability cannot be ensured; continued iteration as suggested by the dynamic model presented in this chapter is needed in order to mitigate volatility in real-time price and ensure a stable market design. In this chapter, guidelines for determining stability with such an iterative exchange of information between the different players are discussed. Beginning with the model of the players (GenCo, ConCo, and ISO) together with their constraints and the optimization goal, the dynamics of the real-time market using the notion of disequilibrium has been captured. A gradient play is used to derive the dynamic evolution of the actions for players and underlying states of the game as dual variables to reach the optimum solution of the real-time market. The stability of the resulting dynamical model of the real-time market is investigated and the region of attraction around the equilibrium of interest is established. This region for which the real-time market is asymptotically stable places an implicit bound on the congestion price. In the same chapter, the stability of the underlying market equilibrium in the presence of uncertainty due to renewable energy and the corresponding region of attraction have been analyzed. The effect of DR as a promising tool for improving robustness of the real-time market due to the uncertainty of RERs is then

quantified.

Numerical results are included that validate the theoretical results using IEEE 30-bus system. The simulation results show how demand curtailment factor due to the real time pricing can mitigate the wind volatility in the wholesale market. The final point that has been presented in this chapter is the placement of a wind generator due to inherent volatility and intermittency. The simulation studies show that self-admittance of the admittance matrix, $|Y_{bus_{ii}}|$, serves as an important guideline for the location of the wind energy in the power network.

A hierarchical Transactive control architecture is proposed in Chapter 5 that combines market transactions at the higher levels with inter-area and unit-level control at the lower levels. This architecture consists of a primary, secondary, and tertiary levels, and operates over time-scales that range from seconds to minutes. A dynamic market mechanism that proposed in Chapter 4 is introduced into the traditional AGC architecture to develop the hierarchical models and controllers. Global asymptotic stability of the overall hierarchical system is established in the presence of uncertainties at all three time-scales. Finally the resulting controller is shown to satisfactorily accommodate perturbations in the wind generation, and result in the desired frequency regulation as well as increased Social Welfare and reducing the integration cost of RERs.

In summary, given the significant impact that increased uncertainties stemming from renewables can have on market transactions, the ideas, concepts and approaches developed in this dissertation significantly advance the state-of-the-art in control and decision making of smart power grid and pave the way for better RERs integration in power systems while overcoming market volatility and inefficiency.

6.2 Future Directions

Uncertainty and intermittency of Renewable Energy Resources (RERs) imply that control methodologies in the future of smart grids must be in real-time and close the loop at various time-scales. Feedback structure leads a new look at market mechanisms with a controls viewpoint enabling a novel framework for analysis and synthesis. Based on the results of this thesis, continuing research in suitable Transactive control design intertwined with market mechanisms design is essential for a successful practical application of the presented methods in this dissertation. There are a number of exciting research directions directly emerging from this thesis, some of which are listed below:

Incorporating Non-convex and Non-rational Participants in Transactive Grid:

Non-convex utility functions, non-rational players, and non-unique equilibrium routinely occur in the wholesale electricity markets. The overall wholesale market model is highly needed so as to include the effects of these realistic features. Each one of these participants has a different utility cost function, which also varies differently with time. Different levels of stochasticity are also associated with each of the participants. By integrating all these participants together, and introducing congestion constraints due to transmission capacity limits, and losses in transmission lines, we can evaluate different market conditions. Suitable

price policies and appropriate information exchange between the different market players can be derived for a stable efficient market under non-convex, an non-rational participants.

Analysis of the Transactive Grid:

Significant potential is anticipated with the expansion of Transactive control to a grid-wise level, in terms of reducing or eliminating the need to build costly thermal resources, reducing the region's carbon footprint, smoothening peaks in electricity use, and integration of intermittent renewable resources. At its core, Transactive control represents a procedure where information is accumulated and forwarded for use over a future horizon, and in essence a closed loop action. A grid-wise deployment of Transactive control implies the introduction of multiple feedback loops, ranging from seconds at the unit-level to seasons at the market level, amidst various latencies and uncertainties, and poses a host of formidable challenges. Concepts of hierarchy, distributed coordination, and cooperative decision-making have to be judiciously introduced in order to simultaneously realize the combined objectives of decarbonization and reliability while meeting capacity, ramp, and security constraints and overcoming market volatility and inefficiency.

Cyber Security and Privacy of Transactive Grid:

Vulnerability analysis of the current market exercise versus the designed dynamic market mechanism due to cyber attacks and exercising market power have to be considered in market mechanism design. Robust dynamic market mechanism designs have a major role to mitigate the effects of these adversities. The proposed market mechanism can be used to perform some interesting analyses such as: (a) How cyber attacks can affect market equilibrium and causes price volatility? (b) How to design a robust market mechanism to deal with such cyber attacks?(c) How to design a Transative control with consumers privacy consideration?

Fair Pricing Mechanisms for Energy and Reserve:

The market mechanism presented in this dissertation needs to be complemented with a fair pricing mechanism for energy and reserve that allows producers to recover generation costs from consumers while guaranteeing revenue reconciliation. How to price commodities in electricity markets is a field of active research. In the context of stochastic security under wind power uncertainty, reserve pricing is a topic of special importance.

To conclude, it should be noted that, apart from the topics for future research outlined in this section, which are directly derived from the problems dealt with in this thesis, feedback notion together with incorporating RERs is expected to pose unique challenges and opportunities in the planning and operation of the electric energy systems in future. This just means several interesting research directions are posed for the current and next generation of researchers in power systems, controls, and economics.

A Appendix

The following Appendix is organized as follows. In Section A.1, the necessary mathematical preliminaries are presented and in Section A.2 the preliminaries of power and frequency control are expressed.

A.1 Mathematical Preliminaries

A.1.1 Lyapunov Stability Theory

In this section, the Lyapunov stability theory is reviewed. A survey of the results that we need in this thesis are presented, with no proofs. The interested reader can refer to [106] and [102], for details.

Basic definitions

Consider a dynamical system which satisfies

$$\dot{x} = f(x,t) \quad x(t_0) = x_0 \quad x \in \mathbb{R}^n. \tag{A.1}$$

We will assume that $f(x,t)$ satisfies the standard conditions for the existence and uniqueness of solutions. Such conditions are, for instance, that $f(x,t)$ is Lipschitz continuous with respect to x, uniformly in t, and piecewise continuous in t. A point x^* is an equilibrium point of (A.1) if $f(x^*,t) \equiv 0$. Intuitively, we say an equilibrium point is locally stable if all solutions which start near (meaning that the initial conditions are in a neighborhood of x^*) remain near x^* for all time. The equilibrium point x^* is said to be locally asymptotically stable if x^* is locally stable and, furthermore, all solutions starting near x^* tend towards x^* as $t \to \infty$. By shifting the origin of the system, we may assume that the equilibrium point of interest occurs at $x^* = 0$. If multiple equilibrium points exist, we will need to study the stability of each by appropriately shifting the origin.

Definition A.1. The equilibrium point $x^* = 0$ of (A.1) is stable (in the sense of Lyapunov) at $t = t_0$ if for any $\epsilon > 0$ there exists a $\delta(t_0, \epsilon) > 0$ such that

$$\|x(t_0)\| < \delta \Rightarrow \|x(t_0)\| < \epsilon, \forall t \geq t_0. \tag{A.2}$$

Lyapunov stability is a very mild requirement on equilibrium points. In particular, it does not require that trajectories starting close to the origin tend to the origin asymptotically. Also, stability is defined at a time instant t_0. Uniform stability is a concept which guarantees that the equilibrium point is not losing stability. We insist that for a uniformly stable equilibrium point x^*, δ in the Definition A.1 not be a function of t_0, so that equation (A.1) may hold for all t_0. Asymptotic stability is made precise in the following definition:

Definition A.2. An equilibrium point $x^* = 0$ of (A.1) is asymptotically stable at $t = t_0$ if

1. $x^* = 0$ is stable, and
2. $x^* = 0$ is locally attractive; i.e., there exists $\delta(t_0)$ such that

$$\|x(t_0)\| < \delta \Rightarrow \lim_{t\to\infty} x(t) = 0. \tag{A.3}$$

As in the previous definition, asymptotic stability is defined at t_0. *Uniform asymptotic stability* requires:

1. $x^* = 0$ is uniformly stable, and
2. $x^* = 0$ is uniformly locally attractive; i.e., there exists δ independent of t_0 for which equation (A.3) holds. Further, it is required that the convergence in equation (A.3) is uniform.

Finally, we say that an equilibrium point is unstable if it is not stable. Definitions A.1 and A.2 are local definitions; they describe the behavior of a system near an equilibrium point. We say an equilibrium point x^* is globally stable if it is stable for all initial conditions $x_0 \in \mathbb{R}^n$. Global stability is very desirable, but in many applications it can be difficult to achieve. Notions of uniformity are only important for time-varying systems. Thus, for time-invariant systems, stability implies uniform stability and asymptotic stability implies uniform asymptotic stability. It is important to note that the definitions of asymptotic stability do not quantify the rate of convergence.

The direct method of Lyapunov

Lyapunov's direct method (also called the second method of Lyapunov) allows us to determine the stability of a system without explicitly integrating the differential equation (A.1). The method is a generalization of the idea that if there is some measure of energy in a system, then we can study the rate of change of the energy of the system to ascertain stability. Let B_ϵ be a ball of size ϵ around the origin, $B_\epsilon = \{x \in \mathbb{R}^n : \|x\| < \epsilon\}$.

Definition A.3. A continuous function $V : \mathbb{R}^n \times \mathbb{R}_+ \to \mathbb{R}$ is a locally positive definite function if for some $\epsilon > 0$ and some continuous, strictly increasing function $\alpha : \mathbb{R}_+ \to \mathbb{R}$,

$$V(0,t) = 0 \;\; and \;\; V(x,t) \geq \alpha(\|x\|) \quad \forall x \in B_\epsilon, \forall t \geq 0. \tag{A.4}$$

A locally positive definite function is locally like an energy function. Functions which are globally like energy functions are called positive definite functions:

Definition A.4. A continuous function $V : \mathbb{R}^n \times \mathbb{R}_+ \to \mathbb{R}$ is a positive definite function if it satisfies the conditions of Definition A.3 and, additionally, $\alpha(p) \to \infty$ as $p \to \infty$.

To bound the energy function from above, we define decreasening function as follows:

Definition A.5 (Decrescent functions)**.** A continuous function $V : \mathbb{R}^n \times \mathbb{R}_+ \to \mathbb{R}$ is decrescent if for some $\epsilon > 0$ and some continuous, strictly increasing function $\beta : \mathbb{R}_+ \to \mathbb{R}$,

$$V(x,t) \leq \beta(\| x \|) \quad \forall x \in B_\epsilon, \forall t \geq 0 \tag{A.5}$$

Using these definitions, the following theorem allows us to determine stability for a system by studying an appropriate energy function. Roughly, this theorem states that when $V(x,t)$ is a locally positive definite function and $\dot{V}(x,t) \leq 0$ then we can conclude stability of the equilibrium point. The time derivative of V is taken along the trajectories of the system:

$$\dot{V}|_{\dot{x}=f(x,t)} = \frac{\partial V}{\partial t} + \frac{\partial V}{\partial x} f.$$

In what follows, by $\dot{V}$ we will mean $V|_{\dot{x}=f(x,t)}$.

Theorem A.1 (Basic theorem of Lyapunov)**.** *Let $V(x,t)$ be a non-negative function with derivative $\dot{V}$ along the trajectories of the system.*

1. *If $V(x,t)$ is locally positive definite and $\dot{V}(x,t) \leq 0$ locally in x and for all t, then the origin of the system is locally stable (in the sense of Lyapunov).*

2. *If $V(x,t)$ is locally positive definite and decrescent, and $\dot{V}(x,t) \leq 0$ locally in x and for all t, then the origin of the system is uniformly locally stable (in the sense of Lyapunov).*

3. *If $V(x,t)$ is locally positive definite and decrescent, and $-\dot{V}(x,t)$ is locally positive definite, then the origin of the system is uniformly locally asymptotically stable.*

4. *If $V(x,t)$ is positive definite and decrescent, and $-\dot{V}(x,t)$ is positive definite, then the origin of the system is globally uniformly asymptotically stable.*

Theorem A.1 gives sufficient conditions for the stability of the origin of a system. It does not, however, give a prescription for determining the Lyapunov function $V(x,t)$. Since the theorem only gives sufficient conditions, the search for a Lyapunov function establishing stability of an equilibrium point could be difficult. However, it is a remarkable fact that the converse of Theorem A.1 also exists: if an equilibrium point is stable, then there exists a function $V(x,t)$ satisfying the conditions of the theorem. However, the utility of this and other converse theorems is limited by the lack of a computable technique for generating Lyapunov functions.

The indirect method of Lyapunov

The indirect method of Lyapunov uses the linearization of a system to determine the local stability of the original system. Consider the system

$$\dot{x} = f(x,t) \tag{A.6}$$

with $f(0,t) = 0$ for all $t \geq 0$. Define

$$A(t) = \frac{\partial f(x,t)}{\partial x}|_{x=0} \tag{A.7}$$

to be the Jacobian matrix of $f(x,t)$ with respect to x, evaluated at the origin. It follows that for each fixed t, the remainder

$$f_1(x,t) = f(x,t) - A(t)x$$

approaches zero as x approaches zero. However, the remainder may not approach zero uniformly. For this to be true, we require the stronger condition that

$$lim_{\|x\|\to 0} \sup_{t\geq 0} \frac{\|f_1(x,t)\|}{\|x\|} = 0 \tag{A.8}$$

If equation (A.8) holds, then the system

$$\dot{z} = A(t)z \tag{A.9}$$

is referred to as the (uniform) linearization of equation (A.1) about the origin. When the linearization exists, its stability determines the local stability of the original nonlinear equation.

Theorem A.2 (Stability by linearization)**.** *Consider the system (A.6) and assume*

$$lim_{\|x\|\to 0} \sup_{t\geq 0} \frac{\|f_1(x,t)\|}{\|x\|} = 0 \tag{A.10}$$

Further, let $A(\cdot)$ defined in equation (A.7) be bounded. If 0 is a uniformly asymptotically stable equilibrium point of (A.9) then it is a locally uniformly asymptotically stable equilibrium point of (A.6).

The preceding theorem requires uniform asymptotic stability of the linearized system to prove uniform asymptotic stability of the nonlinear system. Counterexamples to the theorem exist if the linearized system is not uniformly asymptotically stable. If the system (A.6) is time-invariant, then the indirect method says that if the eigenvalues of

$$A = \frac{\partial f(x)}{\partial x}|_{x=0}$$

are in the open left half complex plane, then the origin is asymptotically stable. This theorem proves that global uniform asymptotic stability of the linearization implies local uniform asymptotic stability of the original nonlinear system. The estimates provided by the proof of the theorem can be used to give a (conservative) bound on the domain of attraction of the origin.

A.1.2 Quadratic Lyapunov Functions for Continues LTI Systems

Constructing a Lyapunov function for an arbitrary nonlinear system is not a trivial exercise. The complication arises from the fact that we cannot restrict the class of functions to search from in order to prove stability. The situation is different for LTI systems as

$$\dot{x}(t) = Ax(t). \tag{A.11}$$

Consider a Lyapunov function candidate of the form

$$V(x) = x^T Px,\ P > 0, \tag{A.12}$$

for the system (A.11). Then

$$\dot{V}(x) = \dot{x}^T P x + x^T P \dot{x} \tag{A.13}$$
$$= x^T A^T P x + x^T P A x \tag{A.14}$$
$$= x^T (A^T P + P A) x \tag{A.15}$$
$$= -x^T Q x, \tag{A.16}$$

where we have introduced the notation $Q = -(A^T P + PA)$; note that Q is symmetric. Now, we see that V is a Lyapunov function if $Q \geq 0$, in which case the equilibrium point at the origin of the system (A.11) is stable. If $Q > 0$, then the equilibrium point at the origin is globally asymptotically stable. In this latter case, the origin must be the only equilibrium point of the system, so we typically say the system (rather than just the equilibrium point) is asymptotically stable. The preceding relationships show that in order to find a quadratic Lyapunov function for the system (A.11), we can pick $Q > 0$ and then try to solve the equation

$$A^T P + PA = -Q \tag{A.17}$$

for $P > 0$. This equation is referred to as a Lyapunov equation, and is a linear system of equations in the entries of P. If it has a solution, then it has a symmetric solution, so we only consider symmetric solutions. If it has a positive definite solution $P > 0$, then we evidently have a Lyapunov function $x^T P x$ that will allow us to prove the asymptotic stability of the system (A.11). The interesting thing about LTI systems is that the converse also holds: If the system is asymptotically stable, then the Lyapunov equation (A.11) has positive definite solution $P > 0$ (which, as we shall show, is unique). This result is stated in the following theorem.

Theorem A.3. *Given the dynamic system (A.11) and any $Q > 0$, there exists a positive definite solution P of the Lyapunov equation*

$$A^T P + PA = -Q \tag{A.18}$$

if and only if all the eigenvalues of A are in the open left half plane. The solution P in this case is unique.

Proof. See [102]. □

A.1.3 Quadratic Lyapunov Functions for Discrete LTI Systems

Consider the discrete LTI system as

$$x(t+1) = Ax(t). \tag{A.19}$$

If

$$V(x) = x^T P x,\ P > 0, \tag{A.20}$$

then

$$\Delta V = V(t+1) - V(t) = x^T A^T P A x - x^T P x \tag{A.21}$$

Thus the resulting Lyapunov equation to study is

$$A^T PA - P = -Q \tag{A.22}$$

The following theorem is analogous to what we presented in the continuos case in Theorem A.3.

Theorem A.4. *Given the dynamic system (A.19) and any $Q > 0$, there exists a positive definite solution P of the Lyapunov equation*

$$A^T PA - P = -Q \tag{A.23}$$

if and only if all the eigenvalues of A have magnitude less than 1 (i.e. are in the open unit disc). The solution P in this case is unique.

A.1.4 Bounded Perturbation and Robustness

In this section, we are interested in studying the stability of linear time-invariant systems of the form

$$\dot{x}(t) = (A + \Delta)x(t) \tag{A.24}$$

where Δ is a real matrix perturbation with bounded norm. In particular, we are interested in calculating a good bound on the size of the smallest perturbation that will destabilize a stable matrix A. Applying the same Lyapunov function as in (A.17) to the perturbed system we obtain

$$\dot{V}(x) = x^T(A^T P + PA + \Delta^T P + P\Delta)x \tag{A.25}$$

It is evident that all perturbations satisfying

$$\Delta^T P + P\Delta < Q, \tag{A.26}$$

will result in a stable system. This can be guaranteed if

$$2\sigma_{max}(P)\sigma_{max}(\Delta) < \sigma_{min}(Q). \tag{A.27}$$

This provides a bound on the perturbation although it is potentially conservative.

Now consider linear time-invariant discrete systems of the form

$$x(t+1) = (A + \Delta)x(t) \tag{A.28}$$

where Δ is a real matrix perturbation with bounded norm. Applying the same Lyapunov function as in (A.21) to the perturbed system we obtain

$$\Delta V(x) = x^T(A + \Delta)^T P(A + \Delta)x - x^T Px \tag{A.29}$$

It is evident that all perturbations satisfying

$$A^T P\Delta + \Delta^T PA + \Delta^T P\Delta < Q, \tag{A.30}$$

will result in a stable system. This can be guaranteed if

$$\sigma_{max}(\Delta) < -\sigma_{max}(A) + \left([\sigma_{max}(A)^2 + \frac{1}{\sigma_{max}(P)}] \right)^{1/2}. \tag{A.31}$$

This provides a bound on the perturbation although it is potentially conservative.

A.1.5 Convex Optimization

In this section, we provide some preliminaries related to the convex optimization. These in turn are directly used in establishing the equilibrium of the wholesale market in Chapter 3. We start with a few basic definitions.

Definition A.6. A set $K \subseteq \mathbb{R}$ is convex if for any two points $x, y \in K$,

$$\alpha x + (1-\alpha)y \in K, \ \forall x, y \in K \text{ and } \alpha \in [0,1]. \tag{A.32}$$

Definition A.7. Given a convex set $K \subseteq \mathbb{R}$ and a function $f(x) : K \to \mathbb{R}$; f is said to be a convex function on K if, $\forall x, y \in K$ and $\alpha \in (0,1)$,

$$f(\alpha x + (1-\alpha)y) \leq \alpha f(x) + (1-\alpha) f(y), \tag{A.33}$$

Furthermore, a function $f(x)$ is concave over a convex set if and only if the function $-f(x)$ is a convex function over the set.

Definition A.8. Given a scalar-valued function $f(x) : \mathbb{R}^n \to \mathbb{R}$ we use the notation $\nabla f(x)$ to denote the gradient vector of $f(x)$ at point x, i.e.,

$$\nabla f(x) = \left[\frac{\partial f(x)}{\partial x_1}, ..., \frac{\partial f(x)}{\partial x_n} \right]^T. \tag{A.34}$$

Definition A.9. Given a scalar-valued function $f(x) : \prod_{i=1}^{I} \mathbb{R}^{m_i} \to \mathbb{R}$ we use the notation $\nabla_i f(x)$ to denote the gradient vector of $f(x)$ with respect to x_i at point x, i.e.,

$$\nabla_i f(x) = \left[\frac{\partial f(x)}{\partial x_i^1}, ..., \frac{\partial f(x)}{\partial x_i^{m_i}} \right]^T. \tag{A.35}$$

Consider a generic optimization problem

$$\begin{aligned} &\text{maximize} \quad f(x) \\ &\text{subject to} \quad g_n(x) = 0, \quad \forall n = 1, \ldots, N \\ &\sum_{n=1}^{N} R_{mn} h_n(x) \geq c_m, \quad \forall m = 1, \ldots L \end{aligned}$$

where $f(x)$ is called the objective function or cost function, R is a matrix of constants and c_m are constants. We assume that $f(x) : \mathbb{R}^n \to \mathbb{R}$ is a convex function to be maximized over the variable x, the functions $g_n(x)$ as equality constraints are affine, and the functions $h_n(x)$ as inequality constraints are cocave. With these assumptions the optimization problem (A.36) is termed a convex optimization problem. In addition, the constraint set for the optimization problem is convex which allows us to use the method of Lagrange multipliers and the Karush Kuhn Tucker (KKT) theorem which we state below [107, 108].

Theorem A.5. *Consider the optimization formulated in (A.36), where $f(x)$ is a convex function, $g_n(x)$ are affine functions, and $h_n(x)$ are cocave functions. Let x^* be a feasible point, i.e. a point that satisfies all the constraints. Suppose there exists constants λ_n and $\mu_m \geq 0$ such that*

$$\begin{aligned} &\nabla f(x^*) + \sum_{n=1}^{N} \lambda_n \nabla g_n(x^*) + \sum_{m=1}^{L} \mu_m (R_{mn} \nabla h_n(x^*) - c_m) = 0 \quad \forall n = 1...N \\ &\mu_m (R_{mn} h_n(x^*) - c_m) = 0 \quad , \forall m = 1, \ldots, L \end{aligned} \tag{A.36}$$

then x^* is a global maximum. If $f(x)$ is strictly concave then x^* is also the unique global maximum.

Proof. see [108]. □

A.2 Active Power and Frequency Control

A generator driven by a steam turbine can be represented as a large rotating mass with two opposing torques acting on the rotation. The mechanical torque, T_{mech}, acts to increase rotational speed whereas the electrical torque, T_{elec}, acts to slown it down. When T_{mech} and T_{elec} are equal in magnitude, the rotational speed, ω, will be constant. If the electrical load is increased so that T_{elec} is larger than T_{mech}, the entire rotating system will begin to slown down. Since it would be damaging to let the equipment slow down too far, preventive action must be done to increase the mechanical torque T_{mech} to restore equilibrium; that is, to bring the rotational speed back to an acceptable value and the torques to equality so that the speed is again held constant.

In the development to follow, we are interested in deviations of quantities about steady-state values which will be designated by a Δ. Before starting let us define ωas rotational speed, α as a rotational acceleration, δ as a phase angle of a rotating machine, T_{net} as a net accelerating torque in a machine, T_{mech} as a mechanical torque exerted on a machine by the turbine, T_{elec} as an electrical torque exerted on the machine by the generator, P_{net} as a net accelerating power, P_{mech} as a mechanical power input, and finally P_{elec} as an electrical power output where all quantities (except phase angle) will be in per unit on the machine base, or, in the case of ω, on the standard system frequency base.

Assume that the machine has a steady speed of ω^{ref}. Due to various electrical or mechanical disturbances, the machine will be subjected to differences in mechanical and electrical torque, causing it to accelerate or decelerate. We are chiefly interested in the deviations of speed, $\Delta\omega$. If the speed of the machine under acceleration is

$$\omega = \omega^{ref} + \alpha t \tag{A.37}$$

then the deviation from nominal speed, $\Delta\omega$, may be expressed as

$$\Delta\omega = \alpha t. \tag{A.38}$$

The relationship between speed deviation and net accelerating torque is

$$T_{net} = I\alpha = I\frac{d}{dt}(\Delta\omega). \tag{A.39}$$

Next, we will relate the deviations in mechanical and electrical power to the deviations in rotating speed and mechanical torques. The relationship between net accelerating power and the electrical and mechanical powers is

$$P_{net} = P_{mech} - P_{elec} \tag{A.40}$$

which is written as the sum of the steady-state value and the deviation term,

$$P_{net} = P_{net_0} + \Delta P_{net} \tag{A.41}$$

where $P_{net_0} = P_{mech_0} - P_{elec_0}$, $\Delta P_{net} = \Delta P_{mech} - \Delta P_{elec}$.
Then

$$P_{net} = (P_{mech_0} - P_{elec_0}) + (\Delta P_{mech} - \Delta P_{elec}). \tag{A.42}$$

Similiarly for torques,

$$T_{net} = (T_{mech_0} - T_{elec_0}) + (\Delta T_{mech} - \Delta T_{elec}). \tag{A.43}$$

Using the basic relationship

$$P_{net} = \omega T_{net}$$

we can see that

$$P_{net} = (\omega^{ref} + \Delta\omega)(T_{net_0} + \Delta T_{net}). \tag{A.44}$$

Substituting Eqs. (A.42) and (A.43), we obtain

$$(P_{mech_0} - P_{elec_0}) + (\Delta P_{mech} - \Delta P_{elec}) = (\omega^{ref} + \Delta\omega)[(T_{mech_0} - T_{elec_0}) + (\Delta T_{mech} - \Delta T_{elec})]. \tag{A.45}$$

Assume that the steady-state quantities can be factored out since

$$P_{mech_0} = P_{elec_0}, \tag{A.46}$$

$$T_{mech_0} = T_{elec_0} \tag{A.47}$$

and further assume that the second-order terms involving products of $\Delta\omega$ with ΔT_{mech} and ΔT_{elec} can be negelected. Then

$$\Delta P_{mech} - \Delta P_{elec} = \omega^{ref}(\Delta T_{mech} - \Delta T_{elec}). \tag{A.48}$$

From Eqs. (A.39), (A.43), and (A.47) the net torque is related to the speed change as

$$\Delta T_{mech} - \Delta T_{elec} = I\frac{d}{dt}(\Delta\omega), \tag{A.49}$$

we then have

$$\Delta P_{mech} - \Delta P_{elec} = \omega^{r}efI\frac{d}{dt}(\Delta\omega) = M\frac{d}{dt}(\Delta\omega). \tag{A.50}$$

This can be expressed in Laplace transform operator notation as

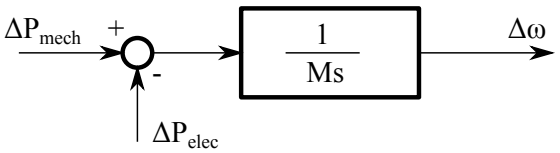

Figure A.1: Relationship between mechanical and electrical power and speed deviation.

$$\Delta P_{mech} - \Delta P_{elec} = Ms\Delta\omega. \tag{A.51}$$

We now consider the effect of loads on the speed deviation $\Delta\omega$. The loads on a power system consist of a variety of electrical devices. Some of them are purely resistive, some are motor loads with variable power-frequency characteristics, and others exhibit quite different characteristics. Since motor loads are a dominant part of the electrical load, there is a need to model the effect of a change in frequency on the net load drawn by the system. This relationship is given by

$$\Delta P_{L(freq)} = D\Delta\omega, \tag{A.52}$$

where D is expressed as percent change in load divided by percent change is frequency, $D = \frac{\Delta P_{L(freq)}}{\Delta \omega}$. For example, if load changed by 1.5% for a 1% change in frequency, then D would equal 1.5. The net change in P_{elec} is

$$\Delta P_{elec} = \Delta P_L + D\Delta\omega \tag{A.53}$$

where ΔP_L is nonfrequency-sensitive load change, and $D\Delta\omega$ is frequency-sensitive load change. Including this in the block diagram in Figure A.1 results in the new block diagram, see Figure A.2

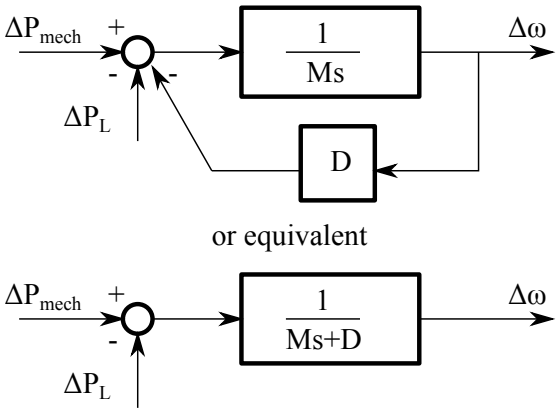

Figure A.2: Block diagram of rotating mass and load as seen by prime-mover output.

A.2.1 Generation Control

Automatic Generation Control (AGC) is the name given to a control system having three major objectives:

(1) To hold system frequency at or very close to a specified nominal value (e.g. 60 Hz).

(2) To maintain the correct value of interchange power between control areas.

(3) To maintain each unitt's generation at the most economic value.

A.2.2 Supplementary Control Action

A load change will produce a frequency change with a magnitude that depends on the droop characteristics of the governor and the frequency characteristics of the system load. Once a load change has occurred, a supplementary control must act to restore the frequency to nominal value. Assume that we are studying a single generating unit supplying load to an isolated power system. The supplementary control action can be accomplished by adding a reset (integral) control to governor, see Figure A.3.

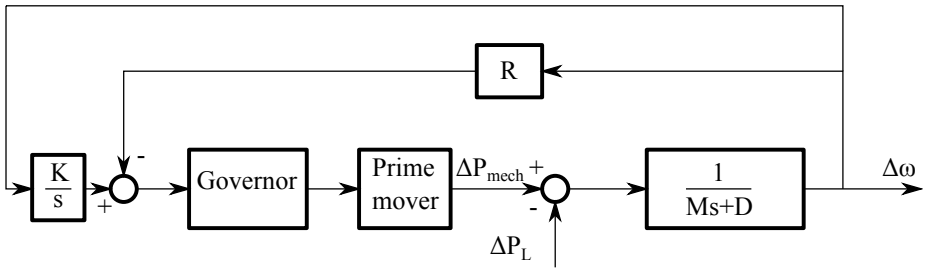

Figure A.3: Supplementary control added to generating unit.

A.2.3 Tie-line Control

When two utilities interconnect their systems, they do so for several reasons. One is to be able to buy and sell power with neighboring systems whose operating costs make such transactions profitable. Further, even if no power is being transmitted over ties to neighboring systems, if one system has a sudden loss of a generating unit, the units throughout all the interconnection will experience a frequency change and can help in restoring frequency.
Consider the hypothetical situation in Figure A.4. Assume both systems have equal gener-

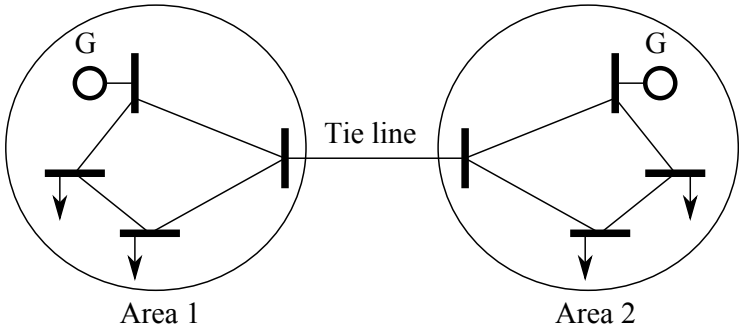

Figure A.4: Two-area system.

ation and load characteristics and, further, assume system in Area 1 was sending 100 MW to system in Area 2 under an interchange agreement made between the operators of each system. Now, let system 2 experience a sudden load increase of 30 MW. Since both units have equal generation characteristics, they will both experience an increase in flow from 100 MW to 115 MW. Thus, the 30 MW increase in Area 2 will have been satisfied by a 15 MW increase in generation in Area 2, plus a 15 MW increase in tie flow into Area 2. This would be fine, except that system 1 contracted to sell only 100 MW, not 115 MW. What is need at this point is a control scheme that recognizes the fact that 30 MW load increase occurred in system 2 and, therefore, would increase generation in system 2 by 30 MW while restoring frequency to nominal value. It would also restore generation in system 1 to its output before the load increase occurred.

We define a control area to be a part of an interconnected system within which the load and generation will be controlled as per tie-line frequency control scheme

(1) If frequency decreased and net interchange power leaving the system increased, a load increase has occurred outside the system.

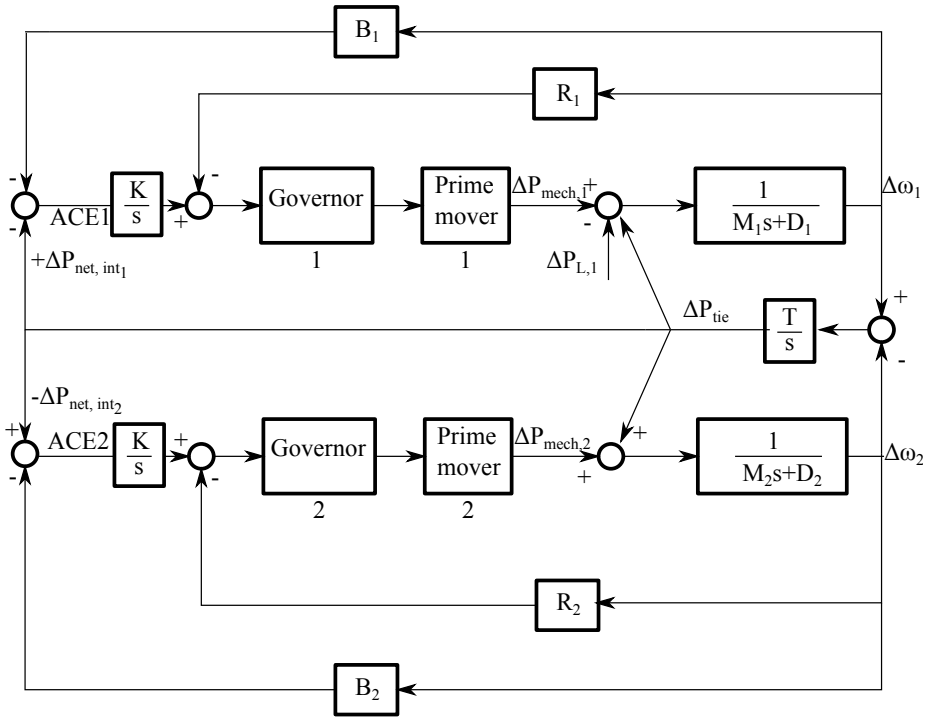

Figure A.5: Tie-line bias supplementary control for two areas.

(2) If frequency decreased and net interchange power leaving the system decreased, a load increase has occurred inside the system.

This can be extended to cases where frequency increases.

This control scheme can be implemented by a control mechanism that weighs frequency deviation, $\Delta\omega$, and net interchange power, $\Delta P_{net,int}$. The frequency response and tie flows resulting from a load change, ΔP_{L1}, in the two-area system in Figure A.4 can be expressed as

$$\Delta\omega = \frac{-\Delta P_{L1}}{\frac{1}{R_1}+\frac{1}{R_2}+D_1+D_2} \tag{A.54}$$

$$\Delta P_{net,int} = \frac{-\Delta P_{L1}\left(\frac{1}{R_2}+D_2\right)}{\frac{1}{R_1}+\frac{1}{R_2}+D_1+D_2} \tag{A.55}$$

The required change in generation, called area control error (ACE), represents the shift in the area's generation required to restore frequency and net interchange to their desired values. The equations for ACE for each area are

$$ACE1 = -\Delta P_{net,int_1} - B_1\Delta\omega, \tag{A.56}$$

$$ACE2 = -\Delta P_{net,int_2} - B_2\Delta\omega \tag{A.57}$$

where B_1 and B_2 are called frequency bias factors

$$B_1 = \left(\frac{1}{R_1}+D_1\right), \quad B_2 = \left(\frac{1}{R_2}+D_2\right).$$

This results in

$$ACE1 = \Delta P_{L1}, \tag{A.58}$$
$$ACE2 = 0. \tag{A.59}$$

This control can be carried out using the scheme outlined in Figure A.5.

A.2.4 Power Generation Basics

In the following sections, generation models which include a synchronous generator all use a form of the swing equation as the generator state equation

$$J\dot{\omega} + D\omega = P_m - P_e,$$

where $P_e \equiv P_G$ is the electrical power output. This generator equation differs for different technologies, since the mechanical power from the turbine, P_m, has a different representation for each turbine type.

A.2.5 Steam-Turbine-Generator

The full set of steam turbine-generator equations is

$$\begin{aligned} M\dot{\omega_G} &= (e_T - D)\omega_G + P_m - P_G \\ T_u\dot{P_m} &= -P_m + k_t a \\ T_g\dot{a} &= -\omega_G - ra + \omega^{ref} \end{aligned}$$

where

- $M = 1.26$ is the inertia constant,
- $e_T = 0.15$ defined by $\frac{\partial P_t}{\partial \omega_G}$ is a coefficient representing the turbine self-regulation,
- $D = 2$ is the damping coefficient,
- $T_u = 0.2$ is the time constant representing the delay between the control valves and the turbine nozzles,
- $k_t = 0.95$ is a proportionality factor representing the control valve position variation relative to the turbine output variation,
- $T_g = 0.25$ is the time constant of the valve-servomotor-turbine gate system,
- $r = 0.05$ is the permanent speed droop of the turbine,
- ω^{ref} is the reference frequency set by the secondary controls, and so is assumed constant in the primary dynamics time scale,
- P_G is the electrical power output defined as the system coupling variable.

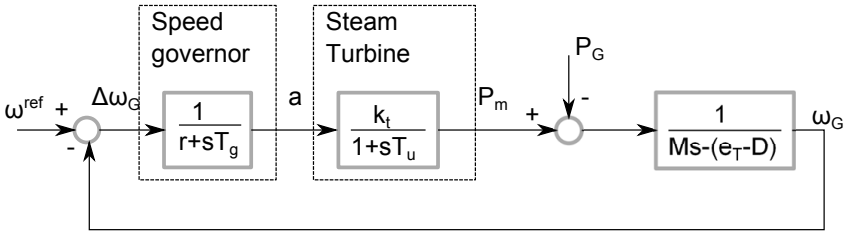

a	Valve position	M	Rotor inertia constant
P_m	Mechanical power	e_T	Turbine self-regulation
P_G	Electrical power	D	Rotor damping constant
ω_G	Rotor speed	ω^{ref}	Reference rotor speed
k_t	Propotionality factor	T_g	Time constant of the valve servomotor-turbine gate system
r	Permanent speed droop		

Figure A.6: Steam-Turbine-Generator.

The block diagram of Steam-Turbine-Generator is shown in Figure A.6. State-space representation

$$\dot{\boldsymbol{x}_G} = \begin{bmatrix} \frac{e_T-D}{M} & \frac{1}{M} & 0 \\ 0 & -\frac{1}{T_u} & \frac{k_t}{T_u} \\ -\frac{1}{T_g} & 0 & -\frac{r}{T_g} \end{bmatrix} \boldsymbol{x_G} + \begin{bmatrix} 0 \\ 0 \\ \frac{1}{T_g} \end{bmatrix} \omega^{ref} + \begin{bmatrix} -\frac{1}{M} \\ 0 \\ 0 \end{bmatrix} P_G$$

where $\boldsymbol{x_G} = \begin{pmatrix} \omega_G & P_m & a \end{pmatrix}^T$ is defined as local state variables.

A.2.6 Hydro-Turbine-Generator

Hydro turbines have a peculiar response due to water inertia: a change in gate position produces an initial turbine power change which is opposite to that sought. For stable control performance, a large transient (temporary) droop with a long resetting time is therefore required. Hence, a slightly more complex set of equations than that for the steam turbine contains governor droop ν as an additional state variable.
The set of equations for a hydro turbine-generator is

$$\begin{aligned} M\dot{\omega}_G &= -(e_H + D)\omega_G + k_q q - k_w a - P_G \\ \dot{q} &= \frac{\omega_G}{T_f} - \frac{q}{T_q} + \frac{a}{T_w} \\ T_e\dot{\nu} &= \nu + r'a \\ T_s\dot{a} &= -\omega_G + \nu - (r_h + r')a + \omega^{ref} \end{aligned}$$

where

- q is penstock flow,
- $M = 1.5$ and $D = 2$ are the inertia and damping constants as above,

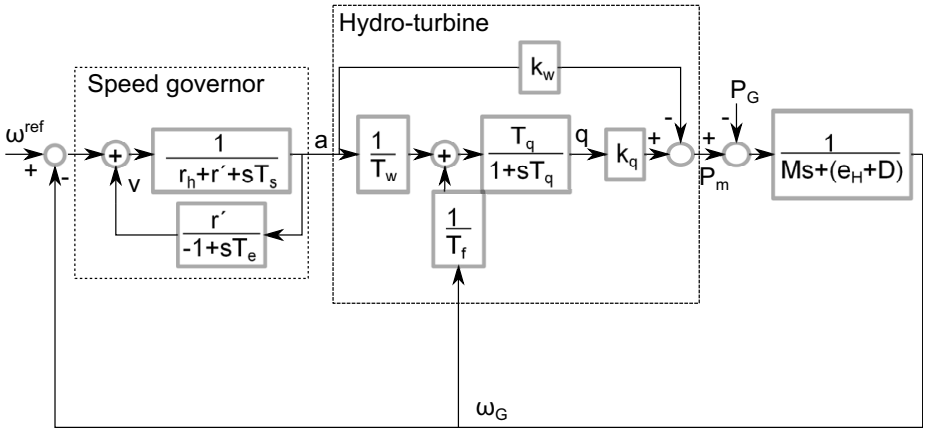

r_h	Permanent speed droop	P_m	Mechanical power	ω_G	Rotor speed
r'	Transient speed droop	P_G	Electrical power	a	Gate position
T_e	Time constant of the valve-turbine gate system	M	Rotor inertia constant	q	Penstock flow
		D	Rotor damping constant	v	Governor droop
T_s	Time constant of the servomotor gate				

T_w, T_q, T_f, e_H, k_q, k_w Ratios of constants from a standard hydro-turbine diagram

Figure A.7: Hydro-Turbine-Generator.

- $e_H = -0.22$, $k_q = 2.78$ and $k_w = 1.52$ are all ratios of constants from a standard hydro-turbine diagram referred to as the universal water turbine steady-state performance diagram,
- $T_f = -3.6$, $T_q = 0.72$, and $T_w = 0.76$ are also all ratios of constants from the same diagram,
- T_c is the time constant of the penstock,
- $T_e = 2$ is the time constant of the valve-turbine gate system,
- $T_s = 0.1$ is the time constant of the servomotor gates,
- $r_h = 0.05$ is the permanent speed droop,
- $r' = 0.4$ is the transient speed droop.

State-space representation

$$\dot{\boldsymbol{x}_G} = \begin{bmatrix} -\frac{e_H+D}{M} & \frac{k_q}{M} & 0 & -\frac{k_w}{M} \\ \frac{1}{T_f} & -\frac{1}{T_q} & 0 & \frac{1}{T_w} \\ 0 & 0 & \frac{1}{T_e} & -\frac{r'}{T_e} \\ -\frac{1}{T_s} & 0 & \frac{1}{T_s} & -\frac{r_h+r'}{T_s} \end{bmatrix} \boldsymbol{x_G} + \begin{bmatrix} 0 \\ 0 \\ 0 \\ \frac{1}{T_s} \end{bmatrix} \omega^{ref} + \begin{bmatrix} -\frac{1}{M} \\ 0 \\ 0 \\ 0 \end{bmatrix} P_G$$

where $\boldsymbol{x_G} = \begin{pmatrix} \omega_G & q & v & a \end{pmatrix}^T$ is defined as local state variables.

A.2.7 Combustion-Turbine-Generator

The typical model of gas turbines in stability studies is presented in Figure A.8. The set of

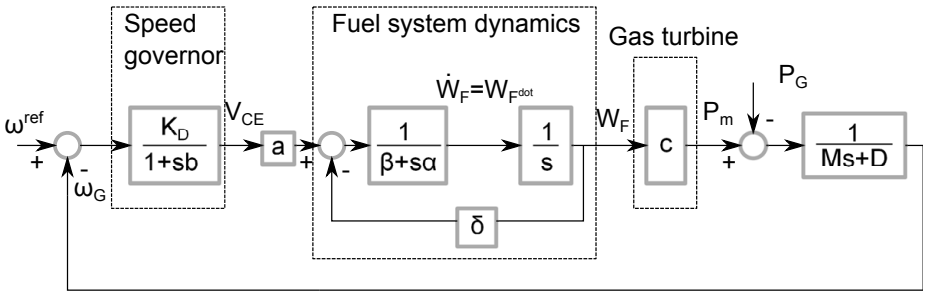

ω^{ref}	Reference rotor speed	$W_{F^{dot}}, W_F$	Fuel flow
ω_G	Rotor speed	P_m	Mechanical power output
V_{CE}	Fuel demand signal (fuel controller)	P_G	Electrical power output
		P_L	Load
M	Rotor inertia constant	D	Rotor damping constant

Figure A.8: Combustion-Turbine-Generator.

equations used for a combustion turbine is

$$\begin{aligned} M\dot{\omega_G} &= -D\omega_G + cW_F - P_G \\ b\dot{V_{CE}} &= -K_D\omega_G - V_{CE} + K_D\omega^{ref} \\ \dot{W_F} &= W_{F^{dot}} \\ \alpha\dot{W}_{F^{dot}} &= aV_{CE} - \delta W_F - \beta W_{F^{dot}} \end{aligned}$$

where

- V_{CE} is fuel controller,
- W_F, $W_{F^{dot}} = \dot{W_F}$ are fuel flow and fuel flow rate respectively,
- $M = 11.5$ and $D = 2$ are the rotor inertia and damping coefficients respectively,
- a, $b = 0.05$ and $c = 1$ are transfer function coefficients for the fuel system,
- $K_D = 25$ is the governor gain,
- $\beta = b + c\tau_F$ and $\delta = c + aK_F$ are algebraic functions of the parameters in the references,
- $\tau_F = 0.4$ is the fuel system time constant,
- $K_F = 0$ is the fuel system feedback gain.

State-space representation

$$\dot{\boldsymbol{x_G}} = \begin{bmatrix} -\frac{D}{M} & 0 & \frac{c}{M} & 0 \\ -\frac{K_D}{b} & -\frac{1}{b} & 0 & 0 \\ 0 & 0 & 0 & 1 \\ 0 & \frac{a}{\alpha} & -\frac{\delta}{\alpha} & -\frac{\beta}{\alpha} \end{bmatrix} \boldsymbol{x_G} + \begin{bmatrix} -\frac{1}{M} \\ 0 \\ 0 \\ 0 \end{bmatrix} P_G$$

where $\boldsymbol{x_G} = \begin{pmatrix} \omega_G & V_{CE} & W_F & W_{F^{dot}} \end{pmatrix}^T$ is defined as local state variables.

A.2.8 Combined Cycle Plant

The combined cycle combustion turbine, CCCT, model

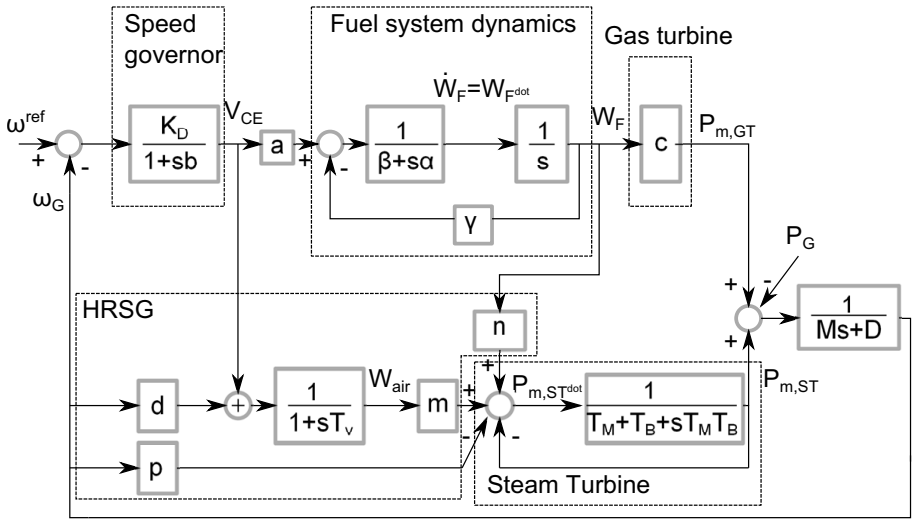

W_F	Fuel flow	V_{CE}	Fuel demand signal (fuel controller)
$W_{F^{dot}}$	Internal state of fuel system	T_v	Vane control time constant
W_{air}	Air flow - Thermodynamic coupling between the turbines	d	Ratio of the fuel flow to rotor speed
$P_{m,ST}$	Mechanical power of steam turbine	T_M, T_B	Time constants for simplified steam turbine
$P_{m,ST^{dot}}$	Internal state of steam turbine	p	Function of the turbine exhaust temperature
$P_{m,GT}$	Mechanical power of gas turbine	HRSG	Heat Recovery Steam Generator
P_G	Electrical power		
m, n	Enthalpy in the mass flow of the air and fuel respectively		

Figure A.9: Combined Cycle Plant.

has equations for both a combustion turbine and steam turbine driving the synchronous generator

$$\begin{aligned}
M\dot{\omega_G} &= -D\omega_G + (P_{m,GT} + P_{m,ST}) - P_G \\
b\dot{V_{CE}} &= -K_D\omega_G - V_{CE} + K_D\omega^{ref} \\
\dot{W_F} &= W_{F^{dot}} \\
\alpha\dot{W}_{F^{dot}} &= aV_{CE} - \gamma W_F - \beta W_{F^{dot}} \\
T_v\dot{W_{air}} &= d\omega_G + V_{CE} - W_{air} \\
\dot{P}_{m,ST} &= P_{m,ST^{dot}} \\
(T_M T_B)\dot{P}_{m,ST^{dot}} &= -p\omega_G + nW_F + mW_{air} - P_{m,ST} - (T_M + T_B)P_{m,ST^{dot}}
\end{aligned}$$

where

- M is the generator inertia constant,

- D is the generator damping constant.

State-space representation

$$\dot{\boldsymbol{x}_G} = \begin{bmatrix} -\frac{D}{M} & 0 & 0 & 0 & 0 & \frac{1}{M} & 0 \\ -\frac{K_D}{b} & -\frac{1}{b} & 0 & 0 & 0 & 0 & 0 \\ 0 & 0 & 0 & 1 & 0 & 0 & 0 \\ 0 & \frac{a}{\alpha} & -\frac{\gamma}{\alpha} & -\frac{\beta}{\alpha} & 0 & 0 & 0 \\ \frac{d}{T_v} & \frac{1}{T_v} & 0 & 0 & -\frac{1}{T_v} & 0 & 0 \\ 0 & 0 & 0 & 0 & 0 & 0 & 1 \\ -\frac{p}{T_M T_B} & 0 & \frac{n}{T_M T_B} & 0 & \frac{m}{T_M T_B} & -\frac{1}{T_M T_B} & -\frac{T_M+T_B}{T_M T_B} \end{bmatrix} \boldsymbol{x_G} + \begin{bmatrix} 0 \\ \frac{K_D}{b} \\ 0 \\ 0 \\ 0 \\ 0 \\ 0 \end{bmatrix} \omega^{ref} + \begin{bmatrix} -\frac{1}{M} \\ 0 \\ 0 \\ 0 \\ 0 \\ 0 \\ 0 \end{bmatrix} P_{m,GT} + \begin{bmatrix} -\frac{1}{M} \\ 0 \\ 0 \\ 0 \\ 0 \\ 0 \\ 0 \end{bmatrix} P_G$$

where $\boldsymbol{x_G} = \begin{pmatrix} \omega_G & V_{CE} & W_F & W_F dot & W_{air} & P_{ST} & P_{ST} dot \end{pmatrix}^T$ is defined as local state variables.

A.2.9 Wind Turbine: Induction Generator

The model for the wind turbine system is specifically developed a model to be used for dynamic studies of dispersed wind turbine applications

$$\begin{aligned} \dot{\omega_G} &= -\frac{D_G - D_T}{M_G}\omega_G + \frac{D_G - D_T}{M_G}\omega_T + \frac{1}{M_G}T_w - \frac{1}{M_G}P_G \\ \dot{\delta} &= -\omega_G + \omega_T \\ \dot{\omega_T} &= \frac{D_T}{M_T}\omega_G - \frac{K}{M_T}\omega_T - \frac{D_T}{M_T}\omega_T + \frac{1}{M_T}T_w \end{aligned}$$

where

- δ is the tortional spring,
- ω_G is the rotor speed of the induction generator,
- T_w defined as the wind torque is an input to the system of equations, as is P_G,
- d is the tortional spring,
- ω_T is the rotor speed of the wind turbine,
- $M_G = 5$, $M_T = 11$, $D_G = 0.8$ and $D_T = 1$ are the generator and turbine inertias and damping coefficients,

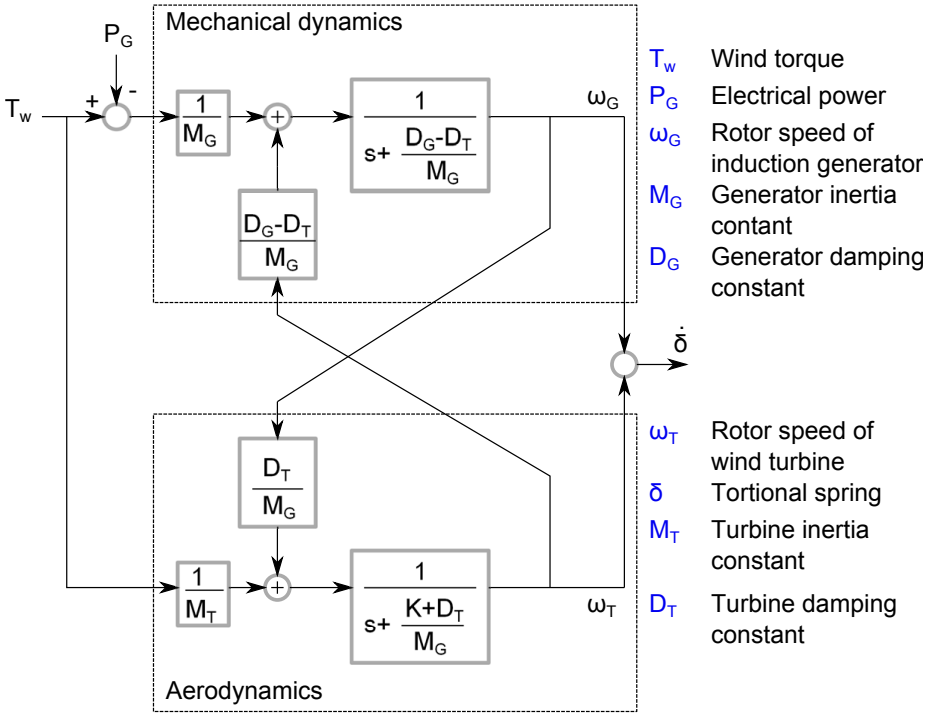

Figure A.10: Wind Turbine - Induction Generator.

- $K = 400$ is the spring constant of the tortional spring used to model the drive train coupling between the two rotors,

State-space representation

$$\dot{\boldsymbol{x_G}} = \begin{bmatrix} -\frac{D_G - D_T}{M_G} & 0 & \frac{D_G - D_T}{M_G} \\ -1 & 0 & 1 \\ 0 & 0 & 1 \\ \frac{D_T}{M_T} & 0 & -\frac{K}{M_T} - \frac{D_T}{M_T} \end{bmatrix} \boldsymbol{x_G} + \begin{bmatrix} \frac{1}{M_G} \\ 0 \\ \frac{1}{M_T} \end{bmatrix} T_W + \begin{bmatrix} -\frac{1}{M_G} \\ 0 \\ 0 \end{bmatrix} P_G$$

where $\boldsymbol{x_G} = \begin{pmatrix} \omega_G & \delta & \omega_T \end{pmatrix}^T$ is defined as local state variables.

B Appendix: Tables

B.1 Tables for Chapter 2

B.1.1 Parameters of GenCos in IEEE 6-bus system used for Example 2.3

Tabular B.1: Cost functions data of Generators

	GenCo1	GenCo2	GenCo3	ConCo1	ConCo2	ConCo3
c_G $[\$/MW^2h]$	1	1.5	1.8	-	-	-
c_D $[\$/MW^2h]$	-	-	-	-1	-0.7	-1.2
b_G $[\$/MWh]$	8.8	9.7	7	-	-	-
b_D $[\$/MWh]$	-	-	-	9.5	12	10.5

B.2 Tables for Chapter 3

B.2.1 Parameters of GenCos in IEEE 30-bus system used for Section 3.5

Tabular B.2: Cost functions data of Generators

Name	Block 1		Block 2	
	SizeMW	Price\$/MW	SizeMW	Price\$/MW
P_{g_1}	12.5	240	40	900
P_{g_2}	12.7	300	40	950
P_{g_5}	12.2	240	80	1200
$P_{g_{11}}$	12.2	240	80	1200
$P_{g_{13}}$	10	40	20	80

B.2.2 Parameters of ConCos in IEEE 30-bus system used for Section 3.5

Tabular B.3: Cost functions data of consumer

Name	Block 1		Block 2	
	SizeMW	Price\$/MW	SizeMW	Price\$/MW
P_{d_7}	11	150	19	600
$P_{d_{15}}$	10	100	21	600
$P_{d_{30}}$	12	170	22	600
P_{d_9}	12	150	24	600
$P_{d_{26}}$	15.5	150	21	600
$P_{d_{27}}$	9.5	150	22	600

Tabular B.4: Fixed load data

Name	Demand	Name	Demand
P_{d_3}	22.31	$P_{d_{14}}$	7.20
P_{d_4}	8.83	$P_{d_{16}}$	4.06
P_{d_8}	13.95	$P_{d_{17}}$	10.46
$P_{d_{10}}$	6.74	$P_{d_{18}}$	3.72
$P_{d_{12}}$	13.01	$P_{d_{19}}$	11.04
$P_{d_{20}}$	2.55	$P_{d_{21}}$	3.39
$P_{d_{23}}$	22.31	$P_{d_{24}}$	10.11
$P_{d_{26}}$	4.06	$P_{d_{29}}$	2.78

B.2.3 Parameters of transmission lines in IEEE 30-bus system used for Section 5.4 and 4.5

Tabular B.5: Transmission Lines Reactance; Line reactances are perunited based on $100MW$

Connected Bus		Reactance (x_{b_k})	Connected Bus		Reactance (x_{b_k})
Bus b	Bus k		Bus b	Bus k	
1	2	0.0575	1	3	0.1652
2	4	0.1737	3	4	0.0379
2	5	0.1983	2	6	0.1763
4	6	0.0414	5	7	0.116
6	7	0.082	6	8	0.042
6	9	0.208	6	10	0.556
9	11	0.208	9	10	0.11
4	12	0.256	12	13	0.14
12	14	0.2559	12	15	0.1304
12	16	0.1987	14	15	0.1997
16	17	0.1923	15	18	0.2185
18	19	0.1292	19	20	0.068
10	20	0.209	10	17	0.0845
10	21	0.0749	10	22	0.1499
21	22	0.0236	15	23	0.202
22	24	0.179	23	24	0.27
24	25	0.3292	25	26	0.38
25	27	0.2087	28	27	0.396
27	29	0.4153	27	30	0.6027
29	30	0.4533	8	28	0.2
6	28	0.0599			

B.3 Tables for Chapter 4

B.3.1 Parameters of GenCos in 4-bus system used for Section 4.3.1

Tabular B.6: Generators Cost and Demand Utilities Coefficients

	GenCo1	GenCo2	ConCo1	ConCo2
c_G $\$/MW^2h$	0.25	0.53	-	-
c_D $\$/MW^2h$	-	-	-0.41	-0.41
τ_G $\$/MW$	10	48	-	-
b_G $\$/MWh$	47.2	48.8	-	-
b_D $\$/MWh$	-	-	70	73
τ_D $\$/MW$	-	-	5	5

B.3.2 Parameters of transmission lines in 4-bus system used for Section 4.3.1

Tabular B.7: Transmission Lines Data

From	To	X $p.u.$	Capacity Limit MW
1	3	0.504	10
1	4	0.372	10
2	3	0.372	15
2	4	0.636	20

B.3.3 Initial conditions in 4-bus system used for Section 4.3.1

Tabular B.8: Initial Conditions

$x_i(0)$	Case 1	Case 2	$x_i(0)$	Case 1	Case 2
$P_{G1}(0)$	20	20	$\rho_1(0)$	57	57
$P_{G2}(0)$	10	10	$\rho_2(0)$	20	20
$P_{D1}(0)$	30	30	$\rho_3(0)$	60	60
$P_{D2}(0)$	35	35	$\rho_4(0)$	10	10
$\delta_1(0)$	0	0	$\gamma_{13}(0)$	10	10
$\delta_2(0)$	8	12	$\gamma_{14}(0)$	10	10
$\delta_3(0)$	2	2	$\gamma_{23}(0)$	10	10
$\delta_4(0)$	8	8	$\gamma_{24}(0)$	10	10

B.3.4 Parameters of GenCos in IEEE 30-bus system used for Section 4.5

Tabular B.9: Parameters of Cost functions for Generators

Name	$P_{G_i}^{min}$	$P_{G_i}^{max}$	τ_g	c_g	b_g
P_{g_1}	0	100	0.6	0.28	47.2
P_{g_2}	0	100	0.2	0.55	53.8
P_{g_5}	0	150	0.6	0.25	40
$P_{g_{11}}$	0	150	0.6	0.25	40
$P_{g_{13}}$	0	100	0.2	0.015	10

B.3.5 Parameters of ConCos in IEEE 30-bus system used for Section 4.5

Tabular B.10: Parameters of Cost functions for Consumers

Name	$P_{Dj}^{min}MW$	$P_{Dj}^{max}MW$	τ_d	c_d	b_d
P_{d_3},$P_{d_{19}}$	15	30	0.1	-0.2	87.2
P_{d_7},$P_{d_{20}}$	30	50	0.1	-0.5	85.5
P_{d_8},$P_{d_{21}}$	30	50	0.1	-0.15	70
P_{d_9},$P_{d_{23}}$	35.0	40	0.2	-0.35	70
$P_{d_{14}}$,$P_{d_{24}}$	10	30	0.2	-0.2	50
$P_{d_{15}}$,$P_{d_{26}}$	15	30	0.2	-0.3	60
$P_{d_{16}}$,$P_{d_{29}}$	6	20	0.2	-0.1	65
$P_{d_{17}}$,$P_{d_{30}}$	15	30	0.2	-0.5	68

Bibliography

[1] The New England Independent System Operator, http://www.iso-ne.com.

[2] The PJM Independent System Operator, http://www.nyiso.com.

[3] New England pool market rules and procedures, http://www.iso-ne.com/mrp/main.html.

[4] The Midwest Independent System Operator, "Real-time wind generation," http://www.midwestiso.org.

[5] Power System Analysis Toolbox (PSAT), http://www.uclm.edu/area/gsee/Web/Federico/software.htm.

[6] A. Kiani and A. M. Annaswamy, "Perturbation analysis of the wholesale energy market equilibrium in the presence of renewables," *Submitted to IEEE Transactions on Smart Grid*, 2012.

[7] A. Kiani and A. M. Annaswamy, "Wholesale energy market in a smart grid: Dynamic modeling, stability, and robustness," *Submitted to IEEE Transactions on Smart Grid*, 2012.

[8] A. Kiani and A. M. Annaswamy, "Control and optimization methods for electric smart grids," in *Control and Optimization Methods for Electric Smart Grids* (A. Chakrabortty and M. D. iIlic, eds.), vol. 3, ch. Wholesale Energy Market in a Smart Grid: A Discrete-time Model, Relation to Nash Equilibrium, and the Impact of Delays, pp. 87–110, Springer Verlag, 2011.

[9] A. Kiani and A. M. Annaswamy, "A hierarchical transactive control architecture for renewables integration in smart grids," *IEEE Conference on Decision and Control (CDC)*, (to appear) 2012.

[10] A. Kiani and A. M. Annaswamy, "Wholesale energy market in a smart grid: Dynamic modeling, and stability," *IEEE Conference on Decision and Control (CDC)*, pp. 2202-2207, 2011.

[11] A. Kiani and A. M. Annaswamy, "The effect of a smart meter on congestion and stability in a power market," *IEEE Conference on Decision and Control (CDC)*, pp. 194-199, 2010.

[12] A. Kiani and A. M. Annaswamy, "Distributed hierarchical control for renewable energy integration in a smart grid," *IEEE (PES) Conference on Innovative Smart Grid Technologies*, pp. 1-8, 2012.

[13] A. Kiani and A. M. Annaswamy, "Perturbation analysis of market equilibrium in the presence of renewable energy resources and demand response," *IEEE Innovative Smart Grid Technologies (ISGT)*, pp. 1-8, 2010.

[14] P. L. Joskow, *Deregulation of Network Industries: What's Next?* Washington DC: Brookings Press, 2000. Deregulation and regulatory reform in the U.S. electric sector.

[15] R. J. Green and D. M. Newbery, "Competition in the british electric spot market," *Journal of Political Economy*, vol. 100, pp. 929 – 953, 1992.

[16] R. J. Green, "Increasing competition in the british electricity spot market," *Journal of Industrial Economics*, vol. 44, pp. 205 – 216, 1996.

[17] R. Green, "The electricity contract market in england and wales," *The Journal of Industrial Economics*, vol. 47, no. 1, pp. 107 – 124, 1999.

[18] S. Borenstein and J. Bushnell, "An empirical analysis of the potential for market power in california's electricity industry," *Second Annual Research Conference of the Program on Workable Energy Regulation (POWER)*, 1997.

[19] P. L. Joskow, "Electricity sector restructuring and competition: Lessons learned," *Cuadernosde Economia (Latin American Journal of Economics),*, vol. 40, pp. 548 – 558, 2003.

[20] K. Skytte, "Market imperfections on the power market in northern europe: A survey paper," *Energy Policy*, vol. 27, pp. 25 – 32, 1999. vol 27 no 1.

[21] M. Kreuzberg, *Spot Prices of Electricity in Germany and Other European Countries*. Munich: Oldenbourg Industrieverlag, 2001.

[22] J. Chandley, S. Harvey, and W. W. Hogan, "Electricity market reform in california," *John F. Kennedy School of Government Harvard University*, 2000.

[23] S. Robinson, "Math model explains volatile prices in power markets," *SIAM News*, 2005.

[24] I.-K. Cho and S. P. Meyn, "Efficiency and marginal cost pricing in dynamic competitive markets with friction," *Theoretical Economics*, vol. 5, no. 2, pp. 215 – 239, 2010.

[25] F. C. Schweppe, M. C. Caramanis, R. D. Tabors, and R. E. Bohn, *Spot Pricing of Electricity*. Kluwer Academic Publishers, 1988.

[26] W. W. Hogan, "Contract networks for electric power transmission," *Journal of Regulatory Economics*, vol. 4, pp. 211 – 242, 1992.

[27] F. F. Wu and P. Varaiya, "Coordinated multilateral trades for electric power networks: theory and implementation," *International Journal of Electrical Power and Energy Systems*, vol. 21, pp. 75 – 102, 1999.

[28] G. C. Chow, *Dynamic economics: Optimization by the Lagrange Method*. Oxford University Press, 1997.

[29] R. D. Christie, B. F. Wollenberg, and I. Wangensteen, "Transmission management in the deregulated environment," *Proceedings of the IEEE*, vol. 88, no. 2, pp. 170 – 195, 2000.

[30] F. Rubio-Oderiz and I. Perez-Arriaga, "Marginal pricing of transmission services: a comparative analysis of network cost allocation methods," *IEEE Transactions on Power Systems*, vol. 15, pp. 448 – 454, 2000.

[31] E. Bompard, P. Correia, and G. Gross, "Congestion-management schemes: a comparative analysis under a unified framework," *IEEE Transactions on Power Systems*, vol. 18, no. 1, pp. 346 – 352, 2003.

[32] F. L. Alvarado, "The stability of power system markets," *IEEE Transactions on Power Systems*, vol. 14, no. 2, pp. 505 – 511, 1999.

[33] H. Glavitsch and F. Alvarado, "Management of multiple congested conditions in unbundled operation of a power system," *IEEE Transactions on Power Systems*, vol. 13, no. 3, pp. 1013 – 1019, 1998.

[34] M. Cain and F. Alvarado, "Implications of Cost and Bid Format on Electricity Market Studies: Linear Versus Quadratic Costs," *Large Engineering Systems Conference on Power Engineering*, June, 2004.

[35] R. J. Green, "The electricity contract market," *Second Annual Research Conference of the Program on Workable Energy Regulation (POWER)*, March 1997.

[36] B. F. Hobbs, C. B. Metzler, and J.-S. Pang, "Strategic gaming analysis for electric power networks: An mpec approach," in *Proceedings of the IEEE Power Engineering Society*, January - February 1999.

[37] M. Liu and G. Gross, "Congestion rents and ftr evaluations in mixed-pool-bilateral systems," *International Journal of Electrical Power and Energy Systems*, vol. 30, pp. 447 – 454, 2008.

[38] J. Yao, I. Adler, and S. Oren, "Modeling and computing two-settlement oligopolistic equilibrium in a congested electricity network," *Operations Research*, pp. 34 – 47, 2008.

[39] J. Yao, S. Oren, and I. Adler, "Two-settlement electricity markets with price caps and cournot generation firms," *european journal of operational research*, pp. 1279 – 1296, 2007.

[40] C. Ruiz and A. Conejo, "Pool strategy of a producer with endogenous formation of locational marginal prices," *IEEE Transactions on Power Systems*, pp. 1855 – 1866, 2009.

[41] X. Hu and D. Ralph, "Using epecs to model bilevel games in restructured electricity markets with locational prices," *Operations Research*, pp. 809 – 827, 2007.

[42] B. F. Hobbs, "Linear complementarity models of nash-cournot competition in bilateral and poolco power markets," *IEEE Transactions on Power Systems*, vol. 16, no. 2, pp. 194 – 202, 2001.

[43] B. Hobbs and J. Pang, "Nash-cournot equilibria in electric power markets with piecewise linear demand functions and joint constraints," *Operations Research*, pp. 113 – 127, 2007.

[44] B. F. Hobbs, C. B. Metzler, and J. S. Pang, "Strategic gaming analysis for electric power systems: An mpec approach," *IEEE Transactions on Power Systems*, vol. 15, no. 2, pp. 637 – 645, 2000.

[45] C. Metzler, B. F. Hobbs, and J. Pang, "Nash-cournot equilibria in power markets on a linearized dc network with arbitrage: Formulations and properties," *Networks and Spatial Theory*, pp. 123 – 150, 2003.

[46] A. C. R. Garcsia and S. Gabriel, "Electricity market near-equilibrium under locational marginal pricing and minimum profit conditions," *European Journal of Operational Research*, pp. 457 – 479, 2006.

[47] H. P. Chao and H. G. Huntington, *Designing Competitive Electricity Markets*. Kluwer Academic Publishers, 1998.

[48] B. F. Hobbs, "Network models of spatial oligopoly with an application to deregulation of electricity generation," *Operations Research*, vol. 34, no. 3, pp. 395 – 409, 1986.

[49] P. D. Klemperer and M. A. Meyer, "Supply function equilibria," *Econometrica*, vol. 57, pp. 1243 – 1277, 1989.

[50] A. Rudkevich and M. Duckworth, "Strategic bidding in a deregulated generation market: Implications for electricity prices, asset valuation and regulatory response," *The Electricity Journal*, 1998.

[51] C. J. Day and D. W. Bunn, "Agent-based simulation of electric power pools: A comparison with the supply function equilibrium approach," in *Proceedings of the 19th Annual North American Conference of the International Association for Energy Economics (IAEE)*, (Albuquerque New Mexico), October 1998.

[52] P. Visudhiphan and M. D. Ilic, "Dynamic game-based modeling of electricity markets," in *Proceedings of the IEEE Power Engineering Society*, 1999.

[53] F. Alvarado, J. Meng, W. Mota, and C. DeMarco, "Dynamic coupling between power markets and power systems," *IEEE Transactions on Power Systems*, vol. 4, pp. 2201 – 2205, 2000.

[54] Y. D. Tang, J. Wu, and Y. Zou, "The research on the stability of power market," *Automation of Electric Power Systems*, vol. 25, pp. 11 – 16, 2001.

[55] L. B. Cunningham, R. Baldick, and M. L. Baughman, "An empirical study of applied game theory: transmission constrained cournot behavior," *IEEE Transactions on Power Systems*, vol. 17, pp. 166 – 172, 2002.

[56] F. L. Alvarado, J. Meng, C. L. DeMarco, and W. S. Mota, "Stability analysis of interconnected power systems coupled with market dynamics," *IEEE Transactions on Power Systems*, vol. 16, no. 4, pp. 695 – 701, 2001.

[57] F. L. Alvarado, "Is system control entirely by price feasible?," in *Proceedings of the 36th annual Hawaii international conference on system sciences*, (Hawaii USA), 2003.

[58] F. L. Alvarado, "Controlling power systems with price signals," *Decision Support Systems*, vol. 40, no. 3, pp. 495 – 504, 2005.

[59] R. Sioshansi and W. Short, "Evaluating the impacts of real-time pricing on the usage of wind generation," *IEEE Transactions on Power Systems*, vol. 24, no. 2, pp. 516 – 524, 2009.

[60] F. Bouffard, F. D. Galiana, and A. J. Conejo, "Market-clearing with stochastic security-part i: Formulation," *IEEE Transactions on Power Systems*, pp. 1818 – 1826, 2005.

[61] F. Bouffard, F. D. Galiana, and A. J. Conejo, "Market-clearing with stochastic security-part ii: Case studies," *IEEE Transactions on Power Systems*, pp. 1827 – 1835, 2005.

[62] E. Bitar, R. Rajagopal, P. Khargonekar, K. Poolla, and P. Varaiya, "Bringing wind energy to market," *IEEE Transactions on Power Systems*, vol. 27, no. 3, pp. 1225–1235 , 2011.

[63] J. Hetzer, D. Yu, and K. Bhattarai, "An economic dispatch model incorporating wind power," *IEEE Transactions on Energy Conversion*, vol. 23, pp. 603 – 611, 2008.

[64] J. Morales, A. Conejo, and J. Pérez-Ruiz, "Economic valuation of reserves in power systems with high penetration of wind power," *IEEE Transactions on Power Systems*, vol. 24, pp. 900 – 910, 2009.

[65] P. Kundur, *Power System Stability and Control*. Mc-Graw-Hill, 1994.

[66] B. R. Herman, N. Zhu, J. Giri, and B. Kindel, "An agc implementation for system islanding and restoration conditions," *IEEE Transactions on Power Systems*, vol. 9, no. 3, 1994.

[67] M. Yao, R. R. Shoults, and R. Kelm, "Agc logic based on nerc's new control performance standard and disturbance control standard," *IEEE Transactions on Power Systems*, vol. 15, no. 2, pp. 852 – 857, 2000.

[68] N. Jaleeli, L. S. VanSlyck, M. M. Yao, R. R. Shoults, and R. Kelm, "Discussion of agc logic based on nerc's new control performance standard and disturbance control standard," *IEEE Transactions on Power Systems*, vol. 15, no. 4, pp. 1455 – 1456, 2000.

[69] T. S. Bhatti and D. P. Kothari, "Variable structure load-frequency control of isolated wind-diesel-microhydro hybrid power systems," *J. Inst. Eng.*, vol. 83, pp. 52 – 56, 2002.

[70] A. A. El-Emary and M. A. El-Shibina, "Application of static var compensation for load frequency control," *Elect. Machines Power Syst.*, vol. 25, no. 9, pp. 1009 – 1022, 1997.

[71] H. Asano, K. Yajima, and Y. Kaya, "Influence of photovoltaic power generation on required capacity for load frequency control," *IEEE Transactions on Energy Conversion*, vol. 11, no. 1, pp. 188 – 193, 1996.

[72] A. Paradkar, A. Davari, A. Feliachi, and T. Biswas, "Integration of a fuel cell into the power system using an optimal controller based on disturbance accommodation control theory," *J. Power Sources*, vol. 128, no. 2, pp. 218 – 230, 2004.

[73] E. Hirst, "Real time balancing operations and markets: Key to competitive wholesale electricity markets," *Technical Report for Edison Electric Institute*, 2001.

[74] A. Wood and B. Wollenberg, *Power Generation Operation and Control*. John Wiley & Sons, 1996.

[75] A. I. M. STUDY, "The future of the electric grid," tech. rep., Massachusetts Institute of Technology, 2011.

[76] F. Wu, P. Varaiya, P. Spiller, and S. Oren, "Folk theorems on transmission access: Proofs and counterexamples," *Journal of Regulatory Economics*, vol. 10, no. 1, pp. 5–25, 1996.

[77] "Final report on the august 14, 2003 blackout in the united states and canada: Causes and recommendations," tech. rep., U.S.-Canada Power System Outage Task Force, 2004.

[78] S. Oren, "Econmic inefficiency of passive transmission rights in congested electrcity systems with competetive generation," *The Energy Journal*, 1997.

[79] J. Bower and D. W. Bunn, "Model-based comparisons of pool and bilateral markets for electricity," *The Energy Journal*, vol. 21, no. 3, pp. 1–29, 2000.

[80] O. Alsac and B. Stott, "Optimal load flow with steady-state security," *IEEE Transactions on Power Systems*, vol. 93, pp. 745 – 751, 1974.

[81] N. P. Padhy, "Unit commitment - a bibliographical survey," *IEEE Transactions on Power Systems*, vol. 19, no. 2, pp. 1196–1205,, 2004.

[82] A. Aoki, T. Satoh, M. Itoh, T. Ichimori, and K. Masegi, "Unit commitment in a large scale power system including fuel constrained thermal and pumped storage hydro," *IEEE Transactions on Power Systems*, vol. 2, no. 4, pp. 1077–1084, 1987.

[83] A. J. Conejo, M. Carrion, and J. M. Morales, *Decision Making Under Uncertainty in Electricity Markets*. International Series in Operations Research and Management Science, Springer, New York, 2010.

[84] R. N. E. Bompard, Y. Ma, and G.Abrate, "The demand elasticity impacts on the strategic bidding behavior of the electricity producers," *IEEE Transactions on Power Systems*, pp. 188 – 197, 2007.

[85] A. J. Conejo, J. M. Arroyo, J. Contreras, and F. A. Villamor, "Self scheduling of a hydro producer in a pool-based electricity market," *IEEE Transactions on Power Systems*, vol. 17, no. 4, pp. 1265 – 1272, 2002.

[86] A. Gabraiel and J. More, *Complementarity and Variational Problems*. SIAM Publication, 1997.

[87] S. Torre, J. Contreras, and A. Conejo, "Finding multiperiod nash equilibria in pool-based electricity markets," *IEEE Transactions on Power Systems*, vol. 19, pp. 643 – 651, 2004.

[88] J. Rosen, "Existence and uniqueness of equilibrium points for concave n-person games," *Econometrica*, vol. 33, pp. 520 – 534, 1965.

[89] D. Fundenberg and J. Tirole, *Game Theory*. MIT Press, 1991.

[90] D. Fudenberg and D. K. Levine, *The Theory of Learning in Games*. Cambridge Massachusetts: The MIT Press, 1998.

[91] X. Chen and S. Xiang, "Perturbation bounds of p-matrix linear complementarity problems," *SIAM Journal on Optimization*, pp. 1250 – 1265, 2007.

[92] S. Meyn, M. Negrete, G. Wang, A. Kowli, and E. Shafieepoorfard, "The value of volatile resources in electricity markets," *IEEE Conference on Decision and Control (CDC)*, 2010.

[93] G. Wang, M. Negrete, , A. Kowli, E. Shafieepoorfard, S. Meyn, and U. V. Shanbhag, "Control and optimization methods for electric smart grids," in *Control and Optimization Methods for Electric Smart Grids* (A. Chakrabortty and M. D. iIlic, eds.), vol. 3, ch. Dynamic Competitive Equilibria in Electricity Markets, pp. 35–62, Springer Verlag, 2011.

[94] M. Roozbehani, M. A. Dahleh, and S. K. Mitter, "On the stability of wholesale electricity markets under real-time pricing," *IEEE Conference on Decision and Control (CDC)*, pp. 1911 – 1918, 2010.

[95] N. Li and J. R. Marden, "Design games for distributed optimization," *IEEE Conference on Decision and Control (CDC)*, pp.2434–2440, 2011.

[96] K. Arrow and L. Hurwicz, "On the stability of the competitive equilibrium," *Econometrica*, vol. 26, pp. 522 – 552, 1958.

[97] A. Nedic and A. Ozdaglar, "Subgradient methods for saddle-point problems," *Journal of Optimization Theory and Applications*, vol. 142, pp. 205 – 228, 2009.

[98] W. Hogan, “Providing incentives for efficient demand respons," prepared for electric power supply association comments on pjm demand response proposals, *Federal Energy Regulatory Commission*, 2009.

[99] M. D. Ilic, “From hierarchical to open access electric power systems,” *Proceedings of the IEEE*, vol. 95, no. 5, 2007.

[100] M. Milligan and B. Kirby, “Utilizing load response for wind and solar integration and power system reliability,” in *Wind Power Conference, Dallas, Texas*, 2010.

[101] A. Keyhani and A. M. Annaswamy, “A new automatic generation control with heterogeneous assets for integration of renewables,” *IEEE (PES) Conference on Innovative Smart Grid Technologies*, 2012.

[102] K. Khalil, *Nonlinear Systems*. Prentice Hall, 3 ed., 2002.

[103] T. Thiringer and J. Luomi, “Comparison of reduced-order dynamic models of induction machines,” *IEEE Transactions on Power Systems*, vol. 16, pp. 119 – 126, 2001.

[104] E. Hinrichsen and P. Nolan, “Dynamics and stability of wind turbine generators,” *IEEE Transactions on Power Apparatus and Systems*, vol. 101, pp. 2640 – 2648, 1982.

[105] S. Heier, *Gid Integration of Wind Energy Conversion Systems,* England: John Wiley & Sons, 1998.

[106] J. Slotine, and W. Li, *Applied Nonlinear Control*. Prentice Hall, 1 ed., 1991.

[107] D. P. Bertsekas, *Dynamic Programming And Optimal Control*. Athena Scientific, 2001.

[108] D. P. Bertsekas, *Nonlinear Programming*. Athena Scientific, 1999.

[109] M. Amin, and A. M. Giacomoni, “Smart grid - safe, secure, self-Healing,” *IEEE Power and Energy Magazine*, vol. 10, pp. 33 – 40, 2012.

[110] YV Makarov, “Incorporating Wind Generation and Load Forecast Uncertainties into Power Grid Operations,” *Report Pacific Northwest National Laboratory*, prepared for the U.S. Department of Energy, 2010.